THE UNIVERSITY OF QUEENSLAND

AUSTRALIA

Mannosylated lipopetides as model vaccines for targeting the mannose receptor

Bita Sedaghat

Pharmacy Doctorate

A thesis submitted for the degree of Doctor of Philosophy at

The University of Queensland in 2016

School of Chemistry and Molecular Biosciences

Abstract

The mannose receptor (MR) is an important component of the immune system and understanding the structural and conformational characteristics of this receptor is a key aspect of targeted vaccine design. Improved understanding of the role of carbohydrate recognition domains (CRDs) 4-7 in recognising glycosylated ligands present on the surface of pathogens such as *C. albicans*, *P. carinii*, *L. donovani*, and *M. tuberculosis* has given new insight into MR vaccine development. Initial studies identified mannan and its derivatives to be important ligands in MR targeting, providing essential knowledge about structural properties of the MR. During the last decade many attempts have been made to target this receptor for applications including vaccine and drug development.

In the present study, a library of vaccine constructs comprising fluorescently-labelled mannosylated lipid dendrimers that contained the ovalbumin $CD4^+$ epitope, $OVA_{323-339}$, as the model peptide antigen were synthesised using fluorenylmethyloxycarbonyl (Fmoc) solid phase peptide synthesis (SPPS). The vaccine constructs were designed with an alanine spacer between the *O*-linked mannose moieties to investigate the impact of distance between the mannose units on receptor-mediated uptake and/or binding in antigen presenting cells.

Mannosylated building blocks were prepared with a Lewis acid reaction and the reaction was successfully modified and monitored for a better yield. This was followed by solid phase synthesis of mannosylated peptides with an azide functional group and a fluorescent tag. Considering the presence of multi-components on the designed mannosylated peptide, different methods of preparation was used and a high yield of the final mannosylated peptides with an azide functional group and a fluorescent tag were prepared. Further, $OVA_{323-339}$ lipopeptides with an alkyne functional group were prepared using microwave assisted peptide synthesis. Final vaccine structures were prepared by attaching azide and alkyne functional groups using click chemistry. The same methods were applied for the preparation of a library of control vaccine structures.

In vitro uptake studies performed on macrophage ($F4/80^+$) and dendritic ($CD11c^+$) cells showed significant uptake and/or binding for vaccine constructs containing mannose and lipid, and also for the lipopeptide vaccine construct without mannose when compared to the controls (containing no lipid, no mannose and no mannose or lipid). Further, *in vitro* mannan competition assays demonstrated that uptake of the mannosylated and lipidated vaccine constructs was MR mediated. To address the specificity of receptor uptake, surface plasmon resonance (SPR) was performed using Biacore technology which confirmed a high affinity of the mannosylated and lipidated vaccine constructs towards the human recombinant MR *in vitro* when compared with vaccine constructs without mannose. These studies also confirmed that both mannose and lipid moieties play significant

roles in receptor-mediated uptake on APCs, potentially facilitating vaccine development. SPR methods were modified for a better quality of study.

In vivo studies with the aim of understanding immune modulatory effects of the mannose and lipid moieties in relation to the structural properties were performed. There have been many studies indicating the ability of the MR in linking the innate immunity (short-term immune response through macrophages and DCs) to adaptive immunity (long-term response by T cell activation and antibody response). This linkage is due to the MR mediated endocytosis of macrophages and dendritic cells (cells of innate immunity) and then antigen presentation to the T cells which isresponsible for a long-term adoptive response. However, it has not been completely disclosed whether uptake by the MR can induce the desired pathways involved in T cell activation. In this study, OT-II T cells were isolated from OT-II transgenic mice (B6.Cg-Tg[TcraTcrb]425Cbn/J) and were adoptively transferred to C57BL/6 mice. Adoptively transferred OT-II cell proliferation was shown to be unaffected by mannosylated lipopetide vaccine constructs. However, antigen specific cytokine release studies done by cytokine bead array and intra cellular staining, showed a relationship between the structural properties and the selection of specific T helper pathways (Th1 and Th2). Here, presence of both mannose and lipid activated cytokines (IL-4, IL-5, IL-13) related to Th2 pathway. On the other hand, the presence of lipid alone on the vaccine structures activated inflammatory cytokines (IL-2 and IFN-γ) that are related to the Th1 pathway. Here, it was also found that structural differences between the vaccine constructs including length of spacers between mannosyl moieties and presence of lipid could affect the levels of cytokine release. Structural differences were also responsible for selective action towards a Th pathway. For instance, two spacers on the vaccine structures with both mannose and lipid were more selective towards the Th2 response, while presence of lipid alone was able to act towards the Th1 pathway. In these studies a positive control group, ovalbumin 323-339 sequence mixed with cholera toxin (OVA+ CT), was used. Here, OVA+ CT, structures with mannose only and structures without mannose and lipid were not significant in the Th1 and Th2 cytokine activation pathways. Finally, antibody measurements following three time vaccinations showed a lack of antibody response against the vaccine constructs and their control groups. Overall, the results suggested activation of APCs by vaccine constructs that was not strong enough to activate a T cell or B cell response but could activate cytokine release.

Mannosylation has been shown to be an effective tool for antigen delivery to the immune system. There are studies that have indicated that mannosylation activates pathways to which the immune system does not react and recognises the antigens as self-antigens. This finding could mean an exciting future for vaccine and drug delivery and has to be further investigated.

Declaration by author

This thesis is composed of my original work, and contains no material previously published or written by another person except where due reference has been made in the text. I have clearly stated the contribution by others to jointly-authored works that I have included in my thesis.

I have clearly stated the contribution of others to my thesis as a whole, including statistical assistance, survey design, data analysis, significant technical procedures, professional editorial advice, and any other original research work used or reported in my thesis. The content of my thesis is the result of work I have carried out since the commencement of my research higher degree candidature and does not include a substantial part of work that has been submitted to qualify for the award of any other degree or diploma in any university or other tertiary institution. I have clearly stated which parts of my thesis, if any, have been submitted to qualify for another award.

I acknowledge that an electronic copy of my thesis must be lodged with the University Library and, subject to the policy and procedures of The University of Queensland, the thesis be made available for research and study in accordance with the Copyright Act 1968 unless a period of embargo has been approved by the Dean of the Graduate School.

I acknowledge that copyright of all material contained in my thesis resides with the copyright holder(s) of that material. Where appropriate I have obtained copyright permission from the copyright holder to reproduce material in this thesis.

Publications during candidature

i. **Peer-reviewed papers**

Sedaghat, B., Stephenson, R., and Toth, I., (**2014**) Targeting the Mannose Receptor with Mannosylated Subunit Vaccines. *Curr Med Chem*. 21 (30):3405-18

Sedaghat, B., Stephenson, R. J., Giddam, A., Eskandari, S., Apte, S. H., Pattinson, D. J., Doolan, D. L., and Toth, I. (**2016**) Synthesis of mannosylated lipopeptides with receptor targeting properties. *Bioconjugate chemistry*. 27 (3), 533-548

ii. Conferences abstract

Oral presentations

Bita Sedaghat, Rachel J. Stephenson, Ashwini Kumar Giddam, Sharareh Eskandari, Simon Apte, David Pattinson, Denise Doolan, and Istvan Toth, Binding and immune modulation properties of mannosylated lipo-peptide vaccines, *Vaccine and vaccination Asia pacific Global summit*, July 27-29, **2015** Brisbane, Australia

Bita Sedaghat, Rachel J. Stephenson, Ashwini Kumar Giddam, Sharareh Eskandari, Simon Apte, David Pattinson, Denise Doolan, and Istvan Toth, Mannosylated lipopeptides with receptor targeting properties, *School of Chemistry and Molecular Biosciences Symposium*, November 18th, **2014,** Brisbane, Australia

Bita Sedaghat, Rachel J. Stephenson, Ashwini Kumar Giddam, Sharareh Eskandari, Simon Apte, David Pattinson, Denise Doolan, and Istvan Toth, Targeting ability and immune modulatory effects of synthetic mannosylated lipopetide vaccines, *School of Chemistry and Molecular Biosciences Symposium*, November 26th, **2015,** Brisbane, Australia

iii. Poster Presentations

B. Sedaghat, R. Stephenson, I. Toth, Syntheis of mannosylated lipopeptides as targets for the mannose receptor, *Control Release Society (CRS)*, **2013**, Sydney, Australia

B. Sedaghat, R. Stephenson, I. Toth, Synthesis of OVA mannosylated peptides for targeting the mannose receptor, *The Brisbane Biological and Organic Chemistry Symposium (BBOCS)*, **2013**, Brisbane, Australia

Sedaghat B., R. Stephenson, A. Giddam, S. Eskandari, I. Toth, Synthesis and characterization of mannosylated lipid core peptides as particulates with targeting properties, *5th International NanoMedicine conference*, **2014**, Sydney Australia

B. Sedaghat, R. Stephenson, A. Giddam, S. Eskandari, I. Toth, mannosylated lipidcore peptides as particulates with targeting properties, *5th International NanoBio Conference*, July, **2014,** Brisbane, Australia

B. Sedaghat, R. Stephenson, A. Giddam, S. Eskandari, S. Apte, D. Pa I. Toth, Complex synthesis of mannosylated lipid core peptides to target the mannose receptor,*15th Tetrahedron Symposium*, June, **2014,** Syngapore

Bita Sedaghat, Rachel J. Stephenson, Ashwini Kumar Giddam, Sharareh Eskandari, Simon Apte, David Pattinson, Denise Doolan, Istvan Toth, mannosylated lipopeptides with receptor targeting properties, *School of Chemistry and Molecular Bioscinces Symposium*, November, **2013**, Brisbane, Australia

Publications included in this thesis

Publication citation – incorporated as part of Chapter 1.

Sedaghat, B., Stephenson, R., and Toth, I., (**2014**) Targeting the Mannose Receptor with Mannosylated Subunit Vaccines. *Curr Med Chem*. 21 (30):3405-18

Contributor	**Statement of contribution**
Bita Sedaghat (Candidate)	Wrote the paper (100%)
Rachel J. Stephenson	Edited paper (60%)
Istvan Toth	Edited paper (40%)

Publication citation – incorporated as part of Chapters 2, 3 and 4.

Sedaghat, B., Stephenson, R. J., Giddam, A., Eskandari, S., Apte, S. H., Pattinson, D. J., Doolan, D. L., and Toth, I. (**2016**) Synthesis of mannosylated lipopeptides with receptor targeting properties. *Bioconjugate chemistry*. 27 (3), 533-548

Contributor	**Statement of contribution**
Bita Sedaghat (Candidate)	Wrote the paper (100%) Designed experiment (10%) Synthesis and method development (100%) *In vitro* uptake study (50%) Confocal study (50%) T cell proliferation study (50%) Size characterization (50%) Surface Plasmon Resonance (100%) Analysis and data interpretation (70%)
Rachel J. Stephenson	Edited paper (60%) Project idea (20%) Design experiment (40%) Analysis and data interpretation (30%)
Ashwini Kumar Giddam	*In vitro* uptake study (50%)
Sharareh Eskandari	Size characterization (50%)
Simon H. Apte	Designed experiment (20%) Confocal study (50%) T cell proliferation study (50%)
David J. Pattinson	Edited paper (5%)
Denise L. Doolan	Edited paper (15%) Designed experiment (10%)
Istvan Toth	Edited paper (20%) Project idea (80%) Designed experiment (20%)

Contributions by others to the thesis

Works and contributions to chapter 1.

Contributor	**Statement of contribution**
Bita Sedaghat (Candidate)	Writing (100%)
Rachel J. Stephenson	Edited (90%)
Istvan Toth	Edited (10%)

Works and contributions to chapters 2, 3, 4 and 5.

Contributor	**Statement of contribution**
Bita Sedaghat (Candidate)	Writing (100%) Designed experiment (10%) Synthesis and method development (100%) *In vitro* uptake study (50%) Confocal study (50%) T cell proliferation study (50%) Size characterization (50%) Surface Plasmon Resonance (100%) *In vivo* animal study (60%) which includes: ➢ Mice vaccination ➢ T cell proliferation ➢ Intracellular staining ➢ Cytokine bead array ➢ ELISA study Analysis and data interpretation (70%)
Rachel J. Stephenson	Edited writing (90%) Project idea (20%) Design experiment (35%) Analysis and data interpretation (30%)
Ashwini Kumar Giddam	*In vitro* uptake study (50%)
Sharareh Eskandari	Size characterization (50%)
Simon H. Apte	Designed experiment (35%) Confocal study (50%)

	T cell proliferation study (50%)
David J. Pattinson	*In vivo* animal study (40%) which includes: ➢ Mice vaccination ➢ T cell proliferation ➢ Intracellular staining ➢ Cytokine bead array ➢ ELISA study
Denise L. Doolan	Designed experiment (10%)
Istvan Toth	Edited writing (10%) Project idea (80%) Designed experiment (10%)

Statement of parts of the thesis submitted to qualify for the award of another degree

"None".

Acknowledgements

There are a number of people without whom this thesis would not have been possible and I would like to give them my deepest appreciation.

First I would like to thank my supervisor Professor Istvan Toth, who gave me an opportunity to start the work and gave me support throughout the time course of my PhD. Further, I would like to thank Dr. Rachel Stephenson who was present during my PhD and has put a lot of effort in revising my writings.

To my husband, Faramarz, who, has been a big support throughout my build up carrier and not only my PhD study. Thank you for giving me comfort when everything seemed impossible. Thanks for fighting with me against the hurdles of life.

To my son, Behrad, who, I adore and cannot live without a day. Thank you for understanding of my long hours of work and my tiredness. I love you and I am very grateful for having you.

To my parents, for being an encouragement for my studies and who have been a comfort in my life by giving me unconditional love. Thanks to my brothers and sister who I can always rely on when everything in life seems hard.

Finally I would like to thank University of Queensland International scholarship for providing me with the opportunity of PhD study.

Thank you.

Keywords

Vaccine, mannosyl, lipopeptide, receptor, targeting, ovalbumin

Australian and New Zealand Standard Research Classifications (ANZSRC)

ANZSRC code: 060110, Receptors and Membrane Biology 60%

ANZSRC code: 111599, Pharmacology and Pharmaceutical Sciences not elsewhere classified, 20%

ANZSRC code: 030406, Proteins and Peptides, 20%

Fields of Research (FoR) Classification

FoR code: 0601, Biochemistry and Cell Biology, 20%

FoR code: 0304, Medicinal and biomolecular chemistry, 50%

FoR code: 1115, Pharmacology and pharmaceutical sciences, 30%

Table of Contents

List of Abbreviations

3-D	three-dimensional
µM	Micromolar
Ac_2O	Acetic anhydride
ANOVA	Analysis of variance
Apa	Antigenic protein
APC	Antigen presenting cells
$BF_3.Et_2O$	Boron trifluoride diethyl etherate
Boc	Benzyloxycarbonyl
BSA	bovine serum albumin
C12	2-aminododecanoic acid
CBA	Cytokine bead array
CD	Cluster of differentiation
CFA	Complete Freund's adjuvant
CLR	C-type lectin receptors
CRD	Carbohydrate recognition domain
CR	Cysteine rich
CT	Cholera toxin
CTLD	C-type lectin like domain
Cu(I)	Copper(I)
CuAAC	Copper-catalysed alkyne-azide cycloaddition reaction
DAAM	Diethylacetamidomalonate
DC	Dendritic cell
DCM	Dichloromethane
DC-SIGN	Dendritic cell-specific intercellular adhesion molecule-3-grabbing non-integrin
Dde	2-Acetyldimedone
Dde-C_{12}-OH	2-(4,4-Dimethyl-2,6-dioxocyclohex-1-ylidene) ethylaminododecanoic acid
DIC	N,N'-Diisopropylcarbodiimide
DIPEA	N,N'-Diisopropylethylamine
DLS	dynamic light scattering
DMAP	4-Dimethylaminopyridine
DMF	N,N'-Dimethylformamide
DMSO	Dimethyl sulfoxide

EDTA	Ethylenediaminetetraacetic acid
ELISA	Enzyme-linked immunosorbent assay
ESI-MS	Electrospray ionization-mass spectrometry
Et2O	Diethylether
EtOAc	Ethyl acetate
FACS	Fluorescence-activated cell sorting
FAM	5(6)-Carboxyfluorescein
FBS	Fetal bovin serum
Fmoc	Fluorenylmethyloxycarbonyl
FNII	Fibronectin type II
GM-CSF	granulocyte macrophage colony-stimulating factor
h	Hours
HATU	1-[Bis(dimethylamino)methylene]-1H-1,2,3-triazolo[4,5-b]-pyridinium 3-oxid hexafluorophosphate
HBTU	O-Benzotriazole-N,N,N’,N’-tetramethyluronium-hexafluorophosphate
HCl	Hydrochloric acid
HEPES	4-(2-hydroxyethyl)-1-piperazineethanesulfonic acid
HOBt	Hydroxybenzotriazole
HPLC	High-performance liquid chromatography
I.V.	Intravenous
ICS	Intra cellular staining
IFN	Interferon
Ig	Immunoglobulin
IgG	Immunoglobulin G
IL	Interlukin
IMDM	Iscove's Modified Dulbecco's Medium
IvDde	(4,4-dimethyl-2,6-dioxocyclohex-1-ylidene)-3-methylbutyl
K_D	Affinity constant
LCP	Lipid core peptide
LAM	Lipoarabinomannan
LPS	Lipopolysaccharide
m/z	mass to charge ratio
MACS	Magnetic-activated cell sorting
Man-BSA	BSA conjugated to mannan

MAP	multiple antigenic peptides
MBHA	4-Methylbenzhydrylamine
MeCN	Acetonitrile
$MgCl_2$	Magnesium chloride
MgSO4	Magnesium sulfate
MHC	Major histocompatibility complex
mM	Millimolar
mmol	Millimole
MPL	Monophosphoryl lipid-A
MR	Mannose receptor
Mtt	4-Methyltrityl
N_2	Nitrogen gas
NaCl	Sodium chloride
NK	Natural killer
NMR	Nuclear magnetic resonance
OVA	Ovalbumin
Pam2Cys	Dipalmitoyl-S-glyceryl cysteine
Pam3Cys	Tri-palmitoyl-S-glyceryl cysteine
PBMC	Peripheral blood mononuclear cell
PBS	Phosphate-buffered saline
PDI	polydispersity index
PEG	Polyethylene glycol
PEGtide	polyethylene glycol peptide
PRR	Pattern recognition receptors
Rmax	maximum analyte binding capacity of the surface in RU
RP-HPLC	Reverse phase high-performance liquid chromatography
RT	Room temperature
Rt	Retention time
RU	Response units
s	Second
S.C.	Subcutaneous
SDS	Sodium dodecyl sulfate
SPPS	Solid phase peptide synthesis

SPR	Surface plasmon resonance
tBu	tert-Butyl
TCR	T cell receptor
TEM	Transmission electron microscopy
TFA	Trifluoroacetic acid
Th	T helper
TIPS	Triisopropylsilane
TLRs	Toll-like receptors
UV	Ultraviolet

List of Figures

Figure 1-5. Mannose receptor and cellular targeting pathway. 1: Attachment of glycosylated ligands (e.g. mannan from the surface of bacteria) to CRD4-8 of the mannose receptor, followed by **2:** internalisation and degradation of ligands by the lysosome for adaptive immune responses. **3:** Presentation of degraded ligands to the surface of the dendritic cell through MHC I and II and co-stimulatory receptors (e.g. CD80/CD86). **4:** Naïve T cell activation through MHC I and II pathways where, **5:** MHC II pathway activates CD4 T cells and achieves, **6:** T-helper response activating cytokine release, or **7:** MHC I pathway activates $CD8^+$ T cells. **8:** Cytotoxic T-lymphocytes response to eliminate infected ligands. The innate pathway activates through **9:** direct release of cytokines through the DC.

Figure 1-6. A typical N-linkage through asparagine (Asn) is highlighted with examples of mannose receptor binding N-linked proteins from *C. albicans* [97], mucin from *Pichia pastoris* [98] and *Saccharomyces cerevisiae* [99]. A typical serine/threonine (Ser/Thr) *O*-linkage is highlighted. Examples of mannose receptor *O*-linked binding proteins include mucin from *Pichia pastoris*, *Saccharomyces cerevisiae* and *M. tuberculosis* [100, 101].

Figure 1-7. **Oxidised and reduced structures of mannose**. Under mild oxidation conditions (e.g. Br_2/H_2O), the C-6 carbon on mannose is oxidised to a carbonyl group forming mannuronic acid; under reducing conditions (e.g. sodium amalgam), mannose is converted to mannitol with the formation of an alcohol at the C-1 carbon. Reduced and oxidised variations of mannan have been used to investigate mannose receptor targeting [92].

Figure 1-8. Schematic of a Manα6Man glycocluster. Frison *et al.* found this structure bound strongly to the mannose receptor resulting in endocytosis of the gycocluster [121].

Figure 1-9. Mannosylated peptides designed to investigate the relationship between the number of mannose groups and their receptor targeting ability. Schematic structure of the mannosylated peptides synthesised by Brimble *et al.* to investigate the relationship between linear and branched mannosylation and receptor targeting [130]. An investigation was carried out using **A:** linear mannosylated peptides separated by alanine spacers, and **B:** di-branched mannosylated peptides separated by alanine spacers. No difference was observed in the targeting ability of linear (**A**) and di-branched (**B**) mannosylated constructs, however spacer length was found to play a role in receptor binding. A fluorescent tag (5(6)-carboxyfluorescein) was included in each glycosylated peptide for bioassay analysis.

Figure 1-10. Oligomannoside clusters synthesised by Bissen *et al.* The structures showing the best affinity for the mannose receptor are **A:** a cluster with five terminal mannoses, and **B:** a cluster with six terminal mannose groups.

Figure 1-11. Lipid core polylysine with multiple epitopes made by Moyle *et al.* Structures contained either *N*-linked mannose or N-linked glucose in both acetylated and deacetylated forms. Both acetylated and deacetylated delivery systems that contained mannose successfully reduced tumour size in mice when compared to glucose delivery systems.

Figure 1-12. Vaccine types. A: Subunit vaccines are prepared by use of part of the pathogen that provokes immune response, this can be based on biological extraction methods (recombinant) or synthetic methods (peptides); **B:** inactivated vaccines are prepared by inactivation of pathogens by heat or chemicals; **C:** live attenuated vaccines are prepared by weakening the pathogen through multiple passages.

Figure 1-13, Schematic diagram of solid phase peptide synthesis. Solid resin support is used to build a peptide chain from individual amino acids where orthogonal Fmoc or Boc protecting groups are used depending on the synthesis conditions, such as the choice of resin. Cleavage of the poly-amino acid chain from the resin generates a peptide in the last step.

Figure 1-14. General Structure of common lipidic adjuvants. These lipidic adjuvants are used in peptide conjugation to enhance immunogenicity; monophosphoryl lipid A (MPLA), di-palmitoyl-S-glyceryl-cystein (Pam2Cys), tri-palmitoyl-S-glyceryl-cystein (Pam3Cys), LCP [159].

Figure 1-15. Toll-like receptor signalling pathway. TLRs are trans-membrane receptors from the family of pattern recognition receptors that exist as both extracellular (TLR-1, 2, 4, 6) and intracellular (TLR-3, 7, 8, 9) molecules. Signalling molecules including IRAK-1-4, TBK1, MyD88s activate a series of nuclear transcription factors (NF-κB, AP-1, NF-IL6 and IRF) causing the cell to produce inflammatory cytokines (TNF, ILs and IFN).

Figure 3-1. Schematic picture of the vaccine construct library. The main library includes vaccine constructs where n is the number of alanine units between each mannose moiety. The sequence for the $OVA_{323-339}$ peptide is a model antigen. Mannose is included into the structures for its mannose receptor targeting ability. The lipid (C12) is added to provide self adjuvanting properties. Designed

final vaccine structures are prepared in two sections **A** and **B**. Section **A** is $OVA_{323-339}$ lipopetide (in case of controls no lipid is on the structure) with alkyne functional group able to be attached to section **B** which is the mannosylated peptide (in case of controls no mannose on the structure) with azido functional group. The final library is provided by an azide-alkyne reaction and formation of a triazole cycle (**C**). The vaccine control library consists of constructs without mannose (D), without lipids (E) and without mannose and lipid moieties (F) and these are used to compare the effect of each moiety on *in vitro* and *in vivo* studies.

Figure 3-2. Scheme for the synthesis of Fmoc-serine mannosylated amino acid building blocks. 1,2,3,4,6-Penta-*O*-acetyl-α,β-$_D$-mannopyranosyl (**1**) was synthesised using $_D$-mannose, DMAP, Ac_2O, 46°C, 24 h, N_2 gas in a 85% yield. N-Fmoc-*O*-(2,3,4,6-tetra-*O*-acetyl-α,β-$_D$-mannopyranosyl)-L-serine (**2**) was synthesised with the addition of Fmoc-serine-OH, $BF_3.Et_2O$, DCM, RT, 4 h in a 42% yield.

Figure 3-3. Mechanism of action for the $BF_3.Et_2O$ Lewis acid reaction. Conjugation of **1** (acetylated mannosyl donor) to Fmoc-Ser-OH using $BF_3.Et_2O$ in DCM at RT for 4 h generated **2** (Fmoc-serine mannosylated amino acid building blocks) as a mixture of α and β due to attack of the Lewis acid from both below (β, 25.44%) and above (α, 74.55%) [230]. For synthesis details see **Chapter 2**, **Section 2.1.2.**

Figure 3-4. Monitoring of the boron trifluoride diethyl etherate ($BF_3.Et_2O$) Lewis acid reaction at 1, 2, 3, 4, 6, and 8 h by analytical RP-HPLC on a C18 column (0 to 100% acetonitrile gradient over 30 min). At 4 h, the optimum yield for the product (**2**, 42%) was observed with a retention time (Rt) of 23.6 min (peak indicated by an arrow) and this eluted at 62% solvent B (**Chapter 2, Section 2.1.1**). Rt 19.3 min is the Fmoc-serine-OH starting material and Rt: 21.5 min is the product missing one acetyl group. The graph was drawn using nudging (overlaying graphs with an angle) in GraphPad Prism.

Figure 3-5. Azide functionalized mannosylated peptide 3. Peptide **3** was synthesised using Method 1 and resulted in a low overall yield of 5%. (a) 20% Piperidine in DMF, RT; (b) Fmoc-lys(IvDde)-OH, HATU, DIPEA; (c) **2**, HATU, DIPEA, DMF; (d) Fmoc-Ala-OH, HATU, DIPEA, DMF; (d*) repeated a and d; (e) 5(6)-carboxyfluorscein (FAM), DIC, HOBt, DMF; (f) 5% hydrazine in DMF on resin (3 × 30 min), RT; (g) azidoacetic acid, HATU, DIPEA, DMF; (h) 95% TFA: 2.5% water: 2.5% TIS. For a detailed synthesis protocol see **Chapter 2**, **Section 2.1.4.1**.

Figure 3-6. HPLC traces of peptides 3 and 4. (A) **3** prepared using Method 1 and obtained in a yield of 5%, Rt=13.69; and (B) **4** prepared using **Method 2** and obtained in a yield of 54%, Rt=20.36. Analytical RP-HPLC: 0-100% acetonitrile gradient over 30 min. For a detailed synthesis protocol see **Chapter 2**, **Section 2.1.4.1**.

Figure 3-7. Reagents and conditions for the synthesis of peptides 4-7: (a) 20% Piperidine in DMF, RT; (a*) 2 cycles of piperidine in DMF; (b) Fmoc-lys(Mtt)-OH, HATU, DIPEA; (c) 2% TFA: 1% TIPS in DCM, 20 cycles; (d) azidoacetic acid, HATU, DIPEA, DMF; (e) N-Fmoc-*O*-(2,3,4,6-tetra-*O*-acetyl-α,β-$_D$-mannopyranosyl)-L-serine, HATU, DIPEA, DMF; (f) Fmoc-Ala-OH, HATU, DIPEA, DMF; (g) 5(6)-carboxyflourscein (FAM), DIC, HOBt, DMF; (h) 95% TFA: 2.5% water: 2.5% TIS. For a detailed synthesis protocol see **Chapter 2**, **Section 2.1.4.2**.

Figure 3-8. Synthesis of the Dde (9) lipid protecting group and the Dde-C12 lipid (10). 2-Acetyldimedone (Dde, **8**) was synthesised using solution synthesis, and was then used to protect the N-terminal of the C12 lipid (**9**) in a reaction with **8** generating the Dde protected C12 lipid (**10**, Dde-C12). For a detailed synthesis protocol see **Chapter 2**, **Section 2.1.5**.

Figure 3-9. Reagents and conditions for microwave-assisted synthesis of peptides 11 and 12; (a) 20% Piperidine in DMF, 20W, 70°C for 2 min + 5 min; (b) Fmoc-Gly-OH; (c) **10**, HATU, DIPEA; (d) 2% hydrazine in DMF (4 x 10 min); (e) Fmoc-Lys-IvDde-OH, HATU, DIPEA; (f) Fmoc-Lys-Fmoc-OH, after deprotection of Fmoc, Ile(Boc) - Ser(tBu) – Gln(Trt) – Ala - Val – His(Trt) - Ala - Ala – His(Trt) - Ala – Glu(OtBu) - Ile – Asn(Trt) – Glu(OtBu) - Ala - Gly – Arg(Pbf) were coupled consequently (in HATU and DIPEA), all amino acids were Fmoc protected and deprotection of Fmoc group was performed as mentioned at (a); (g) 2% hydrazine in DMF on resin (3 × 30 min), RT; (h) pentynoic acid, HBTU, DIPEA, overnight, at RT; (i) 95% TFA: 2.5% water: 2.5% TIS. For a detailed synthesis protocol of peptides **11** and **12** see **Chapter 2**, **Section 2.1.6**.

Figure 3-10. Mannosylated lipopeptide vaccine constructs 13-15, prepared from a copper-mediated click reaction (DMSO, 5 h, RT, N_2 gas) of the lipopeptide-alkyne (**11**) with fluorescently-labelled mannosylated-azides (**4-6**). The formation of the triazole bond in this reaction is highlighted with a square. See **Chapter 2, Section 2.1.7.**

Figure 3-11. Library of fluorescently-labelled mannosylated lipopeptide vaccine constructs (13-15) and control constructs (16-18). The test constructs, containing a variable length alanine spacer between each mannose moiety are **13** (n=0), **14** (n=1) and **15** (n=2). Control constructs for cell-based

studies include **16** (no mannose moieties, n=2), **17** (no lipid moieties, n=2), and **18** (no lipid or mannose moieties, n=2), where n is the number of alanine amino acids. $OVA_{323-339}$ epitope (model antigen) was included as a CD4 T cell epitope. FAM was included in each construct to enable detection in *in vitro* cell studies. The lipid is C12.

Figure 3-12. RP-HPLC trace for the copper-mediated click reaction between peptides 4 and 11 for the formation of vaccine construct 15. (A) **4**, Rt 20.83 min; (B) **15** (a diastereomeric mixture), Rt 21.2 min, 21.6 min, 21.8 min; (C) **11** Rt 23.5 min. Click reaction was performed in DMSO at 50°C under an N_2 atmosphere and stopped after 5 h.

Figure 3-13. TEM images of vaccine constructs 13-18. (A) **13**, (B) **14,** (C) **15,** (D) **16**, (E) **17**, and (F) **18.** The scale bar is 200 nm.

Figure 4-1. *In vitro* uptake/binding and mannan competition study, Vaccine constructs **13-18** (0.5 µM) and control constructs **16-18** (0.5 µM) were assessed in (A) $CD11c^+$ and (B) $F4/80^+$ cells for uptake in the presence or absence of mannan (construct + mannan [1 mg/ml] vs construct alone). Dextran-FITC (1 mg/ml) was the positive control. PBS was the negative control. The study was performed in triplicate and the results were analysed using one-way ANOVA with mean ± SD from three independent experiments, $p<0.0001$.

Figure 4-2. Confocal images, $F4/80^+$ cells (2×10^5) were incubated with vaccine constructs **13**, **15** and **16** (0.5 µM) in the presence or absence of mannan, with commercially available mannan-FITC as the positive control. Cells were plated on culture slides. FAM-labelled vaccine constructs (green) were added to the cells and incubated in the presence and absence of mannan for 4 h at 37°C. Nuclei were stained with Hoechst stain (blue). $F4/80^+$ cells were identified with anti-F4/80 antibody (red). (A) mannan-FITC; (B) vaccine construct **13**; (C) cells pre-incubated with mannan followed by addition of **13**; (D) vaccine construct **15**; (E) vaccine construct **16**. Analysis was performed on a GE DeltaVision Deconvolution confocal microscope at 60x using oil immersion, graphical scales 15µm and 5µm.

Figure 4-3. *In vitro* OT-II spleen proliferation assay. Different dilutions of constructs **13-18** and control peptide, $OVA_{323-339}$ were compared for their ability to stimulate T cell proliferation (5×10^5 cells per well). PBS was used as the negative control. The study was performed in triplicate and the results were analysed with mean ± SD from three independent experiments, $p < 0.0001$.

Figure 4-4. Schematic diagram of SPR performance on a CM-5 chip. CM-5 chips have a dextran surface that enables ligand (the mannose receptor in this study) immobilisation on the surface. The analyte (vaccine constructs in this study) are allowed to pass over the ligand and the resulting interaction and/or binding causes a change in the reflected light from the gold layer on the chip's surface (below the dextran). The optical detection unit converts changes in this reflected light to a readable time-response sensogram. The light source used is plain polarised light.

Figure 4-5. Method development steps. Three steps were taken for method development to ensure accurate measurement of the vaccine constructs to the receptor. Step 1: the MR (ligand) is immobilised on the chip's surface; step 2: surface performance and regeneration scouting are performed to investigate receptor viability and regeneration condition; and step 3: kinetics and affinity measurements are performed to measure binding affinity of vaccine constructs 13-18 (**Chapter 3, Section 3.2.4, Figure 3-11**) .

Figure 4-6. Amine coupling of the MR onto the CM-5 chip. Free carboxylic groups on the dextran-coated CM-5 chip are pre-activated using EDC and NHS (these two provide crosslinking ability by activating the carboxyl groups) to enable covalent binding of the ligand (MR) through the ligands free NH_2 groups.

Figure 4-7. Mannose receptor flow cell immobilisation trace. (A) The MR dissolved in acetate buffer is run over the surface of the chip without pre-activation to scout the level of binding affinity the receptor has for the un-activated dextran ; (B) a solution of ethanolamine is run over the chip's surface to remove any unbound MR from step (A); (C) the dextran surface of the chip is activated with a solution of NHS:EDC; (D1-3) the MR dissolved in acetate buffer is run over the surface of the pre-activated chip in three pulses to reach the desired level of binding (in this instance it is 2000 RU); (E) ethanolamine is run over the chip to remove any excess MR that is not chemically bound from the previous step; and (F) the actual level of MR immobilisation is calculated and compared to the starting baseline level (1850 RU). Letters 's' and 'e' signify the start and end of each injection on the machine, respectively.

Figure 4-7. Mannose receptor flow cell immobilisation trace. (A) The MR dissolved in acetate buffer is run over the surface of the chip without pre-activation to scout the level of binding affinity the receptor has for the un-activated dextran ; (B) a solution of ethanolamine is run over the chip's surface to remove any unbound MR from step (A); (C) the dextran surface of the chip is activated with a solution of NHS:EDC; (D1-3) the MR dissolved in acetate buffer is run over the surface of the

pre-activated chip in three pulses to reach the desired level of binding (in this instance it is 2000 RU); (E) ethanolamine is run over the chip to remove any excess MR that is not chemically bound from the previous step; and (F) the actual level of MR immobilisation is calculated and compared to the starting baseline level (1850 RU). Letters 's' and 'e' signify the start and end of each injection on the machine, respectively.

Figure 4-9. Schematic trace of a surface performance resonance sensogram. (A) starting baseline showing the flow of the running buffer; (B) binding response caused by binding of an analyte to the immobilised ligand (here mannose receptor); (C) dissociation of the analyte from the ligand attributed to a change in the running buffer; (D) regeneration of the ligands surface (removal of all the analyte) by changing the conditions of the buffer (acidic, basic, ionic); and (E) final baseline following regeneration to ensure it is the same as the starting baseline observed in step (A).

Figure 4-10. Regeneration scouting using sodium dodecyl sulfate (SDS 0.05%). An ionic solution of SDS was used as the regeneration solution to assess the MR affinity measurements. (A) the sensogram baseline from the continuous flow of a buffer at 40 µl/min; (B) mannan (10 µg/ml) binding response showing 25 RU; (C) regeneration of the MR by 0.05% SDS solution; (D) an increase in the baseline level is observed following regeneration showing that this was not a successful regeneration. Letters 's' and 'e' signify the start and end of each injection by the machine, respectively.

Figure 4-11. Regeneration scouting using NaOH. A solution of NaOH (pH 9.5) was used as the regeneration solution to assess the MR affinity measurements. (A) The sensogram baseline from the continuous flow of a buffer at 40 µl/min; (B) mannan (10 µg/ml) binding response showing 25 RU; (C) regeneration of the MR using 10 mM NaOH (pH 9.5) solution; (D) a 60 RU down shift in the baseline was observed due to unsuccessful regeneration. Letters 's' and 'e' signify the start and end of each injection by the machine, respectively.

Figure 4-12. Lack of receptor activity following regeneration with NaOH. (A) No binding (an RU of less than 5) was observed when the MR bound to the chip was exposed to mannan (10 µg/ml). This correlates with previous results where the use of a high pH regeneration buffer (10 mM, NaOH, pH 9.5) was shown to change the baseline dramatically. Letters 's' and 'e' signify the start and end of each injection by the machine, respectively. *Note,* the sensogram regeneration stage is not shown.

Figure 4-13. Regeneration scouting using glycine buffer. A glycine buffer (10 mM, pH 2.2) was used as the regeneration solution to assess the MR affinity measurements. (A) The sensogram baseline

from continuous flow of the buffer at 40 µl/min; (B) mannan (10 µg/ml) binding response showing 25 RU; (C) regeneration of the MR using glycine buffer (10 mM, pH 2.2); (D) a small shift in the baseline (± 15 RU) was observed between the baseline at D and the baseline at A.

Figure 4-14. Mass transfer study with mannan. A single concentration of mannan (500 µg/ml) at different flow rates (5, 15 and 75 µl/min) was exposed to the mannose receptor (MR) immobilised on the CM-5 chip. No change was observed in the response level (RU) between each of these runs indicating that mass transfer is not a limiting factor in this study.

Figure 4-15. Binding affinity measurements for vaccine constructs 13-18. Surface plasmon resonance (SPR) analysis for the concentration-dependent binding of mannosylated constructs (**13-15**) and experimental controls (**16-18**) with the immobilised recombinant human macrophage mannose receptor (MR) protein. Solutions of **13-18** (0.78-50 µM concentration range) and mannan (18.75–600 µg/ml) were prepared in running buffer (10 mM HEPES, 1 mM $CaCl_2$, 1 mM $MgCl_2$,150 mM NaCl, 0.005% P20; pH 7.4) and injected over a period of 1.5 min with a dissociation interval of 8 min. The sensogram shows the plotted level of binding in the steady state (Req) against different concentrations of (A) the positive control mannan, and the vaccine constructs (B) **13**, (C) **14**, (D) **15**, (E) **16**, (F) **17**, and (G) **18**. R^2 indicates the fit of the results to the curve with respect to concentration. The affinity constant (K_D) was calculated using the response level at equilibrium (Req) using Equation 1 (**Chapter 2**, **Section 2.2.5**).

Figure 5-1. Dendritic cell (DC) involved in antigen presentation and activation of CD4 and CD8 T cells. Following antigen uptake by pattern recognition receptors (some mentioned in this thesis include: MR, DC-SIGN, TLRs), antigen presenting cells travel to the lymph nodes and present the processed antigen to CD4 and CD8 T cells by MHC II and MHC I, respectively. CD4 or CD8 T cells are activated depending on the antigen type and the following pathways become activated by proliferation: (A) CD8 activation leading to direct antigen elimination through cytotoxic T cells or by inflammatory cytokines in the Th1 pathway (e.g. IL-2, IFN-γ); or (B) humoral pathway where CD4 activates Th2 which is followed by Th2 related interlukin (e.g. IL-6, IL-5, IL-4) production. Upon Th2 activation, B cells are activated and trigger antibody (IgG) production. Memory B cells are produced by B cells.

Figure 5-2. Vaccination groups (G)1-9 used in the *in vivo* study. G1-3 are test compounds used to study immune modulatory properties affected by the differences in the number of alanine spacers between the mannosyl moieties. **G4-8** are controls used to compare a structure-activity relationship

of no mannose (**G4**), no lipid (**G5**), and no mannose and no lipids (**G6**). A mixture of the vaccines' structural components ($OVA_{323-339}$, mannosyl and the lipid, **G7**) was used to compare with the chemically conjugated vaccine constructs (**G1-G6**). The positive control (**G8**) was $OVA_{323-339}$ and CT, and the negative control was PBS (**G9**). All vaccine groups (**G1-9**) were dissolved in PBS (30 µg/100 µl/per mouse) and injected subcutaneously (S.C.) at the tail base. Five mice were used per vaccine group.

Figure 5-3. Schematic diagram of the *in vivo* study. Vaccine groups (**G1-9**) were introduced to mice following the transfer of OT-II $CD45.2^+$ T cells isolated from transgenic mice (B6.Cg-Tg[TcraTcrb]425Cbn/J with OVA sensitive OT-II cells) to C57BL/6 mice. Mice were vaccinated on days 2, 21 and 42. Blood was taken on days 10, 31 and 52 post vaccination. OT-II read outs for flow cytometry and ELISA were performed 10 days post each vaccination. Mice were sacrificed on day 63. ICS and CBA studies were performed on blood samples taken 21 days post dose 3 vaccination.

Figure 5-4. OT-II $CD45.2^+$ $CD4^+$ T cells from OT-II mice do not proliferate in C57BL/6 mice upon vaccination with G1-9. $CD45.2^+$ $CD4^+$ OT-II T cells were purified and 200 µL of suspended cells (0.5×10^6 cells) was injected intravenously at the tail base to $CD45.1^+$ C57BL/6 mice. The percentage of $CD45.2^+$ OT-II cells within the $CD4^+$ population was measured from tail blood taken at days 10, 31 and 42 using flow cytometry. Mean results (±SEM) from five individual mice per time point are shown, (A) at day 10, (B) at day 31, and (C) day 42. Unpaired t-Test was used to show the significance when $p < 0.05$. Here, **G8** is the positive control group vaccinated with $OVA_{323-339}$ + cholera toxin and **G9** is the negative control group vaccinated with PBS.

Figure 5-5. Percentage of $CD62l^{low}$ $CD4^+$ parental T cells. Vaccine constructs **G1-G9** were compared by percentage (%) of $CD62l^{low}$ $CD4^+$ parental T cells following three vaccinations on days 10 (A), 31 (B) and 52 (C). Mean results (±SEM) from 5 individual mice groups are shown. Unpaired t-test was used to show significance when $p < 0.05$. Here, **G8** is the positive control group vaccinated with $OVA_{323-339}$ + CT and **G9** is the negative control group vaccinated with PBS.

Figure 5-6. Schematic process of intra cellular staining. This method is used to measure antigen-specific cytokine release (e.g. IFN-γ, IL-2, TNF). (A) single cell suspensions from vaccination groups' (**G1-9)** lymph nodes and spleen were stimulated by $OVA_{323-339}$ peptide, PMA/ionomycin as experimental positive control and media only as experimental negative control, (B) cells were then incubated at 37°C and 5% CO_2 for 3 days in the presence of protein transport inhibitor, (C) cells were

then permeabilised and fixed, (D) cells were stained with IFN-γ, IL-2 and TNF antibodies. The expression of IFN-γ, IL-2 and TNF was analysed on the $CD4^+$T cells subset using flow cytometry.

Figure 5-7. Intra cellular staining studies on INF-γ, IL-2 and TNF expressing T cells following vaccination. Percentage of CD4 (A, B, C) and CD8 (D, E, F) T cells associated with IFN-γ, IL-2 and TNF upon *in situ* stimulation of draining lymph nodes and spleen cells (isolated 11 days post third vaccination with **G1-G9**) with the $OVA_{323-339}$ peptide and PMA/ionomycin (experimental positive control). Results are normalised against the media per each mouse per group. Mean results (±SEM) from 5 individual mice per group are shown. Unpaired t-Test was used to show the significance when p <0.05. Positive control is **G8** vaccinated with $OVA_{323-339}$ plus CT and negative control is **G9** vaccinated with PBS.

Figure 5-8. Schematic of cytokine bead array measurement. (A) The fluorescent capture beads are conjugated with detection antibodies and are incubated with test samples containing cytokines and secondary antibodies to form (B) sandwich complexes. The sandwich complex is then (C) washed followed by acquisition of sample data using (D flow cytometry. The sample results are generated in graphical and tabular format using the BD CBA analysis software.

Figure 5-9. Antigen specific antibody production following vaccination using ELISA assay. Sera were collected on days 10 (9 days post the first vaccination), 31 (10 days post the second vaccination) and 52 (10 days post the third vaccination). IgG UV intensity was recorded (OD 450) for a 1/200 dilution for all mice groups (**G1-G9**). Mean ± SEM is shown. Unpaired t-Test was used to show significance when p <0.1. Positive control is **G8** vaccinated with $OVA_{323-339}$ plus cholera toxin and negative control is **G9** vaccinated with PBS. There were 5 mice per group.

List of Tables

Table 5-1. Essential cytokines of Th1 and Th2 [345]

Table 5-2. Cytokine bead array results presented as a heat map. Red cells indicate the strongest results while the green cells indicate the weakest results per cytokine for each vaccination group (**G1-G9**).

Chapter 1: Introduction to Vaccine Development and Mannose Receptor Targeting

1.1 Introduction

Vaccination has provided prevention and treatment of many infectious diseases (e.g. smallpox, polio and diphtheria) [1-4]. However, new vaccination strategies are required to overcome immune suppressive diseases, including human immunodeficiency virus (HIV) and malaria infection. The future of vaccine design and development depends on the advanced knowledge of immune system activation pathways and a better understanding of the requirements for specificity and selectivity towards either prophylactic or therapeutic immune pathways. Selecting antigens, inclusion of adjuvants (a moiety that enhances antigen immunogenicity) and addition of targeting moieties, such as mannose, play important roles in all aspects of vaccine development [5].

Vaccine development requires consideration of immunogenicity and efficacy of vaccines. Here, understanding the process of antigens interaction with antigen presenting cells (APCs) which is followed by antigen uptake and processing by these cells can be a crucial factor [6].

Pattern recognition receptors (PRRs), are a large family of receptors that initiate recognition of any invasion of the body. C-type lectins are a sub-family of PRRs and within C-type lectins, the mannose receptor (MR) is an important component of the immune system. The MR has been subject to extensive studies to understand its structure and function. The MR plays an important role in linking both innate (nonspecific defence mechanism) and adaptive (acquired) immunities [7, 8]. Thus, targeting this receptor can be an important part of vaccine design and development. The MR is mainly found on macrophages and dendritic cells (DCs) [9]. Minimal information is available about the mechanisms used by DCs to recognise and internalise pathogens through the MR. However, understanding both the structural and conformational characteristics of this receptor are important aspects to be considered about interactions with this receptor. Earlier studies have found mannan, the primary component in the cell wall of yeast, is a MR ligand. This key finding has allowed researchers to better understand the role of the MR in the uptake, processing and presentation of glycosylated antigens [10, 11].

To date, many strategies have been used to develop vaccines that target the MR. These include using ligands that contain mannan or mannose to increase targeting specificity. However, the actual involvement of the MR in recognition of such mannosylated structures is less studied [9, 12, 13]. Vaccines that target the MR have the potential to elicit different immune responses. Through the analysis of ligand and antibody targeting approaches it is clear that the structural properties of the MR and specificity of the interaction with the MR receptor are crucial factors for determining antigen processing and the resultant immune response.

1.2 Immune system activation pathways

The first interaction of bacteria and microorganisms with the body's immune system is through receptors on the macrophages, DCs and other APCs (Langerhans cells and B lymphocytes). This interaction between fragments of the pathogenic cell wall and phagocytic receptors on APCs generates production of biologically active molecules, including cytokines and chemokines. These biologically active molecules are secreted proteins and are responsible for the regulation of either an anti-inflammatory or pro-inflammatory immune response [14]. The immune system reacts to pathogens in two distinct types of defence: innate and adaptive [15] Here, the innate immune system recognises the nature of infection by providing signals, as a first line host defence, to the adoptive immunity (Figure 1-1). Cells involved in the innate immune system consist of DCs, macrophages and natural killer cells. Each of these components of the innate immune system is able to eliminate the pathogen independently (Figure 1-1). Here, the DCs and macrophages first interaction with the pathogens is through pattern recognition receptors (PRRs), which then internalise the antigen and cause an immediate release of cytokines (Figure 1-1) [16]. Following cytokine release natural killer cells become activated and are able to digest the pathogen with interactions through their surface markers [17].

Furthermore, the innate immune system plays a crucial role in the induction of an adaptive immune response. Unlike the innate immune system, the adaptive immune system becomes activated at a later period, usually 4-7 days post infection, and is associated with the adaptive immune system being involved with antigen recognition through antigen presentation by DCs (Figure 1-1) [18]. One of the important aspects of the adaptive immune system is its ability to generate a range of T and B cells (two types of lymphocytes or white blood cells) and antigen specific receptors including Major Histocompatibility Complex (MHC I and II) receptors and co-stimulatory receptors, in response to DC activation. Here, immature DCs recognise and internalise pathogenic antigens and play an important role in processing the antigenic components and presenting them to T cell receptors.

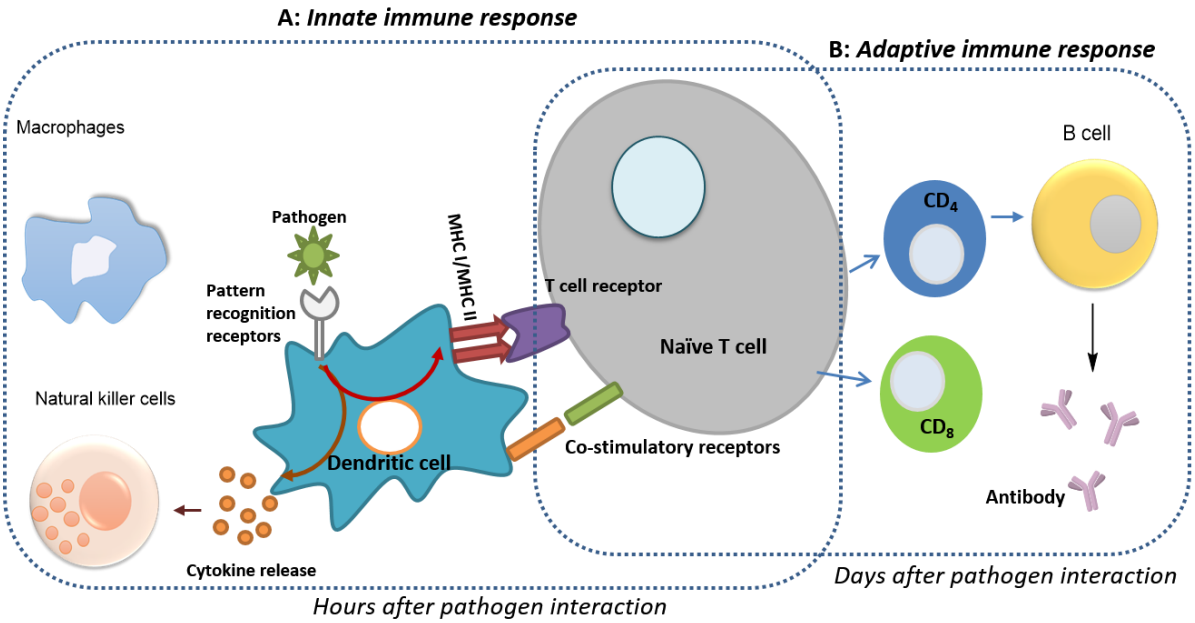

Figure 1-1. Schematic representation of immune factors involved in innate and adaptive immunity. (A) Innate immunity is activated hours post pathogen exposure and involves dendritic cells, macrophages, natural killer cells and pattern recognition receptors; cytokines released in this pathway are antigen independent; (B) Adaptive immunity is activated days after exposure to a pathogen (antigen dependant) and consists of B cells, which lead to an antibody response, and naïve T cells, which lead to CD4 and CD8 T cell proliferation. Naïve T cells represent a common intermediate between innate and adaptive immunity. Here, naïve T cells have the ability to migrate from where they are produced (thymus) to secondary lymphoid organs including the lymph nodes where they become CD4 or CD8 T cells which are the components of the adoptive immune response.

Following antigen uptake, DCs travel to the lymph nodes where T cell activation occurs [15, 19]. One of the key roles of DCs is uptake and presentation of antigens to naïve T cells. Naïve T cells, which are produced in the thymus, travel to secondary lymphoid organs, including the spleen, peripheral lymph nodes and gut-associated lymphoid tissue. In the secondary lymphoid organs naïve T cells recognise CD4 and CD8 co-stimulatory receptors (CD4 and CD8 are transmembrane glycoproteins on the DCs that act as co-receptors for T cell receptor) on the DCs via their T cell receptor (Figure 1-1). Upon encounter between DCs (that have internalised and presented the antigen through CD4 and CD8 receptors) and naïve T cells, CD4 (helper T cells) and CD8 (cytotoxic T cells) T cells are produced activating the B cell response [20].

Intracellular antigens, from tumour or viruses that develop inside body cells, are presented by MHC I molecules which consequently activate cytotoxic CD8 T cells [21]. CD4 T helper cells on the other hand are activated by extracellular antigens that are presented through MHC II molecules.

While two distinct pathways exist for CD4 and CD8 T cell activation, cross presentation is described as a mechanism that allows the extracellular antigens to activate a CD8 T cell response through MHC I molecules (Figure 1-1). It has been suggested that CD4 co-stimulatory receptors play important roles in the production of memory CD8 T cell responses. Sun *et al*., showed that CD8 memory cells produced in the absence of CD4 T cells were not able to respond properly following a second encounter with the same antigen, and this confirmed involvement of CD4 T cells in a CD8 response [22]. In a review by Bourgeois and Tanchot, the importance of CD4 help for a long-term (memory) CD8 response was discussed. Bourgeois and Tanchot concluded that CD4 cells can affect complicated signalling pathways on APCs. They also confirmed the role of CD4 cells on activating CD8 cells causing a secondary immune response [23]. In another study by Bourgeois *et al*., the death of CD8 cells was directly related to the lack of CD4 cells in a vaccinated mouse model indicating the correlation between the CD4 and CD8 activation pathways[24].

1.3 Mannose receptor and structural properties

The MR is a carbohydrate binding receptor expressed by macrophages and DCs [25]. The MR [Cluster of Differentiation (CD); 206] has three other family members: phospholipase A_2 receptor (PLA_2R), Endo180 (CD280) and DEC-205 (CD205). The CD nomenclature was established in 1982 to standardise the naming of cell surface markers to aid identification and characterisation [26]. The MR family are a sub-group of the C-type lectin super-family, a major class of the endocytotic PRRs which promote the attachment, engulfment and destruction of micro-organisms by phagocytosis (Figure 1-2). Unlike other C-type lectin receptors (CLR), the MR family are unique in having multiple carbohydrate recognition domains (CRDs) in a single polypeptide construct [27]. However, from the MR family only the MR and Endo180 are known to recognise and bind monosaccharides [28].

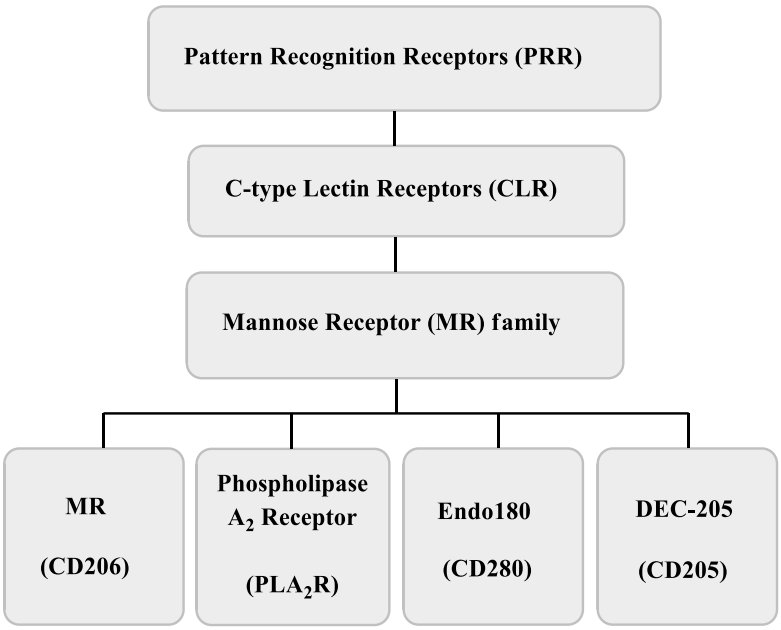

Figure 1-2. Mannose Receptor classifications. Pattern recognition receptors (PRRs) promote the recognition, attachment, and phagocytosis of foreign pathogens via the carbohydrate recognition domain (CRD). CLR is a major class of PRRs which contain one or more CRDs that recognise a wide variety of ligands. Additionally, the entire MR family is able to distinguish self from non-self structures. The mannose receptor (MR) family comprises four members including the MR (CD206), phospholipase A_2 receptor (PLA_2R), Endo180 (CD280), and DEC-205 (CD205).

Wileman *et al.* originally discovered the MR in rabbit alveolar macrophages as a 175 KDa protein by using radio-labelled mannosylated bovine serum albumin (BSA) where it was found to recognise terminal glycosylated chains [29]. A further study by Ezkowits discovered that heteroantisera against human macrophages precipitated a 170 KDa glycoprotein from the cell surface which was confirmed to be the molecular weight of the human MR [30]. In 1990, Taylor *et al.* isolated cDNA clones that covered the entire coding portion of mRNA for the human MR. Sequence analysis confirmed the receptor to be a type I trans-membrane protein with its carboxyl terminal on the cytoplasmic side of the cell membrane (Figure 1-3) [31].

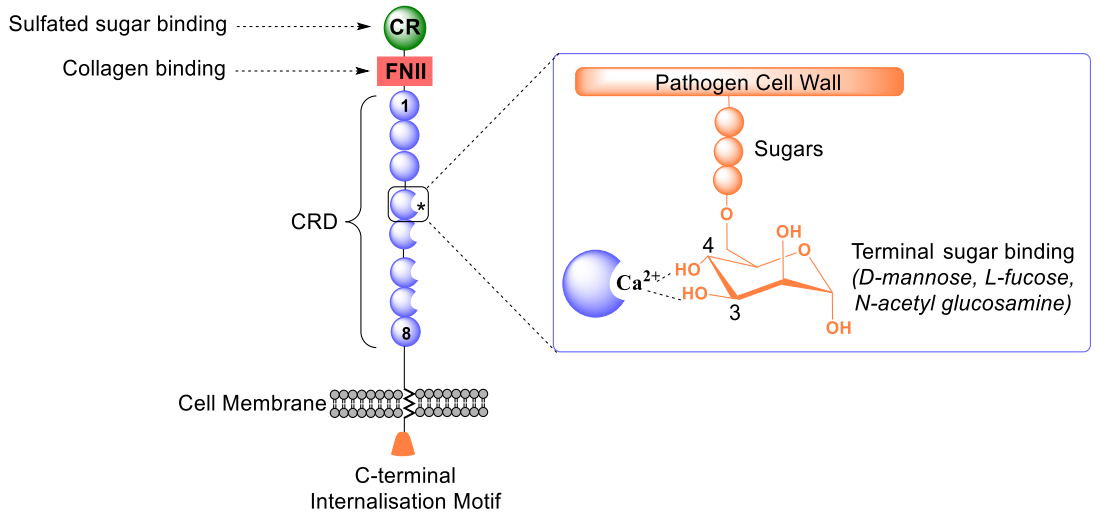

Figure 1-3. Schematic structure showing the organisation of the Mannose Receptor. The Mannose Receptor Cysteine Rich (CR) domain recognises sulfated carbohydrates terminated in N-acetyl glucosamine (15), the Fibronectin type II (FNII) domain binds to collagen I, II, and IV with high affinity and weakly to V [32, 33], and the Carbohydrate Recognition Domains (CRDs) bind complex carbohydrates that terminate in mannose, fucose or N-acetyl glucosamine [32, 34]. Here, CRD4 (*) binds mannosylated ligands found in pathogen cell walls in a calcium-dependent manner. CRD4-7 is essential for high affinity binding to multibranched mannosylated ligands and ligand internalisation. The C-terminal internalisation motif has a role in transferring ligands inside the cell.

The MR exists in both monomeric and multimeric states [31, 32, 35]. Taylor *et al.* expressed the intact receptor in rat fibroblasts and then sedimented the receptor protein confirming it to be a monomer in the cell membrane [36]. However, analysis by Su *et al.* and Boskovic *et al.* provided evidence for the receptor to exist in both states, establishing that the experimental methodology used to study the receptor influences the state that is recovered. Additionally, these results confirmed the presence of multiple carbohydrates in a single polypeptide chain (Figure 1-3) that must cooperate to achieve high-affinity binding of complex ligands [31, 36-39].

The MR is characterised by a N-terminal cysteine rich (CR) domain; a single fibronectin type II (FNII) domain; a carbohydrate recognition domain (CRD) ,which is also referred to as C-type lectin like domain (CTLD), and a C-terminal internalisation motif located at the tail (Figure 1-3). The CR domain acts as a second lectin domain unique to the MR and is comprised of 139 amino acids. This domain is capable of binding sulfated oligosaccharides and has a role in maintaining receptor stability of the ligand endocytosis process at acidic pH [32, 40]. The FNII domain binds collagen and the cytoplasmic tail contains a motif that helps transport bound antigens inside the cell [31, 41]. The CRD consists of eight segments (Figure 1-3) and is responsible for binding glycoconjugates on the surface

of bacteria, parasites, viruses, and fungi that terminate in mannose, fucose or N-acetyl glucosamine [31, 42]. MR family members have evolved different molecular trafficking properties with the receptor found to use both endocytosis and phagocytosis pathways [5]. Although the recognition of glycosylated ligands by MR CRDs is known, a full understanding of their function in the context of vaccine development requires structural knowledge of each domain and how they interact with each other to enable binding and specificity. Further information about the relationship between receptor binding and internalisation is also required.

1.3.1 Carbohydrate recognition domains

Understanding the mechanism of glycopeptide attachment and conformational changes associated with MR CRDs is essential for designing glycosylated ligands that can be used to target this receptor. Pathogen recognition and cellular interactions are mediated through the MR CRD in a calcium dependent manner [8]. An early review by Drickamer shows that the CRDs play an important role in innate immune responses against clinically relevant pathogens including: *Leishmania donovani (L. donovani*), *Plasmodium chabaudi*, and *Pneumocystis carinii (P. carinii) [43, 44]*. These studies showed that the MR participates in opsonin-mediated binding leading to opsonin-independent phagocytosis of pathogens by recognising glycosylated ligands capped with mannose, fucose, or N-acetyl glucosamine, highlighting its important role in the early stages of infection [8, 45].

In 1992, Taylor *et al.* showed that the CR domain, FNII repeat and the first three CRDs were not essential for the binding and endocytosis of glycosylated ligands [11, 36]. Instead, FNII had collagen binding properties that allowed it to play a role in mediating the clearance of collagen fragments or in cell-matrix adhesion. Subsequently, the different types of collagen have been demonstrated to contain glycosylated propeptides, with the propeptide of type I collagen being highly-mannosylated. Here, in addition to the FNII domain, the CRDs of the MR have been shown to bind to this propeptide aiding its clearance from the body. This details a multi-functional role for the MR including roles in tissue remodelling and wound healing [33].

Each CRD consists of approximately 120 amino acids that form eight segments designated CRD1 to CRD8 (Figure 1-3). Multiple CRDs are required to bind complex glycosylated ligands, supporting evidence that they exist as a single polypeptide chain [31, 36, 38, 39, 43]. Site directed mutagenesis, ligand binding and Nuclear magnetic resonance (NMR) analysis confirm that the ligation of CRDs to glycosylated ligands is calcium dependent. A characteristic of this family is the common folding in that each CRD is comprised of two alpha-helices and two small antiparallel beta-sheets held in place by non-covalent and covalent interactions. Four conserved cysteine residues form two disulfide bonds

that stabilise the structure, while contributions from hydrophobic residues make up a hydrophobic core. Calcium is required for carbohydrate binding and receptor activation (Figure 1-3). Understanding the spatial arrangement of the domains and changes induced upon ligand binding is essential to understanding the behaviour of the MR [8, 27, 43].

MR proteolysis experiments showed that CDRs were resistant to degradation in the presence of calcium, which is consistent with a tightly folded structure [32, 36]. *In vitro* analysis was used to determine which of the extracellular domains were engaged in recognition, ligation and endocytosis of glycosylated ligands [11, 36, 43, 46, 47]. These studies confirmed that ligation of the CRDs to these ligands was dependent on the conformation of eight CRD segments and their interaction with the terminal glycans of the ligand [46, 47]. In 1991, Taylor *et al.* reported that CRD1-3 had a weak carbohydrate binding ability while CRD4 was found to have the highest binding affinity. This study concluded that at least three domains (CRD 4, 5 and 7) were required for high affinity binding and endocytosis of multivalent glycoconjugates [11]. It was also shown that CRD4 alone could mimic the saccharide binding ability of all eight CRDs. However, CRD4 binds poorly to multi-glycosylated ligands such as mannan, thus cannot account for the binding of the receptor to natural antigens. For complete affinity of the MR to glycosylated ligands, CRD4-8 must contribute to the binding of oligosaccharides (Figure 1-3) [32, 36].

To determine how the CRD achieves high-affinity glycosylated ligand binding, Taylor and Drickamer produced internal fragments of the receptor using the baculovirus expression system and compared the binding affinity of natural ligands that contained high-mannose oligosaccharides (invertase and mannan) with that of larger protein fragments (BSA conjugated to mannan (man-BSA)). Receptor fragments consisting of CRDs 4-5, 4-6 and 4-7 were purified and subjected to proteolysis studies to determine their affinities for various ligands. It was concluded that the affinity of CRD4-5 for man-BSA did not change after addition of CRD6-7 but when they investigated mannan's affinity for CRD4-5, binding increased when CRD5 was present. This study confirmed that the affinity of the full MR is the same as for CRD4-8 for the studied ligands. Combined, these results indicated that CRD 4-8 recognised terminally mannosylated ligands [11, 36, 46]. Proteolysis experiments supported the idea that CRD4-5 forms a tight ligand binding core essential for high-affinity binding of multivalent ligands but the affinity for mannan increases as more CRDs are present indicating for certain ligands that CRD 6-8 is essential for binding [32].

MR proteolysis experiments showed the resistance of CRD to degradation in the presence of calcium suggested a tight and folded structure. CRD4-5 did not release individual CRDs under proteolytic conditions, indicating that these two domains form extensive contacts implying a fixed orientation to

the binding sites within these two CRDs [36]. In 2006, Boskovic *et al.* explained the three-dimensional (3-D) organisation of the MR showing that the CRDs are packed in pairs as CRD4-5 and CRD7-8 are connected by a single CRD3 and 6 respectively (Figure 1-4A). Electron microscopy studies coupled with 3-D reconstructions and X-ray structures modelled from the Endo180 protein (a member of the MR family) [42], suggested that the conformational properties of the MR were pH dependent, mimicking receptor recycling properties between the plasma membrane and endosome. The CRDs conformation potentially made some points of the receptor more accessible to glycosylated ligands, modelling a structure with the CRD4 domain near the FNII and CR domains in a compact organisation (Figure 1-4A) [32]. Here, all CRD domains have the potential to interact with the ligand (Figure 1-4A), however, it has been shown that only CRD4-7 actually has a role in binding and internalisation. This contradicts a previous model where Napper *et al.* performed hydrodynamic studies of the receptor that suggested a U-shape structural organisation (Figure 1-4B) [48]. In this model, only CRD4 is shown to interact with the ligand. To date, nothing further is known about the spatial alignment of MR CRDs and their interactions with glycosylated ligands. As no complete X-ray structural data is available for the MR, and based on recent evidence and studies, Figure 1-4A represents the most up-to-date accurate structural model for the MR. Further information pertaining to the structural analysis of the MR can be found in published articles [32, 42].

Binding of the MR CRDs to saccharides was studied in the presence of mono- and oligosaccharides of mannose. It was shown that hydroxyl groups on the C3 and C4 position of terminal mannose ligated to calcium to form hydrogen bonds with glutamate and asparagine residues on the CRDs [43, 46, 47, 49]. Drickamer *et al.* reported that the number of CRDs in the receptor would correlate with the ability of the receptor to bind different types of ligands. It was also observed that the multivalent and linear structures of the MRs were two essential properties that allow for recognition of a large number of foreign ligands [43].

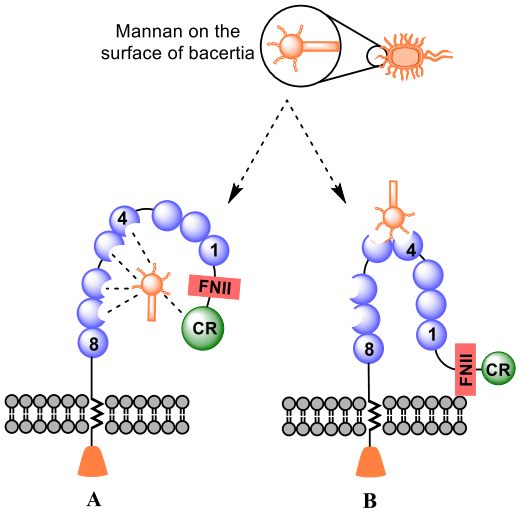

Figure 1-4. A model for the structural organisation of the Mannose Receptor and the attachment of glycosylated ligands. Conformational structure of the mannose receptor with mannan from the surface of bacteria as a model glycosylated ligand. **A** Compact "bent" organisational model proposed by Boskovic *et al.* where the CRD interacts with the CR domain in ligand binding [32, 40]. **B** A U-shaped model proposed by Napper *et al.* suggesting exposure of CRD4-5 in ligand binding [48]. CRD4 has high binding affinity to glycosylated ligands and CRD5-8 in addition to CRD4 is essential in binding multi-glycosylated ligands [32].

1.4 Role of the Mannose receptor in immunity

The MR is a PRR. Unlike single ligand receptors, PRRs are a group of receptors that recognise a broad spectrum of pathogens including yeasts, parasites, bacteria, and viruses [27, 50]. Pathogen recognition is performed by the MR CRDs bound to a variety of microorganisms including *Candida albicans* (*C. albicans*) [30], *P. carinii* [44], *L. donovani* [51], *Mycobacterium tuberculosis* (*M. tuberculosis*) [52] and influenza A virus [53].

The MR is an important part of innate and adaptive immunity [54]. The innate immune system is the body's first non-specific defence mechanism and is responsible for the early detection and acute response to pathogens. Adaptive immunity is antigen specific, allowing for long-term recognition, and enabling the body to create immunological memory after initial exposure to a pathogen. This leads to an enhanced response to subsequent encounters with the same pathogen [7]. Chieppa *et al.* showed that, when exposed to anti-MR monoclonal antibodies, the MRs present on DCs caused DC maturation and increased the level of anti-inflammatory cytokines, which is consistent with the receptors' role in adaptive immunity [55]. Additionally, the MR family (Figure 1-2) has the ability to recognise a diverse range of organisms without interacting with self-structures and although the

mechanism is not fully understood, it is thought to be associated with the CRDs recognising specific patterns (or ligand geometries) of terminal sugars which decorate the surface of microorganisms [27, 56, 57]. Lorenz *et al.* compared the uptake of RNase versus mannosylated-RNase and reported that the latter increased T-lymphocyte stimulation. They proceeded to study the internalisation of soluble yeast mannan compared to mannosylated-RNase by APCs. This study aimed to clarify the ability of the immune system to recognise self from non-self proteins. The enhanced uptake of a foreign antigen was performed through the MR which has specific recognition ability [58]. Recent interest in the ability of MRs to recognise self from non-self has seen studies investigating these properties for potential applications in autoimmune diseases and allergies.

In vitro studies showed that the processing and presentation of antigens was enhanced when the MR was targeted [59]. Research also suggested that ligand binding specificity was the main element that differentiated self from non-self antigens [50]. For example, hexoses (e.g. mannose and fucose) found on the surface of gram positive and negative bacteria have equatorially placed hydroxyl groups at carbons C3 and C4 organised in a branched fashion which were recognised by the receptor, while linear hexoses were not [50]. This indicated that ligand geometry is important in self/non-self recognition by the MR.

Since 1970, mannosylated antigens have been known to effectively potentiate antigen immunogenicity via the MR. Receptor-mediated antigen uptake by DCs and T cell stimulation was shown to be 100 times higher than by pinocytosis [13, 60, 61]. Additionally, mannosylated antigens were also internalised and presented through MHC II, which resulted in up to 10,000 times greater stimulation of T cells [62]. This was supported by Levitz *et al.* who used mannosylated targeting proteins from *Cryptococcus neoformans* to determine the T cell response to MR activation. The resultant antigen-specific immune response via receptor recognition on DCs and subsequent internalisation and presentation through MHC I and II supported the importance of mannosylation for the stimulation of a targeted T cell response [61]. The response (Th1 or Th2) and the cytokine production profile remain largely undefined.

DC maturation occurs after glycosylated ligands bind to the MR and stimulate the internalisation of the glycosylated antigens. The pathway used for antigen degradation and processing is receptor specific [63]. After antigen degradation, lysosomes present the degraded antigen on the surface of mature DCs through MHC I and II resulting in an increased expression of T cell receptor co-stimulatory molecules CD80 and CD86 [64]. In both MHC I and II pathways, CD80/CD86 interact with CD28 on T cells. Activated $CD4^+$-cells differentiate into either Th1 or Th2 cells which release cytokines. The MHC II pathway is responsible for the humoral immune response while the MHC I

pathway is responsible for cytotoxic T-lymphocyte responses (Figure 1-5) [17, 42, 65]. The important role of MR CRDs in promoting an immune response has prompted many clinical *in vivo* and *in vitro* studies [30, 44, 51, 52] and its contribution to disease through the cellular metabolic pathway was highlighted in a recent review [25].

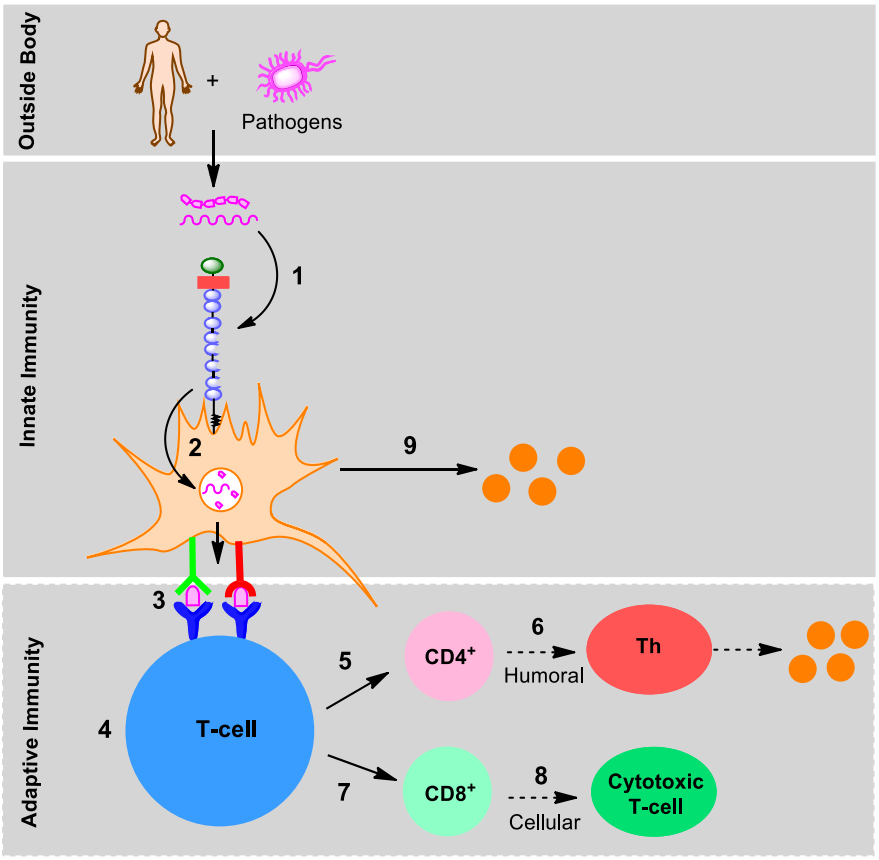

Figure 1-5. Mannose receptor and cellular targeting pathway. 1: Attachment of glycosylated ligands (e.g. mannan from the surface of bacteria) to CRD4-8 of the mannose receptor, followed by **2:** internalisation and degradation of ligands by the lysosome for adaptive immune responses. **3:** Presentation of degraded ligands to the surface of the dendritic cell through MHC I and II and co-stimulatory receptors (e.g. CD80/CD86). **4:** Naïve T cell activation through MHC I and II pathways where, **5:** MHC II pathway activates CD4 T cells and achieves, **6:** T-helper response activating cytokine release, or **7:** MHC I pathway activates $CD8^+$ T cells. **8:** Cytotoxic T-lymphocytes response to eliminate infected ligands. The innate pathway activates through **9:** direct release of cytokines through the DC.

1.5 Subunit vaccines for targeting the mannose receptor

An effective MR-targeting vaccine must successfully deliver epitopes to the CRDs on the MR, helping to ensure optimum processing and presentation to elicit an immune response. A detailed

understanding of receptor-antigen interactions is critical to achieving this aim [66]. MR CRDs have the ability to selectively bind glycosylated ligands resulting in internalisation and processing through MHC I and II pathways, thus it is postulated that any procedure that triggers this cycle has the potential to prompt an effective immune defence. Studies that have targeted the MR have focused on the attachment of mannan or mannose to peptides or proteins to show receptor specificity and affinity. The features of the most prominent experiments have been highlighted in Table 1 and will be discussed throughout the remaining sections.

Table 1-1. Mannosylated subunit vaccine development for targeting the Mannose Receptor

Mannose Receptor Targeting Ligand	Pathogen or Endogenous Ligand	Immune Response	References
Mannan	Lipoarabinomannan	TNF, Th1	[67, 68]
	Oxidised and reduced MUCI	CD8 cytotoxic lymphocyte reaction, Th1/Th2	[54, 69-74]
Mannose	Bovine serum albumin	MHC II presentation	[60, 75]
	Pichia pastoris	MR affinity and DC internalisation	[76]
	Whole OVA protein	Th1/Th2	[73]
	RNase	Ligand specific uptake	[58]
	Polyalanine peptides	T cell response by targeting the MRs CRDs	[77]
	$OVA_{323–339}$	T cell response and APC presentation through the MR	[78]
	PEGtide dendrons	MR targeting and uptake by macrophages	[79]
	Polylysine DNA dendrimers	High affinity to the MR	[80, 81]
	Polylysine dimer	DC internalisation through the MR	[82]

TNF: Tumour Necrosis Factor, MHC: Major Histocompatibility Complex, Th1: T-helper cell type 1, Th2: T-helper cell type 2, OVA: Ovalbumin, MUCI: mucin and carbohydrate associated antigens as tumour markers

Development of a glycosylated subunit vaccine that contained glycan moieties could potentially enable the targeting of a specific receptor [10]. Glycosylated proteins and peptides have been investigated for MR targeting for vaccine development purposes. To date, mannan and mannosylated antigens are one of the most effective ligands for targeting the MR and eliciting an immune response as a result of mannan's strong ability to compete with other ligands for receptor binding [10, 83-87].

1.6 Structural properties of mannan as a mannose receptor ligand

Mannan, a polysaccharide of mannose [88] found in the cell wall of *Sacchaomyces cerevisiae*, (yeast) has been well characterised (Figure 1-6) [89, 90]. Mannan binds to the MR CRDs causing an immune response involving the up-regulation of co-stimulatory molecules (e.g. CD40, CD80 and CD86) and pro-inflammatory cytokines (e.g. IL-12, IL-4), required for Th1 or Th2 cell priming (Figure 1-5) [34, 91]. Extensive studies on mannan and its derivatives have been performed to investigate the important structural properties of mannan that enable recognition by the MR and stimulate an immune response by DCs. The reduction and oxidation of mannose alters the overall structure and functional properties (Figure 1-7) [92]. Consequently, oxidised and reduced forms of mannan have successfully been shown to stimulate Th1 and Th2 responses via different cellular pathways, emphasising the importance of the structural interaction between mannan and the receptor [91]. Since recognising mannan's ability to elicit an immune response, and later its ability to bind to the receptor, vaccine design attempts have investigated the yeast cell wall protein alone [93] or functionalised peptides or proteins with mannan or mannose to mimic the cell wall of a pathogen [71, 72, 74, 94-96].

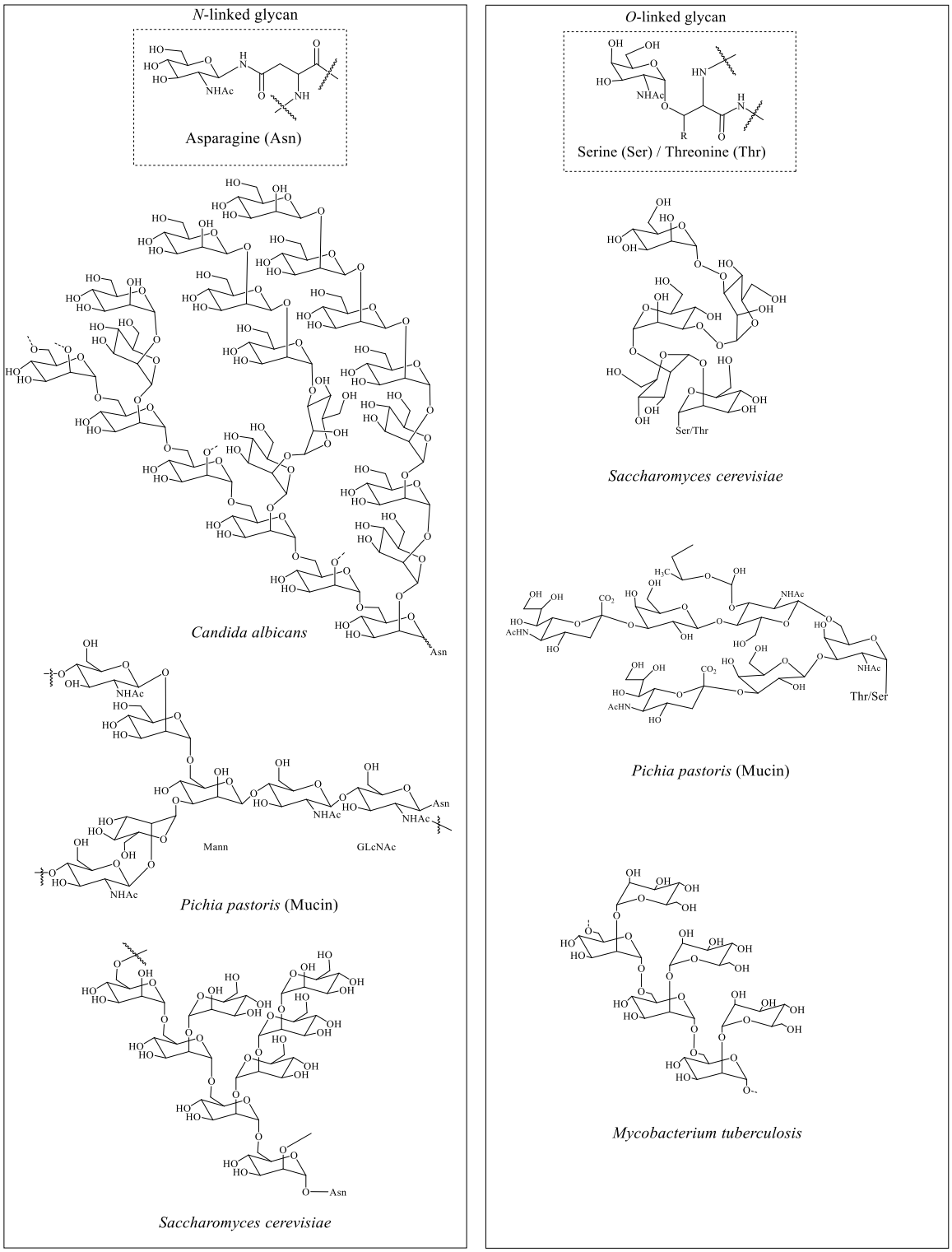

Figure 1-6. A typical N-linkage through asparagine (Asn) is highlighted with examples of mannose receptor binding N-linked proteins from *C. albicans* [97], mucin from *Pichia pastoris* [98] and *Saccharomyces cerevisiae* [99]. A typical serine/threonine (Ser/Thr) *O*-linkage is highlighted. Examples of mannose receptor *O*-linked binding proteins include mucin from *Pichia pastoris*, *Saccharomyces cerevisiae* and *M. tuberculosis* [100, 101].

Apostolopoulos *et al.* found that antigenic MUC1 peptides on the surface of tumour cells attached to oxidised mannan, which stimulated a cellular immune response and CD8 cytotoxic lymphocyte production. Earlier studies from the same group reported an unsuccessful induction of cellular immunity when a diphtheria toxoid carrier was used. These results indicated the importance of oxidised mannan in molecular design, and the effect of targeted specificity towards the MR on the resultant immune response [69, 74]. Oxidised mannan attached to a recombinant MUC1 fusion protein has undergone phase III cancer clinical trials [72, 102, 103]. The results showed that MUC1 attached to oxidised mannan induced tumour-specific CD8 T cell responses but immunisation with reduced mannan-MUC1 conjugates provided poor protection [71]. Additionally, aldehyde mannan-MUC1 elicited a stronger cellular response, inducing INF-γ production and the generation of IgG2a-dominant antibodies [70]. The structural properties of mannan played an important role in receptor uptake and the immune response elicited an important consideration for targeted vaccine design.

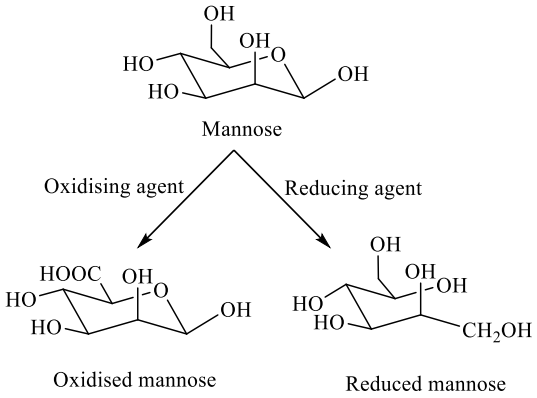

Figure 1-7. **Oxidised and reduced structures of mannose**. Under mild oxidation conditions (e.g. Br_2/H_2O), the C-6 carbon on mannose is oxidised to a carbonyl group forming mannuronic acid; under reducing conditions (e.g. sodium amalgam), mannose is converted to mannitol with the formation of an alcohol at the C-1 carbon. Reduced and oxidised variations of mannan have been used to investigate mannose receptor targeting [92].

Lipoarabinomannan (LAM), derived from *M. tuberculosis* [67, 104], contains terminal mannose residues that are responsible for receptor binding and eliciting secretion of tumour necrosis factor (TNF; a cytokine with anti-microbial activity) by macrophages. Chatterjee *et al.* demonstrated MR binding in competitive inhibition studies that used mannan, mannose-BSA, N-acetyl glucosamine-BSA serum, and antibodies directed against the MR. LAM, derived from the *M. tuberculosis* H37Ra (avirulent) strain, which contains long mannan segments on its cell wall, caused a 100-fold greater secretion of TNF compared to the Erdman strain (virulent), containing shorter mannan segments. These studies described a receptor that was able to discriminate between mannan length isolated from

the virulent and avirulent strains of *M. tuberculosis.* Discrimination between virulent and avirulent strains of *M. tuberculosis* through the secretion of different levels and types of cytokines (e.g. TNF) is also noted in another study [67]. Further, Schlesinger *et al.* demonstrated that macrophages are important in mediating phagocytosis of both virulent and attenuated strains of *M. tuberculosis* but the MR plays an important role in phagocytosis of only the virulent strains [105]. These studies indicate that distinct domains of the MR can vary their modes of interaction with ligands, impacting cellular fate. Also, identification of the structural differences between virulent and attenuated strains, in addition to cellular differences, will enhance the understanding of MR function.

1.7 Carbohydrate based vaccines

In nature, glycosylated proteins occur as both *O*- or *N*-linked glycol moieties (Figure 1-6). Synthetic methods that model this quality are a promising way to produce vaccines with specific targeting ability [106, 107]. Glycosylation is used to increase peptide solubility, oral bioavailability and serum half-life, to gain a broader reactivity, and to provide more conformational properties to synthetic peptides [108]. Biologically, the structural properties of vaccine constructs are important [109]. For instance, the relationship between the structure of glycosylated peptides and their targeting ability plays an important role in an immune response [110, 111].

Variation of the carbohydrate epitopes that target cellular receptors is known to influence cell development and immune responses [112]. Sugar moieties are attached to the peptides or proteins by conjugation to the nitrogen of the asparagine side chain (*N*-linked) and *O*-glycosides are most commonly attached through the hydroxyl group of serine and threonine (Figure 1-6). Glycosylated peptides have roles in vaccine development due to their ability to form new ligands, thus permitting tailoring to meet specific receptor binding properties [112]. Recent advances in the synthesis of complex glycomolecules are due to an increase in experimental studies investigating the interactions between glycosylated ligands and a wide range of immune receptors.

Mannosylation has proved to be an important method for vaccine targeting and design. Common mannosylated vaccine antigen candidates include peptides and proteins. However, other mannosylated systems, such as nanoparticles and liposomes, have also been extensively investigated as vaccine candidates. Here, mannosylation has been shown to effectively increase the uptake and targeting of these systems towards the MR [9, 113], [114, 115]. The primary focus of this thesis will be on mannosylated peptide and protein antigens for vaccine development.

1.7.1 Mannosylated proteins

Initial MR studies investigated the receptors capacity to recognise and internalise various sequences and stimulate a T cell response. However, more recent studies have investigated the binding affinity of the receptor with the aim of developing targeted vaccines [116, 117]. The important role of the MR in the uptake and presentation of ligands to DCs results from the finding that mannosylated ligands are presented more efficiently than non-mannosylated ligands, subsequently generating a greater immune response than non-MR ligands [62, 118, 119]. The exact structural requirements for binding to the MR have not been determined but investigations using polymannan derivatives [91], mannosylated dendrimers [120] and compounds that contain a high number of mannose groups presented to mimic highly branched mannan [121, 122] are promising. Frison *et al.* attached Manα6Man, Manα2Man and Manα3Man to dendrimers. They found that Manα6Man was the optimal ligand, concluding that di-mannose clustered compounds are the best ligands for MR targeting (Figure 1-8) [121].

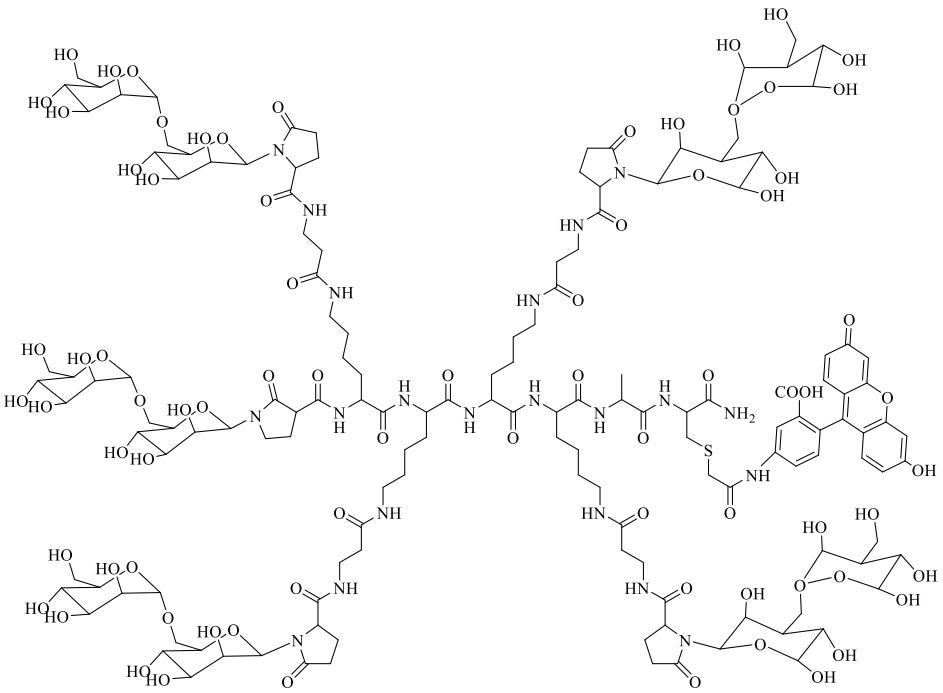

Figure 1-8. Schematic of a Manα6Man glycocluster. Frison *et al.* found this structure bound strongly to the mannose receptor resulting in endocytosis of the gycocluster [121].

Engering *et al.* observed a rapid reappearance of the MR at the cell surface of immature DCs when exposed to mannosylated BSA, suggesting that the receptor efficiently concentrates mannosylated antigens for transport to compartments for processing and peptide loading and also showed that the receptor is recycled to the cell surface [118, 123]. In addition to chemical modification of antigens, natural mannosylation has been used in vaccine development for receptor targeting. A study by Liu *et al.* observed that natural protein *O*-mannosylation was critical to the virulence of *M. tuberculosis* (Figure 1-6) indicating the importance of natural *O*-mannosylation and prevalence of *O*-mannosylated structures in nature [124].

1.7.2 Recombinant *N*- or *O*-linked mannosylation

Glycosylation is a common post-translational modification to the surface of naturally occurring exposed proteins and lipids. Information derived from bacterial genome sequences combined with proteomic and genomic analysis has enabled identification of enzymatic glycosylation machinery. *O*-mannosylated proteins are present in different groups of bacteria and fungi and play a vital role in stimulating an immune response through their interaction with DCs [125].

The affinity of the MR for *N*- or *O*-linked glycopeptides was investigated by Gustafsson *et al.*, who used recombinant proteins with mannose derived from *Pichia pastoris* (Figure 1-6). *P. pastoris* mucin-type fusion proteins (PSGL-1/mIgG2b and AGP/mIgG2b) that predominantly contain α-linked mannose residues in both *N*- and *O*-linked substitutions were used to target the MR. This study demonstrated the receptors high affinity for both *N*- and *O*-linked mannosylated proteins [76].

This affinity was also confirmed when yeast-derived recombinant ovalbumin (OVA) carrying branched *N*- and *O*-linked mannoses was more immunogenic than non-mannosylated OVA [73]. The mannosylation pattern in the cell wall of mutant *C. albicans* (Figure 1-6) was shown to be responsible for increased immunity. In this study, Ifrim *et al.* established that fungal mannan alone did not prime DCs from peripheral blood mononuclear cells for the production of cytokines, concluding that the presence of the *O*- and *N*-linked mannosylated proteins at the *Candida* cell surface is required for a strong immune response [126].

However, effective immunogenicity by glycoprotein-based vaccines does not necessarily correlate to protection, and this is a challenge faced in all areas of vaccine research. Additionally, protection of mannosylated proteins versus un-mannosylated protein-based vaccines is also an important aspect in this field. An example of this is outlined in a paper by Nandakumar *et al.* where the protecting mannosylated antigenic proteins (Apa), secreted by *M. tuberculosis*, induced stronger CD4 T cell responses than un-mannosylated Apa expressed by *E. coli*. However, neither were successful in

providing protective efficacy [127]. Further, Apostolopoulos *et al.* showed that immunisation with MUC1 attached to reduced mannan provided poor protection despite induction of tumour-specific CD8 T cell responses [71]. Studies such as that of Napper and Taylor showed this anomaly in protection versus antibody titre [123], and examples of successful mannosylated versus un-mannosyled-vaccines, whereby protection was obtained, can be found in various articles [128, 129].

1.7.3 Mannosylated peptides

Peptide epitopes from natural proteins have been investigated for their ability to stimulate an immune response [116]. *O*-mannosylated polyalanine peptides were synthesised by Brimble *et al.* in 2007 in an attempt to evaluate the peptides specificity of peptides for targeting MR [130]. A synthetic library was synthesised containing linear or branched *O*-mannosylated serine units, which were placed sequentially in the chain or separated by spacers (Figure 1-9). Binding studies showed that constructs that contained either mono- or branched-mannose groups had the same affinity for the receptor, while increasing the concentration of the mannosylated peptides increased the binding affinity [130, 131].

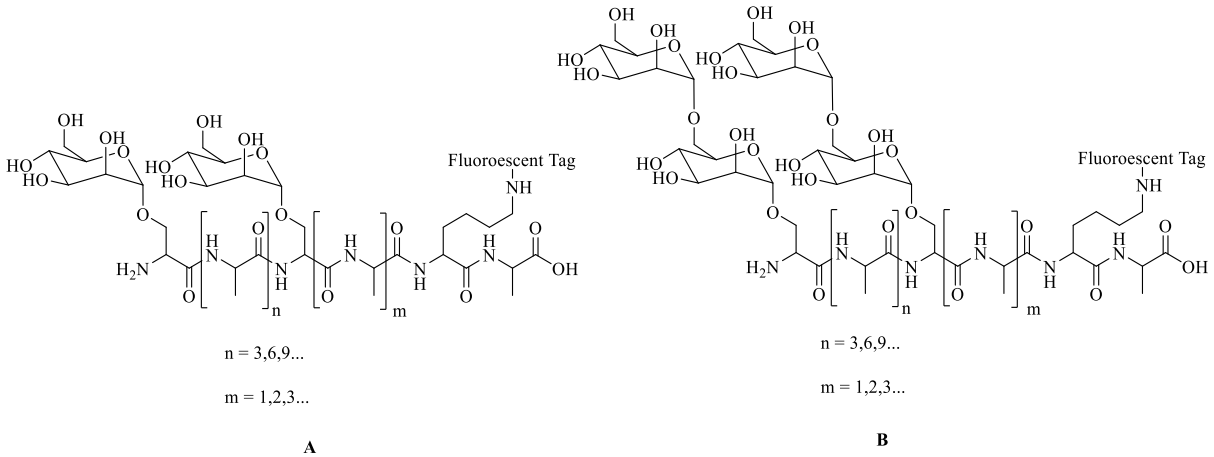

Figure 1-9. Mannosylated peptides designed to investigate the relationship between the number of mannose groups and their receptor targeting ability. Schematic structure of the mannosylated peptides synthesised by Brimble *et al.* to investigate the relationship between linear and branched mannosylation and receptor targeting. [130]. An investigation was carried out using **A:** linear mannosylated peptides separated by alanine spacers, and **B:** di-branched mannosylated peptides separated by alanine spacers. No difference was observed in the targeting ability of linear (**A**) and di-branched (**B**) mannosylated constructs, however spacer length was found to play a role in receptor binding. A fluorescent tag (5(6)-carboxyfluorescein) was included in each glycosylated peptide for bioassay analysis.

Kel *et al.* synthesised a mannosylated $OVA_{323–339}$ epitope and showed that immunisation induced poor T cell effector function despite enhanced antigen presentation when compared to the non-mannosylated epitope, indicating that other pathways were being targeted [78]. To evaluate MR-mediated macrophage targeting, Gao *et al.* synthesised monodispersed polyethylene glycol peptide (PEGtide) dendrons that contained eight mannose groups. Macrophage uptake studies confirmed high uptake of the mannosylated dendrons and showed that an increase in the number of mannose groups resulted in a better DC uptake as confirmed by confocal microscopy in the presence of competitive inhibitor, mannan [79].

Bissen *et al.* investigated the affinity of a library of lysine-based oligomannoside clusters that contained two to six mannose groups (Figure 1-10). This study demonstrated an increase in receptor affinity with an increase in mannose valency [80]. Kinzel *et al.* proposed the use of the same clustered structures with addition of an antigen and plasmid DNA at the C-terminus with the aim of developing a DNA-based vaccine, but, to date, no further information has been published [81]. *O*-linked mannosylated polylysine dendrimers, produced by Kantchev *et al.*,were studied by confocal microscopy for DC internalisation through the MR. This study demonstrated the successful localisation and internalisation of the dendrons, indicating mannosylated-specific targeting [82].

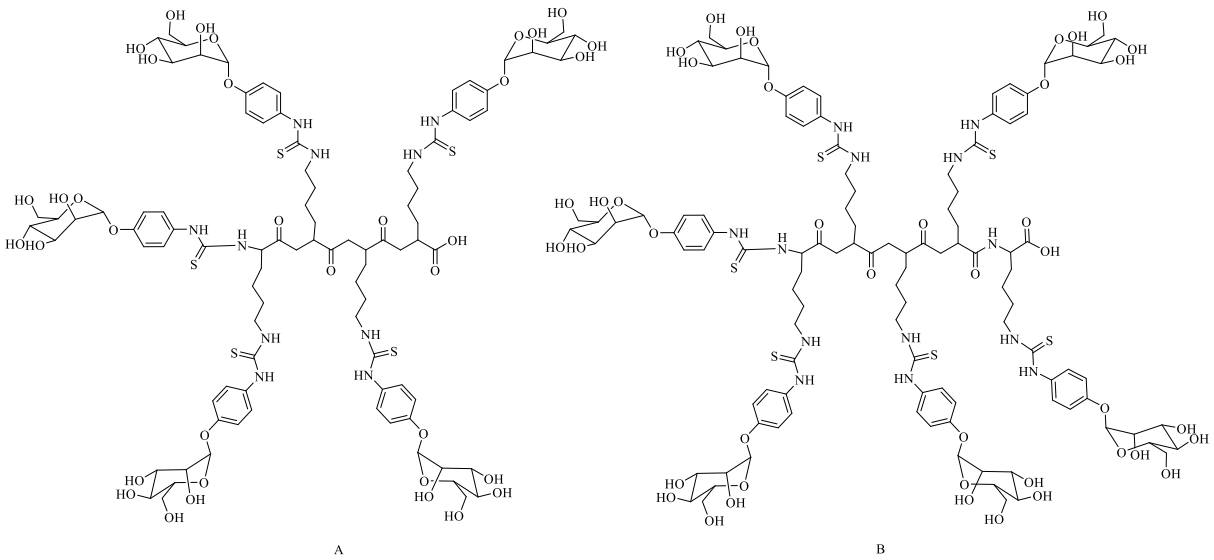

Figure 1-10. Oligomannoside clusters synthesised by Bissen *et al.* The structures showing the best affinity for the mannose receptor are **A:** a cluster with five terminal mannoses, and **B:** a cluster with six terminal mannose groups.

Moyle *et al.* synthesised a vaccine candidate comprised of a human papillomavirus type-16 ($E7_{44-62}$) epitope aimed at treating established cervical cancer. Here they examined the structural placement of mannose groups and epitopes on the ability to target the MR (Figure 1-11). Polylysine dendrimers

that contained a C-terminal lipid core held four $E7_{44-62}$ epitopes with a mannose group attached at the N-terminus (Figure 1-11). This investigation confirmed that mannosylated vaccine candidates successfully reduced cervical cancer size while non-mannosylated candidates did not [132].

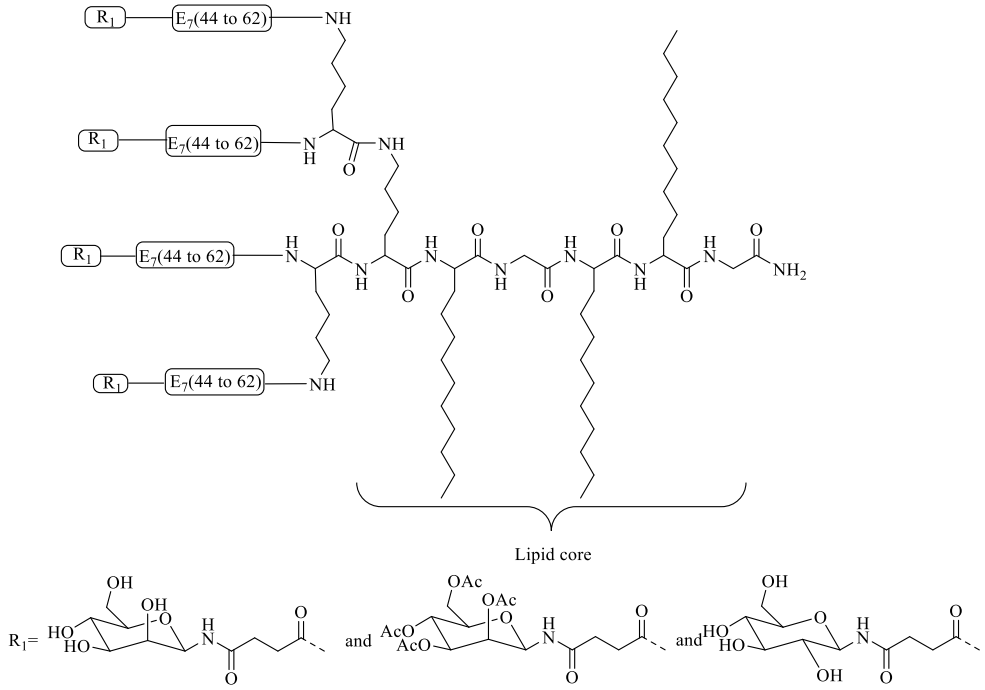

Figure 1-11. Lipid core polylysine with multiple epitopes made by Moyle *et al.* Structures contained either *N*-linked mannose or N-linked glucose in both acetylated and deacetylated forms. Both acetylated and deacetylated delivery systems that contained mannose successfully reduced tumour size in mice when compared to glucose delivery systems.

In 2010, Raiber *et al.* prepared fluorescently labelled derivatives of pepstatin (a selective inhibitor of aspartic proteinases that destroy lysosome antigens) attached to mannose to target DCs. Investigations found that mannosylated constructs selectively targeted, and were internalised by DCs and macrophages, stimulating activation through the MR [133].

All studies have confirmed a requirement of terminal mannose placement in the peptidyl structures enabling MR binding and uptake. Further optimisation in the design of mannosylated peptidyl candidates for effective receptor targeting is still required.

1.8 Peptide-based subunit vaccines

Vaccination is an active immunisation method used to form permanent protection against infections (e.g. against bacteria or viruses) or used in therapies (e.g. cancer) [134]. Common vaccination methods are based on the use of live attenuated (Figure 1-12C), inactivated pathogens (Figure 1-12B),

or the use of a minimal pathogenic part of pathogens (alone or combined with immunogenic compounds) as subunit vaccines (Figurer 1-12A) [135]. In these latter vaccines the immunogenic fraction is only a minimal part of the pathogenic cell wall proteins, toxoids or globulins (Figure 1-12A). This minimal fraction, which is usually an immunologically active peptide (epitope), has been the centre of growing interest due to its many advantages over whole complex pathogenic vaccination (Figure 1-12A) [135, 136]. Many live attenuated vaccines contain infectious material and thus, their preparation steps including culturing and handling may be challenging. However, using peptide-based vaccines can be beneficial in this aspect making preparation steps easier with less risk involved [137].

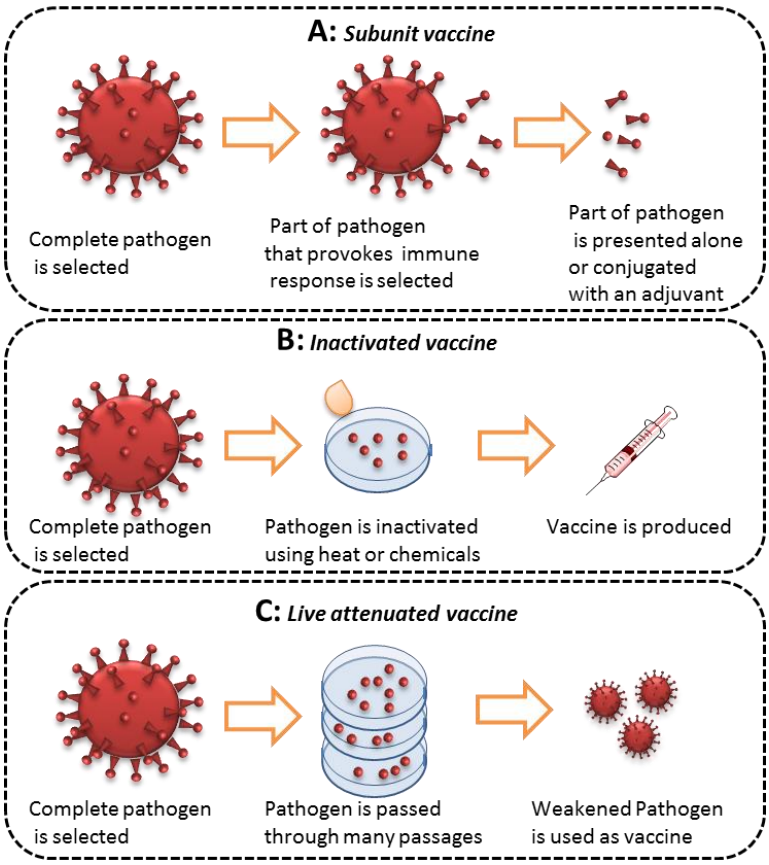

Figure 1-12. Vaccine types. A: Subunit vaccines are prepared by use of part of the pathogen that provokes immune response, this can be based on biological extraction methods (recombinant) or synthetic methods (peptides); **B:** inactivated vaccines are prepared by inactivation of pathogens by heat or chemicals; **C:** live attenuated vaccines are prepared by weakening the pathogen through multiple passages.

Peptide epitopes can be prepared using recombinant technology (e.g. using gene delivery systems for large-scale production) or can be synthetically prepared [138]. Using the minimal antigenic epitope of a pathogenic moiety in a vaccine can provide many advantages, including the exclusion of

unnecessary or harmful sequences. There are some pathogenic moieties where use of the whole pathogen can be oncogenic (e.g. the Epstein–Barr virus) and there are pathogenic moieties where use of the whole pathogenic protein can cause autoimmune disease (e.g. protein from Group A *Streptococci*) [139, 140].

1.8.1 Solid phase peptide synthesis

Solid phase peptide synthesis (SPPS) is a common method used to produce a well-characterised peptide-based subunit vaccine. This method has advantages including the production of highly pure, high yielding and relatively (cost) inexpensive peptide products [141]. In addition, SPPS can be applied for the production of both linear, branched or multi-epitope peptide dendrimers [142]. Peptides have a polyamide backbone where an amine from one amino acid is coupled to the carboxyl group from another amino acid forming a polyamino acid chain (or peptide). In 1903, Emil Fischer was the first to successfully attach two amino acids together using a peptide bond, however, at that time protecting groups were not available and elongation of a peptide chain was not possible [143, 144]. After the development of amino acid protecting groups, including the *t*-benzyloxycarbonyl (Boc) group, and the development of deprotection methods in 1955 by du Vigneaud, the neurohypophyseal nonapeptide hormone, oxytocin, was the first peptide-based hormone analogue synthesised.. For this work, du Vigneaud received the 1955 Nobel Prize in Chemistry [145].

SPPS is primarily based on the use of resins as a solid support for peptide synthesis and has made synthesis methods easier due to an increased stability of the peptide during synthesis [146]. Here, resins are cross-linked polymers and when organic solvents are added to them become swollen and provide a solid support for peptide preparation. Resins have different sizes (80-200µm) and mesh size (polymer number of openings in a square inch – 70-170) and can vary in type (polystyrene, polyamine, tentagel and soluble) depending on the synthesis and cleavage methods chosen for peptide preparation [147]. There are two main types of SPPS and these are based on the N-terminal protecting group employed on the amino acid; Boc and 9-fluorenylmethoxycarbonyl (Fmoc) (Figure 1-13). Boc protection can be useful for providing stability under basic conditions since it is an acid labile protecting group, and can protect the peptide from hydrogenation (Figure 1-13). In this synthesis, the Boc group is deprotected using a strong acid such as hydrofluoric acid (HF) [148]. During the early stages of SPPS development, Boc-SPPS was successfully used in the preparation of many peptides, however, due to dangers involved in the use of HF new studies focused on the development of a newer technique, Fmoc-SPPS which was first introduced in 1970 [149, 150]. Fmoc-SPPS uses milder reaction conditions employing a basic solution to remove the Fmoc protecting group (piperidine) and

the peptide is cleaved from the resin using a milder acid (usually trifluoroacetic acid [TFA]) compared with HF used in Boc-SPPS.

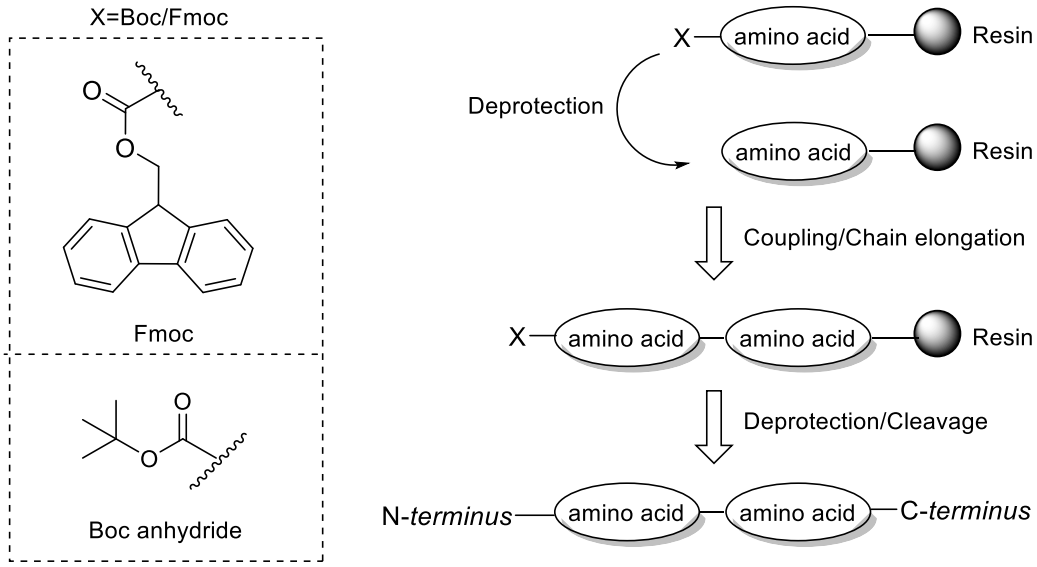

Figure 1-13, Schematic diagram of solid phase peptide synthesis. Solid resin support is used to build a peptide chain from individual amino acids where orthogonal Fmoc or Boc protecting groups are used depending on the synthesis conditions, such as the choice of resin. Cleavage of the poly-amino acid chain from the resin generates a peptide in the last step.

Ease of preparation, drying, purification and storage are some advantages considered for synthetic peptide-based vaccines [136]. However, development of peptide-based vaccines requires further studies to overcome issues including those of optimal immunogenic sequences, choice of efficient delivery systems and low immunogenicity [151].

1.8.2 Lipid incorporation into peptide-based subunit vaccine

Although synthetic peptides have many advantages, including specificity, and ease of synthesis and stability, peptides themselves are poorly immunogenic [152]. Thus, engineering powerful adjuvants such as the inclusion of lipids in the peptide structure can improve their immunogenicity [141]. Therapeutic peptide-based subunit vaccines must overcome biological barriers to achieve receptor targeting. These barriers include chemical stability, stability against enzymatic degradation, reduced toxicity, and improved specificity. Thus, design and modification of peptide epitopes are essential for advanced vaccine development [153].

Adjuvants are described as additions to antigenic moieties that can help increase both cell mediated (cytotoxic T cell) or humoral (cytokine-mediated) immune responses [152]. Commonly studied

adjuvants fall under the categories of recombinant cytokines, oil-emulsions, particulate delivery systems, polysaccharides, alum, cell-based delivery systems and chemical conjugation of lipids to peptides [141, 154]. Recombinant adjuvants including granulocyte macrophage colony-stimulating factor (GM–CSF) and IL-12 have been used in many studies for vaccine development and have reached human based clinical trials [1]. Oil-emulsion adjuvants such as the Montanides are primarily used in cancer vaccine development, however, due to their high toxicity are unlikely to be used in human-based vaccine trials [155]. Particulate delivery systems like liposomes, exosomes and virosomes have been used in combination with peptides for providing both delivery and adjuvant ability and have shown some success in receptor mediated uptake and cellular immune response in clinical/pre-clinical trials for vaccine development [1]. Inulin is a plant-derived polysaccharide that has been shown to produce both cellular and humoral responses [156]. Inulin has been used as an adjuvant in vaccine development with Th1 and Th2 activity [156]. Lastly, the most widely used adjuvant in the vaccine development is Alum. Alum is a well characterised adjuvant that has been shown to activate humoral responses; however, it lacks the ability to enhance a cellular immune response. Further, there are many reports of adverse effects including neurotoxicity, autoimmunity, and long term brain inflammation when Alum has been administered, making it unsuitable for use in humans [2]. Cell-based delivery (by viruses and DCs, *etc.*) has been extensively studied for its use as delivery systems for peptide-based vaccines. However, cell-based delivery systems rely on the cells ability for processing and presenting a peptide antigen and this has been their main limitation due to non-uniformity and problems with reproducibility [157].

There are many modification methods used to increase immunogenicity of peptides, including PEGylation, or the addition of lipids, phosphates or carbohydrate moieties. From these, lipidation has proved to be a successful method in providing lipophilicity and stability for the peptide [158]. Here, lipopeptide vaccines have displayed not only structurally stable and biologically active properties, but also have proved to have effective adjuvanting properties in a variety of vaccines, including those that target Group A *Streptococcus* and cancer [159, 160]. In another study it was shown that glycosylated lipopeptides were successful as peptide delivery systems with self-adjuvanting properties [161]. Diversity in these adjuvanting systems with variable immune responses requires the attention of future studies to advance the development of these adjuvanting systems, thus lipopeptide vaccines with the advantage of being synthetically prepared may be a path to the future in solving a number of debilitating diseases.

1.8.2.1 Peptide-lipids

It is now well-known that in most peptide-based vaccine developments there is a need for increasing immunogenicity by either addition or binding of an adjuvant moiety to peptide epitopes [147, 153]. Lipid core peptides (LCP) are peptide antigens attached to lipid moieties (Figure 1-14). LCPs have been extensively used in the development of subunit vaccine [162]. The idea of using LCPs as self-adjuvanting moieties was first established in the 1980s when it was discovered that addition of lipids to peptides could boost their immunogenicity [163]. Furthermore, it has been shown that different types of lipids influence the antigenic properties of a vaccine, but these are often antigen specific. For example, lipoamino acids incorporated into peptides (LCP), glycolipids (monophosphoryl lipid A [MPL]) and analogues of bacterial lipids inlcuding lipoproteins such as tri-palmitoyl-S-glyceryl cysteine (Pam3Cys) and di-palmitoyl-S-glyceryl cysteine (Pam2Cys) have been investigated as lipid adjuvants (Figure 1-14) [164]. Here, LCP subunit vaccines are known to have self-adjuvanting properties and are generally formed using a minimum of antigenic peptide epitopes necessary for targeting the immune system [165].

Solid and/or solution phase peptides are commonly used to prepare LCPs which are shown to be stable when kept unrefrigerated [166]. To optimise the immune response, the length of the lipid chains, the number of lipids, and the number of spacers between each lipid can be varied. In addition, single or multiple peptide epitopes can be attached in a linear or branched format to the LCP system (Figure 1-14). The LCP system has also been shown to have the ability of targeting DCs and inducing cellular immune activation, including cytotoxic T cell response upon CD4 T cell activation [167]. Further, MPL, Pam2Cys, Pam3Cys are other lipidic structures that have been included in a peptide structure in different studies for their adjuvanting properties [152, 154-156, 159, 160, 162, 164, 166, 168]. However, studies in a mouse model have shown that these lipidic structures conjugated to one peptide epitope (J8), showed similar immune activity when used in conjugation with a greater number of epitopes (J8) [169-171]. Branched lipopeptides have been shown to be resistant to lytic enzymes in the body and are found to give higher T cell stimulation due to their better uptake/presentation by DCs when compared to linear peptides [168, 172]. In a study by Daubersies *et al.* it was shown that when chimpanzees were vaccinated with lipopeptides containing palmitic acid (Figure 1-14) and the malaria antigen LSA-3, they were protected against a challenge with *Plasmodium falciparum* sporozoites [173]. Further, many initial clinical studies have reported success from application of LCP systems as subunit vaccines in the prevention and treatment of cancer, bacteria and parasites (e.g. hookworm) [174].

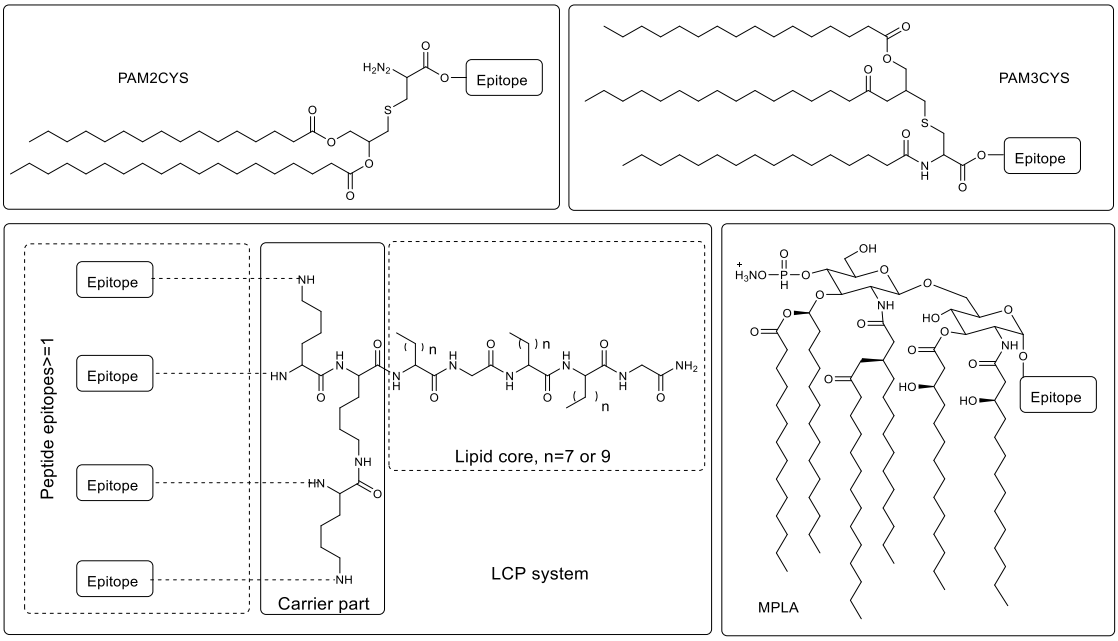

Figure 1-14. General Structure of common lipidic adjuvants. These lipidic adjuvants are used in peptide conjugation to enhance immunogenicity; monophosphoryl lipid A (MPLA), di-palmitoyl-S-glyceryl-cystein (Pam2Cys), tri-palmitoyl-S-glyceryl-cystein (Pam3Cys), LCP [159].

1.8.2.2 Lipidation and receptor binding

Binding of a vaccine structure to a surface molecule on APCs facilitates the transport of antigenic moieties across the cell. Lipidation, depending on where it is located in the peptide chain (N or C terminus) has been shown to affect the immunogenicity of the designed constructs [158]. Here, studies by Lau *et al.* showed that addition of a lipid (cholesterol) to the N-terminus of the HA2 influenza peptide epitope ($HA2_{166\text{-}180}$) increased the cellular (Th1, cytotoxic T cell) immune response in a mouse model [175, 176]. Furthermore, lipid length and lipid type have also been shown to be important factors that affect receptor binding properties. In a study by Zhang *et al.*, lipids with different lengths (C8-C18) were conjugated to galanine (neuropeptide) analogues and tested in a mouse model for their anticonvulsant activity through the galanine receptor. Here, it was concluded that shorter lipids were more successful in receptor targeting, while factors including lipophilicity and charge of the peptide epitope were shown to be involved in the level of anticonvulsant activity [177].

Lipopeptides, lipopolysaccharides and lipoproteins derived from a pathogen's cell wall are recognised by a family of transmembrane proteins called Toll like Receptors (TLRs) present on the surface of macrophages and DCs. TLRs are another subfamily of PRRs and play an important role in innate immunity by their recognition of lipidated structures and activation of inflammatory immune

responses (Figure 1-15) [178]. Ten TLRs (TLR 1-10) have been identified in mammalians and each TLR has been shown to be responsible for ligand recognition [179]. TLR stimulation by invading pathogens sends specific intracellular signals (through signalling molecules like IL-1 receptor associated kinase [IRAK-1-4], tank binding kinase 1 [TBK1], myeloid differentiation factor 88 [MyD88s]) and activates a series of nuclear transcription factors (nuclear factor kappa B [NF-κB], activating protein 1 [AP-1], nuclear factor interlukin [NF-IL6] and interferon regulatory factor [IRF]) that ultimately cause the cell to produce inflammatory cytokines (e.g. interleukins [ILs], interferons [IFN] and TNF) [178]. For instance, TLR-4 was one of the first TLRs to be identified and is responsible for the recognition of lipopolysaccharides [18].

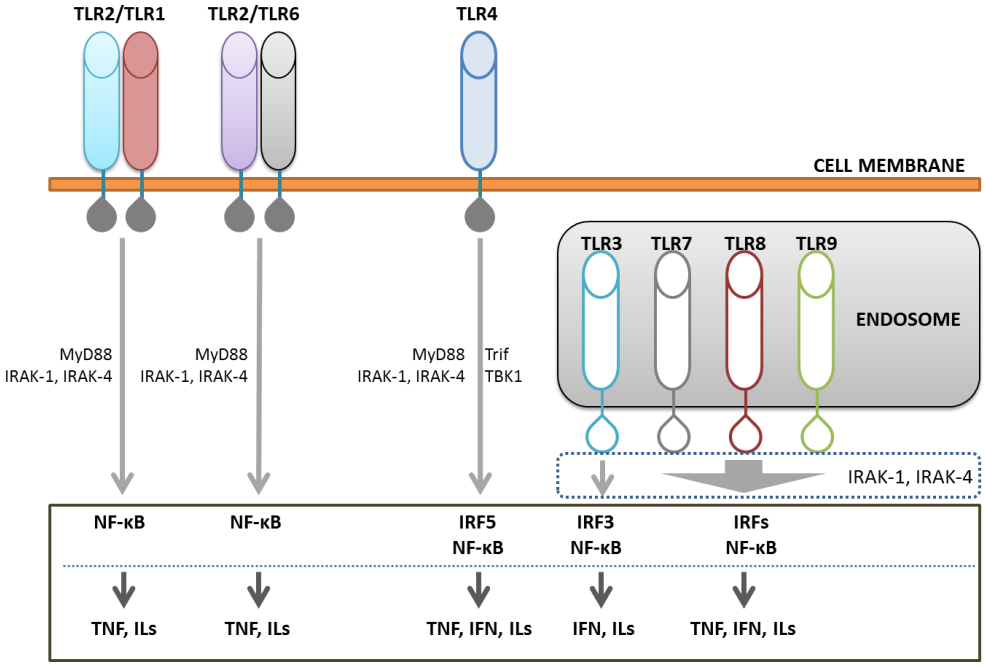

Figure 1-15. Toll-like receptor signalling pathway. TLRs are trans-membrane receptors from the family of pattern recognition receptors that exist as both extracellular (TLR-1, 2, 4, 6) and intracellular (TLR-3, 7, 8, 9) molecules. Signalling molecules including IRAK-1-4, TBK1, MyD88s activate a series of nuclear transcription factors (NF-κB, AP-1, NF-IL6 and IRF) causing the cell to produce inflammatory cytokines (TNF, ILs and IFN).

Further, TLRs-1, 2, 5 and 6 have been shown to recognise other lipidic moieties including bacterial lipopeptides, lipoteichoic acids, flagellin, and glycolipids [15]. Here, TLR interaction with lipidic ligands has been shown to result in the activation of downstream signalling pathways that cause the maturation of DCs (Figure 1-15) [169]. As a result, the discovery and understanding of TLR mechanisms are a crucial factor in the design of vaccine constructs. TLRs, like other pattern

recognition receptors (e.g. the MR), have been shown to be responsible for phagocytosis, activation of the complement system (surface proteins involved in pathogen elimination) and induction of inflammatory signalling pathways [18]. In addition, these TLR activities play key roles in the activation of both innate and adaptive immunities. Mature DCs travel to the lymphatic nodes where they present processed antigens with signalling molecules, through MHC and co-stimulatory molecules (CD80 and CD86), to naïve T cells and initiate a T cell response [18]. Inflammatory cytokines (e.g. IL-12) released as a result of DC maturation can further differentiate T helper (Th) activity into Th1. In a study by Schnare *et al.*, MYD88 (Figure 1-15) deficient mice were immunised by OVA mixed with complete Freund's adjuvant (CFA). No Th1 activity was observed while Th2 activity was unaffected. This confirmed the important role TLRs played in the Th1 activation pathway [180].

1.9 Model antigen selection

There are many known immunogenic antigens, however, only several are used as model antigens, one of which is OVA [181-183]. The OVA protein and epitope $OVA_{323-339}$ is one of the main proteins found in avian egg white [182] and is known to bind to MHC II and cause a T cell response [184]. The OVA protein by itself has been the centre of interest in vaccine design due to its ready availability, and it has been of interest for allergy model studies (asthma, food and dermal allergies) since it is the major protein found in egg white [182]. The OVA protein naturally exists as a glycoprotein, however, it was discovered that the $OVA_{323-339}$ and OVA_{1-10} sequences of the OVA protein bore a B cell epitope that was capable of inducing a T cell response. This discovery was obtained by T cell mediated IgE responses that were observed against an assumed B cell epitope inside $OVA_{323-339}$ and OVA_{1-10} peptides [185]. It is now well-established that the $OVA_{323-339}$ peptide binds to MHC II molecules and appears as a CD4 T cell epitope in T cell activation [186].

The $OVA_{257-264}$ is another epitope derived from the OVA protein and is known to be a CD8 T cell activator through attachment to MHC I molecules, playing an important role in cytotoxic T lymphocyte activation [187]. However, for a successful vaccine, activation of both CD4 and CD8 T cells are necessary. Other structural factors including using different adjuvanting systems, application of multiple epitopes or glycosylation can give selectivity to a specific immune response pathway [188]. A study by Brooks *et al.* showed that application of multiple $OVA_{257–264}$ epitopes in a single delivery system could enhance immune responses in mice by producing an antigen-specific INF-γ response [187]. In this study, multiple antigenic peptides (MAP) conjugated to the $OVA_{257–264}$ (also known as OVA CD8) were compared to non-branched peptides for their ability to generate antigen specific T cells and IFN-γ. It was concluded that the use of cell penetrating delivery systems can

increase the level of immune response in the form of T cell activation and IFN-γ production where $OVA_{323-339}$ was used as a negative control and lacked the ability to produce IFN-γ. Further, Sun *et al.* indicated that in allergenic mice, the $OVA_{323-339}$ epitope (using 300 µg alum as adjuvant) produced a Th1 response but its immunogenicity was limited compared to the full native OVA protein [189]. This confirmed the need for an efficient adjuvant system for small proteins or peptide epitopes as vaccine candidates [190]. OVA was used with biopolymeric carriers to study adjuvanting ability of these carrier systems in C57BL/6 mice by Matzelle and Babensee [191]. Here, the OVA protein delivered with CFA was able to produce high antibody titres compared with OVA delivered with phophate buffered saline (PBS) indicating the importance of applying an adjuvant with a vaccine delivery.

1.9.1 Epitope selection affects the immune pathway

Upon pathogen entrance to the body, an immune response starts with the uptake of extracellular antigens by APCs using different endocytosis methods (one of which includes the MR) [192]. This is followed by presentation of the antigen through MHC molecules to CD4 and CD8 T cells[6]. However, Burgdorf *et al.* demonstrated that the endocytosis pathway involved in antigen uptake plays a crucial role in choosing presentation pathways to either CD4 or CD8 T cells [6]. In this study, the native OVA protein was administered to mice genetically modified to have the MR expressed on DCs and showed that the OVA protein could activate OVA-specific CD8 T cells ($OVA_{257-264}$ sensitive T cells from transgenic mice, OT-I), but was not able to activate OVA-specific CD4 T cells ($OVA_{323-339}$ sensitive T cells from transgenic mice, OT-II). This highlights an important aspect of uptake through the MR that can affect antigen specific T cell response depending on the selection of antigens in a vaccine structure [6, 193]. It is known that CD4 T cells play an important role in CD8 activation. Here, when CD8 T cell responses were studied in the absence of CD4 T cells, CD8 T cells had little proliferation ability and their cytokine level, upon *in vitro* re-stimulation, was very low (similar to naïve T cells) [24]. It is now known that CD8 T cells can function in the processing of an antigen without the presence of CD4 T cells, however, for a memory response, the presence of CD4 T cells is necessary [23]. This theory was observed by Sheldock *et al.* when they used a recombinant vaccinia virus and generated normal $CD8^+$ T cell activity within one week of vaccination, while a re-encounter with the same antigen caused a drastic decrease in the response group when no CD4 T cells were present [194]. All these studies reveal an important and complex relationship between CD4 and CD8 T cells and this has been detailed in Figure 1-5.

1.10 Targeting antigens using particulate delivery

Researchers have been investigating methods for the delivering of antigenic moieties to the immune system to obtain the highest possible immune response against a specific disease [195]. Considering the complexity of the immune system, vaccination can give an unpredicted response (e.g. allergies), however, synthetic design and engineering of peptide structures provides an opportunity to predict the outcome [3]. In the human body, DCs are responsible for constant uptake of antigenic moieties and this uptake is performed through different mechanisms, including phagocytosis of large particles (0.25-10 µm), receptor mediated endocytosis (particles smaller than 500 nm) and pinocytosis which is a term used for any mode of uptake that does not include a receptor [196]. Following vaccine injection (subcutaneously, intradermally, intramuscularly, *etc*), particulate size has been shown to be a limiting factor affecting the uptake and processing of a vaccine by the lymphatic system [134]. Studies have shown that larger particulates (300-500 nm) have smaller diffusion speeds and less ability permeate areas of the extracellular matrix, including areas less crowded by extracellular proteins. However, smaller molecules (less than 50 nm) can easily dissolve into the local matrix and be transported into the APCs or intracellular pathways [197]. When particulates arrive at the lymph nodes, the size effect changes and due to "lymphatic retention", bigger sized particulates stay longer and can target macrophages while smaller particles have more affinity towards DCs and B cells [198]. Antigens designed in a particulate format are known to have the ability to activate CD4 and CD8 T cells through cross-presentation where these particulates can be in the form of nano- and micro-sized delivery systems [197, 199]. When designing particulate vaccine delivery, an important factor that affects the size and delivery ability is the number of antigens bound to a particle. Particles can be aggregations of small antigenic molecules thus the number of antigens can vary in size and concentration [200, 201]. The cross-presentation of antigens delivered as particulates can be size dependant, as suggested in a study by Kovacsovics-Bankowski and Rock, where an optimal cross-presentation was observed by particles with a size of about 3 µm [202]. In another study, Soong *et al.* developed lipid nano-capsules with MPLA that contained a whole protein TLR-4 agonist. Interestingly, they found that their designed delivery system could boost antigen specific T cell responses [200]. All these studies suggest the importance of subunit vaccine delivery in a particulate form and opens future challenges in the design of delivery systems that could efficiently control a desired immune response.

1.11 Conclusion

Knowledge of vaccination has been developed throughout history however, with an ever-demanding need for new treatments and therapies there are still many challenges to be faced. Factors like

selective immune response pathways, targeting, selection of antigenic moieties, adjuvanting properties, and particulate delivery have to be considered for successful vaccine development. From the early encounter of a foreign pathogen by the immune system, the innate immune system is activated, which leads to a long-term memory response, also known as adaptive immunity. An optimum vaccination should be able to activate both these pathways to obtain a desired T cell response.

Studies on the identification of the MR expressed on DCs indicated an important role for this receptor in immunogenicity, while its ability to recognise self from non-self has made it a useful tool in vaccine design and targeting. Studies to understand the targeting and processing involved in the internalisation of pathogenic antigens and antigen presentation through the MR are essential in order to have a better understanding of the function and role of this receptor in an immune response.

A unique feature of this receptor family is the presence of multiple CRDs in a single polypeptide chain. Investigations have found that the CRD is important for glycosylated ligand recognition and internalisation. However, recent studies including computational modelling and microscopy have provided further evidence into the structural and binding features of this receptor. These studies have also confirmed that CRDs 1-3 are not essential for glycosylated ligand binding, with CRD4 having the same ligand biding ability as the whole MR. However, CRDs 5-7 have been shown to be essential for binding to highly glycosylated ligands. This has provided insights into the predicted structural arrangement of the MR with two contradictory models now available. Initially, a U-shaped model was proposed with CRDs 4-5 exposed to the glycosylated ligands, while a more recent investigation suggested a “bent” structure with both CRDs 4-7 and the CR domain playing an important role in the binding of glycosylated ligands (Figure 1-4). These model studies indicate that the structure of the domain is highly related to the experimental design and to date no further information about the structural and spatial arrangement of the CRD domains is known.

The discovery that mannan binds strongly to the MR has enabled receptor binding studies and advanced targeted vaccine development. Vaccine development using mannan as a known ligand, or by the attachment of mannose to proteins and peptides, has been studied extensively. Vaccines derived from mannose exploit the targeting properties of the mannose group while avoiding the stimulation of a mannose-specific immune response because mannose is poorly immunogenic. Mannosylated proteins for vaccine design have included investigating oxidised and reduced mannan. Additionally, recombinant *N*- or *O*-linked mannosylated peptides and proteins have been shown to bind equally and be internalised by the MR receptor. In addition, attaching mannose to a peptide epitope is another approach to enhance receptor targeting. As a result, many strategies have been

employed to develop MR targeted vaccines and through the analysis of ligand and antibody targeting approaches it is clear that the nature and specificity of the antigen interaction with the receptor are critical factors in determining ligand processing and an immune response. However, further information about the organisation of the MR is required to advance/enhance pathogen-specific vaccine development.

Among the different vaccine development methods (including attenuation and inactivation of pathogens or the use of purified macromolecules such as toxoids or immunoglobulins), peptide vaccines have offered the advantage of engineering specific qualities to vaccines, like adjuvanting properties such as lipidation or carbohydrates for targeting. However, peptides as epitopes require a proper adjuvant system that can elevate the immunogenicity of small antigenic peptides. Among the many suggested adjuvanting systems used today, including the most common adjuvant alum, lipidation has shown to be a successful method for the modification of peptide antigens to have self-adjuvanting properties. However, adjuvanting properties caused by lipidation can vary depending on the number and length of the lipid moiety included in a peptide vaccine.

TLRs are found to be a primary receptor responsible for the recognition of lipid moieties. Of the ten TLRs identified in humans, each has been shown to have different properties in the activation of downstream changes in the DCs that can cause a consequent response. Another important factor in vaccine development is the selection of the epitope, essential to obtain the desired cellular or humoral immune response. The $OVA_{323-339}$ and $OVA_{257-264}$ epitopes are two peptide epitopes from the OVA protein which have long been used as model antigens to study CD4 or CD8 T cell responses for vaccine development. Here, studies have shown a cross-presentation effect with the help of these antigenic moieties, with an important relationship identified between a CD4 and CD8 T cell response. Furthermore, delivery systems relying on particulate formation of peptide vaccines have been shown to enhance these immune responses. Many studies have developed delivery systems in the form of nano- and micro-particles and it has been found that the size of a vaccine particulate can affect the speed of travel to the lymph nodes and particulate stability in the lymphatic system before it can be processed by CD4 and CD8 T cells. Overall, size plays an important role in vaccine design and development.

In general, with the current advances in the development of vaccines there are still many unknown aspects that need to be addressed. Further understanding of immune pathways involved in an immune response and a better understanding of the structural relationship in immune activation can be beneficial to advance future vaccine development studies.

1.12 Research Hypothesis

Receptors present on the surface of APCs recognise glycoconjugates and these have been a primary focus of vaccine and drug-targeting research. In the generation of an immune response, receptor mediated antigen uptake is the first crucial step that is followed by a T cell response where subsequent activation of T helper pathways can be achieved. Although it has been proven that the MR can recognise mannosylated peptides and proteins, the structural properties needed for the design of mannosylated peptides with targeting ability, including the spacing or branching of the mannose units that are known to affect receptor targeting and binding, needs to be explored in further detail. To date, most MR targeting studies have focused on the number of mannose moieties. This study focuses on the complex synthesis and analysis of a library of *O*-mannosylated lipo-peptides designed to investigate the MR binding properties for potential use in vaccine design and targeting. Here, the mannosylated lipopetide containing the CD4 ovalbumin epitope ($OVA_{323-339}$) is used as a model antigen to investigate the targeting affinity for the MR. Furthermore, structural properties in relation to T cell activation and cytokine release are evaluated.

Major hypotheses: **mannosylated lipopetides as model vaccines for targeting the mannose receptor**

It was hypothesised that vaccine constructs comprising mannosylated lipid dendrimers containing an ovalbumin epitope as the model peptide antigen and containing an alanine spacer between the *O*-linked mannose moieties could enhance DCs receptor mediated uptake and induce an immune response by T cell proliferation/activation where subsequent activation of T helper pathways could be achieved.

Specific hypotheses 1: **Improvement to the synthesis of fluorescently tagged multicomponent mannosylated lipoeptides.**

Since TLRs were found to be a key element of signalling to immune pathways, lipids of different sources including pathogen cell walls or synthetic forms were found to be able to give adjuvanticity via signalling through TLRs. *O*-mannosyls were also found to be a crucial part of pathogenic cell walls with the ability of targeting the MR. Further, mannose has been used as a tool in the development of structures containing *O*-mannosyls for better receptor targeting and consequently a better uptake to the APCs to achieve a vaccine delivery system. As a result, researchers have -included mannosyls in peptide structures in multiple vaccine development studies. However, many of structures used in vaccine development did not combine a targeting moiety with other components including a lipid adjuvant, model antigenic peptide and a fluorescent tag.

Here, we postulated that although synthesis of multicomponent mannosylated lipopeptides are to be with difficulties we could improve the yields by utilising stepwise synthetic methods. For instance we hypothesised that such complication could be overcome by preparation of building blocks containing mannose and lipid and preparation of small peptides with a final attachment.

Specific hypotheses 2: **Linear placement of mannosyl moieties in the vaccine constructs and an alanine spacer plays a role in antigen presenting cells uptake through enhanced receptor targeting.**

The MR has been shown to recognise mannosylated peptides and proteins, however, the optimal structural properties of these mannosylated peptides with enhanced targeting ability are unknown. This study proves that inclusion of a short spacing or linear placement of the mannose units affect receptor targeting and binding properties.

Specific hypotheses 3: **Structural properties in a vaccine construct could affect the activation immune pathways.**

Studies have revealed a correlation between the structural properties of antigenic peptides and their immunogenicity via T cell and B cell activation [203-205]. Here, T cell proliferation or activation and cytokine release are two of the major immune responses that have been commonly looked into for the determination of a vaccine construct immune activity. In this study, we designed vaccine structures that contained lipidic and sugar moieties and proposed that each component could potentially affect the immunogenicity of a vaccine construct.. In other words, we predicted a relationship between lipidation, glycosylation, particulate size and the immunogenicity of the vaccine.

1.12.1 General Aim

The aim of this study is to synthesise fluorescently-labelled mannosylated lipopeptides as subunit vaccine candidates in order to investigate the effect mannose, lipids and the distance between the mannose units has on immune response and receptor mediated uptake for advanced vaccine development.

1.12.2 Specific Aims

1.12.2.1 Aim 1: Vaccine Candidate Synthesis

1. Synthesise a mannosylated amino acid for use in peptide synthesis; ser-(Ac4-man)-OH.

2. Synthesise a library of azido-functionalised mannosylated lipo-peptide building blocks containing a fluorescent tag [5(6)-carboxyfluorescein] and a different number of alanine spacers between the mannose moieties.
3. Synthesise alkyne-functionalised $OVA_{323-339}$ lipo-peptide building blocks.
4. Produce solution phase copper-mediated azide-alkyne cycloaddition (CuAAC or click reaction) for conjugation of the mannosylated and $OVA_{323-339}$ lipo-peptide building blocks to form vaccine candidates.
5. Synthesise a library of control peptides, including vaccine constructs without lipid and/or mannose moieties.

1.12.2.2 Aim 2: Physiochemical Evaluation and In vitro Receptor Binding Study

1. Analyse each vaccine construct using Dynamic light Scattering (DLS) and transmission electron microscopy (TEM) to assess the size and shape of the particles.
2. Investigate receptor-mediated uptake and mannan inhibition studies on splenocytes ($F4/80^+$ and $CD11c^+$ cells) using flow cytometry and confocal microscopy.
3. Investigate receptor-mediated uptake using surface performance resonance (SPR) technology on the extracellular part of the MR to study receptor binding and affinity.
4. Investigate the T cell stimulatory activity of each vaccine construct for antigen specific T cell proliferation.

1.12.2.3 Aim 3: In vivo Study

1. Isolate and purify $CD45.2^+$OT-II cells and adoptively transfer to C57BL/6 mice to investigate T cell proliferation following vaccination of the vaccine candidates.
2. Investigate the up-regulation of interferon gamma (IFN-γ) and antibody production using enzyme-linked immunoSpot (ELISPOT) and enzyme-linked immunosorbent assay (ELISA) techniques, respectively.
3. Investigate immune cell cytokine production using the cytokine bead array (CBA) assay.
4. Investigate the cytokine producing T cells using an intra cellular staining (ICS) assay.

1.13 Thesis Outline

Chapter 1. **Introduction to Vaccine Development and Mannose Receptor Targeting**

This chapter provides an introduction to the immune pathways involved in antigen recognition, the structural properties of the MR, mannnosylation of peptides and proteins, and lipidation and selection of antigenic epitopes.

Chapter 2. **Experimental Section**

This chapter includes general material and methods used for the preparation of vaccine constructs, and *in vitro* studies and *in vivo* studies are discussed.

Chapter 3. **Synthesis of Mannosylated Lipopeptides**

This chapter describes the synthesis of a library of mannosylated lipopeptides. The designed vaccine library contains the $OVA_{323-339}$ epitope, lipids to increase adjuvanticity, a fluorescent tag [5(6)-carboxyfluorescein, FAM] for visualisation in cell uptake studies, and two *O*-mannosyl groups for MR targeting. The synthesis and purification of an acetyl protected mannosylated building block [ser-(Ac4-man)-OH] is the first step followed by inclusion of the pure compound in the mannosylated peptides with FAM. This is followed by synthesis of the lipidated-$OVA_{323-339}$ peptide. This lipidated-$OVA_{323-339}$ peptide and the manosylated peptides are then attached using click chemistry. The final library of mannosylated lipopeptides (vaccine constructs) contains 0, 1 and 2 spacers of alanine between the mannose moieties to study the targeting of these vaccine constructs towards the MR in relation to the structural properties of designed vaccine constructs **(Chapter 3, Figure 3-1)**. A library of control peptides is also prepared to study the effect mannose and/or lipid moieties play in vaccine construct targeting and immunogenicity.

Chapter 4. ***In vitro*** **Evaluation of Mannosylated Lipopeptide Vaccines**

An uptake/binding study is performed on splenocytes isolated from naïve mice (6 weeks old). Cells are stained with anti-CD11c and anti-F4/80 antibodies to investigate the uptake/binding by $F4/80^+$ and $CD11c^+$ subsets of cells. The uptake study is performed on all vaccine constructs. Dextran-FITC is the positive control and PBS is the negative control. A mannan inhibition assay is performed to indicate the proportion of receptor mediated uptake. Vaccine constructs are characterised for their size using DLS to enable size and uptake correlations. Confocal imaging supports the uptake/binding data observed for the vaccine constructs. Further, a SPR study is performed using Biacore technology where CM-5 chips are used to immobilise the human recombinant MR. Here, the affinity of the vaccine constructs to this human recombinant MR is measured. Lastly, the *in vitro* T cell stimulatory activity of the vaccine constructs is measured using flow cytometry in splenocytes isolated from OT-II mice following stimulation with the vaccine constructs.

Chapter 5. In vivo Studies on Mannosylated Lipopeptide Vaccines

Immune properties of the vaccine constructs are measured using purified CD45.2^{+}OT-II cells that have been transferred to C57BL/6 mice. Mice are immunised with the vaccine constructs at 1, 21 and 42 days. Blood specimens for the OT-II proliferation read out are collected and ELISA performed 10 days post each immunisation. To measure cytokine release associated with the vaccine constructs, mice are sacrificed on day 63 after the last immunisation and ICS and CBA assays performed.

Chapter 6. Conclusion and Future Directions

This chapter contributes to the overall findings of the studies presented in this thesis and provides suggestions for future directions of this study.

Chapter 2: Experimental Section

2.1 Synthesis of mannosylated lipopeptides

2.1.1 General Materials and Equipment

All reagents used were of the highest grade available. Diethyl acetamidomalonate 1-bromodecane, dimedone, triethylamine, ethyl acetate (EtOAc), n-hexane, N,N'-diisopropylcarbodiimide (DIC), triisopropylsilane (TIS), 4-dimethylaminopyridine (DMAP), boron trifluoride diethyl etherate ($BF_3.Et_2O$), copper wire, FAM and diethylacetamidomalonate (DAAM) were provided from Sigma-Aldrich (St. Louis, MO, USA). Protected amino acids were purchased from Novabiochem (Laufelfingen, Switzerland) and Mimotopes (Melbourne, Australia). N,N'-dimethylformamide (DMF), TFA, methanol (MeOH), N,N'-diisopropylethylamine (DIPEA), 1-[bis(dimethylamino)methylene]-1H-1,2,3-triazolo[4,5-b] pyridinium 3-oxide hexafluorophosphate (HATU), N,N,N′,N′-tetramethyl-*O*-(1H-benzotriazol-1-yl)uronium hexafluorophosphate O-(benzotriazol-1-yl)-N,N,N′,N′-tetramethyluronium hexafluorophosphate (HBTU), hydroxybenzotriazole (HOBt), piperidine, and dichloromethane (DCM) were obtained from Merck (Hohenbrunn, Germany). Sodium hydrogen carbonate ($NaHCO_3$), magnesium sulfate ($MgSO_4$) and acetic anhydride (Ac_2O) were supplied by Chem-Supply (Gillman, South Australia, Australia). High-pressure liquid chromatography (HPLC)-grade acetonitrile (MeCN) was purchased from RCI Labscan Ltd. (Bangkok, Thailand).

Analytical reverse phase high-performance liquid chromatography (RP-HPLC) was carried out on a Shimadzu instrument with an LC-20AB pump, a SIL-20AHT auto-sampler and an SPD-M10A detector set to a wavelength of 214 nm. Preparative RP-HPLC was carried out on a Shimadzu system equipped with a CBM-20A controller, LC-20AT pump, SIL-10A auto-sampler and SPD-20A UV/Vis detector set to a wavelength of 214 nm and a FRC-10A fraction collector. Both analytical and preparative HPLC were performed using flows of solvent A (0.1% TFA in water) and solvent B (90:10:0.1% MeCN:water:TFA).

NMR studies were performed in $CDCl_3$ (unless otherwise specified) on a Bruker Avance 300 MHz instrument (Bruker Biospin, Germany). Electrospray ionisation mass spectrometry (ESI-MS) was performed on a PE SCIEX AP13000 triple quadrupole mass spectrometer operated with a constant flow of 1:1 mixture of solvent 1 (0.1% acetic acid in water) and solvent 2 (90:10:0.1% MeCN:water:acetic acid) at a rate of 0.5 ml/min. Synthesis of lipopeptides was carried out using a CEM Discovery® microwave (20 W, CEM Corporation, Matthews, NC, USA) with temperature-resistant, open vessels from CEM Corporation (Matthews, NC, USA). In the case of manual synthesis, shaking was performed on a WS/180° shaker (Glas-Col, IN, United States). Size measurements were performed using DLS technology via a Zetasizer Nano ZP instrument (Malvern Instruments, UK).

TEM was performed using a JEM-1010 TEM (JEOL Ltd., Japan). TEM images were analysed using AnalySIS® software (Soft Imaging Systems, Megaview III, Munster, Germany).

2.1.2 *S*ynthesis of mannosylated building block

2.1.5.1 *Synthesis of αβ-$_D$-mannose pentaacetate (1)*

The synthesis of α-$_D$-mannose pentaacetate (**1**, **Chapter 3**, **Section 3.2.1**; **Figure 3-2**) was carried out as per Kowalczyk *et al.* [206]. Briefly, a solution of $_D$-mannose (6.00 g, 33.30 mmol) in Ac_2O (16.00 mL, 169.85 mmol) was refluxed (46°C) under a N_2 atmosphere followed by the addition of a catalytic amount of DMAP (600 mg, 4.91 mmol) after 3 hours. After 24 hours, the solvent was removed *in vacuo*. The residual oil was dissolved in EtOAc (20 mL) and washed with $NaHCO_3$ (saturated) (2 × 10 mL), H_2O (2 × 10 mL) and brine (2 × 10 mL). The organic phase was dried with anhydrous $MgSO_4$, filtered and concentrated *in vacuo* to afford a racemic mixture (α:β) of **1** as a yellow oil (11 mg, 85%). NMR data was as follows:
(1): Yield = 85%. ^{1}HNMR (500 MHz, $CDCl_3$): δ = 2.01 (s, 3H), 2.06 (s, 3H), 2.10 (s, 3H), 2.18 (s, 3H), 2.18 (s, 3H), 3.80-3.89 (dd, 1H), 4.061-4.11 (dd, 1H) and 4.25-4.38 (dd, 1H), 5.19 (d, 1H), 5.36-5.37 (m, 2H), 6.09 (d, 1H).

2.1.5.1 *Synthesis of N-Fmoc-O-(2,3,4,6-tetra-O-acetyl-α,β-$_D$-mannopyranosyl)-L-serine (2)*

The Fmoc-serine mannosylated amino acid, N-Fmoc-*O*-(2,3,4,6-tetra-*O*-acetyl-α,β-$_D$-mannopyranosyl)-L-serine (**2**, **Chapter 3**, **Section 3.2.1**; **Figure 3-2**) was synthesised by first acetylating the mannose hydroxyl groups to form α,β--$_D$-mannose pentaacetate using a previously published method (**1**, **Chapter 2, Section 2.1.2.1**) [206]. This intermediate was then coupled with Fmoc-serine-OH in a BF_3 Lewis acid catalysed reaction to generate N-Fmoc-O-(2,3,4,6-tetra-O-acetyl-α,β-$_D$-mannopyranosyl)-L-serine (**2**) [207]. Compound **2** was purified to a 28% overall yield using preparative RP-HPLC on a C18 column using a gradient of 20-80% over 45 min with a Rt of 23.6 min. NMR and mass spectrometry data was consistent with previously published results :
(**2**): Yield = 42%. ^{1}HNMR (500 MHz, $CDCl_3$): δ 7.75-7.60, 7.40–7.36, 7.32–7.28, (8H, ArH), 6.17 (d, 1H, *O*-ester), 5.77 (d, 1H, NH), 5.37 (t, H4), 5.32 (bs, H2), 5.26 (dd, 1H), 4.58 (bd, 1H, CH), 4.25 (complex, H6), 4.17 (bd, 1H, CH), 4.13 (bd, 2H, H5, H6), 3.98 (bd, 1H), 2.19, 2.10, 2.03, 2.01 (4s, 12H, $4CH_3$); ESI-MS *m/z*: exact mass: $[M+H]^+$ calc. 657.62 found 658.4, $[M+2H]^{2+}$ calc. 329.81 found 331.4

2.1.3 General method for glycosylated solid phase peptide synthesis

2.1.5.1 *Resin loading*

Fmoc SPPS was assisted using a manual shaker on a Rink amide MBHA resin. Resin was swollen in DMF overnight before use.

2.1.5.1 *Fmoc-deprotection*

Each Fmoc-deprotection consisted of resin treatment with 20% piperidine in DMF followed by extensive DMF washing For microwave synthesis (2 x 5 min, 50°C, 20W), and for manual synthesis (2 × 30 min at room temperature [RT]), deprotection cycles with piperidine (20%) followed by DMF washing were performed.

2.1.5.1 *1-(4,4-dimethyl-2,6-dioxo-cyclohexylidene)-3-methyl-butyl (IvDde) deprotection*

The IvDde protecting group was removed manually by treatment of the resin with a 2% hydrazine in DMF solution (12 × 15 min) followed by extensive washing with DMF.

2.1.5.1 *Amino acid coupling*

For manual synthesis, N-Fmoc-protected amino acids (4.2 eq.) were pre-activated with HATU (4 eq.) and DIPEA (5 eq.) for 5 min and coupled to the resin twice for at least 30 min. Lipoamino acids (4.2 eq.) were prepared by dissolving them in HATU (4.0 eq.) and DMF solution followed by addition of DIPEA (6.2 eq.) and double coupling to the resin for 30 min.

2.1.5.1 *5(6)-Carboxyfluorescein (FAM) coupling*

FAM (1.5 eq.) was coupled to the resin manually using HOBt (2.5 eq.) and DIC (2.5 eq.) in DMF in the dark overnight. Removal of the unwanted FAM ester-bond was achieved by treating the resin with 20% piperidine (6 × 5 min or until no more yellow colour was observed in the DMF washes) followed by extensive washing with DMF [208].

2.1.5.1 *Resin Cleavage*

At the completion of peptide synthesis and when the terminal Fmoc group had been removed, the resin was washed with DMF, MeOH, and DCM, and dried *in vacuo* overnight. The crude peptides were cleaved from the resin with 95% TFA, 2.5% TIS and 2.5% water for 3 h at RT. All cleaved peptides were precipitated, filtered and washed thoroughly with ice-cold diethyl ether. The

precipitated compounds were dissolved in MeCN:water (1:1) that contained 0.1% TFA and lyophilised overnight to give amorphous powders.

2.1.4 General methods for the synthesis and characterisation of mannosylated and un-mannosylated azido peptides (3-7)

2.1.4.1 Synthesis of mannosylated peptide 3

For the synthesis of **3**, manual Fmoc SPPS as described in **Method 1** in **Chapter 3**, **Section 3.2.2.1** was employed. Briefly, Fmoc amino acids were coupled to the resin following activation with HATU (4.0 eq.) and DIPEA (6.2 eq.) in DMF. The Fmoc-Lys-OH side chain was protected with IvDde. 2,3,4,6-Tetra-*O*-acetyl-α,β-$_D$-mannopyranosyl (**2**, 1.5 eq.) building blocks were coupled manually using HATU (1.5 eq.) and DIPEA (4.5 eq.) in DMF for 12 h followed by washing with DMF (3 × 5 min). A subsequent coupling was performed when the ninhydrin testing indicated it was required [209]. FAM (1.5 eq.) was coupled to the resin using HOBt (2.5 eq.) and DIC (2.5 eq.) in DMF overnight. Removal of the unwanted FAM ester-bond was achieved by treating the resin with 20% piperidine (6 × 5 min) followed by extensive washing with DMF [208]. The resin was then treated with 5% hydrazine in DMF on resin (3 × 30 min) to deprotect the lysine side chain protecting group, ivDde. This was followed by coupling of azidoacetic acid (4.2 eq.) which was synthesised according to a previously published method [210] using HATU (4.0 eq.) and DIPEA (6.2 eq.) in DMF overnight. Cleavage (as detailed in **Chapter 2**, **Section 2.1.3.6**) of the crude peptides was achieved by dissolving the crude products in solvent B that were then purified by preparative RP-HPLC on a C8 column with a gradient of 30% to 80% solvent B over 45 min. Due to complications as outlined in **Chapter 3**, **Section 3.2.2.1**, a low yield was obtained.

2.1.5.1 *Synthesis of mannosylated peptides 4-7*

For the synthesis of vaccine constructs **4-7** (**Chapter 3**, **Section 3.2.2.2**, **Figure 3-7**), manual Fmoc SPPS as described in **Method 2** in **Chapter 3**, **Section 3.2.2.2** was employed. Here, peptides were assembled on Rink amide MBHA resin (0.1 mmol scale) using the *in situ* neutralisation protocol for Fmoc SPPS [211]. After loading the resin with Fmoc-lys(Mtt)-OH, the 4-methyltrityl group (Mtt) was deprotected using TFA:TIS:DCM (1:2:97) using 20 cycles (5 min/cycle) and the resin was washed well with DCM after each the cycle. Following Mtt deprotection, azidoacetic acid (4.2 eq.) was coupled using DIPEA (6.2 eq.) in DMF overnight. **2** (1.5 eq.) was coupled (×2) to the resin using HATU (1.5 eq.) and DIPEA (4.5 eq.) in DMF for 12 h followed by washing with DMF (3 × 5 min). A subsequent coupling was performed when ninhydrin testing indicated it was required. FAM

coupling (**Section 2.1.3.5**) and resin cleavage (**Section 2.1.3.6**) were performed. Yield and ESI-MS results are described in **Chapter 1**, **Section 3.2.2.2**, **Table 3-2**.

2.1.5 Lipopeptide Synthesis

2.1.5.1 *Synthesis of 2-acetyldimedone (Dde-OH) (8)*

Synthesis of 2-acetyldimedone (Dde-OH, **8**) was carried out as per Ross *et al.* [212]. Briefly, dimedone (15 g, 107 mmol) was dissolved in DCM (100 ml). DMAP (2.61 g, 21 mmol) and triethylamine (30 ml, 215 mmol) were added and the mixture was stirred for 10 min at RT. Ac_2O (9.38 ml, 1.6 mmol) was added to the mixture and the reaction was stirred for 2 days under a N_2 atmosphere. Ac_2O was removed in *high vacuo* and the crude product was dissolved in EtOAc and washed with 5% HCl (3 × 300 ml). The organic phase was combined and dried over $MgSO_4$ and the solvent was removed *in vacuo*. The resulting crude oil was purified using a silica column and n-hexane:EtOAc (3:2) as eluent to afford the title compound (**8**) with the following yield and NMR:
(**8**): Yield = 84%. ^{1}H NMR (300 MHz, $CDCl_3$): 1.08 (6H, s, $C(CH_3)_2$), 2.36 (2H, s, H-5a, H-9a), 2.54 (2H, s, H-5b, H-9b), 2.61 (3H, s, CH_3).

2.1.5.2 *Synthesis of [(4,4-Dimethyl-2,6-dioxocyclohex-1-ylidene)ethylamino]-D,L-dodecanoic Acid: (C12) (9)*

The synthesis of 4,4-dimethyl-2,6-dioxocyclohex-1-ylidene)ethylamino]-D,L-dodecanoic acid (C12, **9)** was carried out as per Ross *et al*. [212]. Briefly, to a dry round-bottomed flask containing sodium ethoxide (6.8 g, 100 mmol), DAAM (21.3 g, 100 mmol) was added followed by addition of 1-bromodecane (41.7 ml, 140 mmol). The reaction mixture was refluxed for 24 h under an atmosphere of N_2 gas. The reaction was stopped by removing the mixture from the reflux heat, cooling to RT and pouring into crushed ice to precipitate the aminodiester product (**9**, **Chapter 3**, **Section 3.2.3.1**, **Figure 3-8**). The product was collected using a Buchner funnel and dried in a desiccator overnight. DMF (14 ml) and fuming HCl (120 ml of 37%) were added to the dried product and refluxed for 3 days. The reaction was stopped by removing the heat. The mixture was cooled to RT, then poured into crushed ice to precipitate the product. The product was collected using a Buchner funnel and dried overnight in a desiccator to yield the final product (**9**) with the following yield and NMR:
(**9**): Yield = 42%. ^{1}H NMR (500 MHz, CDCl3) d 13.70 (1H, d, H-bonded NH), 11.74 (1H, br s, COOH), 4.37 (1H, m, a-CH), 2.52 [3H, s, C(NH)CH3], 2.39 (4H, s, 2CH2CO), 2.02-1.87 (2H, m, b-CH2), 1.43-1.23 (16H, m, 8CH2), 1.01 [6H, s, C(CH3)2], 0.85 (3H, t, CH3)

2.1.5.3 *Synthesis of 2-(4, 4-Dimethyl-2, 6-Dioxocyclohex-1-ylidene) ethylaminododecanoic acid (Dde-C12-OH) (10)*

The synthesis of 2-(4, 4-dimethyl-2, 6-dioxocyclohex-1-ylidene) ethylaminododecanoic acid (Dde-C12-OH, **10**) was performed as per Ross *et al.* [212]. Briefly, **8** (9.76 g, 53.6 mmol) was dissolved in ethanol to which **9** (12.3 g, 48.7 mmol) and TEA (7.44 ml, 53.4 mmol) was added. The mixture was refluxed under an atmosphere of N_2 for 2 days with TLC monitoring (EtOAc: n-hexane, 20:30) where the product had an Rf of 0.9. The solvent was removed using co-evaporation with EtOAc *in vacuo*. The resultant crude product was dissolved in EtOAc and washed with 5% HCl (3 × 200 ml). The combined organic phase was dried over $MgSO_4$ and the solvent was removed *in vacuo*. The product was triturated twice with diethyl ether to afford the pure product as a white solid with the following yield and NMR:

(**10**): Yield = 30%. ^{1}H NMR (500 MHz, $CDCl_3$): 0.86 (3H, t, CH3), 1.05 (6H, s, $C(CH_3)2$), 1.43-1.23 (16H, m, $8CH_2$), 2.02-1.87 (2H, m, CH_2), 2.42 (4H, s, $2CH_2CO$), 2.55 (3H, s, $C(NH)CH_3$), 4.38 (1H, m, CH).

2.1.6 Synthesis and characterisation of $OVA_{323-339}$ lipopeptide (11) and peptide alkynes (12)

2.1.6.1 *Resin loading for microwave synthesis*

Fmoc SPPS was assisted by a CEM Discovery microwave peptide synthesiser on Rink amide MBHA resin. The resin was swollen in DMF overnight before use.

2.1.6.2 *Fmoc-deprotection for microwave synthesis*

Each Fmoc-deprotection consisted of resin treatment with 20% piperidine in DMF (2 x 5 min, 50°C, 20W) followed by extensive washing with DMF.

2.1.6.3 *1-(4,4-dimethyl-2,6-dioxyacyclohexylidene)ethyl (Dde) deprotection*

The Dde protecting group was removed manually by treatment of the resin with 2% hydrazine in DMF solution (12 × 15 min) followed by extensive DMF washing.

2.1.6.4 *Amino acid coupling for microwave synthesis*

N-Fmoc-protected amino acids (4.2 eq.) were pre-activated with HATU (4 eq.) and DIPEA (5 eq.) for 5 min and coupled to the resin (2 x 5 min, 70°C, 20W). The coupling of Fmoc-Arg(pbf)-OH was

carried out at 25°C for 10 min and 50°C for 10 min, respectively. For the peptide dendrimers, the quantities of amino acids and coupling agents were used in ratios relative to the number of branches. Lipopeptide **11** (**Chapter 3**, **Section 3.2.3**, **Figure 3-9**) was synthesised using microwave-assisted Fmoc SPPS on Rink Amide resin (0.2 mmol) using an *in situ* neutralisation protocol [211]. Synthesis of **8** was achieved as per Gibbons *et al.* [213] and **9** and **10** were synthesised as described by Ross *et al.* [212]. Branching of peptide **11** was achieved using Fmoc-lys(Fmoc)-OH followed by the consecutive addition of the $OVA_{323-339}$ epitope by sequential coupling of Fmoc-Arg(Pbf)-OH, Fmoc-Gly-OH, Fmoc-Ala-OH, Fmoc-Glu(OtBu)-OH, Fmoc-Asn(Trt)-OH, Fmoc-Ile-OH, Fmoc-Glu(OtBu)-OH, Fmoc-Ala-OH, Fmoc-His(Trt)-OH, Fmoc-Ala-OH×2, Fmoc-His(Trt)-OH, Fmoc-Val-OH, Fmoc-Ala-OH, Fmoc-Gln(Trt)-OH, Fmoc-Ser(tBu)-OH, and Boc-Ile-OH. Removal of ivDde was performed on-resin (**Chapter 3, 3.2.3**) followed by addition of pentynoic acid (4.2 eq.) which was coupled overnight to the resin using HBTU (4 eq.) and DIPEA (6.2 eq.). Following cleavage (detailed in **Section 2.1.3.6**), the crude lipopeptide was purified by preparative RP-HPLC with a 20% to 80% gradient of solvent B over 45 min generating **11** as a fluffy white solid. Synthesis of **12** (**Chapter 3**, **Section 3.2.3.2**, **Figure 3-9**) was achieved using a similar method to **11**; however, lipids were omitted from the synthesis generating **12** as a fluffy white solid. Yields and ESI-MS data for **11** and **12** are shown in **Chapter 3**, **Section 3.2.3**, **Table 3-3**.

2.1.8 Copper-mediated azide-alkyne cycloaddition (13-18)

Fluorescently-labelled mannosylated lipopeptide vaccine constructs (**13-18**, **Chapter 3, Section 3.2.4**, **Figure 3-10**) were prepared using copper-wire mediated click chemistry [214]. Briefly, purified fluorescently-labelled mannosylated-peptide-azides **4-6** (1.16 µmol, **Section 3.2.2**) were dissolved in separate vials that contained a solution of lipopeptide-alkyne **11** (1.1 µmol, **Section 3.2.3**) in DMSO (500 µL). Copper wires (60 mg) were added and the reaction was protected from light with aluminium foil and stirred under an atmosphere of N_2 gas for 5 h at 45°C. The reaction was monitored by analytical RP-HPLC (20% to 80% gradient of solvent B over 45 min, C8 column). Upon completion of the reaction, copper wires were removed by filtration, washed with DMSO (1 ml), and the reaction was quenched by addition of Millipore water (2 ml). Crude products were purified by preparative RP-HPLC (20% to 80% gradient over 45 min, C8 column) and lyophilised to afford pure vaccine constructs **13-15** as pale yellow solids. Characterisation was achieved by ESI-MS (**Chapter 3, Section 3.2.4, Table 3-4**). Vaccine constructs **16-18** were synthesised by coupling **7** to **11**, **6** to **12**, and **7** to **12**, respectively using the same method as described in **Chapter 3, Section 3.2.4**.

2.1.8 Size characterisation

2.1.8.1 *Dynamic light scattering (DLS)*

The size of the particles formed by vaccine constructs **13-18** was measured in PBS (pH 7.4) using a non-invasive backscatter technique using a DLS instrument with DLS software. The measurement was performed in triplicate at 25°C in disposable cuvettes with a scattering angle of 173°.

2.1.8.2 *Transmission electron microscopy (TEM)*

TEM was operated at 100 kV. Vaccine constructs **13-18** were dissolved in PBS (0.5 µM, pH 7.4) and allowed to equilibrate at 25°C for at least 12 h, and used within 20 h. They were dropcast onto the 200 mesh carbon-coated grids for 2 min, excess liquid was soaked away using filter paper and the dried samples were imaged within 24 h.

2.2 *In vitro* evaluation of mannosylated lipopeptide vaccines

2.2.1 General Materials and Equipment

Phenol free IMDM Glutamax medium, 2-mercaptoethanol and streptomycin was purchased from Gibco® (Life Technologies, VIC, Australia). Anti-mouse CD11c Alexa Fluor® 700, FITC anti-mouse CD4, PE anti-mouse T cell receptor Vα2 and APC/Cy7 anti-mouse F4/80 antibody were purchased from (Biolegend, Pacific Heights Blvd, San Diego, CA, USA). 1-Ethyl-3-(3-dimethylaminopropyl)carbodiimide (EDC), N-hydroxysuccinimide (NHS), ethanolamine, 2-[4-(2-hydroxyethyl)piperazin-1-yl]ethanesulfonic acid (HEPES), and $CaCl_2$, were purchased from Sigma-Aldrich (NSW, Australia). Eri-lysis buffer and FACS buffer (PBS, 0.02% sodium azide, 0.5% BSA) were purchased from BD Biosciences (North Ryde, NSW, Australia). LSR II flow cytometer (BD Biosciences, San Jose, CA, USA) was used for *in vitro* uptake studies. 8-Well polylysine-treated µ-slides (ibidi GmbH, Germany) were used for confocal microscopy (GE DeltaVision Deconvolution microscope). Biacore experimentation was performed using Biacore 3000 instrumentation (BIAcore, GE Healthcare, NSW, Australia) on a CM-5 chip provided from GE Healthcare-Australia (Silverwater, NSW, Australia). Glycine, $MgCl_2$ and NaCl were obtained from Chem-Supply (Gillman, South Australia). Surfactant P20 was obtained from GE Healthcare-Australia (Silverwater, NSW, Australia). The recombinant human macrophage mannose receptor (catalogue number 2534-MR/CF) was purchased from In Vitro Technologies Pty. Ltd. (Brisbane, QLD, Australia).

2.2.2 *In vitro* uptake

Single-cell suspensions of splenocytes isolated from mice were prepared by passing the spleen through a 40 µm cell strainer [215]. Erythrocytes were then lysed with erylysis buffer. The remaining cell population was re-suspended in complete phenol free IMDM Glutamax medium, supplemented with 10% foetal bovine serum, 50 µM 2-mercaptoethanol, 100 U/ml penicillin, and 100 µg/ml streptomycin and added to sterile 12-well plates at a density of 2×10^5 cells per well. After 4 h incubation, cells were treated with vaccine constructs **13-18** at a concentration of 0.5 µM. After 24 h at 37°C in a humidified atmosphere of 5% CO_2 and 95% air, the adherent cells were scraped from the plate, centrifuged and resuspended in PBS buffer that contained anti-CD11c (0.125µg/100µl) and anti-F4/80 (25µg/100µl) antibodies for 30 min at 4ºC [215]. The cells were centrifuged and resuspended in FACS buffer (0.5 mL) and analysed using a LSR II flow cytometer [215]. To investigate receptor-mediated uptake, a mannan competition assay was performed [216]. Following isolation, plating and 4 h incubation of the cells (as described previously), cells were treated with mannan (1 mg/ml) 1 h prior to incubation with the vaccine constructs (**13-18**, 0.5 µM). Cell washing, processing and antibody staining was performed as stated previously. Data are presented as mean ± standard deviation for triplicate samples. Differences between vaccine groups were determined using a one-way analysis of variance (ANOVA) followed by a Tukey test and were considered statistically significant if the P value was <0.0001.

2.2.3 Confocal Imaging

Splenocytes were isolated as per **Section 2.2.2**. Cells were re-suspended in IMDM media with 5% foetal bovine serum in sterile plates at a density of 2×10^5 cells per well. Cells were treated with vaccine constructs **13-18** at concentrations of 0.5 µM in a humidified atmosphere of 5% CO_2 and 95% air for 4 h, at 37°C. IMDM was then removed and adhered cells were stained with anti-F4/80 antibody (25µg/100µl) and Hoechst (1 µg/100µl) stain, incubated for 30 min, and washed with IMDM (300 µl). Cells were observed with a GE DeltaVision Deconvolution microscope using band-pass filters 505 ± 36 nm, 531 ± 40 nm and 411 ± 48 nm to detect green, red and blue fluorescence, respectively. Receptor-mediated uptake was investigated by treating cells with mannan (1 mg/ml) at 37°C in a humidified atmosphere of 5% CO_2 and 95% air 1 h prior to incubation with vaccine constructs **13-18** at a concentration of 0.5 µM. Cell washing, processing, and antibody staining was performed as per **Section 2.2.2**.

2.2.4 *In vitro* OT-II Proliferation assay

A single cell suspension of OT-II mice splenocytes was prepared by passing the spleen through a 40 µm cell strainer, erythrocytes were lysed using erylysis buffer, and after centrifuging (600 g for 4 min at -4°C) the remaining cell populations were re-suspended in complete phenol free IMDM Glutamax medium containing supplements and antibiotics, as described in **Section 2.2.2**. Cells were plated in sterile 96-well plates at a density of 5×10^5 cells per well and incubated at 37°C in a humidified atmosphere of 5% CO_2 and 95% air with serial dilutions (5, 1.7, 0.5, 0.18, 0.06, and 0.02 µM) of vaccine constructs (**13-18,** dissolved in PBS) in triplicate. After 72 h, the cells were stained with anti-mouse CD4and anti-mouse T cell receptor Vα2 antibodies. The cells were centrifuged (600 g for 4 min at -4°C) and resuspended in FACS buffer (0.5 mL). The results were read on a LSR II flow cytometer.

2.2.5 Real-time surface plasmon resonance (SPR)

Step 1: Immobilisation: The recombinant human macrophage MR was immobilised on a CM-5 research grade sensor chip using amine coupling chemistry according to the Biacore manufacturer's instructions (**Chapter 4**, **Section 4.5.1.1**). In a typical procedure, activation of the chip's surface was achieved using EDC (400 mM) and NHS (100 mM) in a 1:1 ratio at a flow rate of 20 µl/min for 8 min. The MR was dissolved in sodium acetate buffer (10 mM sodium acetate in water, pH 4.4) at a concentration of 50 µg/ml and immobilised at 20 µl/min for 7 min to reach a final response unit (RU) of 20,000. The remaining reactive groups were blocked using ethanolamine (1 M, pH 8.5) at a flow rate of 20 µl/min for 7 min.

Step 2: Surface performance and regeneration scouting: A surface performance test was performed to test the viability of the immobilised receptor using mannan (10 µg/ml) as per **Chapter 4**, **Section 4.5.1.2**. To revive the MR from the bound mannan following regeneration buffers; sodium dodecyl sulphate (SDS) 0.05%, NaOH 10 mM (pH: 9.5) and glycine 10mM (pH: 2.2) were used to check their regeneration ability. As described in **Chapter 4**, **Section 4.5.1.2**; glycine (10 mM, pH 2.2) was chosen for the regeneration of MR following exposure of the chip to vaccine constructs **13-18**.

Step 3: Binding affinity measurement: Vaccine constructs **13-18** (50 µM to 0.78 µM) were dissolved in running buffer (10 mM HEPES, 1 mM $CaCl_2$, 1 mM $MgCl_2$, 150 mM NaCl, 0.005% P20 in water, pH 7.4) to reach the optimum concentration. Kinetic cycle analysis was performed using mannan (18.75-600 µg/ml) dissolved in running buffer and was used as a positive control (**Chapter 4**, **Section 4.5.1.3**). Each running cycle consisted of 3 steps: i) injection of the vaccine construct (or mannan) for

1.5 min at 40 µl/min, ii) an 8 min dissociation step at 40 µl/min with running buffer, and iii) injection of the regeneration buffer (10 mM glycine, pH: 2.2) for 5 min at 40 µl/min. One control flow cell, used as a blank sensogram for subtraction of the bulk refractive index, was also activated by EDC-NHS and then blocked using ethanolamine (as described in **Chapter 4**, **Section 4.2.4.1.1**). All solutions were filtered using polytetrafluoroethylene membrane syringe filters (0.22 µm) and degassed prior to use. For binding studies, the temperature was kept at 25°C. The immobilised MR performance was analysed after each regeneration step using a surface performance test with mannan (30 µg/ml) to verify that the surface was still active.

The K_D (an affinity constant, used to measure the strength of binding of a single molecule to its ligand) was calculated using the binding response level at equilibrium (R_{eq}) for each vaccine construct (analyte) as outlined by Burkhard and Shapiro using Equation 1 (Eq. 1) [217]. Here, K_A is the association constant, C is the analyte concentration (µM), R_{max} is the response at saturation, and n is the number of binding sites determined by the type of fitting chosen. The steady state response level was chosen to show the validity of the results using BIAevaluation 4.1 software. Analysis of replicate experiments allowed the data to be analysed using a one-site binding model [217, 218].

$$R_{eq} = \frac{K_A C R_{max}}{1 + K_A C_n} \qquad \text{(Eq. 1)}$$

2.3 *In vivo* studies on mannosylated lipopeptide vaccines

2.3.1 General Materials and Equipment

Pathogen free C57BL/6 (Animal Resources Centre, Perth, Australia) and OT-II (Walter and Eliza Hall Institute of Medical Research, Melbourne, Australia) mice were bred at QIMR Berghofer and used at 5-6 weeks of age. All animal studies were approved by the QIMR Berghofer's Animal Ethics Committee. All methods were followed from previously set protocols used in Professor Doolan's laboratory at the QIMR Berghofer Institute [219]. Cell culture media (consisting of 10% foetal calf serum [FCS], 2-Mercaptoethanol, glutamin, knockout Dulbecco's-modified Eagle's media [KDMEM]), magnetic cell sorting buffer (MACS; consisting of phosphate buffer saline, 2% fetal calf serum) and the OVA protein and $OVA_{323-339}$ peptide were also provided by Professor Doolan's laboratory at the QIMR Berghofer Institute.

Antibodies used for in vivo OT-II cell proliferation assay: Vβ Biotin (T cell receptor, MR9-4),α-CD4 BV510 (OT-II) and red cell lysis buffer were obtained from Biolegend (San Jose, CA, USA). CD45.2 PE, CD45.1 FITC (anti-mouse), α-Vα2 APC, α-CD8 APC/CY7 (anti-mouse) and Strepavidin PerCP/Cy5.5 were purchased from Biolegend (San Diego, CA). $CD4^+$ (L3T4) microbeads were

obtained from Miltenyi Biotec (Bergisch Gladbach, Germany). FACSCalibur was used with CellQuest version 3.1f software (BD Biosciences, San Jose, CA, USA). Flo Jo analysis of data was performed post run by V9.1 (Treestar, Ashland, OR, USA). Flow Check® microbeads were purchased from Polysciences Inc. (Warrington, PA, USA).

Intra Cellular Staining (ICS): Phorbol 12-myristate 13-acetate (PMA) and ionomycin was obtained from Sigma-Aldrich (NSW, Australia), Golgiplug™ and TNFα (rat α-mouse TNFα FITC) from BD Biosciences (NSW, Australia). IFNγ (rat α-mouse IFNγ APC), IL-2 (rat α-mouse IL-2 PE) were obtained from Biolegend (San Diego, CA, USA). A LSR II flow cytometer from BD Biosciences (NSW, Australia) was used in this study.

Cytokine Bead Array (CBA): A CBA mouse Th1/Th2/Th17 cytokine kit was obtained from BD Biosciences (NSW, Australia). The CBA assay was performed on a FACSarray cytometer equipped with the CellQuest Pro and CBA software (BD Biosciences).

Enzyme-Linked Immunosorbent Assay (ELISA): NUNC maxisorp 96-well plates were purchased from eBioscience (San Diego, CA, USA), biotinylated donkey anti-mouse IgG was purchased from Life Technologies (VIC, Australia), tetramethylbenzidine (TMB), stop reagent and Tween 20 were obtained from Sigma Aldrich (NSW, Australia), and strepavidine-peridinin chlorophyll was from BD Pharmingen (NSW, Australia). The VERSAmax micro plate reader was from Molecular Devices (CA, USA).

2.3.2 OT-II cells cell preparation process, adoptive transfer

Five OT-II female mice were sacrificed and CD4 splenocytes and lymphocytes were purified using $CD4^+$ (L3T4) microbeads. CD4 purified cells were stained with α-CD4 (OT-II) FITC (1:200) and α-Va2 PE (1:200) using $CD4^+$ (L3T4) microbeads and the purity was checked using a FACSCalibur. The relative number of live cells was normalised by a count of Flow Check® microbeads (Polysciences Inc., Warrington, PA, USA) as described previously [220]. Cells were then diluted in PBS (9 mL) and prepared for injection. Each mouse (C57BL/6) received 200 µL of suspended cells (0.5×10^6 cells) by intravenous (I.V.) injection at the tail base.

2.3.3 Vaccination with vaccine constructs

Vaccine groups **G1-8** were dissolved in PBS (30 µg/100µl) and injected subcutaneously (S.C.) after the adaptive transfer of OT-II cells. Here, a control PBS group (**G9**) was used as the negative control. Immunisation was repeated 2 more times at 14 day intervals as per **Chapter 5.2.1, Figure 5-3**.

2.3.4 OT-II proliferation activation assay

Blood samples (5 µl) were taken from the tip of the tail two weeks after each immunisation. Samples were centrifuged and stained with a cocktail of antibodies (Table 2-1). Cells were washed and lysis buffer was added followed by storing for 10 min at 37°C. Cells were then washed with 2% media (containing 2% FCS) and then resuspended in MACS buffer (100 µl) and analysed using a flow cytometer (FACS BD LSRFortessa™). Single stained cells were used to set the compensation level for the results. Results shown in **Chapter 5**, **Section 5.2.1**, **Figure 5-4**.

Table 2-1. Antibodies used for the CD4 proliferation assay

Marker	Fluorescent	Dilution
CD8	APC-Cy7	1:400
CD4	BV510	1:1000
CD45.1	FITC	1:200
CD45.2	PE	1:200
CD44	PE/Cy7	1:800
CD62L	BV605	1:800

2.3.5 Preparing cells for intracellular staining and the cytokine bead array

Vaccinated mice (**G1-9**, **Chapter 5**, **Section 5.1**, **Figure 5-2**) were sacrificed and the spleens were removed. Spleens were strained through a 100 µm plastic mesh and cells were suspended in 10 ml of 2% media (contained 2% FCS) and centrifuged (600 g, 4 min at -4°C). The supernatant was removed and the cells were resuspended in lysis buffer (5 ml). After 5 min, 2% media was added, the cells were centrifuged (600 g, 4 min at -4°C) and following removal of the supernatant, 10% media (10 mL) was added to resuspend the cells for a total count per well of 5×10^5. The cells were counted using FACS BD LSRFortessa™.

2.3.6 Intra-cellular staining (ICS)

Splenocytes from a single cell preparation (5×10^5) of spleens, isolated from sacrificed mice 11 days post immunisation (day 63), were added to the wells of 96-well plates (5×10^5) and incubated in the presence of GolgiPlug (1 µl/ml), and in the presence or absence of the $OVA_{323-339}$ peptide (10 µg/ml). Pre-mixed PMA (5 ng/ml) and ionomycin (500 ng/ml) were used as the positive control. After 3 days incubation (37°C and 5% CO_2), cells were stained for IFN-γ (rat α-mouse IFNγ APC. 0.2 mg/ml), IL-2 (rat α-mouse IL-2 PE, 0.2 mg/ml) and TNFα (rat α-mouse TNFα FITC, 0.5 ml/ml). The total number of IFN-γ, IL-2 and TNF positive CD4 and CD8 cells was determined using a LSR II flow cytometer and by subtracting the unstimulated controls from the peptide stimulated cells. Results are shown in **Chapter 5**, **Section 5.2.2.1**, **Figure 5-7**.

2.3.7 Cytokine bead array (CBA)

Cytokine measurements were performed using the supernatant of single suspensions of splenocytes using the Th1/Th2 kit (BD 560485) according to the manufacturer's guidelines (BD Biosciences). Cytokines (IL-2, IL-4, IL-5, IL-6, IL-10, IL-12p70, IL-13) were measured in the supernatant of antigen-stimulated (OVA protein) splenocytes, unstimulated splenocytes (experimental negative control) and splenocytes stimulated with Con A (experimental positive control). Analysis was performed by a FACSarray cytometer equipped with CellQuest Pro and CBA software and the results are shown in **Chapter 5**, **Section 5.2.2.2**, **Table 5-2**.

2.3.8 ELISA

Blood samples (200 µl) were collected from individual mice (**G1-9**) 1 week post immunisation. Sera IgG was measured for both pooled and individual mice. 96-Well NUNC maxisorp plates were coated overnight at 4°C with the OVA protein (10 µg/ml, 50 µl) dissolved in bicarbonate coating buffer (0.05 M Na_2CO_3, pH 9.6). The wells were then blocked with 5% skim milk powder in PBS (100 µl/well) for 1 h at 37°C. This step was performed to prevent non-specific binding. The plates were then washed with 0.05% Tween 20 in PBS (PBST) and the sera dilutions were added to the wells followed by 1 h incubation at 37°C. The plates were washed 3 times with 0.02% Tween in PBS. Biotinylated donkey anti-mouse IgG (8 µl) diluted in 100 µl PBS was added to each well and incubated for 1 h at 37°C. The plates were washed 4 times with PBST (0.02%). Streptavidin-horseradish peroxidase (HRP) (160 µl) was added to each well, incubated for 1 h, and the plates were washed with PBST (0.02%). Plates were developed by adding RT tetramethylbenzidine (TMB, 50

µl/well), incubating for 10 min followed by addition of RT TMB stop reagent (50 µl/well). The optical density (OD) was measured at 405 nm using a micro plate reader.

2.4 Data analysis and statistics

Data were analysed using Prism v5.0a software (GraphPad, La Jolla, CA, USA). Statistical analysis was carried out using an unpaired Student's t-test (nonparametric, Mann-Whitney), or by ANOVA followed by a Tukey post-test where indicated. Differences were considered to be significant when $P<0.05$ otherwise P was reported.

Chapter 3: Synthesis of Mannosylated Lipopeptides

3.1 Introduction

Therapeutic peptides must overcome biological barriers to achieve cellular targeting. These barriers include chemical stability, stability against enzymatic degradation, reduced toxicity, and improved specificity. To achieve this, modification of peptide epitopes are inevitable procedures essential for vaccine development [153]. Despite the many attempts to design peptide-based vaccines for a variety of diseases, many of these vaccines have fallen short due to the lack of peptide stability, targeting ability or low immune-stimulation. However, such problems can be overcome by the addition of structural and immunological active components to the vaccine design.

For instance, the lipidation of peptides is an effective method for increasing the immune-stimulatory properties of a peptide-based vaccine [164, 221]. Additionally, glycosylation has also been shown to increase the specificity of vaccine candidates towards the desired cellular target, making a combination of lipidation and glycosylation potentially effective vaccine attributes in a targeted vaccine design strategy [222]. To produce a well-characterised peptide subunit, vaccineSPPS is a commonly used synthesis method. Here, SPPS has advantages over solution synthesis methods, including the production of a highly pure, high yielding and relatively (cost) inexpensive vaccine. SPPS methodology can be applied for the production of both linear or branched peptide dendrimers [142]. In this study, lysine will serve as the branching moiety enabling incorporation of lipids, peptide epitopes and glycosyl moieties (mannose) into a single peptide vaccine construct [15,16]. The lipoamino acid attached to the OVA peptide is designed to function as the lipidic self-adjuvanting moiety [223].

This chapter details the synthesis of linear *O*-linked mannosylated lipopeptides (Figure 3-1). Here, functionalisation of the serine side chain with mannose using solution synthesis enabled the step-wise addition of an *O*-mannosylated building block using SPPS techniques. Research has shown that *O*-linked glycoproteins, where the glycosyl moiety is attached through a serine or threonine, are the most common glycoproteins found in nature [100] and are commonly isolated from the cell walls of yeast and bacteria [16, 224]. In this study, this *O*-mannosylated serine amino acid was used to target the C-type lectins on APCs. Here, functionalisation of the serine side chain with mannose enabled the step-wise addition of an *O*-mannosylated building block during SPPS. Fully protected mannose-serine building blocks were used in peptide synthesis to help the stability of sugar in the process of peptide synthesis and also to increase sugar solubility in organic solvents which are used in SPPS [225]. For this purpose, hydroxyl groups on the mannose moiety were protected in a method with a good yield and then were coupled to serine. The mannosylated amino acid has been shown to successfully generate high-yielding peptides in Fmoc SPSS [207].

In this study, the $OVA_{323-339}$ peptide epitope was included in the peptide vaccine structure as a model antigen with the prospect of CD4 T cell activation. Here, recombinant OVA *O*-mannosylation has been shown to be effective in MR targeting [190]. However, in a previous study, the $OVA_{323-339}$ epitope produced a Th1 response in mice but its immunogenicity was limited compared to the full OVA protein [189] confirming the need for an adjuvant system for small proteins or peptide epitopes as vaccine candidates.

The final library of vaccine constructs (**Figure 3-1**) was designed to contain different length spacers (0, 1, 2 alanine units) between the two mannose moieties to gain information about the relative spatial requirements of the sugars on their uptake by APCs (**Chapter 1, Section 1.4, Figure 1-5**). An increase and/or decrease of space between each mannosyl moiety was postulated to play a role in the binding of these vaccine constructs to the MR, and give an increased understanding on the binding requirements. A fluorescent tag (FAM) was included in the vaccine structures to enable detection in *in vitro* cell studies. For more information on the selection and role of each moiety included in the vaccine constructs, please refer to **Chapter 1**, **Sections 1.7-1.8**.

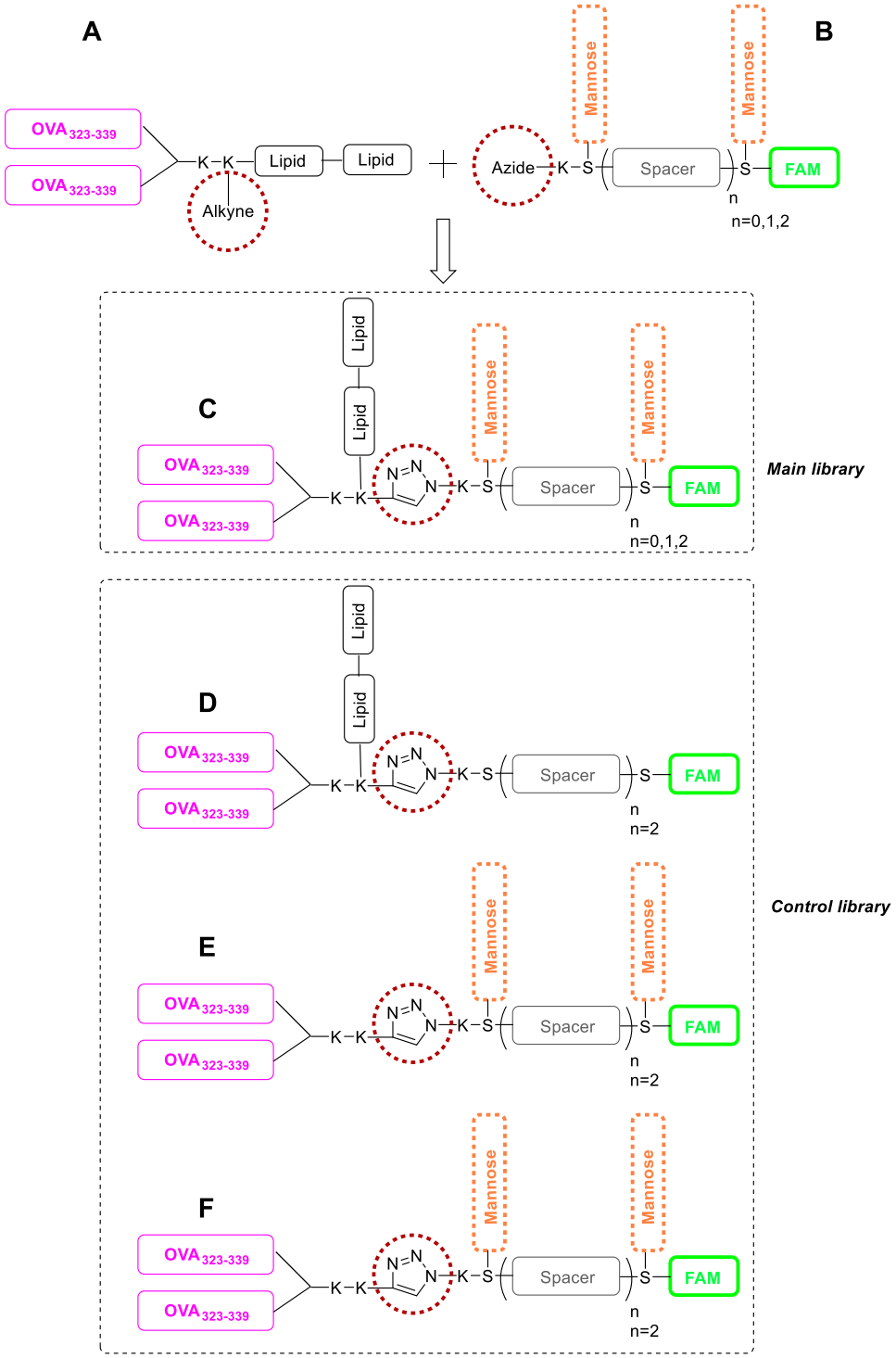

Figure 3-1. Schematic picture of the vaccine construct library. The main library includes vaccine constructs where n is the number of alanine units between each mannose moiety. The sequence for the $OVA_{323-339}$ peptide is a model antigen. Mannose is included into the structures for its mannose receptor targeting ability. The lipid (C12) is added to provide self adjuvanting properties. Designed final vaccine structures are prepared in two sections **A** and **B**. Section **A** is $OVA_{323-339}$ lipopetide (in case of controls no lipid is on the structure) with alkyne functional group able to be attached to section **B** which is the mannosylated peptide (in case of controls no mannose on the structure) with azido

functional group. The final library is provided by an azide-alkyne reaction and formation of a triazole cycle (**C**). The vaccine control library consists of constructs without mannose (D), without lipids (E) and without mannose and lipid moieties (F) and these are used to compare the effect of each moiety on *in vitro* and *in vivo* studies.

The synthesis of multi-functional glycosylated peptides that contained two mannose moieties, an azido functionality (to enable conjugation to the OVA antigen using azido-alkyne click chemistry), and a fluorescent tag (Figure 3-1A) was challenging and required selective deprotection/protection strategies to ensure high yields and increased stability. Microwave-assisted SPPS was utilised for the preparation of vaccine constructs /building blocks (Figure 3-1A). Here, microwave synthesis was used as it is known to generate long peptides in a faster time compared with manual synthesis [226]. Manual preparation of vaccine constructs (Figure 3-1B) was used to prepare the glycosylated peptides to achieve a good level of coupling ensuring a high yielding product. Throughout each synthesis, micro-cleavages were performed to confirm successful elongation of the peptide chain, ensuring a successful synthesis especially important with long peptide sequences. Herein, different approaches for the synthesis of the vaccine constructs including the main library (Figure 3-1C) and the control library (Figure 3-1D, E and F) are presented and discussed.

3.2 Results and Discussion

In nature, a large proportion of proteins are glycosylated, and the synthetic approach has provided the chance of preparing pathogens cell wall mimics [227, 228]. Although synthetic methods like the application of enzymes in carbohydrate preparation can quickly provide pure products, they are more efficient in the preparation of large scale glycosylated products [227].Hence, chemical synthesis, specially SPPS used for the preparation of glycosylated constructs with specific properties and less unwanted problems of natural sources, are more likely under investigation [229, 230]. In general, the preparation of glycoproteins is a difficult task with complications in regards to the formation of a reproducible glycoprotein, although the preparation of glycopeptides using SPPS gives a chance of designing an engineered active product [231].

In nature, *O*-Linked mannose is naturally available attached to a serine or threonine amino acid [222]. Further studies are needed to include *O*-mannosyl serine/threonine building blocks in vaccine peptides with preservation of the mannosyl targeting properties found in nature (**Chapter 1, Section 1.6, Figure 1-6**). Special arrangements of the *O*-mannosyl building blocks, such as the space needed between the glycosylic moieties in a peptide for a better receptor attachment, have rarely been investigated. As a result, this has prompted the exploration of the synthesis optimisation and

conformational properties of *O*-linked mannosylated peptides for use in biological and immunological studies with the aim of advancing vaccine development through increased targeting of APCs. Several studies have reported the preparation of *O*-mannosyl serine or threonine building blocks for application in peptide synthesis [208, 225]. However, these *O*-mannosyl serine or threonine building blocks have rarely been incorporated into peptides [208, 230].

3.2.1 Design and Synthesis of Mannosylated Building Blocks

The Fmoc-serine mannosylated amino acid **2** (N-Fmoc-*O*-(2,3,4,6-tetra-*O*-acetyl-α,β-$_D$-mannopyranosyl)-L-serine, Figure 3-2) was synthesised from acetylated $_D$-mannose (**1**, Figure 3-2) as a building block for use in the synthesis of mannosylated peptides. One of the advantages of using this Fmoc-serine mannosylated amino acid building block is the ease of addition to a growing peptide chain using Fmoc SPPS. It was previously reported that 1,2,3,4,6-penta-*O*-acetyl-α,β-D-mannopyranosyl with a carboxylic pentafluorophenyl protecting group successfully generated high-yielding peptides (63%) using Fmoc SPSS, however, the presence of the ester protecting group required an extra deprotection step under acidic conditions when used at the *N*-terminus of the peptide [207, 232]. Other methods for preparation of mannosyl building blocks, including application of a carboxylic-protected serine using t-butyl or pentaflurophenyl protecting groups also required additional deprotection steps. These additional deprotection steps increased the overall synthesis time or required the use of solution-based deprotection strategies, which could not be applied to the linear addition of more than one building block [207, 230]. Conjugating chlorine or bromide at the anomeric position of mannose before attachment to the amino acid can also add an extra step to the preparation of a final mannosylated building block [230]. Therefore, the two-step preparation of a Fmoc-serine mannosylated amino acid building block with an unprotected carboxylic acid at the C-terminus (**2**, Figure 3-2) provided an ease of application in peptide chain elongation using Fmoc SPPS. Here, the hydroxyl groups of $_D$-mannose were acetylated to ensure stability of the sugar moiety during peptide synthesis and to avoid acylation (Figure 3-2). Without this hydroxyl protection, the glycosidic bond was susceptible to degradation [207]. Further, Lewis acid reaction (Figure 3-2) was chosen due to the ease of access to starting materials and shorter reaction times regarding the steps taken compared to other methods available for preparation of a mannose-serine building block.

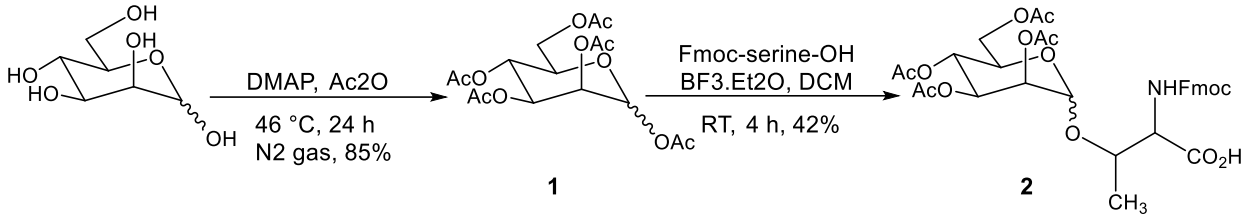

Figure 3-2. Scheme for the synthesis of Fmoc-serine mannosylated amino acid building blocks. 1,2,3,4,6-Penta-*O*-acetyl-α,β-$_D$-mannopyranosyl (**1**) was synthesised using $_D$-mannose, DMAP, Ac_2O, 46°C, 24 h, N_2 gas in a 85% yield. N-Fmoc-*O*-(2,3,4,6-tetra-*O*-acetyl-α,β-$_D$-mannopyranosyl)-L-serine (**2**) was synthesised with the addition of Fmoc-serine-OH, $BF_3.Et_2O$, DCM, RT, 4 h in a 42% yield.

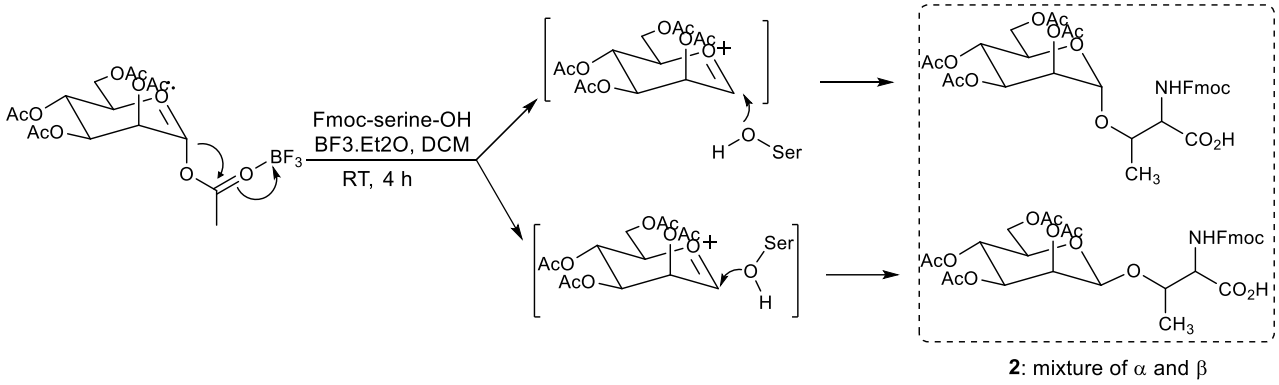

Figure 3-3. Mechanism of action for the $BF_3.Et_2O$ Lewis acid reaction. Conjugation of **1** (acetylated mannosyl donor) to Fmoc-Ser-OH using $BF_3.Et_2O$ in DCM at RT for 4 h generated **2** (Fmoc-serine mannosylated amino acid building blocks) as a mixture of α and β due to attack of the Lewis acid from both below (β, 25.44%) and above (α, 74.55%) [233]. For synthesis details see **Chapter 2**, **Section 2.1.2.**

The synthesis of **1** was performed as previously described (33) and is detailed in **Chapter 2**, **Section 2.1.2**. Here, Lewis acid (BF_3) was used as a promoter for the attachment of the serine hydroxyl group to the anomeric carboxyl group on per *O*-acetylated mannose. It is postulated that an intermediate oxonium is formed and depending on the angle of interaction, both α or β isomers are formed (Figure 3-3) [233].

The synthesis of **2** was optimised by monitoring the Lewis acid reaction using analytical RP-HPLC. Here, a 4 h reaction was found to give a maximum yield of 42% while longer reactions resulted in degradation of the product (Figure 3-4). This product degradation was observed 4 h after the reaction was started in analytical RP-HPLC and is postulated to be associated with the rearrangement of the glycosyl group and formation of new subsidiary structures (Figure 3-4) [230]. Additionally, two peaks

were observed for the product that were attributed to α- (74.55%) and β- (25.44%) analogues of the sugar (Figure 3-4). Furthermore, as the Fmoc-serine amino acid was used in excess in this reaction, it was expected that this peak would be present at the conclusion of the reaction (Figure 3-4). At 21.5 min (Figure 3-4) a peak was observed relating to the final product (**2**) without one acetyl group. This was also reported by Wang *et al.* and was explained to be related to the thermolytic condition of the BF_3 reaction [233]. Previous studies have also reported 18 h reactions using the same reaction conditions described here ($BF_3.Et_2O$, DCM, RT, Fmoc-ser-OH) generating a pure yield of 5% [230]. Here, preparative RP-HPLC was used with a C18 column, product **2** was purified with a 30-70% gradient of acetonitrile over 45 min and was characterised by ESI-mass spectrometry and NMR (Appendix 1).

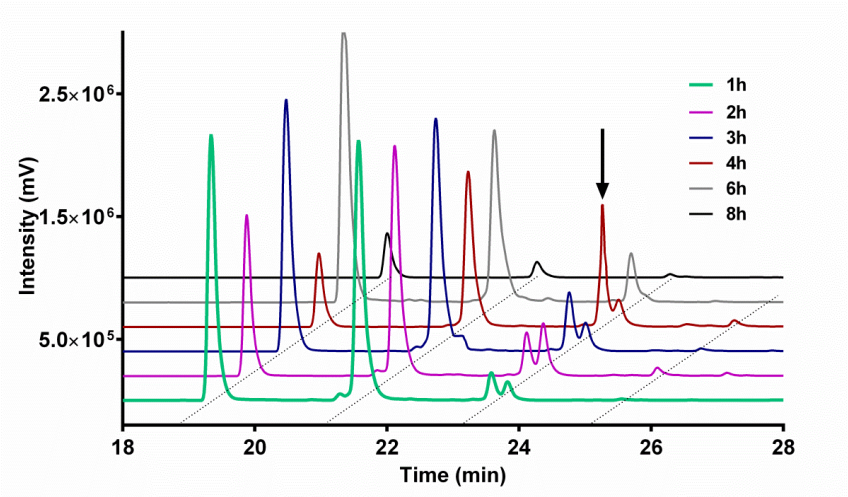

Figure 3-4. Monitoring of the boron trifluoride diethyl etherate ($BF_3.Et_2O$) Lewis acid reaction at 1, 2, 3, 4, 6, and 8 h by analytical RP-HPLC on a C18 column (0 to 100% acetonitrile gradient over 30 min). At 4 h, the optimum yield for the product (**2**, 42%) was observed with a retention time (Rt) of 23.6 min (peak indicated by an arrow) and this eluted at 62% solvent B (**Chapter 2, Section 2.1.1**). Rt 19.3 min is the Fmoc-serine-OH starting material and Rt: 21.5 min is the product missing one acetyl group. The graph was drawn using nudging (overlaying graphs with an angle) in GraphPad Prism.

3.2.2 Synthesis and characterisation of fluorescently-labelled mannosylated (and un-mannosylated) peptide azides

Mannosylated peptides that contain more than one mannose moiety and are widely spaced have been shown to have increased affinity for the MR, present on APCs [234]. However, it has also been argued that less distance between these mannose moieties can also enhance affinity and binding towards the MR [131]. Further, studies have reported that a dimannoside cluster was better at recognising CRDs

of the MR, while single mannose-BSA was better recognised by a DC-SIGN receptor (a C-type lectin receptor with one CRD and with affinity towards glycosylated structures) with a single CRD, suggesting that linearity and spacing should be considered in the design of MR ligands [121]. Thus, the aim was to investigate the role of distance between the mannose units and the effect this had on binding and affinity towards the MR. Here, mannose units were used arranged linearly (non-clustered) in peptide vaccine constructs. Inclusion of an alanine spacer between each mannose unit has also been shown to minimise unwanted steric interactions Depending on the hydrophilicity or lipophilicity of these spacers in the structure, different sizes and conformations can be obtained [121, 235]. Here, two synthesis strategies (Method 1 and Method 2) were detailed for preparation of mannosylated peptides using Fmoc SPPS to obtain a final library of mannosylated peptides in high yields to be tested as potential vaccine constructs (Figure 3-1).

3.2.2.1 Method 1:

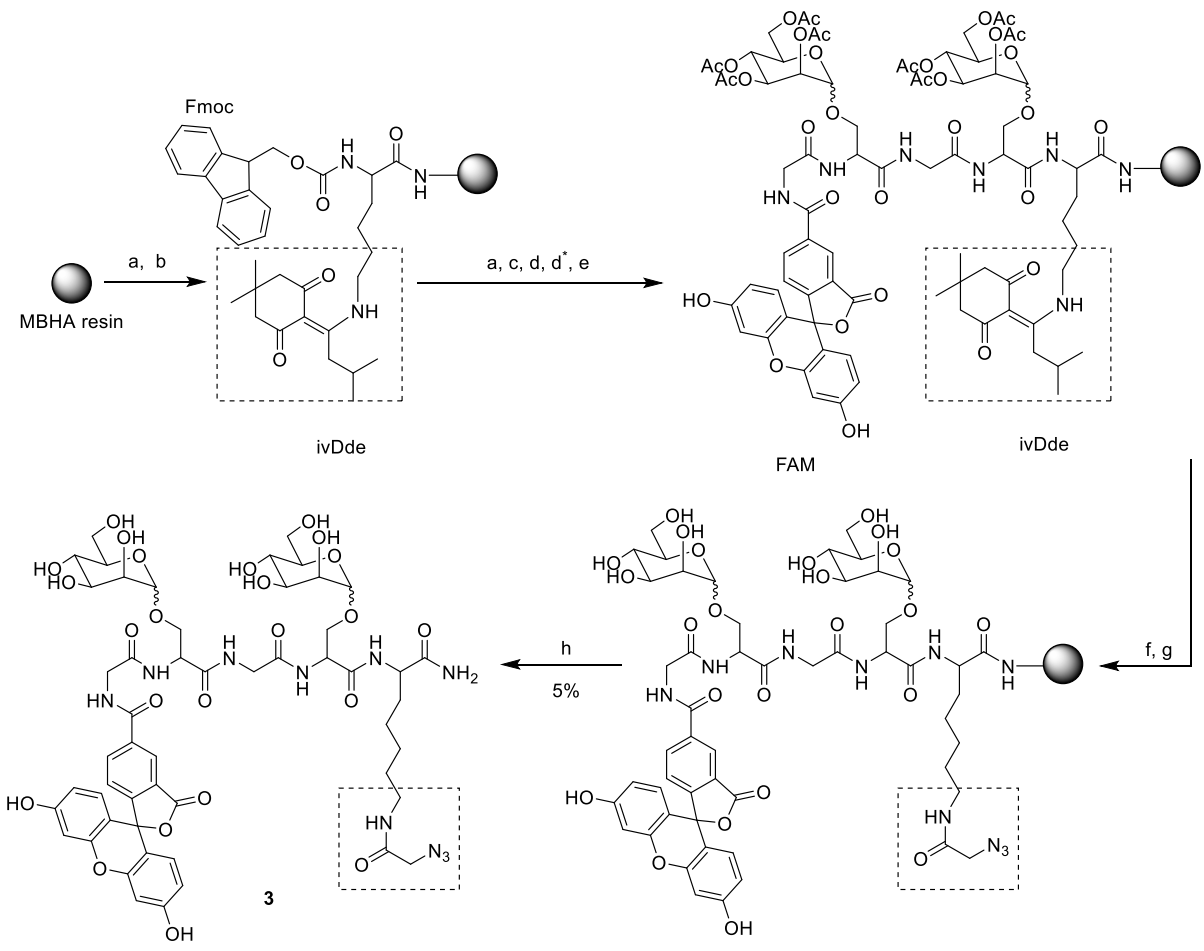

Figure 3-5. Azide functionalized mannosylated peptide 3. Peptide **3** was synthesised using Method 1 and resulted in a low overall yield of 5%. (a) 20% Piperidine in DMF, RT; (b) Fmoc-lys(IvDde)-OH, HATU, DIPEA; (c) **2**, HATU, DIPEA, DMF; (d) Fmoc-Ala-OH, HATU, DIPEA, DMF; (d*)

repeated a and d; (e) 5(6)-carboxyfluorscein (FAM), DIC, HOBt, DMF; (f) 5% hydrazine in DMF on resin (3 × 30 min), RT; (g) azidoacetic acid, HATU, DIPEA, DMF; (h) 95% TFA: 2.5% water: 2.5% TIS. For a detailed synthesis protocol see **Chapter 2**, **Section 2.1.4.1**.

Peptide **3** (Figure 3-5) was synthesised using manual Fmoc SPPS. Here, Fmoc-lys(IvDde)-OH was first coupled to the peptide chain. Peptide elongation was continued by addition of 2,3,4,6-tetra-*O*-acetyl-α,β-D-mannopyranosyl-serine building blocks (**2**, Figure 3-2) with addition of 2 alanine spacers between each mannose unit. Fmoc amino acids were coupled by activation with HATU and DIPEA in DMF. HATU has been shown to be an efficient coupling reagent for generating products with high reactivity and low racemisation [236]. Following addition of the last amino acid in sequence, FAM was coupled and excess ester-bound FAM removed by treatment with 20% piperidine. Addition of FAM enables visualisation in *in vitro* cell studies [208]. The resin was then treated with 5% hydrazine in DMF on resin (3 × 30 min) to remove the lysine side chain protecting group, IvDde, along with acetyl protecting groups on the mannosyl moieties, to enable coupling of an azido-functional group. This azido group enabled coupling of additional functional groups (e.g. peptides) using an azido-alkyne click reaction at a later stage in the project. Here, mannosylated peptide **3** was released from the solid support by treating the resin with a mixture of TFA, TIPS and water. All the acid-labile amino acid side chain protecting groups were removed concomitantly. The resulting crude peptide was purified by preparative RP-HPLC (0-100% solvent B) on a C8 column and characterised using ESI-MS (Table 3-1). For a detailed synthesis protocol see **Chapter 2**, **Section 2.1.4.1**.

Table 3-1. ESI-MS data, RP-HPLC Rt and yield for mannosylated peptide 3

Peptide	ESI-MS *m/z*			Rt	Yield
	Ionization	Calculated	Found	(min)	(%, column)
3	$[M+H]^{+1}$	1212.4	1214.1	13.69	5, C8

Crude peptide **3** showed multiple peaks in the HPLC trace (Figure 3-6) and was obtained in a very low yield (5%). This is proposed to be due to the incomplete removal of the IvDde group and or acetyl protecting groups on the mannose. The multiple observed peaks in Figure 3-6 represent peptide **3** without 2 acetyl groups, without 1 mannose unit, without the FAM moiety, and with IvDde still present post-cleavage.

The analysis of these results clarified that a couple of factors had occurred as reported in previous studies: 1) Hydrolysis of the fluorescent tag under basic conditions had occurred [237]; and 2) IvDde is a hydrophobic side chain protecting group and there have been reports on the difficulty of removing this protecting group and its presence in the product confirms this result [238]. Considering the low yield observed and also considering the amount of peptide required for the vaccine studies, a new method (Method 2) was proposed to overcome these problems and ultimately achieve higher product yields.

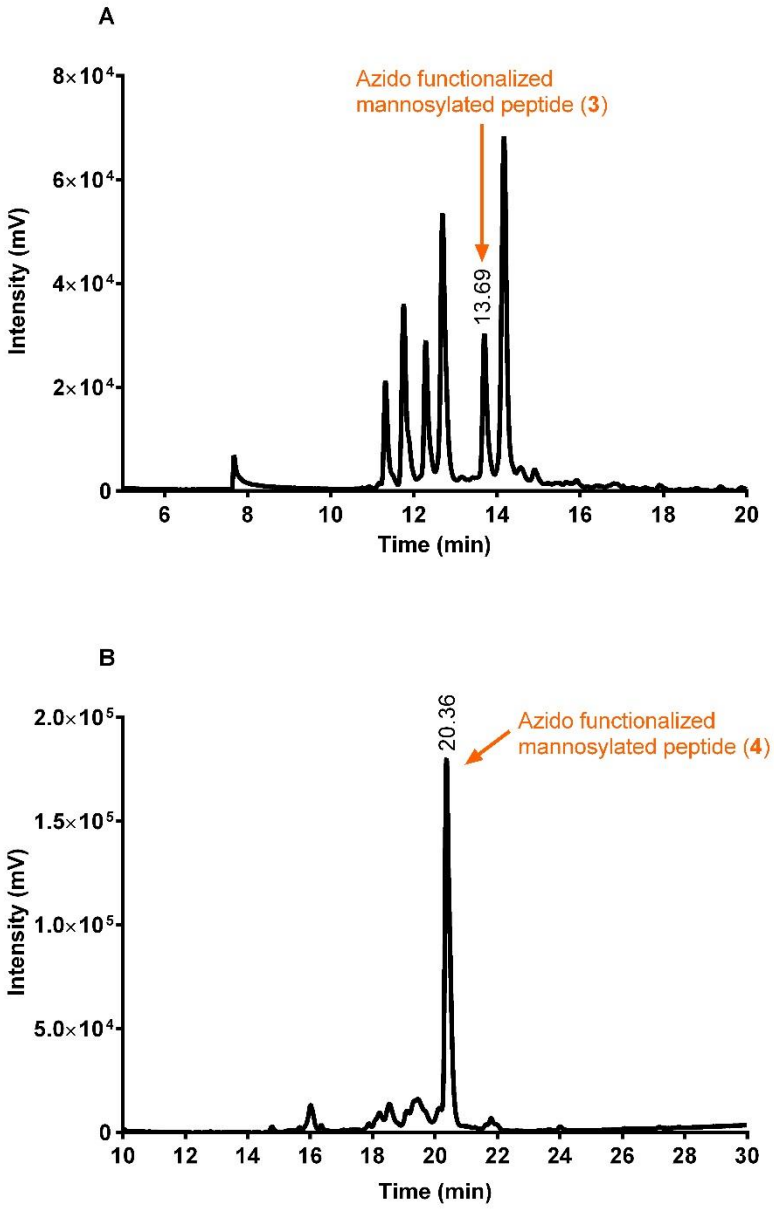

Figure 3-6. HPLC traces of peptides 3 and 4. (A) **3** prepared using Method 1 and obtained in a yield of 5%, Rt=13.69; and (B) **4** prepared using **Method 2** and obtained in a yield of 54%, Rt=20.36. Analytical RP-HPLC: 0-100% acetonitrile gradient over 30 min. For a detailed synthesis protocol see **Chapter 2**, **Section 2.1.4.1**.

3.2.2.2 Method 2:

By changing the strategy from Method 1 (**Section 3.2.2.1**) to Method 2 for the preparation of azido-functionalised mannosylated peptides, it was hoped that the complications observed with the IvDde removal and fluorescent tag stability observed in Method 1 (**Section 3.2.2.1**, Figure 3-6) were overcome. This was achieved by changing the lysine side chain protecting group from IvDde to Mtt (Figure 3-7).

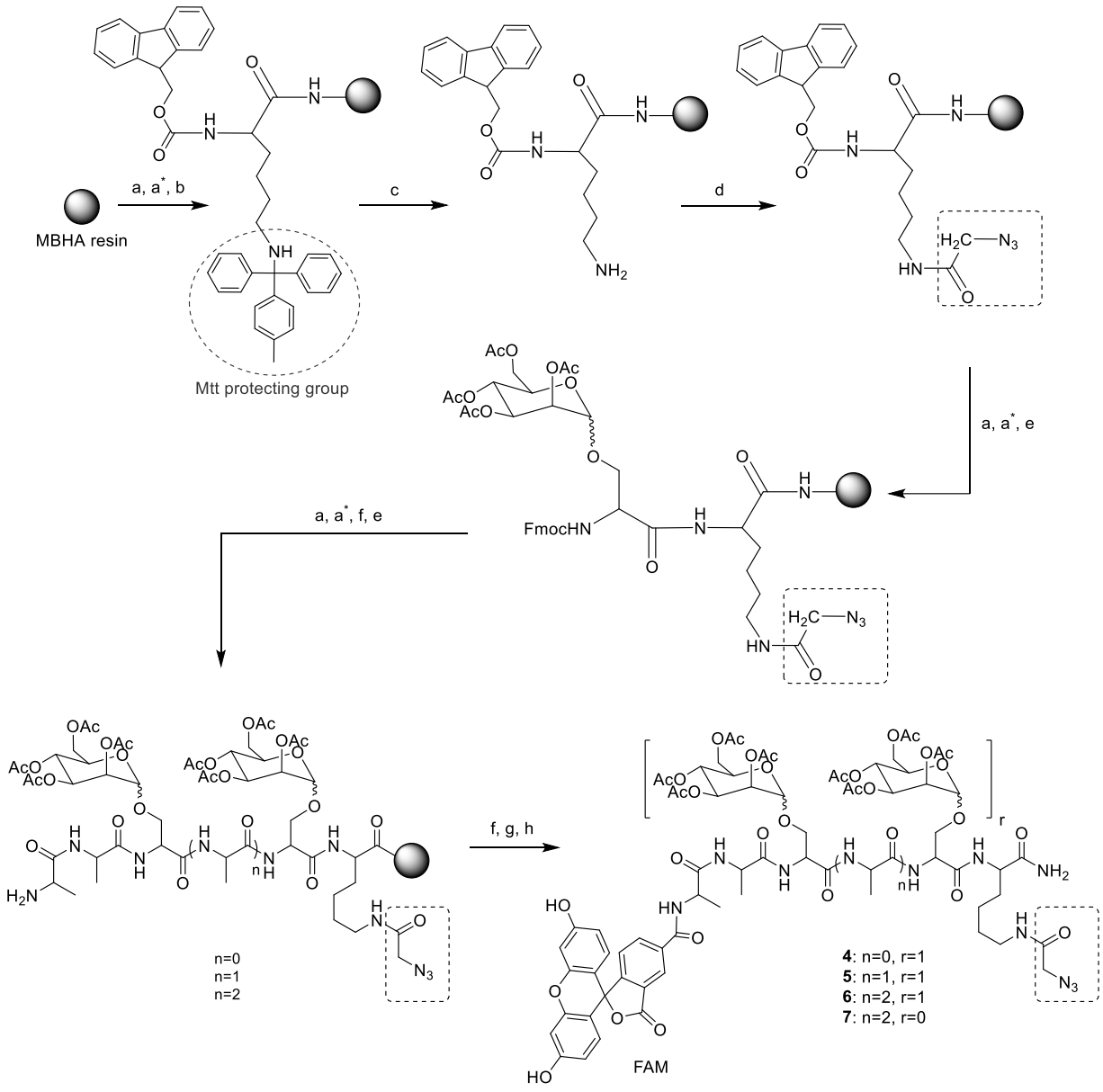

Figure 3-7. Reagents and conditions for the synthesis of peptides 4-7: (a) 20% Piperidine in DMF, RT; (a*) 2 cycles of piperidine in DMF; (b) Fmoc-lys(Mtt)-OH, HATU, DIPEA; (c) 2% TFA: 1% TIPS in DCM, 20 cycles; (d) azidoacetic acid, HATU, DIPEA, DMF; (e) N-Fmoc-*O*-(2,3,4,6-tetra-*O*-acetyl-α,β-$_D$-mannopyranosyl)-L-serine, HATU, DIPEA, DMF; (f) Fmoc-Ala-OH, HATU,

DIPEA, DMF; (g) 5(6)-carboxyflourscein (FAM), DIC, HOBt, DMF; (h) 95% TFA: 2.5% water: 2.5% TIS. For a detailed synthesis protocol see **Chapter 2**, **Section 2.1.4.2**.

Azido-functionalised mannosylated peptides **4-7** (Figure 3-7, Table 3-2) were synthesised using manual Fmoc SPPS. The orthogonal Mtt side chain protecting group was removed from the lysine using mildly acidic conditions (Figure 3-7) and azidoacetic acid was coupled to allow for functionalisation with the $OVA_{323-339}$ lipo-peptide after cleavage. Mtt was chosen to protect the orthogonal lysine group because it is easily deprotected on-resin using 1% TFA and scavenger (1% TIS) in DCM [239]. Following this, the Fmoc group from the lysine was removed and the Fmoc-serine-mannose amino acid (**2**, Figure 3-1) was coupled using standard *in situ* Fmoc coupling procedures [240]. Un-mannosylated fluorescent peptide **7** was synthesised using the same procedure as compounds **4-6**, however, the Fmoc mannosylated serine amino acid (**2**) was replaced with Fmoc-serine(tBu)-OH (Figure 3-7). Peptide **7** contains two alanine amino acids employed as a spacer between each mannose unit (Figure 3-7) and was used as a control for *in vitro* studies to investigate the role of mannose on receptor binding. For a detailed synthesis protocol for peptides **4-7** using Method 2 see **Chapter 2**, **Section 2.1.4.2**.

Table 3-2. ESI-MS data, RP-HPLC Rt and yields for peptides 4-7

Construct	ESI-MS *m/z*			C8: Rt (min)	C18: Rt (min)	Yield (%)
	Ionization	Calculated	Found			
4	$[M+H]^{+1}$	1563.45	1565.0	20.83	20.64	54
5	$[M+H]^{+1}$	1634.53	1634.5	20.57	20.51	62
6	$[M+H]^{+1}$	1705.61	1706.6	20.50	20.49	68
7	$[M+H]^{+1}$	1044.39	1045.8	15.04	12.16	48

3.2.2.3 Comparison of Method 1 with Method 2

Method 1 gave a very low yield (5%) for the synthesis of peptide **3** and this was proposed to be due to the instability of FAM and acetyl groups due to a reaction to hydrazine and further difficulties in the removal of IvDde on the lysine side chain as explained in **Section 3.2.2.1**. The advantage of Method 2 was that FAM was added as the last functional group at the N-amino end of the peptide chain so it was intact and stable. It was previously shown that FAM can be unstable in the presence of hydrazine and it was postulated that this could be the reason for the low yield obtained in Method 1 [208]. Further, IvDde was not completely removed which could be associated with its high hydrophobicity [241].

The revised synthesis method of first removing the Mtt protecting group on the lysine side chain, improved the yield by 4-5 times higher than Method 1 (Figure 3-6). As can be seen in Figure 3-6, the number of crude peaks observed in analytical RP-HPLC was considerably reduced in Method 2 (Figure 3-6B) compared with Method 1 (Figure 3-6A).

3.2.3 Synthesis and characterization of $OVA_{323-339}$ lipopeptide and peptide alkynes

Lipid moieties included in peptide (or proteins) constructs are efficient in improving their bioavailability by increasing the lipophilicity and have the potential to overcome enzymatic barriers [221]. Inclusion of lipid moieties in peptide vaccines has been shown to increase passive diffusion of peptides across epithelial barriers as well as increase uptake in lymphatic systems [221]. LCP (**Chapter 1, Figure 1-13**) vaccines are known to have self-adjuvanting properties and contain minimum epitopes necessary for targeting cells [165]. The LCP systems with 2 or 3 lipid moieties are known to target DCs and induce cellular activation by attachment to TLRs [167]. It has been shown that LCPs along with Pam3Cys and Pam2Cys are ligands for TLR2 and when incorporated into an antigenic moiety have been shown to elicit cellular and humoral immune responses [242]. Previous studies have shown that incorporation of long chain lipoamino acids into a peptide chain can change the size of the peptide particles and this is known to affect its immunogenic properties [243]. The alkyl chain in a lipoamino acid could vary in length, but the most common number of carbon atoms used in vaccine studies is between 12 and 16. In this study, C12 was chosen as this has been shown to have an adjuvanting effect when attached to the peptide epitope [244].

The $OVA_{323-339}$ epitope of OVA is known to bind to MHC II causing a T cell response [182, 184]. This $OVA_{323-339}$ epitope is a common antigenic peptide reported to be used in the design of peptide vaccines for a T cell response [245, 246]. T cells are activated when T cell receptors interact with an antigenic epitope and generate the release of cytokines, inducing T cell proliferation [245]. In this study, two copies of the $OVA_{323-339}$ epitope was incorporated into the peptide vaccine constructs with the ultimate goal of designing a prophylactic vaccine with T helper response. Increasing the number of epitopes attached to a lysine core dendron can improve peptide size uniformity and has been shown to enhance the *in vivo* activity of peptides [247].

In this project, alkyne-functionalised peptides containing two lipid moieties (C12) and two branches of the $OVA_{323-339}$ peptide as the model antigen were synthesised using microwave-assisted Fmoc SPPS (Figure 3-8). The design of a branched peptide vaccine has the advantage of presenting multiple copies of an epitope to the immune system in one single entity. Here, the lysine amino acid, containing

both α and ε amino groups, provides branching points for the attachment of multiple peptide epitopes in one construct [248].

3.2.3.1 Synthesis of lipid building blocks

It has been previously shown that the addition of lipid moieties to a peptide chain increases its stability and immunogenicity by increasing the lipophilicity and inducing formation of peptide particles [153]. Using self-adjuvanting lipopeptide vaccines has the advantage of being safe and reproducible (detailed in **Chapter 1**, **Section 1.8.2**) [153, 249, 250]. In this project, two lipid moieties were incorporated into the peptide chain. This has been shown to give the most promising antibody response in relation to the structural activity by improving the adjuvanting properties of the vaccine constructs [142].

Synthesis of the C12 lipid (**9**, Figure 3-8) and subsequent protection using the Dde protecting group (**8**, Figure 3-8) was performed using previously published procedures [212, 251] and is detailed in **Chapter 2**, **Section 2.1.5**. Here, Dde was chosen as a protecting group for lipoaminoacids as it is compatible with Fmoc SPPS and can be selectively removed on resin [212, 252]. Further, the Dde-C12 (**10**) was prepared by a reaction of the C12 (**9**) with Dde (**8**, Figure 3-8).

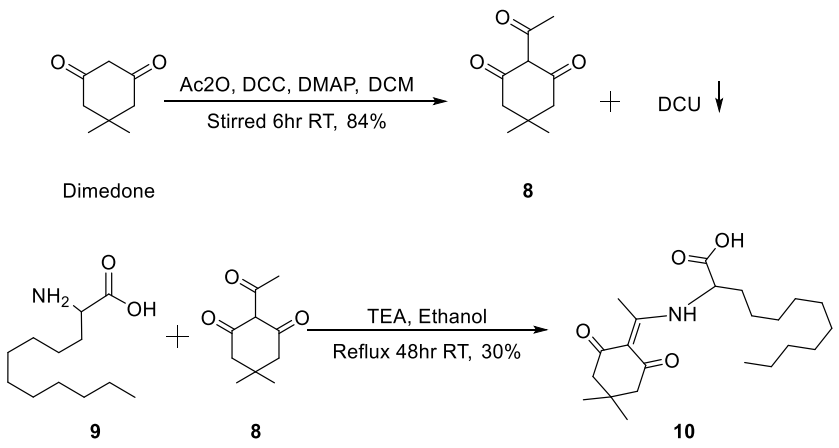

Figure 3-8. Synthesis of the Dde (9) lipid protecting group and the Dde-C12 lipid (10). 2-Acetyldimedone (Dde, **8**) was synthesised using solution synthesis, and was then used to protect the N-terminal of the C12 lipid (**9**) in a reaction with **8** generating the Dde protected C12 lipid (**10**, Dde-C12). For a detailed synthesis protocol see **Chapter 2**, **Section 2.1.5**.

3.2.3.2 Synthesis of OVA$_{323-339}$ peptides

Microwave-assisted Fmoc SPPS was used for synthesis of peptides **11** and **12** on Rink amide MBHA resin. Following coupling of the Dde-C12 (**10**, Figure 3-8), the Dde protecting group was manually removed by treating the resin with 2% hydrazine in DMF. Branching and concurrent addition of two OVA peptides (Figure 3-9) was achieved using Fmoc-lysine(Fmoc)-OH. Standard microwave-assisted Fmoc SPPS protocols were used for the synthesis of peptide **11**, with amino acid activation using HATU and DIPEA. Each amino acid (listed in Figure 3-9) coupling was followed by Fmoc deprotection using two cycles (5 min/cycle) of 20% piperidine in DMF. The IvDde protecting group on the side chain of lysine was removed manually and functionalised with an alkyne functional group. Peptide **12**, which contained no lipid moieties, was synthesised as a control for the cell-based assays using a similar method to peptide **11**, without inclusion of the lipids. Purification details for peptides **11** and **12** are reported in Table 3-3. For a detailed synthesis protocol of peptides **11** and **12** see **Chapter 2**, **Section 2.1.6**.

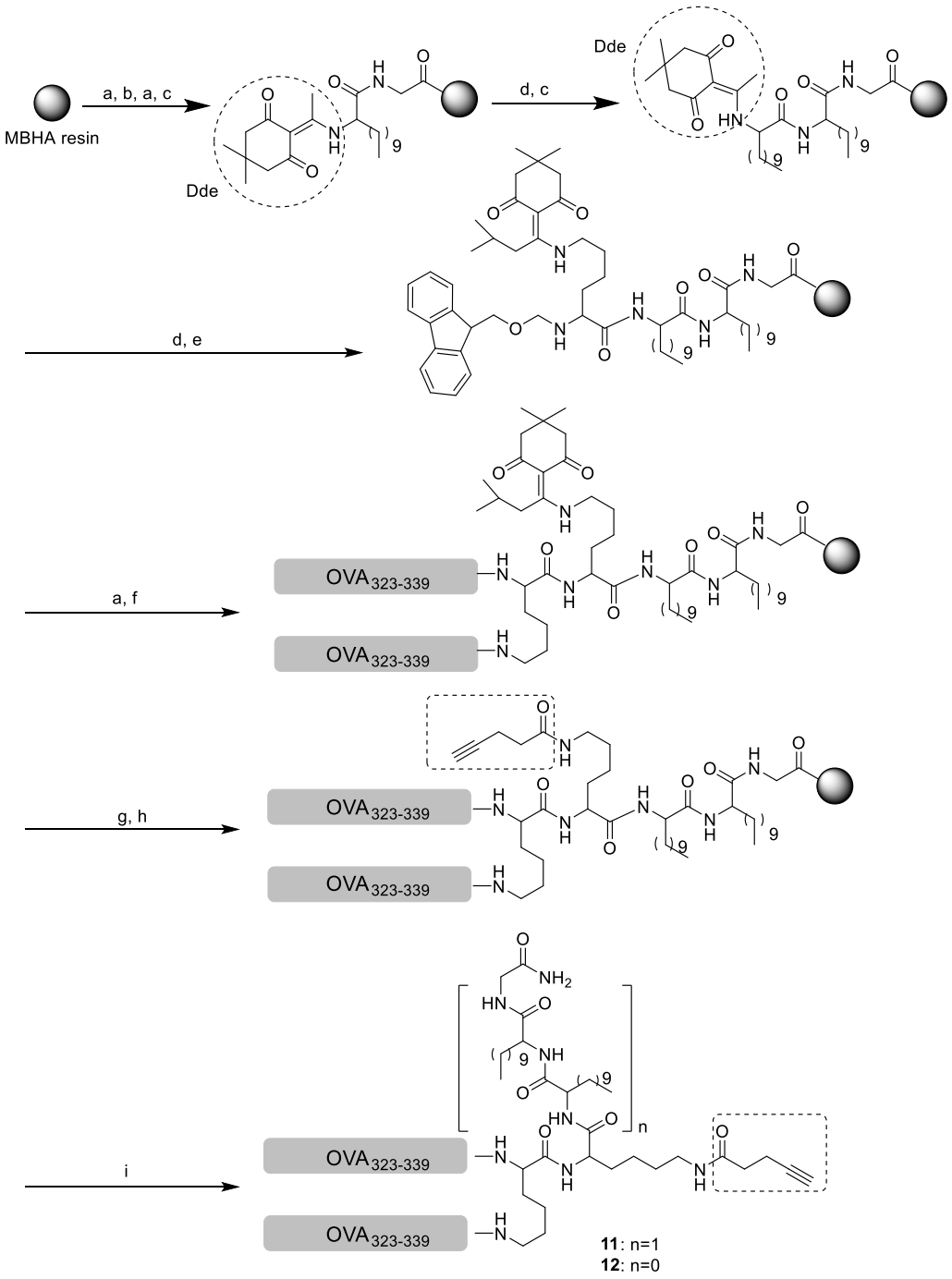

Figure 3-9. Reagents and conditions for microwave-assisted synthesis of peptides 11 and 12; (a) 20% Piperidine in DMF, 20W, 70°C for 2 min + 5 min; (b) Fmoc-Gly-OH; (c) **10**, HATU, DIPEA; (d) 2% hydrazine in DMF (4 x 10 min); (e) Fmoc-Lys-IvDde-OH, HATU, DIPEA; (f) Fmoc-Lys-Fmoc-OH, after deprotection of Fmoc, Ile(Boc) - Ser(tBu) – Gln(Trt) – Ala - Val – His(Trt) - Ala - Ala – His(Trt) - Ala – Glu(OtBu) - Ile – Asn(Trt) – Glu(OtBu) - Ala - Gly – Arg(Pbf) were coupled consequently (in HATU and DIPEA), all amino acids were Fmoc protected and deprotection of Fmoc group was performed as mentioned at (a); (g) 2% hydrazine in DMF on resin (3 × 30 min), RT; (h) pentynoic acid, HBTU, DIPEA, overnight, at RT; (i) 95% TFA: 2.5% water: 2.5% TIS. For a detailed synthesis protocol of peptides **11** and **12** see **Chapter 2**, **Section 2.1.6**.

Table 3-3. ESI-MS data, RP-HPLC Rt and yields for peptides 11-12

Construct	ESI-MS *m/z*			Rt	Yield
	Ionization	Calculated	Found	(min)	(%, Column)
11	$[M+3H]^{+3}$	1439.98	1440.1	17.47, 17.28, 16.96	73, C4
12	$[M+2H]^{+2}$	1962.10	1962.1	17.79	83, C18

3.2.4 Conjugation of mannosylated peptide azides to lipopeptide alkynes using copper-mediated azido-alkyne click chemistry

Large dendritic peptides with complex branched structures can be difficult to synthesise and purify in a single step. However, there are a number of techniques available to assist in their synthesis [253, 254]. In this study, copper-mediated azide-alkyne cycloaddition reaction or "click chemistry" was employed due to its safety, reliability, and high yielding reaction (Figure 3-10). Furthermore, cell-based assays found that the triazole bond formed between the two products in this reaction had an increased stability against proteolytic degradation and was able to mimic a native peptide bond [253, 254].

In this study, the $OVA_{323-339}$ lipopeptide-alkyne (**11**) was conjugated to fluorescently-labelled mannosylated-azides (**4-6**), forming a library of mannosylated vaccine constructs (**13-15**, Figure 3-10) designed to test the impact of distance between the mannosyl groups on cell uptake. The click reaction was performed in DMSO, which easily dissolved each reaction component. The reaction was monitored by analytical RP-HPLC to quantify the optimal reaction duration and product identification was achieved using ESI-MS. Here, the reactions were found to be completed in 5 h where formation of the product did not proceed any further when reaction times were increased. In some cases, when the reaction was left longer (24 h), there was no change in the product yield and by-products had started to form, potentially due to the breakdown of the sugar moiety from lengthy exposure to elevated temperatures (50°C). In this study, copper wire was used as the source of the copper catalyst because of its advantages over traditional sources of copper, which require the use of use N-based ligands or the reduction of Cu^{II} to Cu^{I} *in situ:* copper wire also facilitates the easy removal of excess copper from the reaction [214]. At the completion of the reaction, the copper wire was removed by filtration, the reaction was quenched with water and lyophilised to obtain the crude test vaccine constructs (**13-15**, Figure 3-10).

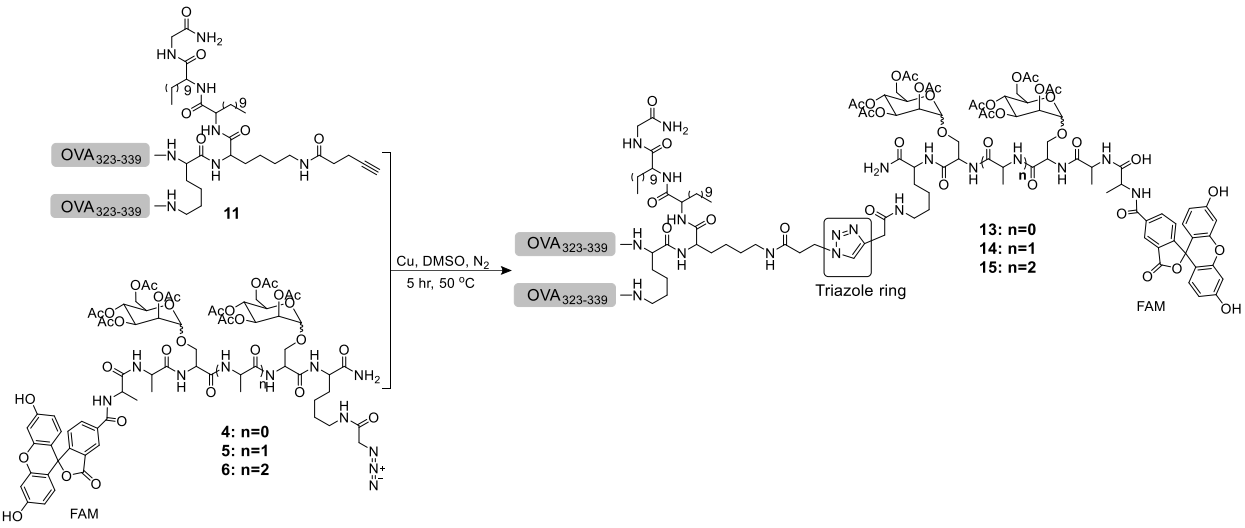

Figure 3-10. Mannosylated lipopeptide vaccine constructs 13-15, prepared from a copper-mediated click reaction (DMSO, 5 h, RT, N_2 gas) of the lipopeptide-alkyne (**11**) with fluorescently-labelled mannosylated-azides (**4-6**). The formation of the triazole bond in this reaction is highlighted with a square. See **Chapter 2, Section 2.1.7.**

Vaccine constructs used as controls in *in vitro* and *in vivo* studies were also synthesised (**16-18**, Figure 3-11). Here, conjugation of **7** to **11** generated **16** (Figure 3-11) which contained no mannose moieties. Furthermore, a mannosylated construct that contained no lipids (**17**, Figure 3-11) and a construct that contained no lipids or mannose (**18**, Figure 3-11) were generated by conjugation of **12** with **6**, and **12** with **7**, respectively. Constructs **16-18** were designed to test the role of lipids and/or mannose in cell binding/uptake studies as well as immune modulation properties.

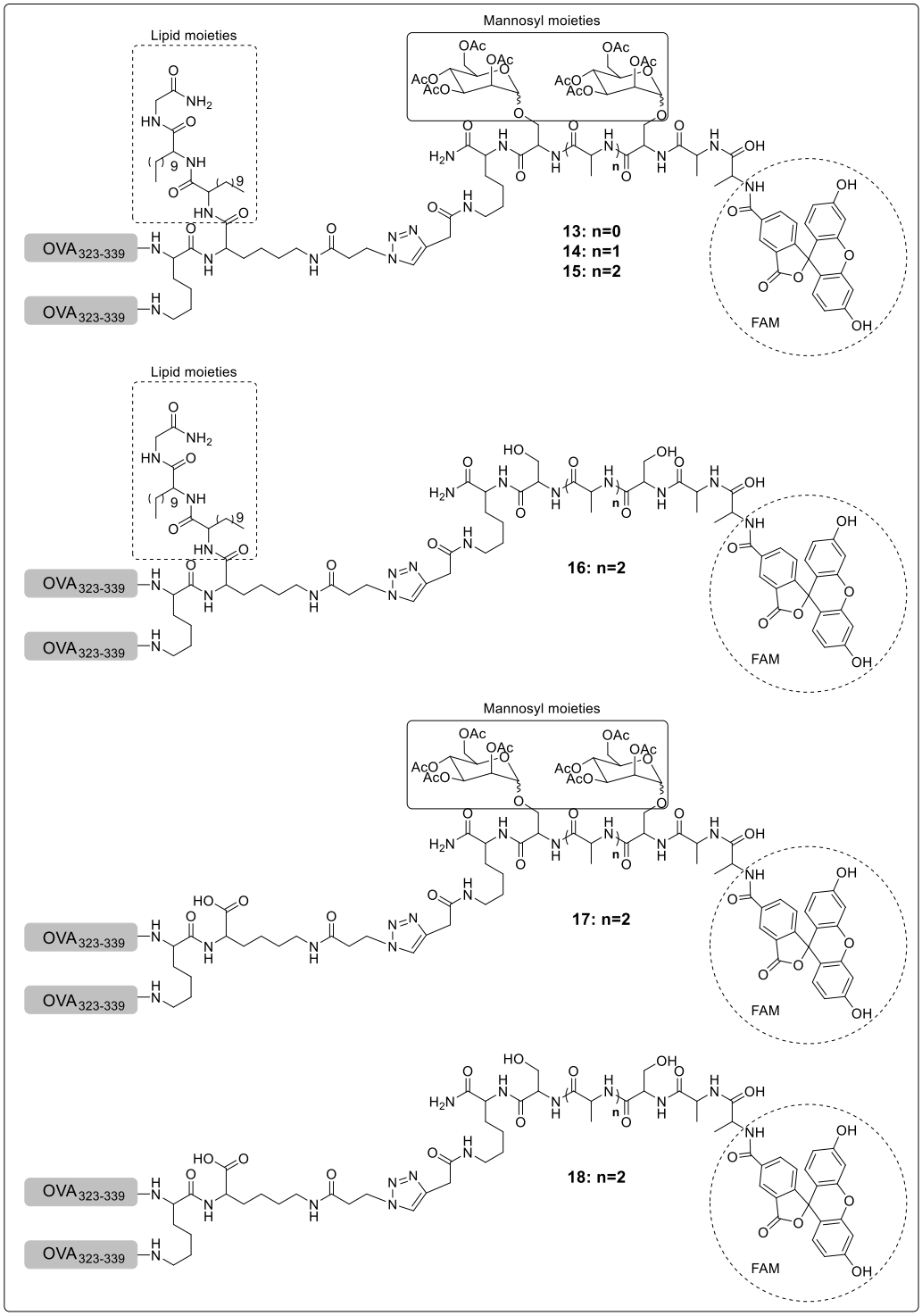

Figure 3-11. Library of fluorescently-labelled mannosylated lipopeptide vaccine constructs (13-15) and control constructs (16-18). The test constructs, containing a variable length alanine spacer between each mannose moiety are **13** (n=0), **14** (n=1) and **15** (n=2). Control constructs for cell-based studies include **16** (no mannose moieties, n=2), **17** (no lipid moieties, n=2), and **18** (no lipid or mannose moieties, n=2), where n is the number of alanine amino acids. $OVA_{323-339}$ epitope (model antigen) was included as a CD4 T cell epitope. FAM was included in each construct to enable detection in *in vitro* cell studies. The lipid is C12.

Vaccine constructs **13-18** (Figure 3-11) were purified by preparative RP-HPLC on a C8 column and isolated in yields of 34-51% (Table 3-4). The retention times were slightly longer than that of the reacting peptide building blocks due to their larger molecular size and higher hydrophobicity (Table 3-2). Figure 3-12 shows the RP-HPLC trace for construct **15** as an example. The peak of product (**15**, Figure 3-12) and the lipopeptide starting material (**11**, Figure 3-12) are multivalent because the lipids are present as a diastereomeric mixture in accordance to previous reports [255]. Construct **15** also contained a mixture of both α- and β-stereochemistries for the mannose units (Figure 3-11). Here, broad peaks are observed for all mannosylated peptides (**4-6**) and lipidated peptides (**10-11**) due to the anomeric mixture of the mannose moieties and the diastereoisomeric mixture of the lipids, respectively (Appendices 9-12). As a result, multiple peaks were observed for the vaccine constructs **13-16** (Appendices 9-12).

For all constructs, the number of peaks observed in RP-HPLC is less than that expected and this can be attributed to each diastereoisomer having a similar retention time, and hence the broader RP-HPLC peaks observed. Furthermore, the mannosylated peptide azide (**4**), was present at the conclusion of the reaction (Figure 3-12A). Vaccine constructs that contained the mannose groups had been acetylated for peptide synthesis (**13-15 and 17**, Figure 3-11) and these acetyl groups were not removed before the cell-based assays. Previous studies have shown that acetylation of these glycosyl groups (including mannose) increased cell uptake and that the acetyl groups were subsequently removed by esterases inside the cell [231, 256]. Previous studies have also confirmed no significant differences in biological activity between acetylated and non-acetylated mannosylated peptides [257]. In addition, studies show that both acetylated and non-acetylated hexoses inhibit the binding of mannan to mannose binding lectins [258]. Hence, in this study, the acetyl protecting groups on mannose were not removed.

Table 3-4. ESI-MS data, RP-HPLC, Rt and yields for vaccine constructs 13-18

Vaccine Construct	ESI-MS *m/z*			C8: Rt (min)	C4: Rt (min)	Yield (%)
	Ionization	Calculated	Found			
13	$[M+4H]^{+4}$	1471.09	1472.0	21.68, 21.94, 22.42	20.40, 20.65, 21.94, 21.62	33
14	$[M+4H]^{+4}$	1488.86	1489.3	21.26, 20.56, 21.97	21.24, 22.20, 23.87	35
15	$[M+4H]^{+4}$	1506.63	1506.3	19.88, 20.11, 20.47	21.31, 20.60, 20.79, 22.28	34
16	$[M+4H]^{+4}$	1341.48	1341.5	20.13, 20.41, 21.36	16.81, 17.16, 17.54, 17.85	45
				C8: Rt (min)	C18: Rt (min)	
17	$[M+4H]^{+4}$	1407.97	1408.1	13.50	20.53	51
18	$[M+4H]^{+4}$	1242.82	1244.1	14.35	---	35

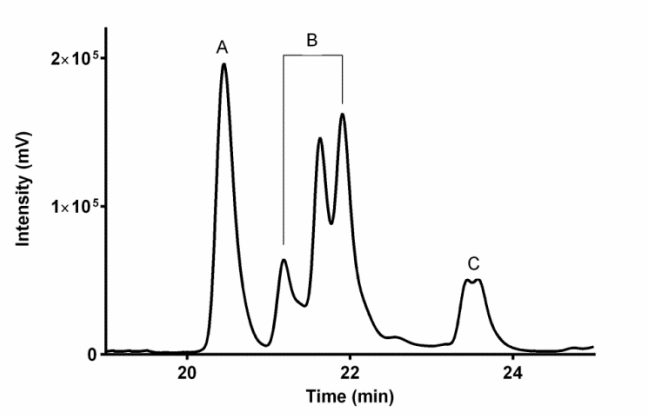

Figure 3-12. RP-HPLC trace for the copper-mediated click reaction between peptides 4 and 11 for the formation of vaccine construct 15. (A) **4**, Rt 20.83 min; (B) **15** (a diastereomeric mixture), Rt 21.2 min, 21.6 min, 21.8 min; (C) **11** Rt 23.5 min. Click reaction was performed in DMSO at 50°C under an N_2 atmosphere and stopped after 5 h.

3.2.5 Size characterisation

Vaccine constructs **13-18** were investigated for their self-assembly and particle formation in PBS. Here, the hydrophilic $OVA_{323-339}$ peptide conjugated to the hydrophobic lipid created amphiphillic constructs that self-assembled in aqueous media to form particles, providing access to peptide nanoparticles with discrete sizes. Self-assembled nano-sized particulate vaccines have been shown to possess many advantages, including enhanced stimulation of immune responses owing to improved presentation of multivalent antigens on the surface of the particle and increased *in vitro* stability [5]. Furthermore, particle formation has been shown to enhance receptor accessibility to the targeting mannose moieties [9]. In this study, DLS measurements of vaccine constructs **13-15** showed a size range of 150 ± 50 nm with a polydispersity index (PDI) of 0.4-0.6 (Table 3-5).

Particles in the vaccine formulations have size range of <5µm similar to pathogen characteristics and their uptake by APCs is proved to be via receptor mediated or receptor independent pathways. Self-assembly of peptide particles is possible for a size range of nano to micron [259, 260]. Peptide assembly happens by presence of hydrophilic and hydrophobic amino acids in a peptide structure. These hydrophilic and hydrophobic forces can create a network between the peptides and form particulates [261]. Monomers participate in formation of a self-assembled particles and these particles can contain secondary structures like micelles [259]. If positive or negative charge forces are present between particles multilayer formations can be created and more than 50 constructs can participate in formation of such multilayer formations [262].

Table 3-5. DLS size measurements of vaccine constructs 13-18

Vaccine construct	Size (nm)	PDI	SD
13	100.2 ± 25	0.37	0.069
14	208.3 ± 25	0.43	0.129
15	111.6 ± 25	0.59	0.072
16	376 ± 25	0.22	0.142
17	376.9 ± 25	0.46	0.019
18	216 ± 25	0.286	0.029

TEM imaging of these constructs showed a smaller size range (80 ± 50 nm, Figure 3-13A-C) which has been attributed to the drying step during sample preparation [263]. TEM of **13-15** showed a size range of 40 ± 10 nm (Figure 3-13D-F). This smaller size can be associated with the lower molecular weight of control peptides and the absence of lipids. However, DLS results showed a larger size range for control vaccine constructs **16-18,** due to aggregations forming in water.

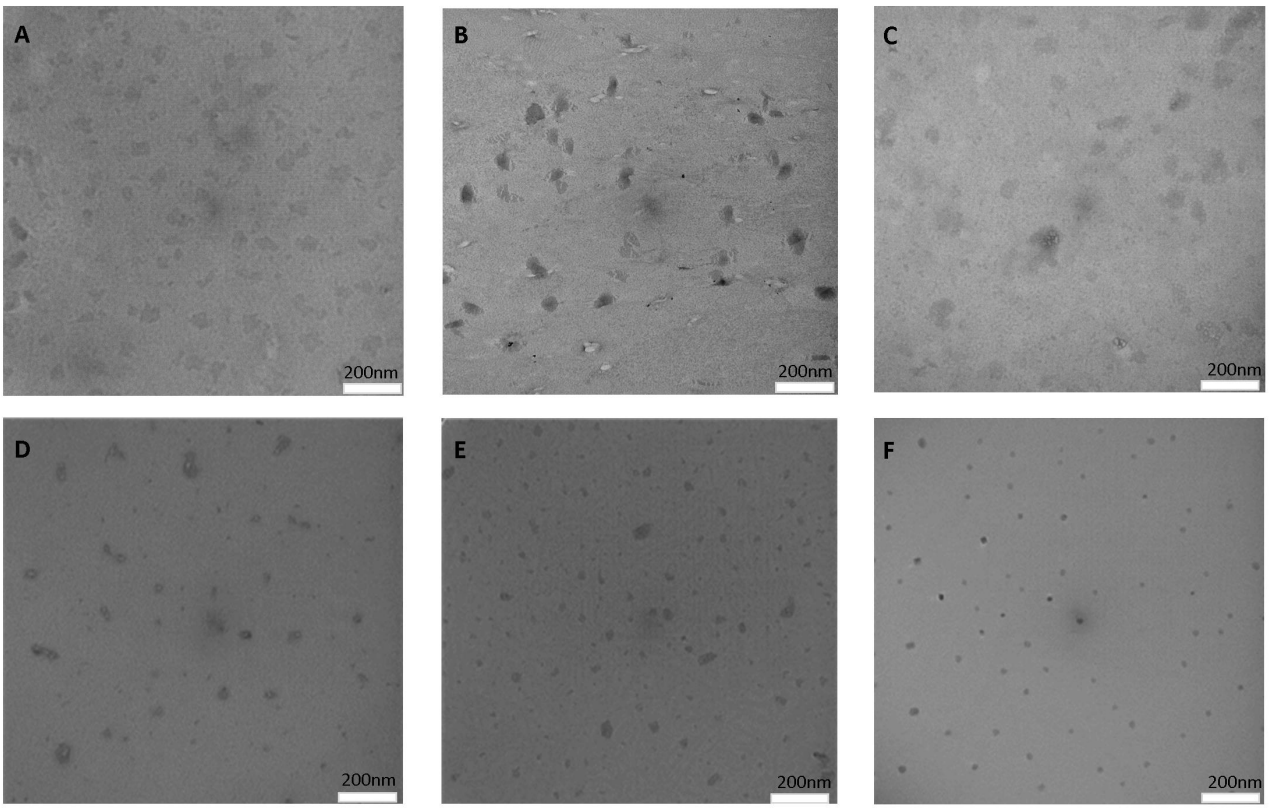

Figure 3-13. TEM images of vaccine constructs 13-18. (A) **13**, (B) **14,** (C) **15,** (D) **16**, (E) **17**, and (F) **18.** The scale bar is 200 nm.

3.3 Conclusion

O-mannosyl-serine acetyl protected building blocks (**2**) were successfully synthesised and two copies were included linearly into azido-functionalised peptides. Alanine units (0, 1 or 2) were included between these two mannose moieties using Fmoc SPPS. A fluorescent tag was included in the designed azido-functionalised mannosylated peptides (**4-7**) to allow for visualisation in *in vitro* studies. Synthesis of azido-functionalised mannosylated peptides was modified by changing the lysine side chain protecting group from IvDde to Mtt, and as a result, a 10% improvement in the overall yield was achieved. Lipoamino acids containing 12 carbons in the alkyl chain were synthesised and two copies were incorporated into the alkyne functionalised $OVA_{323-339}$ -branched peptide antigen **11**. Click chemistry was used to join azido-functionalised (**4-7**) and alkyne-functionalised peptides (**11-12**) to obtain a final library of vaccine constructs (**13-18**). The click reaction was monitored to the point where the final product (**13-18**) was achieved and no further progress was observed in the reaction after 5 h. The final library of vaccine constructs was characterised for their size properties. DLS and TEM confirmed particle formation where a smaller particle size was observed for the control library (**16-18**) due to their smaller molecular weights.

Chapter 4: *In vitro* Evaluation of Mannosylated Lipopeptide Vaccines

4.1 Introduction

APCs are specialised for presentation of an antigen to T cells (**Chapter 1, Section 1-2, Figure 1-1**) [264, 265]. It is known that for T cell activation, antigenic moieties are processed into peptides for further presentation to MHC I and II molecules. DCs and macrophages are cell populations present in splenocytes that have been the centre of cell targeting studies for vaccine development. Among APCs, DCs have the ability to uptake and process antigens and subsequently maturate as effective APCs with T cell (Th1, Th2, Th17, and Treg) activating properties [63, 266]. Activation and processing of antigenic moieties varies depending on the properties of the antigenic moiety (e.g. presence of targeting moieties such as glycosyl groups) and the presence of the adjuvant in the vaccine. These all affect the affinity towards the APC receptors by the antigen and a consequent immune response [63]. Thus, targeting antigens to specific receptors on the APCs is an appropriate method to enhance an immune response. The MR and some of the other C-type lectins have been identified on the surfaces of both macrophages and DCs and have been the subject of vaccine targeting strategies for many decades [128]. The presence of the large numbers of the MRs on the surface of macrophages and DCs is known to be evidence for their significant role in antigen presentation [192, 267].

The MR contains eight extracellular CRDs and the conformation of these CRDs has been shown to play an important role in the recognition of glycosylated ligands [25, 31, 268]. The structural properties of the MR CRDs have been studied extensively, but the relationship between the antigen and receptor binding and recognition, and the properties that preferentially target the antigen towards this receptor are lesser known [12, 269, 270].

Glycosylation, in particular mannosylation, has been shown to be an effective method for the targeting of antigenic peptides or protein vaccines to the MR, increasing the vaccines antigenic potential by enhancing uptake and processing by APCs [13, 25, 271]. Although the exact binding requirements of the MR remain to be elucidated, studies aimed at targeting this receptor have reported that poly-mannan derivatives, mannosylated dendrimers, and compounds that mimic a dendritic branched structure, known as the cluster effect, were often found to be antigenic [12, 121, 216]. Furthermore, it was shown that branching, multimerisation, and the number of mannose moieties all affect receptor binding [12, 121, 216]. In 2008, Kowalczyk *et al.* showed that bis-mannose compounds that contained a PEG spacer were taken up by human monocytes better than mono-mannosylated compounds. However, they also identified a mono-mannosylated compound that showed similar binding, suggesting that the incorporation of a second mannose group in the peptide

chain was not essential [77, 131]. Studies by Frison *et al.* showed that the linear arrangement of the MR's CRD (**Chapter 1, Section 1-3, Figure 1-3**) led to specific and high affinity binding between the MR and synthetic compounds that contained di-mannose clusters and/or end-standing single mannose units [12, 121]. The MR has been shown to bind to mannosylated ligands with different branching and spacing arrangements in the presence of other functional groups. Nevertheless, the exact binding requirements of the MR have not been clearly defined [12, 269].

This chapter presents an *in vitro* investigation into the effect the distance between the mannose units has on receptor-mediated binding and uptake by APCs. Here, a library of *O*-mannosylated lipopeptides that contain a linear arrangement of mannose and the model $CD4^+$ antigen and $OVA_{323-339}$ (**Chapter 3**, **Figure 3-1**) were synthesised as detailed in **Chapter 3**.

In the present work, these vaccine constructs were designed to mimic the linear arrangement and *O*-linked properties of glycoconjugates found in nature [272]. Studies on structural properties of such *O*-glycans was discussed in **Chapter 1, Section 1.6**. Here, an alanine spacer was inserted between the mannose units to study the structural properties of the mannosylated vaccine in relation to APC uptake. The alanine spacer was chosen as previous studies had reported that the distance between the mannose groups played an important role in the uptake of mannosylated compounds through the MR on monocytes [12, 131, 269]. In a study by Kowalczyk *et al.*, the optimal uptake of mannosylated compounds was achieved when three alanine amino acids were inserted between the linearly attached *O*-mannose groups compared with structures with greater numbers of spacers between the mannosyl groups [130]. In addition, two mannose units have been included in each vaccine construct in this study, as previous studies have shown that synthetic constructs that contained two mannose units could target the MR with high affinity confirmed by a higher level of uptake [12, 77, 206, 269]. Additionally, shorter spacers between the mannose units have been shown to be effective at targeting the MR [206]. Therefore, this aspect was investigated relative to the presence of lipids and a peptide antigen, which are known to enhance self-adjuvanting properties and induce particulate formation [9, 12, 206]. Amphiphillic moieties have been shown to enhance nanoparticle formation and the change in nanoparticle size was found to affect uptake [214].

$CD11c^+$ (a common discriminator of spleen-derived DCs from other APCs found in the spleen) and $F4/80^+$ (a common discriminator of spleen-derived macrophages from other APCs found in the spleen) cells from splenocytes were used to study the uptake of the vaccine constructs *in vitro* using confocal microscopy and flow cytometry. Further, SPR was optimised and used to study the specific binding properties and i*n vitro* T cell proliferation was studied as a preliminary indication of

immunomodulatory properties of vaccine constructs. The studies presented here are based on the *in vitro* targeting of the mannosylated lipopeptide vaccines **13-18** and their synthesis procedure is described in **Chapter 3**.

4.2 Results and Discussion

4.2.1 Flow cytometry cell uptake study

DCs capture, process and present antigens to naive T cells. Antigen presentation by DCs develops in the context of MHC I and II, however, the resulting immune response, to a large extent, depends on the identity of the antigenic moiety [17]. Factors including the type of targeted receptor on the DCs and the presence of adjuvant on the delivered antigen can both affect the final immune response [273]. Spleen-isolated DCs are heterogeneous and two subsets of DCs are identified by their surface markers (subset 1: $CD11c^+$, $DEC\text{-}205^+$, $CD24^+$, $CD11b^-$, $33D1^-$, $CD4^-$; and subset 2: $CD11c^+$, $DEC205^-$, $CD24^-$, $CD11b^+$, $33D1^+$, $CD4^-$). However, both subsets are known to express CD11c [274]. $CD11c^+$ DCs are commonly studied for their antigen uptake ability. In a study by Bond *et al.*, it was shown that $CD11c^+$ DCs had a higher ability of antigenic uptake compared with other dermal DCs. In their study, they compared fluorescently labelled OVA protein and dextran to track the ability of different human DCs in antigenic uptake [275]. They found that $CD11c^+$ DCs had a significantly higher ability in the uptake of fluorescently labelled OVA and dextran, when compared to other subsets of DCs from skin [275] . In another study by Narenderan *et al.*, it was shown that DCs were a better target for mannosylated-antigenic uptake than peripheral monocytes [276]. Here, they found that mannosylation of proinsulin antigen did not improve T cell proliferation but was able to increase the uptake of autoimmune antigens. F4/80 is known to be highly expressed on tissue macrophages, including macrophages found in cells isolated from the spleen [277]. Hu *et al.* chose the $F4/80^+$ subset of macrophages to study the T cell activation by macrophages. They found that macrophages have different subsets and their T cell activation ability varies due to their different surface receptors [278]. Overall these studies indicate the importance of $CD11c^+$ and $F4/80^+$ cells and the vital role they have in antigen uptake for advancing vaccine development.

In vitro uptake and targeting of the mannosylated vaccine constructs (**13-18**, **Chapter 3**, **Figure 3-1**) were tested using two subsets of APCs ($CD11c^+$ DCs and $F4/80^+$ macrophages) isolated from the spleens of naive C57BL/6 mice (Figure 4-1). Cells were isolated as a mixed population of APCs, including macrophages and DCs, using a standard protocol [215] and were used immediately. Fluorescently-labelled vaccine constructs (0.5 µM) dissolved in PBS were added to the isolated cells and allowed to incubate for 4 h before washing the cells to remove any excess or non-specifically

bound compound. The washing step in this procedure is known to remove unbound peptides from the surface of the cells [161, 279]. The vaccine constructs were labelled with a fluorescent tag (FAM) to facilitate cell tracking. Cells were then stained with anti-CD11c and anti-F4/80 antibodies which bound to cells that contained CD11c and F4/80 markers. CD11c is present in high levels on DCs and F4/80 on macrophages [280, 281]. Dextran has been shown to bind strongly to the MR and was used as a positive control for both subsets of cells [282]. The concentration of each vaccine construct was optimised (data shown in Appendix 15).

Changing the distance between the mannose moieties from no alanine units (**13**, Figure 4-1) to two alanine units (**15**, Figure 4-1) resulted in a negligible difference in uptake by both $CD11c^+$ and $F4/80^+$ cells (Figures 4-1A and 4-11B, respectively). Results also confirmed a higher level of uptake by **13-16** in $CD11c^+$ positive cells compared to $F4/80^+$ cells. Here, vaccine constructs **16-18** are controls designed with only lipids (**16**), only mannose moieties (**17**) and no mannose or lipids (**18**). However, a significantly lower binding was observed in both subsets of cells for the control peptides **16-18** that contained no lipid and/or no mannose moieties (Figures 4-1A and B).

Mannan is a known ligand of the MR [216]. Mannan is a polycarbohydrate with the ability to block the uptake of the vaccine constructs by saturating the receptors involved in their uptake [283, 284]. A mannan inhibition study was performed to confirm receptor-mediated uptake of the constructs on the surface of $CD11c^+$ and $F4/80^+$ cells. Following pre-incubation of the cells with mannan (1 mg/ml), the cells were incubated for 4 h with the vaccine constructs (**13-18,** 0.5 µM) before separately washing and staining the $CD11c^+$ or $F4/80^+$ cells (Figure 4-1).

Flow cytometry results showed a significant reduction in the uptake/binding for all constructs when the cells were pre-incubated with mannan (Figure 4-1), implying that mannan specifically blocked the receptor-mediated uptake of these compounds. A significant difference in mannan inhibition studies was observed in the binding and/or uptake of constructs **13-15** in both $CD11c^+$ and $F4/80^+$ cells with increased binding observed when a longer spacer was employed between the mannose units. However, no significant difference was observed for constructs **13-15** in the binding and uptake studies in the absence of mannan (Figure 4-1). From these lipidated and mannosylated constructs (Figure 4-1), binding inhibition in the presence of mannan was higher for construct **15** compared with constructs **13** and **14**. It could only be concluded that **15** is the best mimic of mannan for $CD11c^+$ and $F4/80^+$ cells (**15**, Figures 4-1A and B). Interestingly, even the constructs that contained no mannose units in their structure (**16** and **18**) had a lower uptake in the competition assay, indicating that the peptide and/or lipids have non-specific binding and/or uptake into these cells (Figure 4-1), although

in the case of **14**, this difference was not significant. It has been shown that lipids can target and bind the CRDs on the CLRs [285]. Unlike **15** (lipids present in the structure) whose high binding ability was significantly inhibited in the presence of mannan, the binding of **17** (no lipids) was not inhibited (Figures 4-1A and 4-1B). This indicated that lipids, and not the antigen, directed the binding and uptake of the tested cell lines.

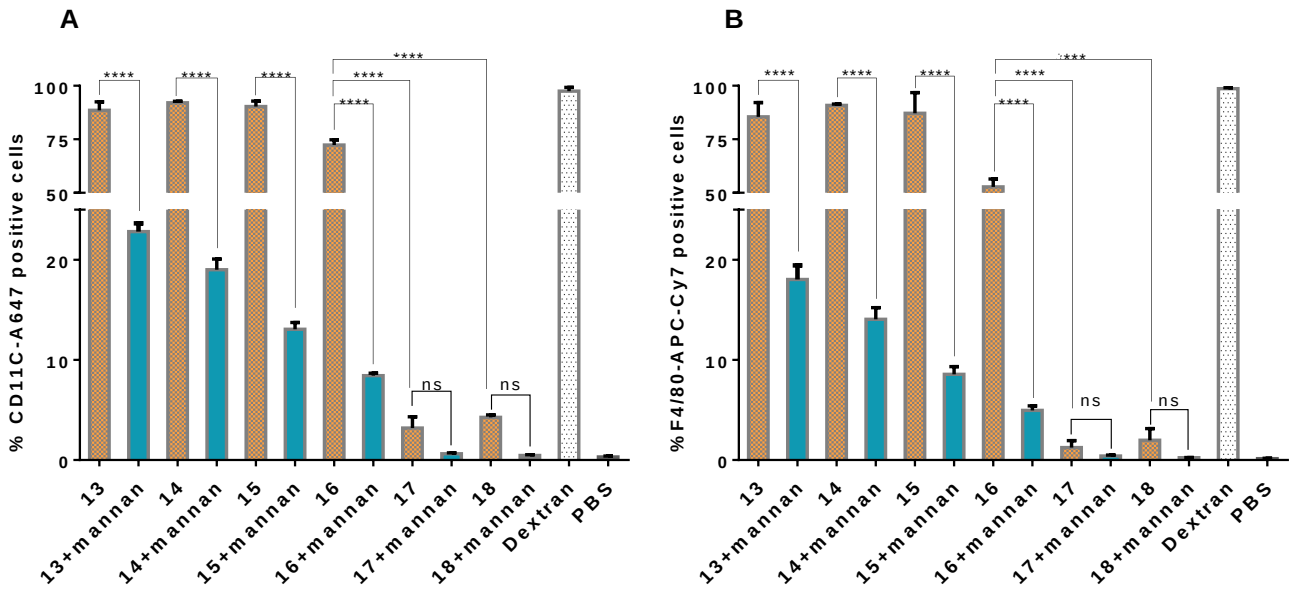

Figure 4-1. ***In vitro*** **uptake/binding and mannan competition study**, Vaccine constructs **13-18** (0.5 µM) and control constructs **16-18** (0.5 µM) were assessed in (A) $CD11c^+$ and (B) $F4/80^+$ cells for uptake in the presence or absence of mannan (construct + mannan [1 mg/ml] vs construct alone). Dextran-FITC (1 mg/ml) was the positive control. PBS was the negative control. The study was performed in triplicate and the results were analysed using one-way ANOVA with mean ± SD from three independent experiments, $p<0.0001$.

The results showed that the uptake of vaccine constructs that contained both mannose and lipid moieties (**13-15**, Figure 4-1) was higher than that of constructs that contained no lipids (**17**) or no lipid and mannose moieties (**18**). However, **16** that did not have any mannose units in its structure had a higher uptake than **13** or **14**. The addition of hydrophobic moieties (such as lipids) has been shown to increase non-specific binding to the surface of cells, which could account for the higher level of cell-binding observed for **16** (Figure 4-1) [255]. The non-specific binding observed for peptide **16** could be associated with the affinity of the vaccine candidates for non-CLRs (including TLRs) as previous studies on lipidated peptides have confirmed this finding [178]. The mannan inhibition study indicated that receptor-mediated uptake through a mannan-inhibited receptor (e.g. MR) is likely. However, as uptake was not completely inhibited, other receptors and mechanisms

contributed to the uptake [286]. Overall, results from this study suggest that both mannose and lipids play important roles in the uptake of vaccine constructs, with both structural features affecting receptor-mediated uptake.

4.2.2 Confocal imaging

Confocal imaging was used to confirm the uptake and/or binding of the vaccine constructs to F4/80$^+$ cells. Constructs **13**, **15** and **16** (0.5 µM) were incubated with cells for 4 h followed by staining with an anti-F4/80 antibody. The cell nucleus was stained with Hoechst stain. Mannan-FITC was used to show the association of mannan to the cell-surface receptors (Figure 4-2A).

The results showed that construct **13** was localised both at the periphery of the cell and inside the cell, shown as punctate granules in the cytoplasm (Figure 4-2B). This was consistent for vaccine construct **15** (Figure 4-2D). Construct **16** showed primarily peripheral localisation that confirmed non-specific binding to the surface of the cells hypothesised in the flow cytometry uptake results (Figure 4-2E). To confirm receptor-mediated uptake, cells were pre-incubated with mannan (20 times excess to make sure that all lectin receptors were saturated as per previous studies done on mannan inhibition) before incubation with **13** [283]. Pre-incubation significantly reduced the uptake with the compound predominantly localised on the cells' surface (Figure 4-2C). This correlated with the mannan competition assay results reported in Figure 4-1. Here, differences observed in the light emission by **15** when compared to **13** can be associated to resolution limitations in confocal microscopy [287].

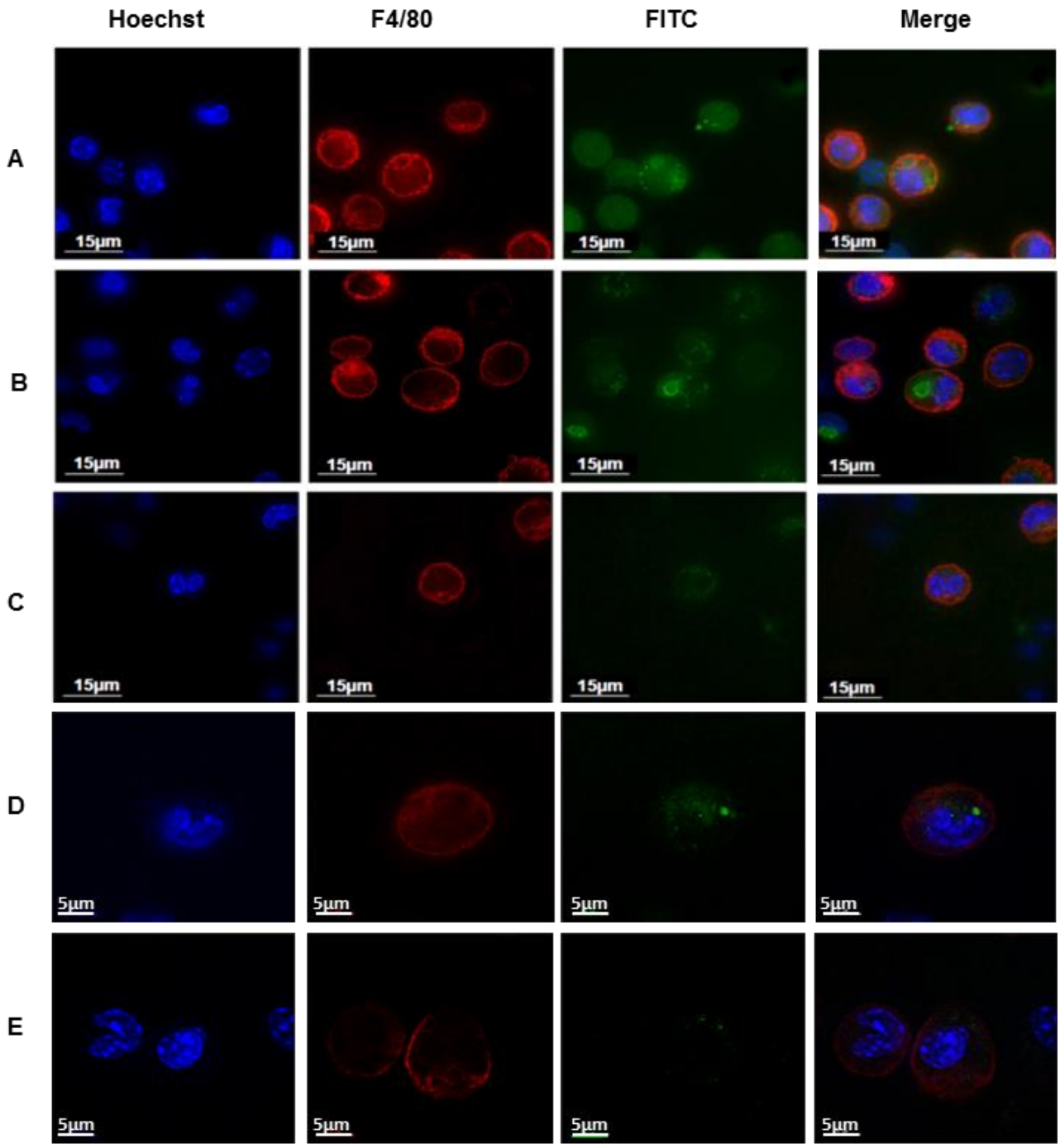

Figure 4-2. Confocal images, F4/80^{+} cells (2×10^{5}) were incubated with vaccine constructs **13**, **15** and **16** (0.5 µM) in the presence or absence of mannan, with commercially available mannan-FITC as the positive control. Cells were plated on culture slides. FAM-labelled vaccine constructs (green) were added to the cells and incubated in the presence and absence of mannan for 4 h at 37°C. Nuclei were stained with Hoechst stain (blue). F4/80^{+} cells were identified with anti-F4/80 antibody (red). (A) mannan-FITC; (B) vaccine construct **13**; (C) cells pre-incubated with mannan followed by addition of **13**; (D) vaccine construct **15**; (E) vaccine construct **16**. Analysis was performed on a GE

DeltaVision Deconvolution confocal microscope at 60x using oil immersion, graphical scales 15µm and 5µm.

4.2.3 OT-II splenocyte proliferation assay

OVA-specific, αβ T cell receptor (T cell receptors that have αβ domain of T cell receptor) transgenic mice (OT-II mice) were used to investigate whether uptake of constructs **13-18** caused *in vitro* T cell proliferation. T cells obtained from OT-II mice spleens express transgenic OVA-specific αβ T cell receptors and are designed to recognise the $OVA_{323–339}$ peptide fragment from the OVA antigen for a T cell dependant B cell activation [288]. When APCs take up and process antigenic peptides they present the antigenic components through MHC molecules. T cell activation occurs when they interact with these antigenic fragments. This activation results in cytokine production and T cell proliferation [245]. A successfully designed immunological vaccine requires being uptaken and further presented to T cells by APCs. In this *in vitro* assay the proliferation of OT-II mice spleen T cells was measured in response to different dilutions of constructs **13-18** (Figure 4-3).

Results showed that all constructs had higher proliferation properties compared to the $OVA_{323-339}$ peptide, with constructs **13**, **15** and **16** stimulating the highest effector T cell proliferation (Figure 4-3). This confirmed the previous results where constructs **13-16** had the highest receptor-mediated uptake (Figure 4-1). Here, it was further concluded that constructs **13-15** had a tendency of showing differences in T cell stimulation due to their structural differences. However, T cell proliferation seems to be independent of the presence of mannosyl moieties and probable structural conformations had played a more important role on the T cell activation. There have been many recent studies that have indicated that although the presence of mannosyl moieties could increase the uptake in APCs, T cell activation is mostly dependant on the antigen type and the adjuvanting moiety [9].

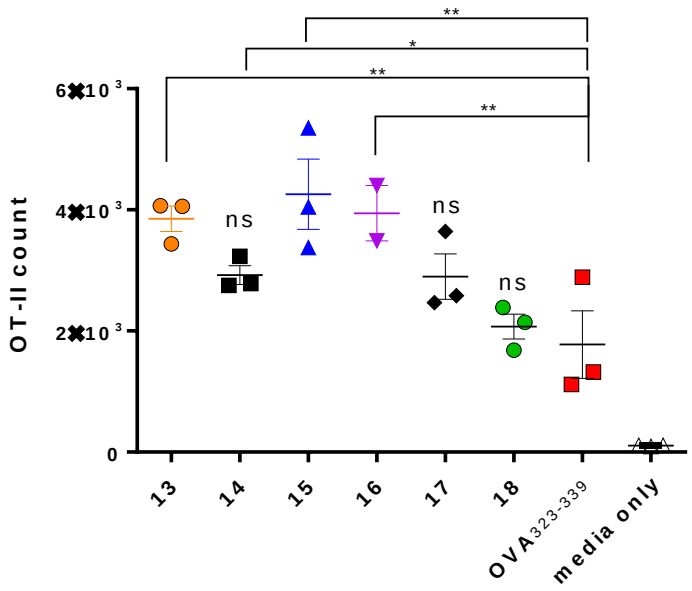

Figure 4-3. *In vitro* OT-II spleen proliferation assay. Different dilutions of constructs **13-18** and control peptide, $OVA_{323-339}$ were compared for their ability to stimulate T cell proliferation (5×10^5 cells per well). PBS was used as the negative control. The study was performed in triplicate and the results were analysed with mean ± SD from three independent experiments, $p < 0.0001$.

4.2.4 Real-time surface plasmon resonance (SPR)

SPR is a technology developed to study molecular interactions. Measuring kinetic constants by optical biosensors based on molecular interactions is a common valid method applied in many studies [287, 289, 290]. Among these presented studies, Biacore appears to be the most widely used instrument to assess binding affinity of variable constructs [287].

The SPR method used in the Biacore machine includes immobilisation of a ligand (in this case, the mannose receptor) onto a chip surface, then passing an analyte (in this instance the vaccine constructs) over this chip in which the resulting interactions and bindings can be studied with a high level of detectability. SPR answers many questions, including the specificity of molecular interactions identified through the extent of binding, and it also provides the affinity of an interaction through time response curve results (Figure 4-4).

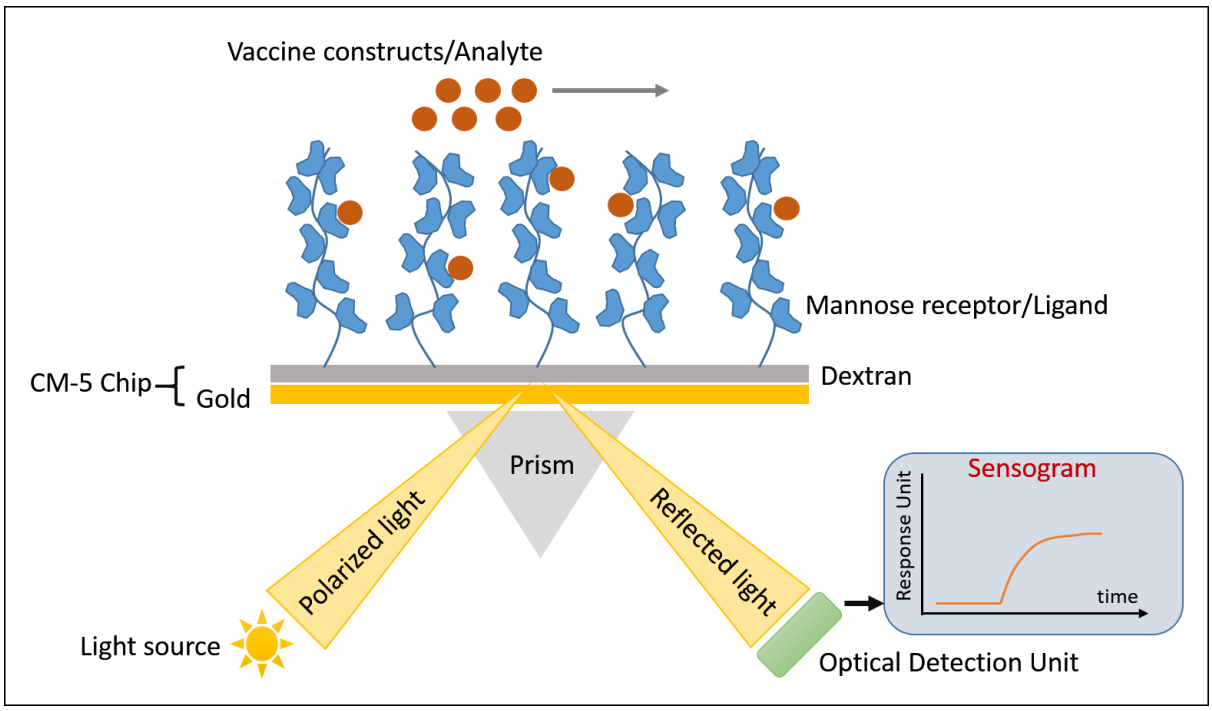

Figure 4-4. Schematic diagram of SPR performance on a CM-5 chip. CM-5 chips have a dextran surface that enables ligand (the mannose receptor in this study) immobilisation on the surface. The analyte (vaccine constructs in this study) are allowed to pass over the ligand and the resulting interaction and/or binding causes a change in the reflected light from the gold layer on the chip's surface (below the dextran). The optical detection unit converts changes in this reflected light to a readable time-response sensogram. The light source used is plain polarised light.

The advantage of SPR compared to some of the other methods available (e.g. ELISA) for ligand binding interactions, includes having less steps and faster results, however, experimental execution can sometimes be a challenge [291]. SPR is based on changes in the refractive index of a gold plate due to surface absorption or desorption (Figure 4-4). Here, changes in the electromagnetic properties of the metal surface allow evanescent wave absorption. Light wave coupling to the surface is the method used in a Biacore machine for measuring the angle of light that strikes the surface and resonance occurs. This method is called resonant wavelength SPR [292]. Here reflected light from a metal surface gives a graph (sensogram) that can be analysed for the binding properties of the analyte with ligand depending on the intensity of the reflected light. A sensogram is based on the level of interaction response unit (RU) against time. Analysis of this SPR sensogram provides information on the binding affinity (K_D) of an analyte to an immobilised ligand on the surface of the chip [292]. The following sections describe the method development studies performed in this study to investigate the interaction of the vaccine constructs with the mannose receptor using Biacore SPR technology, and the results from this investigation.

4.2.4.1 Method development

SPR was performed on a BIAcore 3000 system. Here, three major steps were used to measure the binding affinity of the vaccine constructs to the receptor bound to the chip's surface. Step 1: immobilisation method used to bind the MR to the chip's surface; step 2: surface performance was used to check receptor binding viability and regeneration scouting was performed to find the best condition for reviving the receptor after each binding; and step 3: affinity measurements were performed to measure binding affinity of vaccine constructs **13-18** (Figure 4-5).

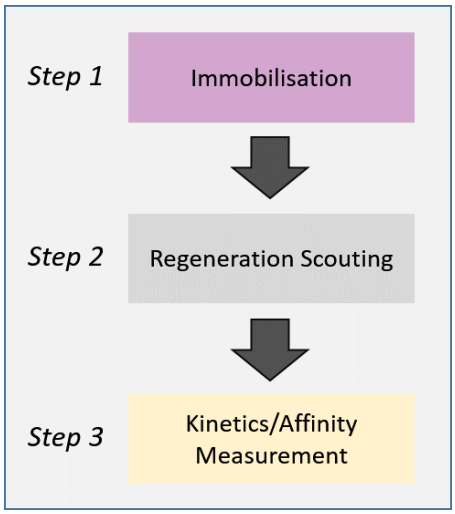

Figure 4-5. Method development steps. Three steps were taken for method development to ensure accurate measurement of the vaccine constructs to the receptor. Step 1: the MR (ligand) is immobilised on the chip's surface; step 2: surface performance and regeneration scouting are performed to investigate receptor viability and regeneration condition; and step 3: kinetics and affinity measurements are performed to measure binding affinity of vaccine constructs 13-18 (**Chapter 3, Section 3.2.4, Figure 3-11**).

4.2.4.1.1 Step 1: immobilisation

Recombinant human macrophage mannose receptor (MMR, Catalogue number 2534-MR/CF) was immobilised on a CM-5 research grade sensor chip containing a carboxymethylated dextran surface using a standard amino-coupling method (Figure 4-6). Running buffer used in this experiment consisted of HEPES (4-(2-hydroxyethyl)-1-piperazineethanesulfonic acid, 10 mM), $CaCl_2$ (1 mM), $MgCl_2$ (1 mM), $NaCl_2$ (150 mM) and 0.005 % surfactant P20 all in deionized water at pH 7.5. The receptor was dissolved in sodium acetate buffer (20 µg/ml) and immobilised at 10 µl/min for 7 min on a flow cell. Gustafson *et al*. found acetate buffer (pH 4.5, 10mM) to be a suitable buffer for running the MR [293]. In general, the pH of the immobilisation buffer should be low enough to ensure electrostatic adsorption of the ligand (here the MR) onto the chip's surface is achieved [294]. In this

reaction, the primary amino-groups on the recombinant MR protein are covalently bound to the carboxyl groups on the dextran-coated chip (Figure 4-6).

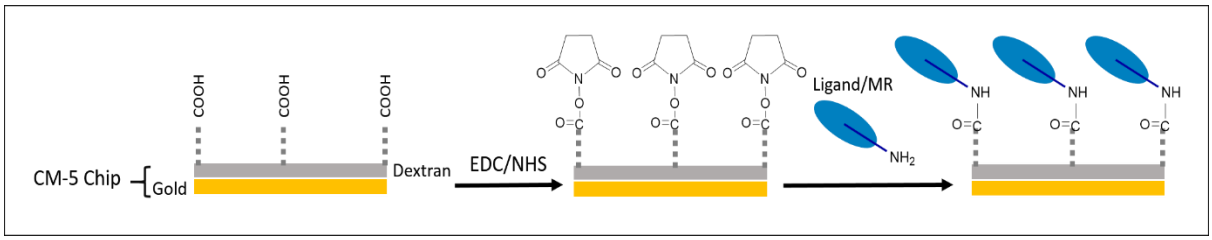

Figure 4-6. Amine coupling of the MR onto the CM-5 chip. Free carboxylic groups on the dextran-coated CM-5 chip are pre-activated using EDC and NHS (these two provide crosslinking ability by activating the carboxyl groups) to enable covalent binding of the ligand (MR) through the ligands free NH_2 groups.

The immobilisation method consisted of a binding scouting stage (Figure 4-7A) where the Biacore instrument measured the binding ability of the receptor to the dextran surface on the chip without preliminary activation (Figure 4-7A). The second stage was removal of bound receptors with a short injection of ethanolamine (Figure 4-7B). The third stage was surface activation with NHS:EDC at a 1:1 ratio (Figure 4-7C) followed by the fourth stage which was a receptor injection for achieving the desired binding level which here is about 2000 RU. Finally, the un-functionalised active groups from dextran were deactivated using ethanolamine (20 µl/min) for 7 min (Figure 4-7D). The amount of binding of the MR to the chip was calculated by subtracting the baseline at the end of cycle (Figure4-7F) from the starting baseline.

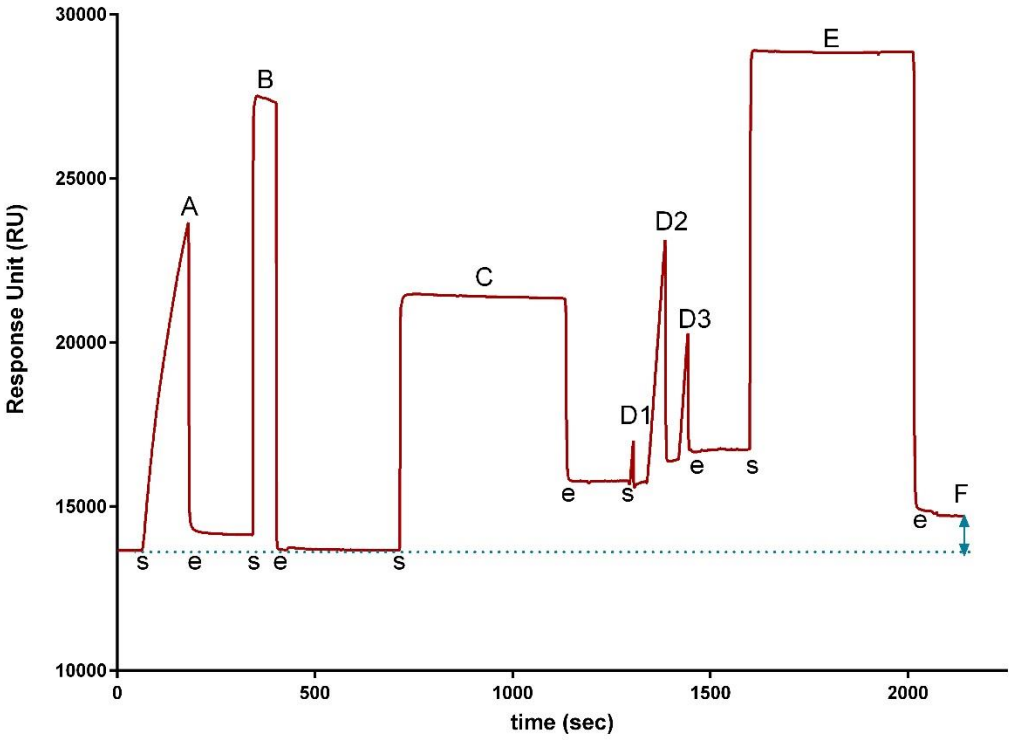

Figure 4-7. Mannose receptor flow cell immobilisation trace. (A) The MR dissolved in acetate buffer is run over the surface of the chip without pre-activation to scout the level of binding affinity the receptor has for the un-activated dextran ; (B) a solution of ethanolamine is run over the chip's surface to remove any unbound MR from step (A); (C) the dextran surface of the chip is activated with a solution of NHS:EDC; (D1-3) the MR dissolved in acetate buffer is run over the surface of the pre-activated chip in three pulses to reach the desired level of binding (in this instance it is 2000 RU); (E) ethanolamine is run over the chip to remove any excess MR that is not chemically bound from the previous step; and (F) the actual level of MR immobilisation is calculated and compared to the starting baseline level (1850 RU). Letters 's' and 'e' signify the start and end of each injection on the machine, respectively.

A reference flow cell was then activated using NHS:EDC but the surface was blocked using ethanolamine without any receptor binding (Figure 4-8). For each SPR cycle, two flow cells (reference flow cell and MR flow cell) were used concurrently to ensure that during the affinity measurements the results were not affected by non-specifically bound analyte found in the buffers, and that the results could be normalised between runs. This normalisation was performed through the deduction of results obtained in the reference flow cell (without the MR) from the MR flow cell (containing the MR), which are presented as the affinity results in this study.

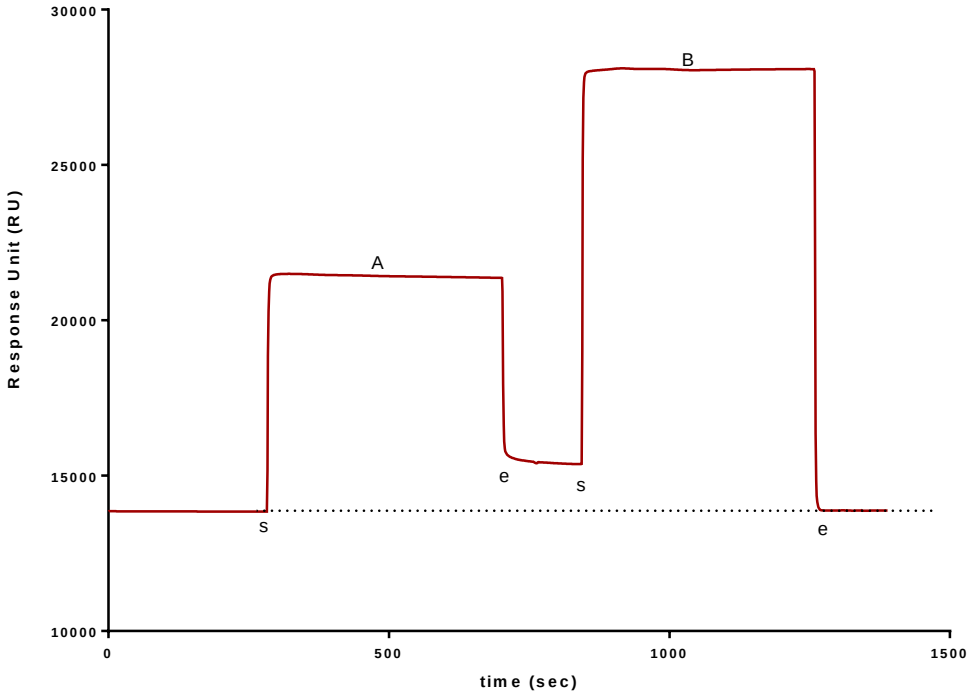

Figure 4-8. Reference flow cell immobilisation trace. (A) The dextran surface on the CM-5 chip is activated using a solution of NHS:EDC, and (B) a solution of ethanolamine is run over the chip's surface to block the activated sites. The treated reference flow cell is used as a reference flow cell to normalise the results from the mannose receptor (MR) flow cell. Letters's' and 'e' signify the start and end of each injection on the machine, respectively.

4.2.4.1.2 Step 2: Surface performance and regeneration optimization

A general SPR sensogram consists of (A) a starting baseline, (B) binding/association, (C) dissociation, (D) regeneration, and (E) final baseline as shown in Figure 4-9.

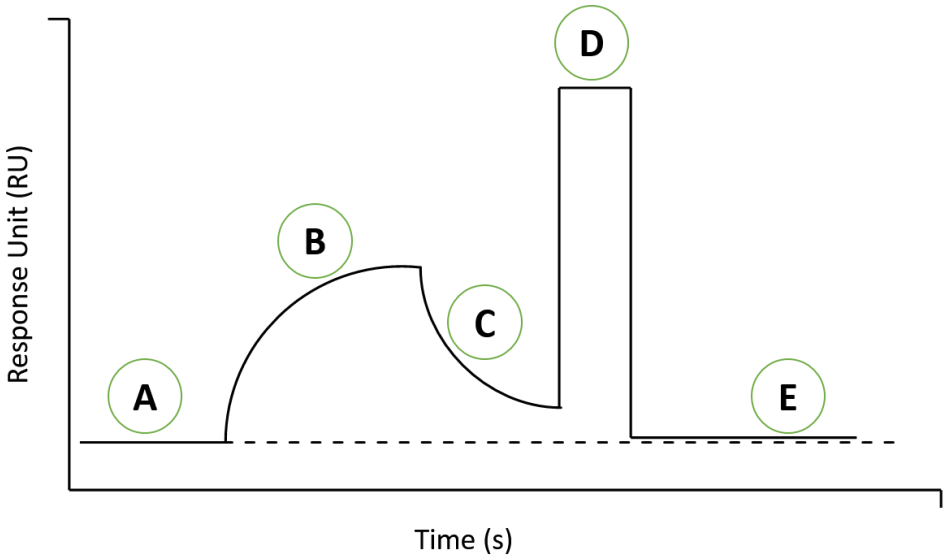

Figure 4-9. Schematic trace of a surface performance resonance sensogram. (A) starting baseline showing the flow of the running buffer; (B) binding response caused by binding of an analyte to the immobilised ligand (here mannose receptor); (C) dissociation of the analyte from the ligand attributed to a change in the running buffer; (D) regeneration of the ligands surface (removal of all the analyte) by changing the conditions of the buffer (acidic, basic, ionic); and (E) final baseline following regeneration to ensure it is the same as the starting baseline observed in step (A).

Here, a starting baseline is identified by exposing the chip to the running buffer and ensuring no binding or association is observed (Figure 4-9A). The analyte dissolved in the running buffer is then run over the bound ligand to measure binding and affinity (Figure 4-9B). It is important to dissolve the analyte in running buffer that is the same as the buffer that runs over the flow cells, since differences in the two can result in shifts in the sensogram [294]. Choice of running buffer is also very important since it has a role in keeping the immobilised receptor in natural condition [295]. After this association step (Figure 4-9B), the machine stops the analyte injection and the bound analyte starts to dissociate from the ligand in the presence of running buffer. This stage is called dissociation (Figure 4-9C). A regeneration step is required to detach the receptor from any bound analytes to enable the chip to be used a number of times for the same and/or different analyte samples (Figure 4-9D). In this case, the baseline should return to the initial level (Figure 4-9E). Optimisation of the regeneration conditions is discussed by applying different regeneration solutions with different pHs as shown in Table 4-1.

Table 4-1. Regeneration scouting solutions

Regeneration Solution	pH
Sodium dodecyl sulfate (SDS)	Ionic
NaOH 10 mM	9.5
Glycine 10mM	2.2

A surface performance test is an essential method to understand the affinity of a targeting moiety. In this study, a surface performance test was performed using mannan (10 µg/ml), a known MR binding ligand, to check the receptor activity following MR immobilisation [296]. Regeneration is an important step in which the receptor is revived from previous binding to be prepared for a new binding cycle [297]. It is essential to have a baseline at the same level of the initial baseline following each regeneration, otherwise, the next measurement cycle is inconsistent and the results cannot be trusted [294]. Here, acidic, basic and ionic regeneration solutions were used to find the optimal conditions for regenerating the MR following MR binding to the constructs (Table 4-1).

As shown in Figure 4-10, following mannan (10 µg/ml) injection (Figure 4-10B) and surface regeneration with a 0.05% solution of SDS (Figure 4-10C), the end baseline level (Figure 4-10D) was compared to the start baseline (Figure 4-10A). The results show that mannan had a binding level of 25 RU which, at the end point of the injection of mannan injection, only 50% of the total binding was lost in the dissociation phase (where only running buffer passes over the MR, Figure 4-9C) while regeneration with SDS (0.05%) was not able to cause any further dissociation. The importance of a successful regeneration solution is based on the fact that a change in the level of baseline is carried forward into the next cycle of measurement and thus having an unstable baseline affects the results [294].

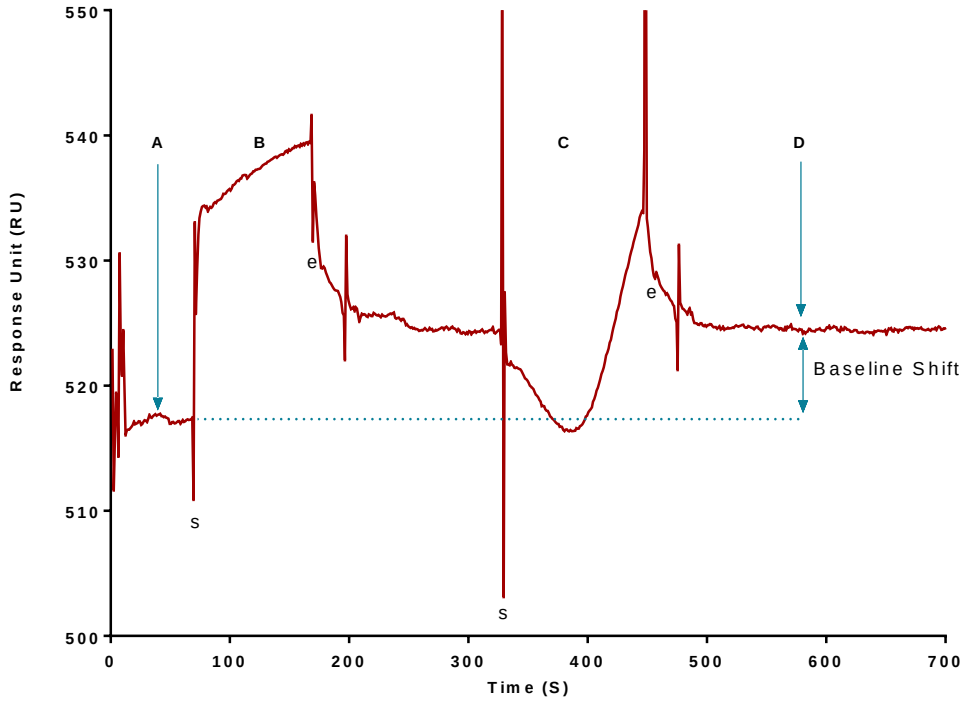

Figure 4-10. Regeneration scouting using sodium dodecyl sulfate (SDS 0.05%). An ionic solution of SDS was used as the regeneration solution to assess the MR affinity measurements. (A) the sensogram baseline from the continuous flow of a buffer at 40 µl/min; (B) mannan (10 µg/ml) binding response showing 25 RU; (C) regeneration of the MR by 0.05% SDS solution; (D) an increase in the baseline level is observed following regeneration showing that this was not a successful regeneration. Letters ‘s’ and ‘e’ signify the start and end of each injection by the machine, respectively.

As shown in Figure 4-10, regeneration using SDS (0.05%) was unable to remove mannan, while regeneration using stronger basic conditions (NaOH, pH 9.5) caused a down drift in the baseline

(Figure 4-11) due to potential denaturation of the MR protein and loss of receptor activity (Figure 4-12).

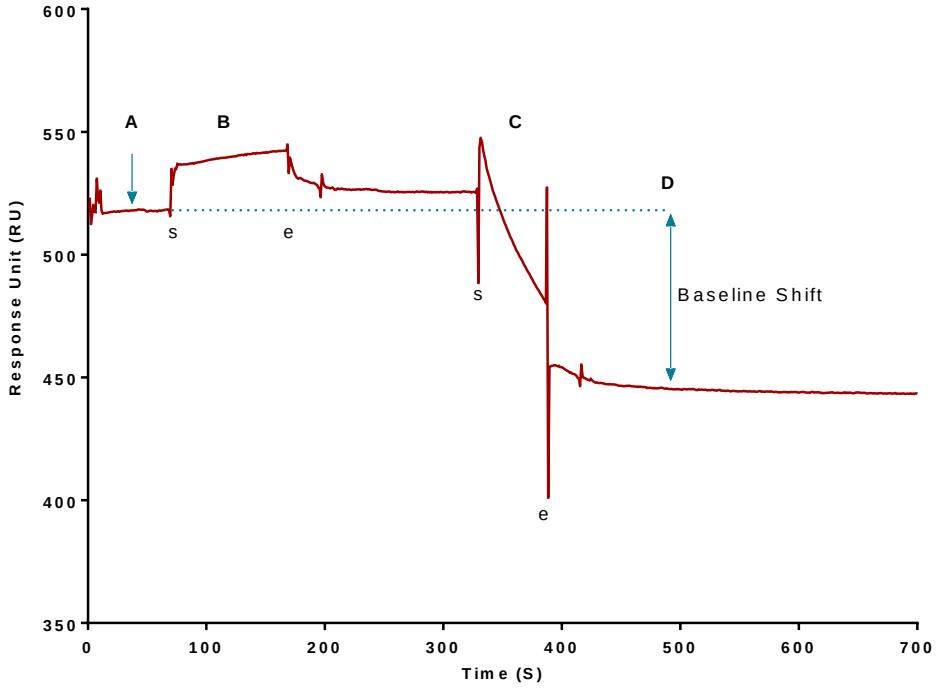

Figure 4-11. Regeneration scouting using NaOH. A solution of NaOH (pH 9.5) was used as the regeneration solution to assess the MR affinity measurements. (A) The sensogram baseline from the continuous flow of a buffer at 40 µl/min; (B) mannan (10 µg/ml) binding response showing 25 RU; (C) regeneration of the MR using 10 mM NaOH (pH 9.5) solution; (D) a 60 RU down shift in the baseline was observed due to unsuccessful regeneration. Letters ‘s’ and ‘e’ signify the start and end of each injection by the machine, respectively.

Another attempt at regeneration scouting was performed using NaOH (10 mM, pH 9.5). A surface performance test was performed using mannan as the standard ligand for the MR (Figure 4-11) to check the surface activity of the MR protein. The observed results showed a lack of receptor activity, and this was potentially due to denaturation of the receptor protein due to the high pH conditions of regeneration with NaOH (Figure 4-12). Olson *et al.* have shown that conformational changes happen in the MR CRDs at pHs over 7.5, and they predicted no binding would occur at that pH, however, they did not perform SPR studies [298].

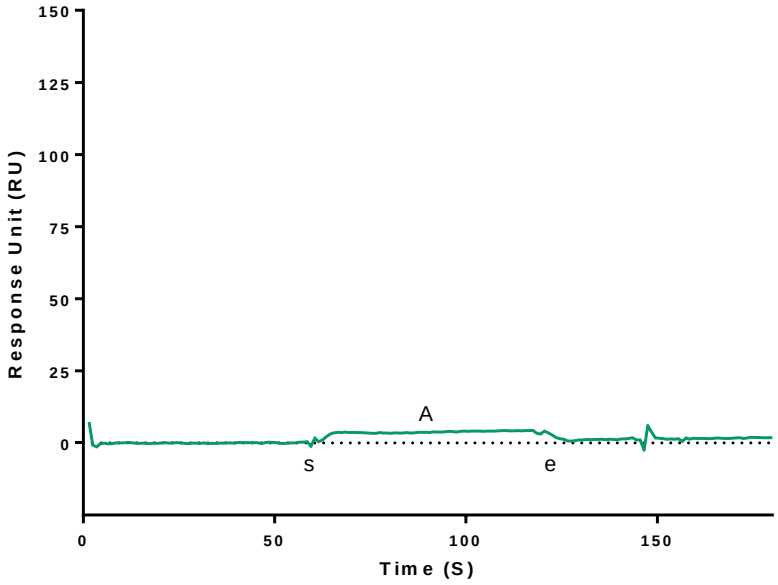

Figure 4-12. Lack of receptor activity following regeneration with NaOH. (A) No binding (an RU of less than 5) was observed when the MR bound to the chip was exposed to mannan (10 µg/ml). This correlates with previous results where the use of a high pH regeneration buffer (10 mM, NaOH, pH 9.5) was shown to change the baseline dramatically. Letters 's' and 'e' signify the start and end of each injection by the machine, respectively. *Note*. the sensogram regeneration stage is not shown.

As a result of a lack of receptor activity, this particular flow cell could no longer be used and a new flow cell was loaded with the MR. Here, glycine buffer (10 mM, pH adjusted to 2.2 using HCl) was used for receptor regeneration following mannan binding. As observed in Figure 4-13, using this glycine buffer as the regeneration solution showed little change in the end baseline when compared to the start baseline (Figure 4-13). This confirmed a successful MR regeneration condition and was used throughout the rest of the study for regeneration of the receptor between individual runs.

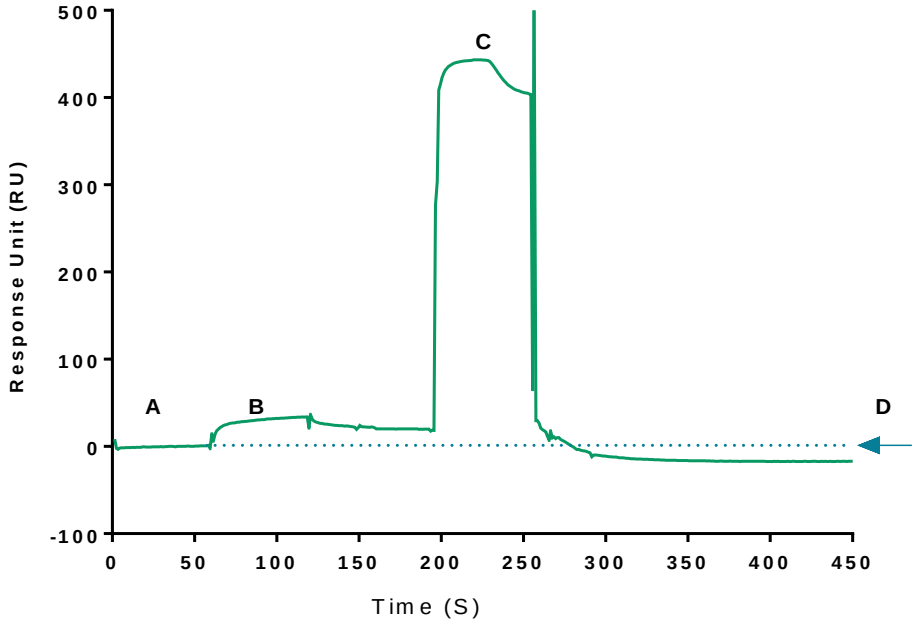

Figure 4-13. Regeneration scouting using glycine buffer. A glycine buffer (10 mM, pH 2.2) was used as the regeneration solution to assess the MR affinity measurements. (A) The sensogram baseline from continuous flow of the buffer at 40 µl/min; (B) mannan (10 µg/ml) binding response showing 25 RU; (C) regeneration of the MR using glycine buffer (10 mM, pH 2.2); (D) a small shift in the baseline (± 15 RU) was observed between the baseline at D and the baseline at A.

It was concluded that due to the properties of the MR protein (180 K_D, with multiple binding sites) an acidic pH is the best condition for regenerating the protein binding sites. Optimisation of the regeneration buffer has rarely been presented in studies but there are studies that have used different conditions on the MR. Gustafsson *et al.* reported studies on human recombinant MR using glycine buffer (pH 2.2) for receptor regeneration following affinity measurements using *O*-glycan proteins extracted from *P. pastoris* (yeast) [293]. In another study, Duverger *et al.* used domains 1–8 of the human macrophage MR to study the carbohydrate-lectin interaction. Here, a 0.3 M α-methyl mannoside was added to the running buffer and used as the regeneration solution [294].

4.2.4.1.3 Step 3: Binding affinity measurement

The recombinant MR has 8 CRDs (**Chapter 1**, **Section 1-3, Figure 1-3**) that have been proven to have one (or two binding motifs) involved in the binding of carbohydrates [293]. The relative distance between the two mannose moieties in each construct and the presence (or absence) of lipids on the constructs affect the binding ability to this recombinant human macrophage MR protein. This was investigated and affinity measurements (K_D) describe the binding of a ligand (MR) to an analyte (vaccine constructs **13-18**).

A concentration dependant binding affinity measurement was carried out using mannan as a positive control for comparing the binding affinity of vaccine constructs **13-18** (Figure 4-15). Five concentrations (Figure 4-15A) were chosen to run affinity measurements where Rmax was reached at 600 µg/ml with 47 RU (Figure 4-15A). To plot a steady state affinity graph it is necessary to run affinity measurements for different concentrations of mannan (Figure 4-15A). Additionally, as detailed above, a glycine buffer was used between each cycle, as this buffer was optimised and shown to give the best results for regeneration of the MR receptor.

Binding interactions between the ligand (MR) and analyte (vaccine constructs) occur in two steps. In the first step known as 'mass transfer', the analyte diffuses from the buffer to the surface of the chip [299]. The second step is when the actual binding occurs. Mass transfer is one of the limiting factors in the application of SPR when the analyte concentration is too high and is known to affect the accuracy of affinity calculations. Our previous studies had shown large particulate formation by vaccine constructs **13-18**, as a result possibility of mass transfer limitation was to be addressed. Furthermore, the flow rate has been shown to be an essential factor for determination of mass transfer. An ideal binding of an analyte to a ligand occurs when the magnitude of the binding does not change due to changes in the flow rate (called mass transfer). Here, a mass transfer study was performed (Figure 4-14). One concentration of mannan (500 µg/ml) was chosen to run at three different flow rates (5, 15 and 75 µl/min) to check if changes in the flow rate affected the response level (RU). As observed in Figure 4-14, there is no difference in the RU level between the three individual runs with different flow rates suggesting that the surface is not mass-transport limiting in the presence of mannan.

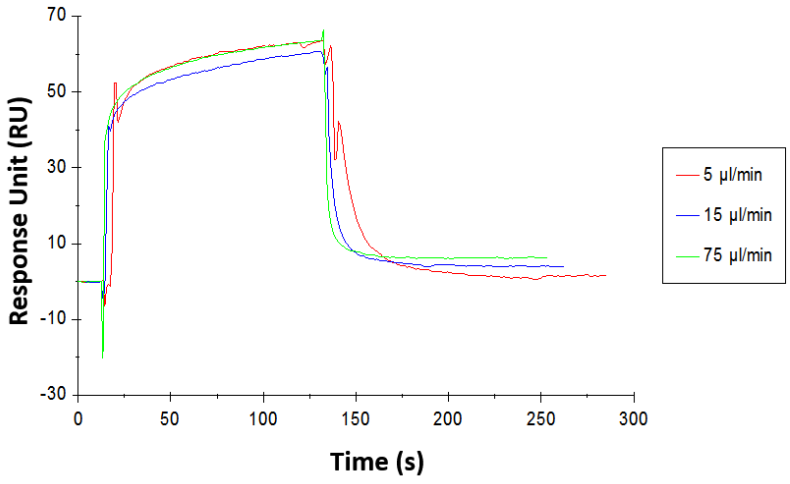

Figure 4-14. Mass transfer study with mannan. A single concentration of mannan (500 µg/ml) at different flow rates (5, 15 and 75 µl/min) was exposed to the mannose receptor (MR) immobilised

on the CM-5 chip. No change was observed in the response level (RU) between each of these runs indicating that mass transfer is not a limiting factor in this study.

To achieve an accurate binding affinity calculation, an equilibrium binding coefficient was performed on vaccine constructs **13-18** to determine the steady state binding to the MR protein (Figure 4-16) [217, 300]. Results are presented of the steady state binding level (Req) as a function of analyte concentration (Figure 4-15) and the K_D. Mannan has a reported high binding affinity to the macrophage MR and has also been used as an activity control for binding assays on the recombinant human MR protein [293, 301]. In this study, mannan was used as the positive control and, for the first time using Biacore technology, was shown to have a strong K_D of 0.15 µm with a R^2 value of 0.9943 (Figure 4-16A).

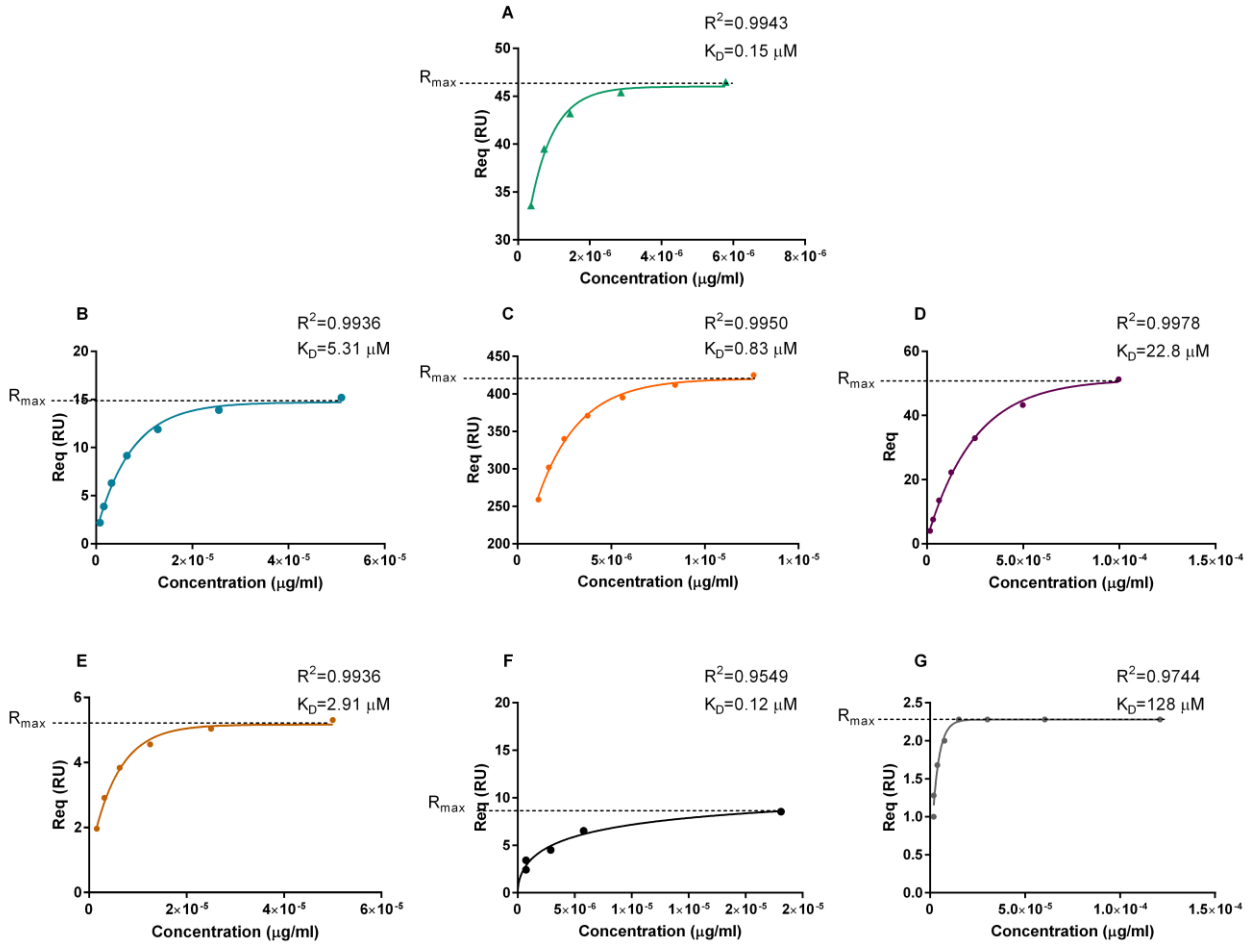

Figure 4-15. Binding affinity measurements for vaccine constructs 13-18. Surface plasmon resonance (SPR) analysis for the concentration-dependent binding of mannosylated constructs (**13-15**) and experimental controls (**16-18**) with the immobilised recombinant human macrophage mannose receptor (MR) protein. Solutions of **13-18** (0.78-50 µM concentration range) and mannan (18.75–600 µg/ml) were prepared in running buffer (10 mM HEPES, 1 mM $CaCl_2$, 1 mM $MgCl_2$,150

mM NaCl, 0.005% P20; pH 7.4) and injected over a period of 1.5 min with a dissociation interval of 8 min. The sensogram shows the plotted level of binding in the steady state (Req) against different concentrations of (A) the positive control mannan, and the vaccine constructs (B) **13**, (C) **14**, (D) **15**, (E) **16**, (F) **17**, and (G) **18**. R^2 indicates the fit of the results to the curve with respect to concentration. The affinity constant (K_D) was calculated using the response level at equilibrium (Req) using Equation 1 (**Chapter 2**, **Section 2.2.5**).

The results indicated that vaccine construct **14** (K_D = 0.83, R^2 = 0.9950, Figure 4-16C) had the highest level of binding (Rmax value) and affinity (K_D value) when compared with vaccine constructs **13-16** which had binding affinities between 2.9 and 22.8 (Figures 4-15B, D-E). Here, the lower the K_D the better the affinity of the construct to the receptor. Furthermore, the consistency of the results at varying concentrations was indicated by the R^2 values with a good value being close to 1.00. These results suggest that the optimal affinity and binding was dependent upon the compounds' structural properties. Here, construct **14,** containing only one alanine spacer between the mannose moieties, was shown to have a similar range of particle size as constructs **13** and **15**, **14** (**Chapter 3**, **Section 3.2.4**, **Figure 3-11**). Therefore, this increase in binding level can be associated with other factors, including conformation and structural properties (length of spacer, particle size, *etc*).

Furthermore, construct **16** (control) containing only lipids in the structure (no mannose) also showed a very high K_D of 128 (R^2 = 0.9744, Figure 4-15G) (low affinity) when compared to constructs **13-15**. It is well known that the MR binds to the lipoarabinomannan structures, exogenous glycolipid antigen moieties found on the cell walls of mycobacteria [302]. The MR has also been shown to play an important role in the uptake of lipidic structures [303]

Interestingly, these results indicate that even with an absence of mannose in the vaccine constructs, control compound **17**, which contains two mannose moieties in close proximity and no lipids, had a strong affinity to the recombinant MR protein (Figure 4-15F). However, it can be observed from the R_{max} that the level of binding is low (Figure 4-15F). Additionally, construct **18** containing no mannose and no lipids also showed a very low affinity (K_D of 128 µM, R^2 = 0.9744, Figure 4-15G). Overall, the poor level of binding obtained for constructs **16-18** suggests that for a better interaction with the MR, OVA-based vaccine constructs need to contain both mannosyl and lipidic moieties.

Overall, interesting findings were obtained from this SPR study supporting observations made in the uptake and binding studies performed using flow cytometry and confocal microscopy experiments on DCs and macrophage isolated from the spleens of mice (Figures 4-1 and 4-2, respectively). *A*

tabulation of *in vitro* OT-II proliferation, K_D and R_{max} is presented in **Appendix 17** showing the correlation between MR binding affinity, binding level and OT-II proliferation.

Both mannose and lipidic moieties appear to be necessary for the enhanced uptake and binding of these vaccine constructs to the MR. It was also confirmed that structural properties, such as the distance between the mannose units, play an important role in binding.

4.3 Conclusion

The presence of both mannose and lipids in the vaccine constructs was shown to increase their uptake in both DCs and macrophages. Furthermore, a receptor competition study by mannan confirmed that the uptake of vaccine constructs **13-16** was receptor mediated. Investigation into the ability of these vaccine constructs in T cell proliferation indicated that the presence of lipids in vaccine construct **16** significantly increased T cell proliferation, while constructs **13** and **15** showed similar potency as **16** in T cell activity. This indicated that the presence of a mannosyl moiety did not affect T cell proliferation properties. Further investigations were developed by SPR to assess the binding ability of vaccine constructs to the MR. Glycine buffer with pH 2.2 was chosen as the effective receptor regenerator. The SPR results indicated that all vaccine constructs had affinity for the MR while the highest affinity for the MR was observed for constructs **14** and **17**. Overall, the results indicate that a higher affinity for the MR is correlated with lower T cell proliferation ability.

Chapter 5: *In vivo* Studies on Mannosylated Lipopeptide Vaccines

5.1 Introduction

This chapter aims to investigate synthetic peptide-based subunit vaccines and the impact lipids and glycosylic (mannose) moieties have on T cell orientation (Figure 5-2). More specifically, the purpose of this study is to design vaccine constructs that bear lipidic and mannose moieties in a linear arrangement and investigate their impact on the immune response in a murine model. Particularly, the structural properties (effect of distance between each mannose unit, and the presence or absence of lipids and mannose) that affect the activation of different Th pathways through the study of T cell expansion and cytokine release are investigated.

The $OVA_{323-339}$ peptide epitope has long been studied for its immune activating properties [189, 304]. In this study, the vaccine constructs contained a double branched $OVA_{323-339}$ epitope conjugated to mannose (for MR targeting) and lipids moieties (for self-adjuvanting properties) and the design, synthesis and *in vitro* analysis of these was outlined in **Chapters 3-4**. There have been some studies that have included a glycosylic or lipidic moiety on the $OVA_{323-339}$ epitope, however, co-presence of both the targeting and adjuvanting moieties on a single peptide epitope has rarely been studied for their immune stimulating properties [93, 288, 305].

The innate immune system recognises pathogen cell walls through PRRs and responds through APCs. Activation of APCs causes the adaptive immune system to respond according to the type of threat by producing cytokines or cytotoxic T cells, as detailed in **Chapter 1, Section 1-2**. Here, development of constructs that could activate these responses can be valuable for a better understanding of immune pathways.

Prophylactic and therapeutic vaccinations are successful methods for the elimination of infectious and cancerous cells with the ability to produce cellular or humoral responses [4, 188]. PRRs are the front line receptors activated during these infections and are primarily involved in the innate immune response (**Chapter 1**, **Section 1-4**, **Figure 1-5**).

An innate immune response is activated through antigen uptake by DCs at the site of infection, including the epithelial layer, non-lymphoid tissues, *etc* [306]. DCs deliver the processed antigen to the lymph nodes where the antigen is then presented to naïve T cells. Here, T cell activation (called an adaptive immune response) involves both cellular and humoral responses (B cell activation) [306]. The T cell receptor (located on lymphocyte T cells) is recognised as a key receptor in T cell activation and immune responses produced by vaccine constructs. First line T cell activation is based on the

antigen presentation by APCs to MHC molecules. Thus, peptides and proteins with different targeting properties (glycosyl or lipidic moieties, or specific antigens) are uptaken by APCs and this can lead to MHC I or II activation and a consequent difference in the resulting T cell response (Figure 5-1) [307]. T cell activation is further recognised by Th polarisation into Th1 and Th2 T cells, and this polarisation is determined by cytokine secretion assays (Figure 5-1) [308]. Lectins with the ability to recognise carbohydrates moieties are important surface receptors on APCs [305]. Lectins play an important role in the selective recognition of carbohydrates and are essential in pathogen neutralisation [309].

The MR, an important member of the lectin family, is known to recognise mannosylated components of pathogenic antigens and process these antigens into the lysosomal compartments in APCs. Here, the antigen is processed and can be presented through MHC I and MHC II molecules to $CD8^+$ and $CD4^+$ T cells for cellular or humoral responses (Figure 5-1) [9]. It is known that mannosylation of different epitopes, for the purpose of MR-targeted vaccine design and development, have been shown to be an effective method for studying both innate and adaptive immune responses [310, 311]. The MR on APCs is known to be involved in antigen uptake that is followed by antigen presentation through MHC molecules (**Chapter 1, Section 1.4, Figure 1-5**). In a study performed by Turner *et al*. it was shown that defects in the levels of MR in serum caused recurrent infections in children showing the important role of the MR in the control of infection. [312]. Although there have been many studies indicating the link between the MR and innate immunity to adaptive immunity, it is not yet completely elucidated whether uptake by the MR can induce the desired pathways involved in T cell activation. For instance, antigen mannosylation has shown variable immune responses due to the cross-reaction with other PRRs, including TLRs and DC-SIGN [313]. Studies by Apostopolus *et al.* have indicated that mannan-bound peptides are internalised and presented by both MHC I and II molecules [314]. However, vaccines that are designed to target the MR can also overlap with these other lectin receptors (e.g. DC-SIGN). Also, TLRs can also be targeted due to presence of lipids on the vaccine structures (Figure 5-1) [315].

The MR is also reported to have an important role in the elimination of endogenous (produced in the body) mannosylated peptides, causing a downstream increase of pro-inflammatory cytokines that are produced by Th1 (a subset of $CD4^+$ T cells) activation [316]. In general, adding mannose moieties to a vaccine structure can be a selective tool to enhance the targeting of specific pathways in the immune system, and more studies on this combination can benefit future vaccine design and development.

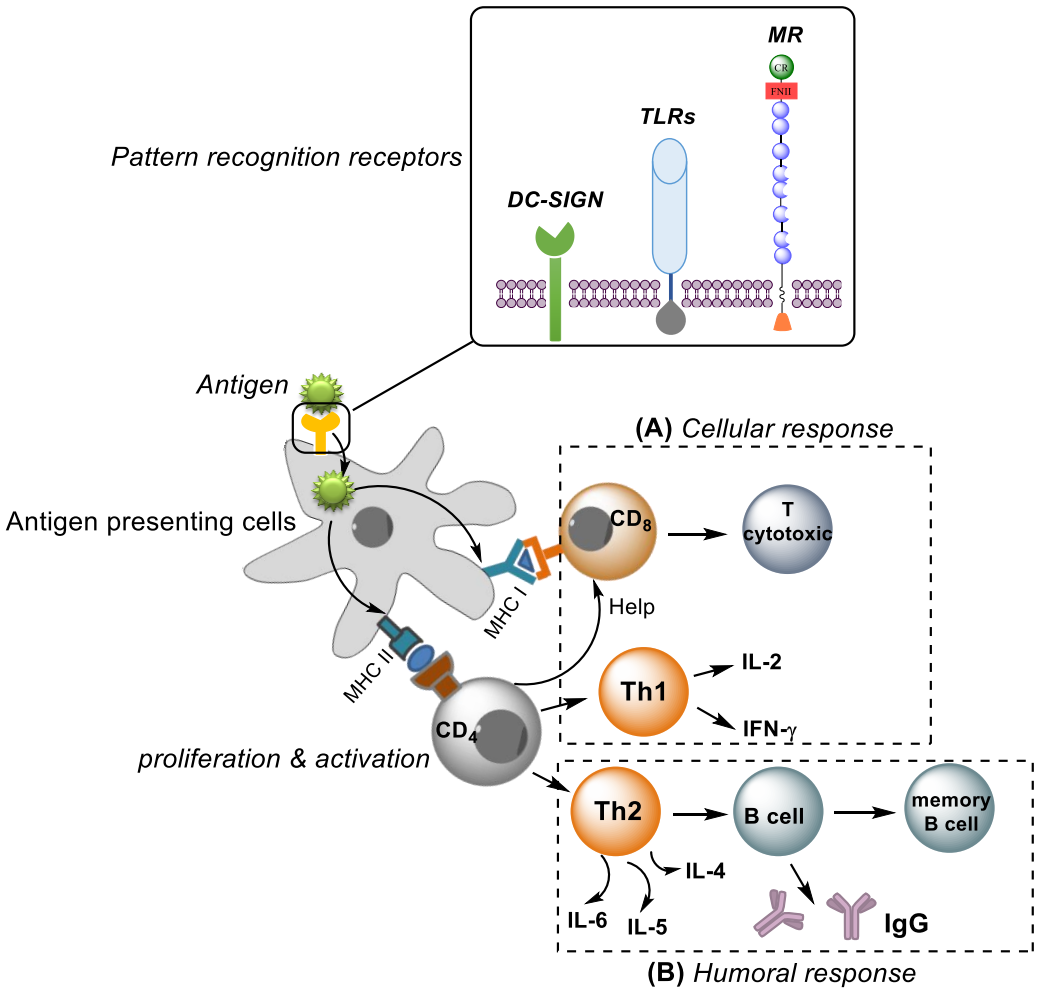

Figure 5-1. Dendritic cell (DC) involved in antigen presentation and activation of CD4 and CD8 T cells. Following antigen uptake by pattern recognition receptors (some mentioned in this thesis include: MR, DC-SIGN, TLRs), antigen presenting cells travel to the lymph nodes and present the processed antigen to CD4 and CD8 T cells by MHC II and MHC I, respectively. CD4 or CD8 T cells are activated depending on the antigen type and the following pathways become activated by proliferation: (A) CD8 activation leading to direct antigen elimination through cytotoxic T cells or by inflammatory cytokines in the Th1 pathway (e.g. IL-2, IFN-γ); or (B) humoral pathway where CD4 activates Th2 which is followed by Th2 related interlukin (e.g. IL-6, IL-5, IL-4) production. Upon Th2 activation, B cells are activated and trigger antibody (IgG) production.

Recent studies have shown lipidic moieties have lectin receptor targeting properties that aidg the immunogenicity of peptide antigens through the activation of TLRs [317]. TLRs have been widely studied for their ability to modulate immunestimulatory (adjuvanting) responses [318, 319]. Vaccine constructs that target TLRs have been shown to generate the desired Th1 response. A Th1 response is measured by the production of IL-2, INF-γ, macrophage activation and elimination of antigens [320]. On the other hand, a Th2 response is characterised by cytokine release and B cell activation (IL-4, 5, 13) (Figure 5-1) [320].

Addition of lipids to vaccines has been shown to induce self-adjuvanting properties through TLR recognition and/or activation [153, 162, 223]. Here, peptidoglycans attached to the synthetic lipid (Pam3/2Cys) have been shown to stimulate a Th2 response via TLR-2 activation [321]. Lipopolysaccharides extracted from the bacterial cell wall were able to stimulate TLR-4 and activate both Th1 and Th2 pathways [322]. Furthermore, lipid moieties incorporated into peptide-based vaccines have been shown to enhance the hydrophobic properties of the peptide epitope, aiding the epitopes stability and delivery to the site of action [158].

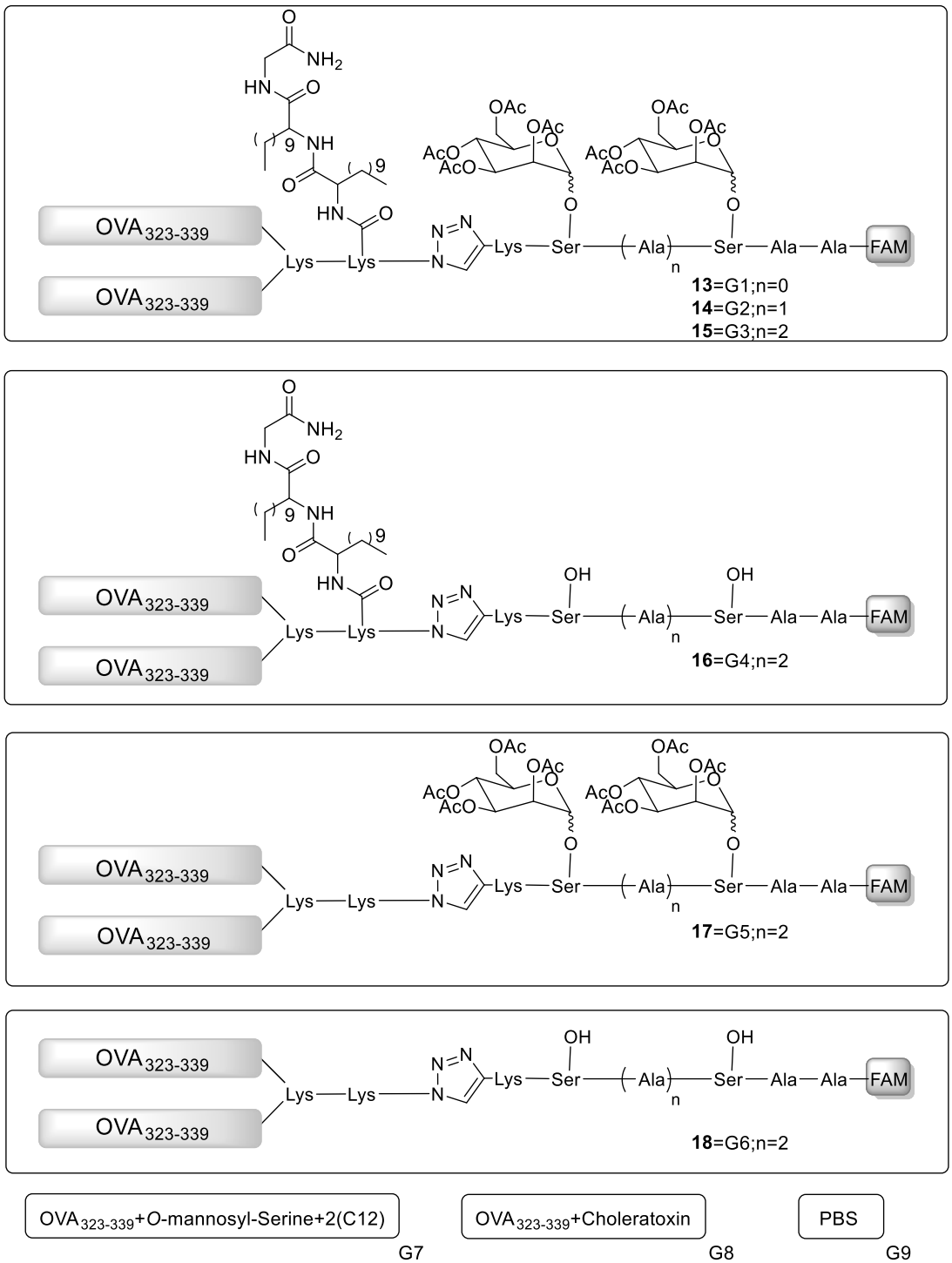

Figure 5-2. Vaccination groups (G)1-9 used in the *in vivo* study. G1-3 are test compounds used to study immune modulatory properties affected by the differences in the number of alanine spacers between the mannosyl moieties. **G4-8** are controls used to compare a structure-activity relationship of no mannose (**G4**), no lipid (**G5**), and no mannose and no lipids (**G6**). A mixture of the vaccines' structural components ($OVA_{323-339}$, mannosyl and the lipid, **G7**) was used to compare with the chemically conjugated vaccine constructs (**G1-G6**). The positive control (**G8**) was $OVA_{323-339}$ and CT, and the negative control was PBS (**G9**). All vaccine groups (**G1-9**) were dissolved in PBS (30 µg/100 µl/per mouse) and injected subcutaneously (S.C.) at the tail base. Five mice were used per vaccine group.

Vaccine constructs **13-18** used for the vaccination of mice (now called **G1-6** where G stands for groups, Figure 5-2) were prepared as per **Chapter 3**. Here, **G1-3** contained two C12 lipid moieties and two mannose units separated by 0 (**G1**), 1 (**G2**) or 2 (**G3**) alanine units between each mannose moiety (Figure 5-2). Experimental controls to check the structure-activity relationship included **G4** (no mannose), **G5** (no lipid) and **G6** (no mannose and lipid). In addition, a physical mixture of the $OVA_{323-339}$ peptide with the mannose and lipid moieties (1:1:1) in PBS (**G7**) was used to study the relationship between a physical mixture of the vaccine components and the chemically-bound constructs (**G1-G6**). $OVA_{323-339}$ pre-mixed with CT in PBS (**G8**) was used as the positive control, and PBS (**G9**) was used as a negative control (Figure 5-2). This mannosylated lipopeptide vaccine library is examined in *in vivo* immune pathways for T cell activation (OT-II study) and cytokine release (ICS/CBA studies) (Figure 5-3).

5.2 Results and Discussion

5.2.1 In vivo CD4 T-cell proliferation/activation

Overall, there are two different pathways involved in $CD4^+$ T cell activation, i) an antigen dependant pathway (Figure 5-1), and ii) an antigen independent pathway (**Chapter 1, Section 1.2, Figure 1-1**). The antigen dependant pathway occurs when the T cell receptor binds to antigens presented by MHC molecules [323]. The antigen-independent pathway, however, is a cytokine dependant pathway characterised by T cell activation through cytokine release and occurs in the early stages of an immune response when DCs encounter an antigenic moiety (**Chapter 1, Section 1.2, Figure 1-1**) [323]. It has been shown that only a negligible percentage of T cell activation occurs along the antigen-independent pathway. A huge advantage of infections and vaccines successful in targeting the antigen through the antigen dependant pathway is the production of very specific antigen-related immune

responses [324, 325]. Antigen dependant CD4 T cell activation primarily occurs in secondary lymphoid organs (lymph nodes, spleen and skin). Within the lymph nodes, activation of CD4 occurs through antigen recognition presented on MHC II molecules. There are three professional APCs with the ability of MHC II presentation and subsequently CD4 activation: macrophages, DCs and B cells. Since macrophages are mostly located in non-lymphoid tissues that do not include the areas in which T cells exist, activation of APCs and MHC II presentation is unlikely to happen through this cell subset. Furthermore, studies with macrophage knock-out mice have shown a normal T cell activation [265, 323]. B cells on the other hand, have been shown to contribute to MHC II presentation. Early studies demonstrated that B cells lacking antigen-specific surface immunoglobulin were inefficient at taking up the antigen and presenting the subsequent antibody response. It was concluded that B cells required help from T cells to be efficient in antigen elimination [326].

In this study, T cell proliferation was assessed in order to understand the T cell activation ability of vaccine constructs (**G1-6**) along with experimental controls (**G7-9**) upon APC presentation. In **Chapter 4, Section 4.2.1, Figure 4-1** it was shown that the vaccine constructs **13-16** were successfully taken up through DCs and macrophages in a receptor mediated pathway *in vitro* meaning the designed vaccine constructs could potentially initiate an adoptive long-term immune response. Thus, further investigate was needed to determine whether these vaccines were able to activate T cells (OT-II T cells specific for $OVA_{323-339}$ epitope) in an *in vivo* murine model. Hence, OT-II (CD4, $CD45.2^{+}$) cells were separated from transgenic mice (B6.Cg-Tg[TcraTcrb]425Cbn/J) to be adoptively transferred to C57BL/6 mice. OT-II cells are T cells with the ability to recognise and activate constructs containing the $OVA_{323-339}$ epitope. Upon adoptive transfer of OT-II cells to C57BL/6 mice, vaccination with vaccine constructs (Figure 5-2) was performed on C57BL/6 mice using S.C. injection on days 2, 21 and 42 (Figure 5-3). OT-II proliferation results and ELISA was performed on days 10, 31 and 52. Ten days post vaccination of **G1-9**, mice were sacrificed (day 63) and cytokine measurement assays including ICS and CBA, were performed *ex vivo* (Figure 5-3). Figure 5-3 shows the schematic *in vivo* study that is presented in this chapter.

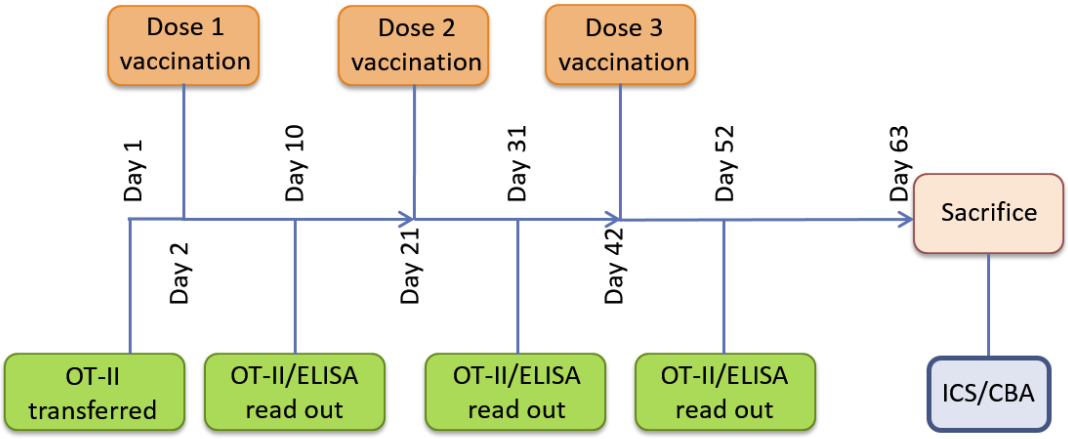

Figure 5-3. Schematic diagram of the *in vivo* study. Vaccine groups (**G1-9**) were introduced to mice following the transfer of OT-II CD45.2^{+} T cells isolated from transgenic mice (B6.Cg-Tg[TcraTcrb]425Cbn/J with OVA sensitive OT-II cells) to C57BL/6 mice. Mice were vaccinated on days 2, 21 and 42. Blood was taken on days 10, 31 and 52 post vaccination. OT-II read outs for flow cytometry and ELISA were performed 10 days post each vaccination. Mice were sacrificed on day 63. ICS and CBA studies were performed on blood samples taken 21 days post dose 3 vaccination.

5.2.1.1 Immunisation by mannosylated peptides resulted in an impaired T cell response

$OVA_{323-339}$ epitope is known to activate OVA specific T cells through MHC II molecules. It is also argued that this epitope also bears at least one B cell epitope (323-339), however, there is only one study that has mentioned the presence of the B cell epitope [327]. In a study by Sun *et al.*, it was shown that 50% of the B cell response generated by the OVA protein was antibody specific to the $OVA_{323-339}$ epitope [327]. It is well-established that upon antigen activation CD4^{+} T cells differentiate into Th1 or Th2 T cells (Figure 5-1) [328]. This differentiation is mainly characterised by the type of cytokine produced. Th1 activation is known by the production of IFN-γ and IL-2, while Th2 activation can be characterised by IL-4, 5 and 13 cytokines (Figure 5-1). Th2 is also involved in B cell activation (Figure 5-1). APCs activate a CD4 response that consequently activates a Th2 response which in turn activates a B-cell response, detected by IgG antibody production (Figure 5-1).

As the vaccine structures (**G1-6**) contain the CD4 epitope ($OVA_{323-339}$), the *in vivo* ability of vaccine structures (**G1-9**) for a T cell activation proliferation was assessed. Here, OT-II proliferating cells are considered to be activated when T cells expressing CD45.2 increase in percentage over the total parental CD4^{+} T cells [329]. For this purpose, OT-II cells (CD45.2 CD4^{+} T cells) were purified and injected (I.V.) into C57BL/6 mice to study the T cell population. Vaccine constructs **G1-6** were prepared by mixing 30 µg of each construct with 100 µl of PBS. One day post OT-II T cell adoptive transfer, mice were immunised with the vaccine constructs (**G1-9**) (Figure 5-3). Vaccination was

performed 3 times at 21 days intervals. On days 10 (Figure 5-4A), 31 (Figure 5-4B) and 52 (Figure 5-4C), blood was collected from the mouse tail and the proliferation of $CD45.2^+$ OT-II cells was quantified using flow cytometry (Figure 5-4). Here, $CD45.2^+$T cells (OT-II) were identified and their percentage over the total parental T cells was measured.

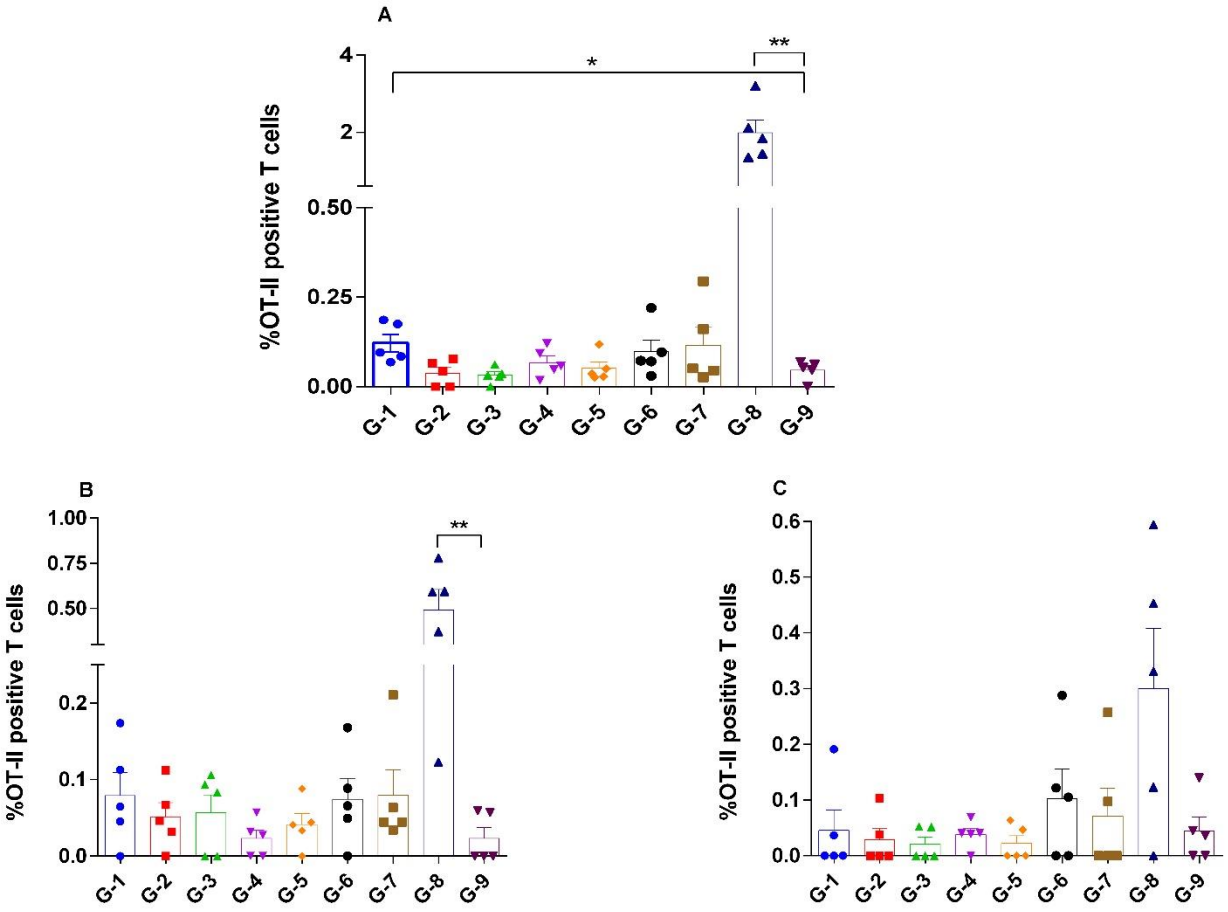

Figure 5-4. OT-II $CD45.2^+$ $CD4^+$ T cells from OT-II mice do not proliferate in C57BL/6 mice upon vaccination with G1-9. $CD45.2^+$ $CD4^+$ OT-II T cells were purified and 200 µL of suspended cells (0.5×10^6 cells) was injected intravenously at the tail base to $CD45.1^+$ C57BL/6 mice. The percentage of $CD45.2^+$ OT-II cells within the $CD4^+$ population was measured from tail blood taken at days 10, 31 and 42 using flow cytometry. Mean results (±SEM) from five individual mice per time point are shown, (A) at day 10, (B) at day 31, and (C) day 42. Unpaired t-Test was used to show the significance when $p < 0.05$. Here, **G8** is the positive control group vaccinated with $OVA_{323-339}$ + cholera toxin and **G9** is the negative control group vaccinated with PBS.

In the immune system $CD4^+$ T cells have the role of maturation and also providing B cell activation. As a result, it is important for a successful vaccine to have the ability of $CD4^+$ T cell activation to generate a subsequent antibody response [330]. Figure 5-4 shows the percentage of $CD4^+$ $CD45.2^+$ OT-II for each group of mice immunised with the vaccine constructs (**G1-9).** Here, an impaired T cell response was observed for vaccine groups **G1-7** and no OT-II expansion was observed. As can be seen in Figure 5-4, the percentage of OT-II cells was significantly higher after the first vaccination dose (day 10) for **G1** and **G8** (positive control) when compared to the PBS group (Figure 5-4A), however, following the second (Figure 5-4B) and third (Figure 5-4C) vaccinations, no significant difference was observed between mice groups (**G1-G7**) and the PBS control group (**G9**). Here, a low percentage of $CD4^+$ $CD45.2^+$ OT-II cells (less than 1%) indicates a lack of antigen presentation and a consequent decrease in the number of $CD4^+$ $CD45.2^+$ OT-II cells. For a T cell proliferation and B cell activation, CD4 cells should recognise the CD4 epitope in the immunogen, however, sometimes epitope suppression occurs and can cause a non-detectable T cell proliferation due to tolerance to the epitope [330, 331].

Further, the observed reduction of the proliferation responses, associated with a diminishing percentage of $CD4^+$ $CD45.2^+$ OT-II cells post vaccination, could be caused by a lack of antigen recognition or presentation in an *in vivo* model as was reported by Trépanier *et al.* [332]. Other factors also play a role in this observed decline of the $CD4^+$ $CD45.2^+$ OT-II cell population. One possible explanation for a lack of OT-II proliferation might be that significant proliferations might have had happened at earlier time points than a week, for example, at days 3 or 4 post vaccination [246]. Simerska *et al.* reported OT-II proliferation 4-7 days after vaccination by LCPs containing the $OVA_{323-339}$ epitope [246]. These results could have been better observed at an earlier time point after vaccination, due to possible proliferation that might have occurred at earlier time points rather than 10 days after vaccination.

Another explanation for the diminishing percentage of $CD4^+$ $CD45.2^+$ OT-II cells is associated with a lack of migratory properties of APCs to the lymph nodes (where the antigen is presented to the T cells), which caused a reduction in the number of OT-II cells and subsequently lack of T cell activation. This has been reported by Mirenda *et al*. [333]. They reported that partial T cell activation can cause T cell unresponsiveness (anergic T cells) due to the defects caused on the T cells migratory ability [333, 334].

Further, OT-II proliferation has been shown to affect Th1 polarisation, and only a completely polarised Th1 can affect inflammation [335]. The results presented in Figure 5-4 show that

vaccination with the vaccine constructs (**G1-G6**) stops the proliferation and differentiation stage in OT-II cells. This lack of OT-II activation was previously reported to be a result of mannosylation, where mannosylation has been shown to inhibit T cells from recognising antigenic moieties [335]. However, the irresponsiveness of the T cells was not observed in *in vitro* studies performed on splenocytes for the $CD4^+$OT-II T cell activation proliferation (detailed in **Chapter 4**, **Section 4.2.3**). This *in vitro* proliferation study showed a significant increase in effective CD4 proliferation response for constructs **G1-G4** when compared with the $OVA_{3232-339}$ peptide alone. These observations are in line with previous reports on the decreased *in vivo* T cell response despite increased *in vitro* T cell proliferation by mannosylated antigenic peptides [311, 335].

5.2.1.2 CD62L precursor of memory T cell

CD 62L is from the family of L selectin proteins expressed on the surface of memory T cells [336]. Previous studies have demonstrated that memory T cells express low amounts of CD62L ($CD62L^{low}$) on their surface. $CD62L^{hi}$ T cells are referred to as "central memory" T cells, while $CD62L^{low}$ T cells are referred to as "effector" memory T cells [337]. CD62L positive T cells are activated in the lymph node by APCs. In this process, CD62L is cleaved by enzymes including disintegrin and metalloprotease [338]. Studies have shown that CD62L shedding plays an important role in T cell activation in the lymph nodes. Further, it is confirmed that although CD62L is present on memory T cells its shedding is not essential for the production of memory T cells or T cell immigration to the infection site, thus, the lack of shedding can affect the viral elimination effect [339].

In this study, measurement of the percentage of $CD4^+CD62L^{low}$ T cells was performed with OT-II readout flow cytometry study at time points mentioned in Figure 5-4 (days 10, 31 and 52). As can be seen in Figure 5-5, the results only showed a significant increase (**, p <0.008) in the percentage of $CD4^+CD62L^{low}$ cells (of total $CD4^+$ T cells) for **G8** (positive control) when compared to **G9** (negative control) that was consistent after the second (Figure 5-5B, day 31) and third vaccinations (Figure 5-5C, day 52). It can be observed that following the final vaccination the OT-II readout from day 52, **G7** had the highest percentage of $CD4^+CD62L^{low}$ proliferation (**, p <0.008) compared with the vaccination groups **G1-6** which did not show significance when compared to the PBS control group (**G9**). This indicated that **G7** contained unattached moieties of mannose, lipid and $OVA_{323-339}$. This is consistent with a previous study by Sun *et al.* where it was demonstrated that OVA protein conjugated to CT had failed to induce a T cell proliferation/activation; they showed that the results were weaker when $OVA_{323-339}$+ CT was injected [340].

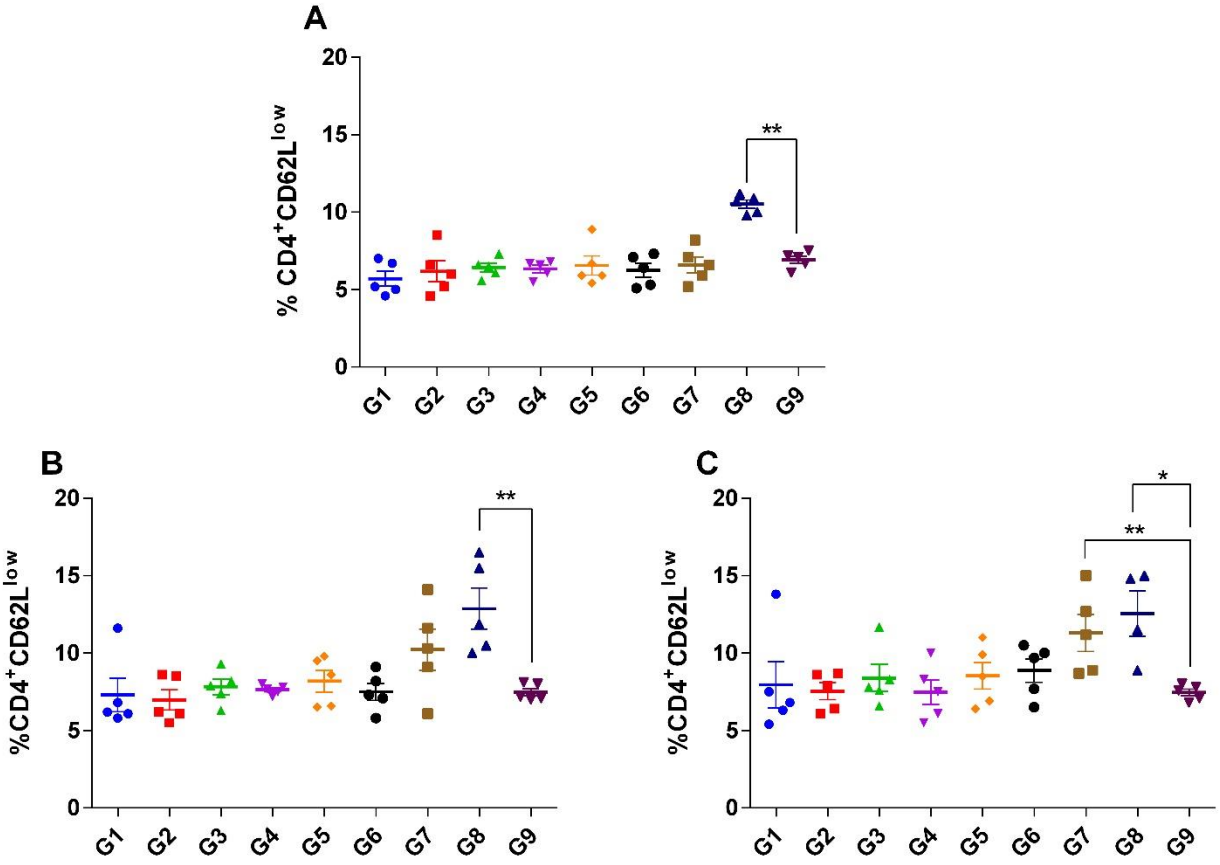

Figure 5-5. Percentage of CD62l^{low} CD4^{+} parental T cells. Vaccine constructs **G1-G9** were compared by percentage (%) of CD62l^{low} CD4^{+} parental T cells following three vaccinations on days 10 (A), 31 (B) and 52 (C). Mean results (±SEM) from 5 individual mice groups are shown. Unpaired t-test was used to show significance when p <0.05. Here, **G8** is the positive control group vaccinated with $OVA_{323-339}$ + CT and **G9** is the negative control group vaccinated with PBS.

All vaccinated groups (**G1-G6**, Figure 5-5) showed no increase in the percentage of CD62L^{low}CD4^{+} following the second (Figure 5-5B) and third (Figure 5-5C) vaccinations, and the results were not significant. Following the third vaccination, all groups except **G7** failed to increase the percentage of CD62L^{low}CD4^{+} when compared to the PBS group (**G9**). Overall, these results suggest that lipidic and mannosyl moieties may perform better for a memory T cell response only when are physically mixed together (**G7**) (Figure 5-5). Overall, the mannosylated lipopetide vaccines were not able to change their percentage of CD62l^{low} CD4^{+} parental T cells. A lack OT-II *in vivo* proliferation/activation by mannosylated peptides ($PLP_{139-151}$) was also observed in a study by Kel *et al.*[341].

5.2.2 Th activation pathway and cytokine release

Vaccine constructs **G1-G9** were screened for their ability to induce cytokine production by $CD4^+$ cells in vaccinated C57BL/6 mice 11 days after the final vaccination (day 63). The study of cytokines released was performed to help clarify the Th pathway(s) involved in an immune response by these vaccine constructs. Both subsets of $CD4^+$ cells, Th1 and Th2, are necessary components of a successful long-term immune response, and hence study of the relation between structural properties of vaccine constructs and the consequent activated immune pathway are important aspects of vaccine development [342]. To enable this part of the study, ICS (**Chapter 2, Section 2.3.6**) and CBA (**Chapter 2, Section 2.3.7**) assays were used to measure post vaccination cytokine production. Development of techniques including ICS and CBA has provided an ability to investigate the specific pathways that vaccines activate. It has been established that upon activation of $CD4^+$ T cells, Th1 and Th2 cells are differentiated (Figure 5-1). Here, Th1 is responsible for the production of IFN-γ, TNF and IL-2, while Th2 is responsible for the production of IL-4, IL-5, IL6, IL-10 and IL-13 (Table 5-1) [343, 344].

Table 5-1. Essential cytokines of Th1 and Th2 [345]

Th1	IFN-γ	Activates cytotoxic T cells
	IL-2	Promotes T cell development
	TNF	Involved in protection and cure
Th2	IL-4	Promotes T cell differentiation into Th2, regulates antibody production
	IL-5	Involved in humoral immunity against parasites
	IL-6	T cell and B cell activation and differentiation
	IL-10	Inhibits inflammatory cytokines (TNF) production
	IL-13	Inhibits inflammatory cytokines (IFN-γ and IL-2) production

T helpers (Th1 and Th2) are the most important cells in an adaptive immune response (Table 5-1) [307]. T helpers have been shown to activate B cells and enable production of antibodies or activation of cytotoxic T cells. T cells are activated by the markers on the surface of APCs which present antigens (Figure 5-1). Upon APCs' antigen presentation to the T cells, T cell activation occurs through two separate recognition pathways, recognition of antigens presented by the MHC molecule and recognition of antigens along the APCs' intracellular pathway. If a T cell receives only one of these

two signals it will progress along the apoptosis pathway and cannot be activated [307, 346]. Upon activation effector T cells then produce IL-2. IL-2 is a cytokine that after attaching to its receptor and activating intracellular signalling can cause further T cell proliferation (Figure 1-5).

5.2.2.1 Cytokine release study by intra cellular staining

Antigen-specific T cell responses and recognition of activated pathways (Th1, Th2) depends on the type of cytokines released. The ICS assay has been applied in immunological studies for the purposes of specifying the type of cytokines produced (Figure 5-6) [347].

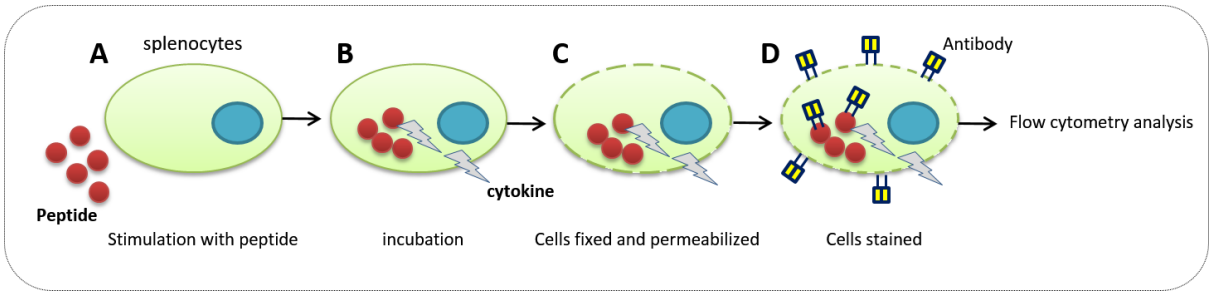

Figure 5-6. Schematic process of intra cellular staining. This method is used to measure antigen-specific cytokine release (e.g. IFN-γ, IL-2, TNF). (A) single cell suspensions from vaccination groups' (**G1-9)** lymph nodes and spleen were stimulated by $OVA_{323-339}$ peptide, PMA/ionomycin as experimental positive control and media only as experimental negative control, (B) cells were then incubated at 37°C and 5% CO_2 for 3 days in the presence of protein transport inhibitor, (C) cells were then permeabilised and fixed, (D) cells were stained with IFN-γ, IL-2 and TNF antibodies. The expression of IFN-γ, IL-2 and TNF was analysed on the $CD4^+$T cells subset using flow cytometry.

The ICS (Figure 5-6) assay was performed (as detailed in **Chapter 2**, **Section 2.3.6**) to characterise antigen specific T cells immune-cytokine responses induced by vaccination groups **G1-9**. At day 63 **G1-9** mice were sacrificed (Figure 5-3) and two tests were performed. Lymph nodes and spleens were collected and *in situ* recall response was performed on the T cells in the presence of $OVA_{323-339}$ peptide. Also cells from lymph nodes and spleens were used to prepare single cell suspensions for cytokine release measurement. This was followed with excitation of splenic and lymphatic cells by the $OVA_{323-339}$ peptide. A positive experimental control (PMA/ionomycin) and a negative experimental control (media only) were used to validate the experiment. Cells were then cultured for 3 days in the presence of protein transport inhibitor, which results in accumulation of cytokine (detailed in **Chapter 2**, **Section 2.3.6**). Following this cells were permeabilised and fixed and anti-cytokine antibodies added before flow cytometry analysis was performed (Figure 5-6).

The desired aim of preparing the vaccine constructs (**G1-6**) was an immune activity either through a T cell activation or cytokine release. Here, cytokines indicative of a CD4 Th1 response include IL-2, IFN-γ and TNF. Th1 cells are known to secrete IL-2, IFN-γ and TNF which have been shown to eliminate intra-cellular pathogens that have entered macrophage lysosomes by activating macrophage lysosomal killing [307]. IFN-γ is also known to prohibit IL-4 production by blocking the activation of Th2 [343]. IL-4 is a cytokine involved in the up-regulation of the MR. This argument has already been proven by studies showing that IFN-γ affects MR mediated uptake of antigens [348].

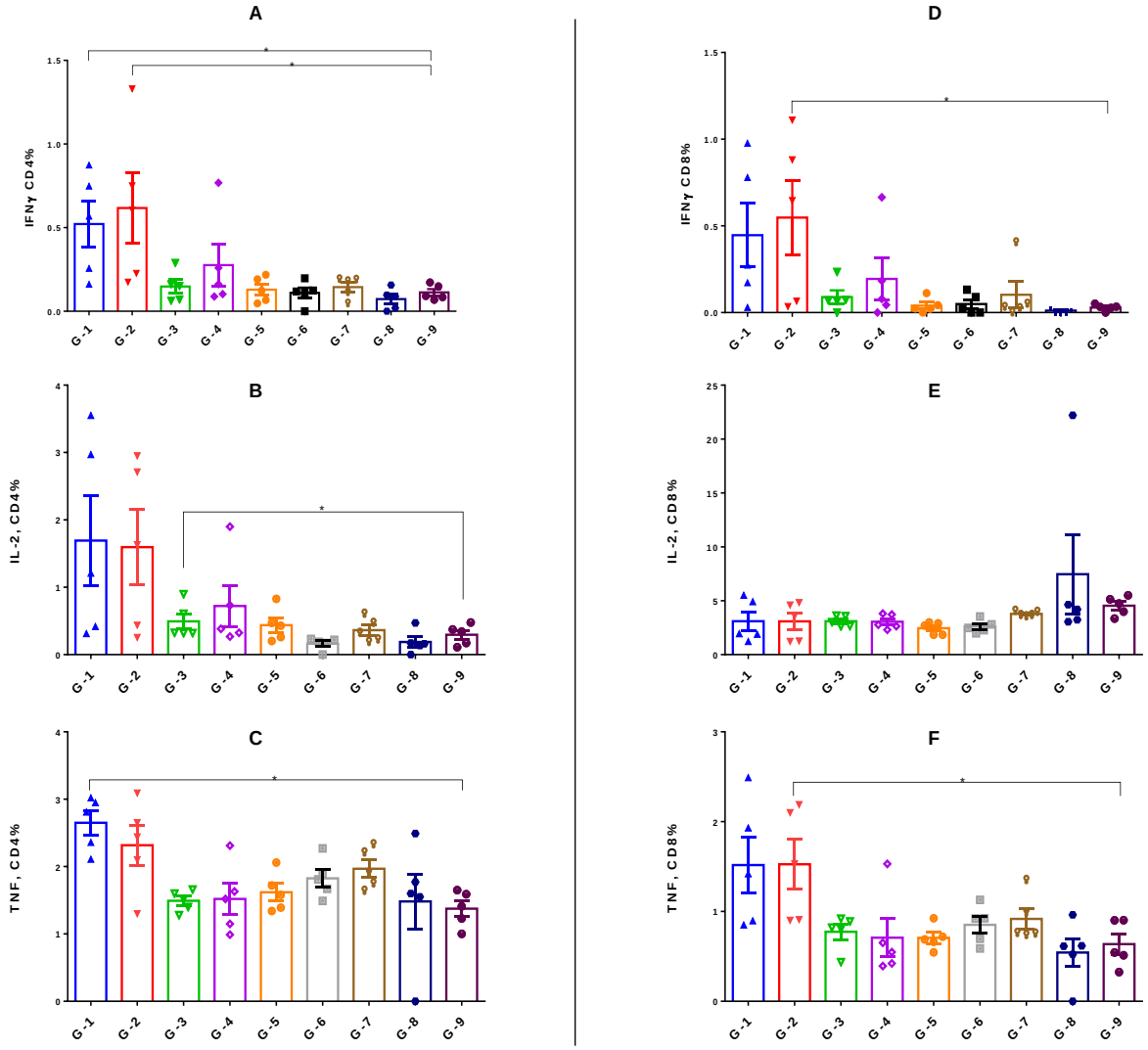

Figure 5-7. Intra cellular staining studies on INF-γ, IL-2 and TNF expressing T cells following vaccination. Percentage of CD4 (A, B, C) and CD8 (D, E, F) T cells associated with IFN-γ, IL-2 and TNF upon *in situ* stimulation of draining lymph nodes and spleen cells (isolated 11 days post third vaccination with **G1-G9**) with the $OVA_{323-339}$ peptide and PMA/ionomycin (experimental positive control). Results are normalised against the media per each mouse per group. Mean results (±SEM) from 5 individual mice per group are shown. Unpaired t-Test was used to show the significance when

p <0.05. Positive control is **G8** vaccinated with $OVA_{323-339}$ plus CT and negative control is **G9** vaccinated with PBS.

The ICS assay (Figure 5-7) indicated CD4 and CD8 T cells were expressing antigen specific cytokines including INF-γ, IL-2 and TNF(Figure 5-7). Here, **G4** had a significantly (*) higher CD4/IL-2 production than **G9** (negative PBS vaccinated group), while differences between **G1-G3** were not significant for IL-2 production (Figure 5-7B). In an study by Zhu *et al.*, palmitoyl attached lipopeptides (herpes simplex virus type 1 peptide was used as the model antigen) could induce higher T cell related IL-2 production when compared with their control glycopeptide [175]. **G1-G2** indicated significantly higher ($^{*}p$ <0.05) CD4/IFN-γ production than **G9** which is an indicator of activation of the Th1 pathway as detailed by Bettahi *et al.* (Figure 5-7A) [349]. Bettahi *et al.* used glycol lipopeptides to vaccinate C57BL/6 mice and the results showed a significant antigen specific IFN-γ production in comparison with the negative PBS vaccinated mouse group [349]. **G1** CD4 associated TNF production (Figure 5-7C) was also significantly higher than **G9** (negative PBS group). **G1's** ability to induce pathways involved in CD4/TNF and CD4/IFN-γ links this vaccination group to the Th1 activation pathway. A previous study by Braumuller *et al.* showed that combining TNF and IFN-γ permanently stopped cancer cells from growing [350]. By comparing the CD4 associated cytokine release (Figure 5-7) with T cell proliferation results, the significance in the OT-II cells proliferation by **G1** when compared to the negative control, **G9** (Figure 5-4A), was observed indicating activation of the pathway that results in production of IFNγ cytokine, which was consistent with the OT-II proliferation results (day 10, Figure 5-4A). An overview of the results (Figure 5-7) indicated a significant production of CD4 linked IL-2 and IFN-γ by **G1** when compared to the negative control group (Figure 5-7A and B). **G2,** on the other hand, activated $CD8^{+}$ linked INF-γ and TNF (Figure 5-7D and F). Here, the difference between **G1** (vaccinated with **13**, 0 space between mannosyl groups in the structure) and **G2** (vaccinated with **14**, 1 space between mannosyl groups in the structure) is the number of alanine spacers. IL-2 and IFN-γ are mediators of CD8 activation and cellular response, where activation of CD8 (cellular response) may occur by the cross-presentation of antigens to MHC I molecules upon uptake by the MR [330]. **G2's** level of CD8/IL-2 (Figure 5-7D) was significantly (*) higher than the control **G9** group, indicating a cross-presentation of this vaccine group upon its high affinity to the MR as was indicated before in **Chapter 4, Section 4.2.4.** Here, **G8** failed to show CD4 or CD8 linked IL-2, IFN-γ and TNF activation. In general, there are different observations for OVA+ CT; while some studies have shown a lack of T cell proliferation, others have indicated Th1 and Th2 activated cytokine release following vaccination [327, 340, 351].

5.2.2.2 Inflammatory cytokine measurement

It has been established that antigen mannosylation can enhance the pathways involved in antigen presentation to MHC II molecules [352]. Many studies have sought an antibody response through B cell activation with the help of CD4 that provides activation of Th2 cells. Upon T cell antigen specific activation, Th1 or Th2 pathways get activated (Figure 5-1) [344]. The advantage of Th2 activation is that it generates long-term memory immunity, compared with Th1 which gives an immediate cellular response [330]. However, an advantage of Th1 activation is its involvement in cytotoxicity enabling the elimination of a specific pathogen [307]. Thus, studies of cytokines involved in Th1 and Th2 pathways requires detection of cytokines released by splenic and lymphatic cells following vaccination with, in this case, **G1-9**. In this study, the designed vaccine structures were assessed for their ability to produce a Th response and consequent cytokine production.

The $OVA_{3233-339}$ peptide has been previously studied and is known to have the ability of both Th1 and Th2 related cytokine release (IL-2, IL-4, IL-5 and IFN-γ) through OVA-specific $CD4^+$ T cells extracted from BALB/c mice [353]. Here, the structural differences affecting cytokine secretion pertaining to both Th1 and Th2 pathways using CBA methodology were studied. CBA methodology is a useful technique to analyse small volumes of samples for several cytokines in a single well [354].

In this experiment, the supernatant (collected from the spleen and lymph node of a mouse) was combined with antibody-labelled microspheres (Figure 5-8A) that were designed to bind specifically to certain cytokines (listed in Table 5-2). Streptavidin–phycoerythrin bound to secondary antibodies was used for detection of the cytokines (Figure 5-8B). This was followed with washing to remove unwanted molecules (Figure 5-8C) (including non-specifically bound antibodies). Cytokine production was identified by fluorescence intensity on a flow cytometer (Figure 5-8D).

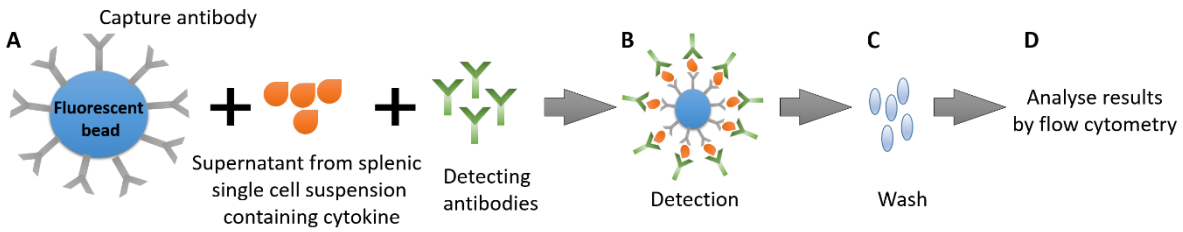

Figure 5-8. Schematic of cytokine bead array measurement. (A) The fluorescent capture beads are conjugated with detection antibodies and are incubated with test samples containing cytokines and secondary antibodies to form (B) sandwich complexes. The sandwich complex is then (C) washed

followed by acquisition of sample data using (D flow cytometry. The sample results are generated in graphical and tabular format using the BD CBA analysis software.

Results from this CBA study showed that application of vaccine structures bearing the $OVA_{323-339}$ epitope along with both mannose and lipidic moieties (**G1-G2**) activated pathways involved in the activation of Th1 (IL-2) and Th2 (IL-4, IL-5, IL-6, IL-10, IL-13) immune responses. **G3** (which also contained the $OVA_{323-339}$ epitope, mannose and lipids but had the longest distance between each mannose moiety) showed increased selectivity towards the Th2 pathway through the generation of cytokines, however, no IL-2 response was observed. Here, IL-2, as a pro-inflammatory cytokine, has been shown to play a role in the suppression of the MR whereas IL-4, an anti-inflammatory cytokine, has a role in the up-regulation of the MR [348]. Further, additional cytokines released through Th2 activation (e.g. IL-13 and IL-10) were shown to up-regulate the MR [355]. This could increase uptake through the MR on APCs. It was previously shown (**Chapter 4, section 4.2.4.1.3, Figure 4-16**) that **G2** had a high binding and affinity to the MR.

Table 5-2. Cytokine bead array results presented as a heat map. Red cells indicate the strongest results while the green cells indicate the weakest results per cytokine for each vaccination group (**G1-G9**).

G	IL2	IL4	IL5	IL6	IL10	IL12p70	IL13	TNF
1	15.65	1.78	34.49	10.21	0.00	0.00	48.50	0.00
2	8.87	2.89	15.44	14.98	21.71	0.00	6.36	0.00
3	0.00	0.00	2.35	0.00	17.53	2.08	33.58	11.20
4	6.28	0.00	5.88	20.68	12.76	9.85	0.00	0.00
5	3.37	1.45	0.00	17.95	0.00	0.00	0.00	11.67
6	4.28	0.00	1.36	0.00	17.04	0.00	0.00	0.00
7	20.93	0.00	4.95	41.93	6.83	15.97	18.17	12.87
8	2.28	0.00	0.00	0.00	0.00	20.00	0.00	0.00
9	0.00	0.00	0.00	0.00	0.00	0.00	0.00	0.00

By comparing the mannosylated (**G1, G2 and G3**) and non-mannosylated (**G4** and **G6**) vaccine constructs, **G1-G2** which were involved in the uptake by MR (indicated in **Chapter 4**, **Section 4.2)**, activated production of IL-4, 5 and 13 (Table5-2). These three cytokines have been shown to be involved in a Th2 type immune response. Interestingly, **G3** was the strongest in the level of Th2 antigen specific cytokines measured in this study (highest level of IL-5 and 13, Table 5-2). However,

G1 and G2 were also able to activate Th1 due to IL-2 production (Table 5-2). Further, it can be postulated that factors affecting conformational properties of a vaccine structure (e.g. the number of alanine spacers between mannosyl moieties) could affect the Th actvation pathway. As can be seen, **G1-G3** only varied by their number of alanine spacers but had different levels of cytokine production. The CBA results further showed that **G4** with no mannose on the structure showed no IL-4 production but showed comparatively higher levels of IL-2, showing a tendency to activate the Th1 pathway (Table 5-2). The positive control **G8** showed a high level of IL-2 and TNF (Table 5-2). Another study by Fabienne *et al.* showed that when OVA protein was injected subcutaneously it could generated cytokines related to the Th1 pathway [356]. In general, all vaccine constructs **G1 and G2** and **G4-8** were able to induce cytokines related to Th1 pathway, however, **G3** was more selective towards the Th2 pathway with no IL-2 production.

TLRs 2 and 4 have been shown to be involved in binding to lipopolysaccharides on bacterial cell walls and consequently activating Th1 cytokines (including TNF and IL-12) resulting in varying levels of cytokines depending on the structural properties of the selected lipopolysaccharides [357]. Further, it has been shown that TLR activation can consequently activate Th1 while a lack of TLR activation can result in the production of cytokines responsible for Th2 [357].

These results are exciting due to the fact that differences in the structure, including presence or absence of lipid has been able to affect the cytokine production pathway and this could enlighten the future of targeting specific immune pathway. There has been a growing interest in the application of cytokines and vaccine constructs that activate specific cytokine pathways for cancer therapy [358-360].

Comparing the results from ICS and CBA shows that **G1** and **G2,** which had shown significance in the level of IFN-γ produced, had a relatively high IL-2 response in the CBA assay confirming activation of Th1.

5.2.3 Antibody production

Antibody measurements are generally performed to estimate the level of humoral response resulting from B cell activation through a Th2 pathway (Figure 5-1) [361]. Antibody production is essential to the immune system for pathogen deactivation. In this study, sera from vaccinated mice were collected at days 10, 31 and 52 following 1, 2 and 3 vaccinations, respectively. An ELISA was performed whereby ELISA plates were coated in OVA protein (dissolved in PBS) to capture the IgG specific

antibody response found in the vaccinated mice sera (Figure 5-8). Experimental details are described in **Chapter 2**, **Section 2.3.8**.

The ELISA results (Figure 5-9) indicated that the B cell epitope in the $OVA_{323-339}$ epitope that is hypothesised to activate a B cell response through polarisation of CD4 to Th2 did not give strong activation for a B cell response to produce antibodies. Antibody production for the vaccine constructs (**G1-G9**) was analysed by ELISA (Figure 5-9). Results were significant ($p<0.1$) for an IgG response of **G4** (no mannose, Figure 5-9) when compared to **G1 and** G**2** and **G5-G7**, **G8** and **G9** following the first, second and third vaccination. Antibody production by OVA protein injected with CT is previously reported to be very low [356].

Comparing **G1** ELISA results with the cytokine production study in **Section 5.2.2** implies that **G1** has a tendency to activate the Th1 pathway and is further confirmed by a lack of antibody response.

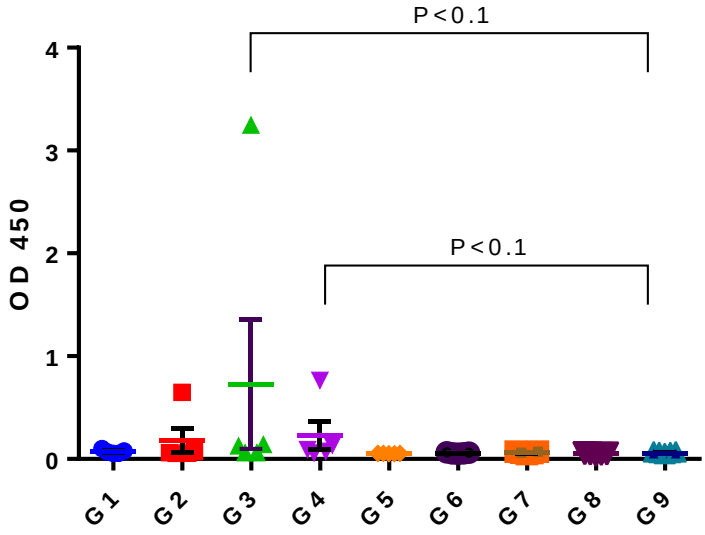

Figure 5-9. Antigen specific antibody production following vaccination using ELISA assay. Sera were collected on days 10 (9 days post the first vaccination), 31 (10 days post the second vaccination) and 52 (10 days post the third vaccination). IgG UV intensity was recorded (OD 450) for a 1/200 dilution for all mice groups (**G1-G9**). Mean ± SEM is shown. Unpaired t-Test was used to show significance when p <0.1. Positive control is **G8** vaccinated with $OVA_{323-339}$ plus cholera toxin and negative control is **G9** vaccinated with PBS. There were 5 mice per group.

An antibody response is known to be correlated to the Th2 activation pathway which is followed by B cell activation (Figure 1-5) [341]. Although **Section 5.2.2** results indicated that addition of mannose to these constructs caused selectivity towards a Th2 pathway activation, this activation was not

confirmed with antibody production after each vaccination dose. This was also observed by Junda *et al.,* who reported that mannosylated $OVA_{323-339}$ administered with CFA impaired antibody response [341]. In a study done by Anjuere *et al.* it was observed that cholera toxin B transdermal injection could activate Th1 cytokines while supressing antibody production [356].

Further, in this study, lipids alone on a vaccine construct (**G4**) caused a B cell response which was confirmed with antibody production (Figure 5-9). Thus, lipidic and mannosyl moieties present with the $OVA_{323-339}$ on the vaccine structures (**G1-3**) have failed to help in IgG production.

In addition, **G2** and **G3** showed a relatively higher antibody titre following the third vaccination (Figure 5-9), however, when the vaccinated groups (**G1-9**) were tested for the amount of antibody production per mouse per group (Figure 5-9), only one mouse per group gave a high antibody response showing immune variations in the inbred mouse [362].

In general, antibody production by the vaccination groups **G1-8** was considered to be not significant in comparison with the negative control (vaccinated with PBS). Previous studies on OT-II transgenic or wild-type C57BL/6 mice immunised with $OVA_{323-339}$ had reported failure of IgG production in the vaccinated mice sera when compared to negative control (saline) [363]. In another study by Kel *et al.,* it was reported that vaccination with mannosylated $OVA_{323-339}$ resulted in significantly lower levels of IgG antibody compared to the negative control group (PBS) [335]. This reduction in the IgG level was used as a positive aspect for control of hypersensitivity [335]. Future studies with more numbers of mice may produce more reliable results which may indicate a better understanding of structural variations on antibody response. In general, the results showed a lack of an antibody response following vaccination with **G1-9** as well as a lack of T cell proliferation (**Section 5.2.1**).

5.3 Conclusion

This chapter presented *in vivo* results to determine the structural relation of **G1-6** to immunity pathways activated following vaccination. This was assessed through T cell proliferation studies on adoptively transferred OT-II T cells in C57BL/6 mice, following vaccination by **G1-G9**. **G7-9** were the control vaccination groups where **G7** was a non-conformed vaccination group containing a mixture of $OVA_{323-339}$, mannose and lipid. **G8** was $OVA_{323-339}$ plus CT as a positive control and **G9** was a negative control (PBS).

Mannosylated OVA peptides have long been investigated for their cellular and immunological properties [120]. $OVA_{323-339}$ is known to be presented through MHC II molecules on DCs. Here, the structural relationship of *O*-mannosylated $OVA_{323-339}$ lipopeptides was investigated by observing the immune response in the mice. Interestingly, the *in vivo* OT-II proliferation ability remained unchanged following vaccination by mannosylated lipopeptides, due to possible partial activation, however, the same vaccine constructs **13-16** were able to activate OT-II cells proliferation *in vitro* (**Chapter 4, Section 4.2.3**). This contrast shows the need of better mouse models for the study of CD4 T cell activation where adopted T cells do not diminish in a short period of time. Along with a lack of OT-II production ability, vaccine groups 1-6 failed to show significance of $CD62L^{low}CD4^{+}$ cells responsible for recall.

ICS and CBA assay results showed antigen specific cytokine release linked to $CD4^{+}$ T cells. **G1** and G**2** (mannosylated lipopeptides with 1 and 2 alanine spaces between mannosyl moieties) had the ability to activate the pro-inflammatory cytokines involved in Th1 and Th2 pathways (Figure 5-7, Tables 5-1, 5-2). Among all the studied vaccination groups (**G1-9**), **G4** was the most selective towards the release of cytokines involved in the Th1 pathway, however, the level of cytokine for **G4** was not significantly high. **G3** showed no Th1 activation but showed Th2 activation. The overall results showed that cytokine release indicated that presence of mannosyl moiety on the vaccine structure, which in turn shows a tendency towards cytokine production along the Th2 pathway. Lipidation, on the other hand, showed cytokine production related to the Th1 pathway. Further, it was found that structural differences including the number of spacers between mannosyl moieties could affect specificity towards different Th pathways.

Selectivity towards the activation of T helpers is an important aspect of vaccine designs. **G3** showed selectivity towards Th2 pathway to release cytokines but showed no Th1 activation. This finding is interesting since the difference between **G1**, G**2** and G**3** was the space between the mannosyl moieties, indicating that a bigger space between the mannosyls produces selectivity towards Th2 activation pathway. This change in the number of spaces was shown in **Chapter 4** to affect the *in vitro* results. A possible conformational change could be responsible in the antigen position in the formed particles.

IgG production was studied by ELISA assay (Figure 5-9). Here, lipid moiety alone on the vaccine structures was relatively helpful in antibody production by activating B cell antigen recognition while it was concluded that addition of mannosyl and lipid moiety (**G1-5**) to the $OVA_{323-339}$ peptide failed to increase IgG to a significant level when compared to the negative control. Positive control group

G8 showed no success in activating an antibody response which was in line with its Th1 activated cytokines (results from ICS and CBA assays). This lack of antibody response and activation of Th1 pathway was previously reported [356].

In general, the designed structures showed selectivity towards different Th response pathways, which provides progress towards the future design of peptide-based subunit vaccines.

Chapter 6: Conclusion and future prospects

In the area of vaccine development for immune modulation, targeting specific receptors on cells involved in the immune system's front line of defence has been shown to enhance an immune response. Here, within the family of C-type lectins, the MR is a key front line receptor in the body's defence against pathogens [270]. This receptor is located on DCs and macrophages which form the first barrier when foreign pathogens enter the body. APCs have been well-documented in the removal of pathogens from the body and their role in the immune response. Targeting these specific cells and their surface receptors is seen as a promising way of advancing vaccine design.

Many studies have investigated the enhanced development of vaccines (and delivery systems) through the targeting of the MR. The most common approach has been achieved through glycosylation of antigens to mimic the pathogen's cell surface, for a better recognition and a consequent internalisation. However, there are many unknown aspects of targeted vaccine design, including the structure of the receptor, the required arrangement of targeting moieties and spatial arrangement of CRDs, making this receptor an important focus for researchers investigating advanced vaccine design. It is known that glycosylated antigens, in particular mannosylated, have enhanced binding and targeting of the MR and research has recently focused on this approach for enhancing vaccine development. This stems from glycosylation being present on the surface of pathogens that researchers want to mimic this in their research. This approach has been common for the targeting of peptide and protein-based vaccines for a number of diseases. However, due to the unknown conformation of the MR, there are many questions surrounding the conformational properties and structure of a glycosylated vaccine required for effective receptor targeting, and these are yet to be addressed [268].

Synthetic peptide vaccines, due to their stability and their easily modifiable structure, are found to be an important part of vaccine development studies. Tailoring of these peptide vaccines through the inclusion of antigenic moieties, addition of lipids and/or glycosyl units, and addition of one or more epitopes enables researchers to develop a vaccine for a particular disease with defined structural properties, potentially enhancing the desired immune response. This synthetic approach also offers the ability to target specific cell surface receptors, such as the MR, through inclusion of mannose units, potentially advancing vaccine development.

This thesis aimed to develop mannosylated lipopeptides that could target the MR and activate the immune system.

A library of mannosylated lipopeptides was designed that included an $OVA_{323-339}$ epitope as a model epitope, two lipid moieties to give adjuvanting properties, and two mannose moieties. The constructed

library was designed to investigate the effect the distance between the two mannose units had on MR affinity (*in vitro* and *in vivo*) and to achieve this an alanine spacer (0, 1, or 2 alanine amino acids in length) was inserted between each mannose moiety. A fluorescent tag was also included in each construct to enable tracking in *in vitro* cell studies. A library of control vaccine constructs was also prepared to study the role of lipid and/or sugar moieties on the targeting of this receptor (*in vitro*) and immune response (*in vivo*). This thesis aimed to test three hypothesis; hypotheses 1: Improvement of the synthesis of fluorescently tagged multicomponent mannosylated lipoeptides; hypotheses 2: Linear placement of mannosyl moieties in the vaccine constructs and an alanine spacer plays a role in antigen presenting cells uptake through enhanced receptor targeting, and hypotheses 3: structural properties in a vaccine construct could affect the activation immune pathways.

To answer hypotheses 1: Synthesis of this multi-component vaccine construct library (containing mannose, lipids, OVA epitope, and a fluorescent tag) and the control library (containing either/or mannose, either/or lipids, OVA epitope, and a fluorescent tag) was carried out using a combination of manual methods and microwave assisted solid phase peptide synthesis. To enable successful synthesis of a complex library, the constructs were prepared as two building blocks which were then conjugated. This has been shown to give higher yields and purity when compared with a linear synthesis of such large and multi-complex molecules. In this study, the peptides were prepared as two sections; 1) azido-functionalised mannosylated peptides with a fluorescent tag, and 2) alkyne $OVA_{323-339}$ lipopeptides. In addition to this, the synthesis of *O*-mannosylated serine building blocks was prepared using a Lewis acid reaction to enable the easy addition of the mannose moieties into each construct using the peptide synthesis methodology. This Lewis acid reaction was successfully monitored and optimised to obtain a better yield than that reported in the literature (42% compared with 5%, respectively).

The method for the synthesis of the azido-functionalized mannosylated peptides was also optimised to ensure high yields although it was complicated by the presence of many different functional groups in a single moiety (azide moiety [for conjugation and formation of the final vaccine constructs at a later stage in the project], mannose units, fluorescent tag). Here, the order of functional group addition and type of side chain protecting groups present on the lysine amino acid (which enables the addition of multiple functional groups) was optimised and overall, high yielding peptides were achieved (**4**-**6**, 54-68%).

The alkyne $OVA_{323-339}$ lipopeptides were prepared using microwave assisted SPPS which enabled a faster synthesis compared with manual synthesis without compromising yield or purity (**11**-**12**, 73-

83%). In these constructs, the alkyne moiety was added to enable conjugation and formation of the final vaccine constructs at a later stage in the project.

Following successful synthesis of the building blocks, alkyne $OVA_{323-339}$ lipopeptides and azido-functionalised mannosylated peptides, the final vaccine constructs were prepared using azido-alkyne copper mediated 'click' chemistry. In this reaction, formation of a triazole bond was generated which has been shown to be stable chemically and metabolically. This 'click' reaction was performed using copper wire and monitored using RP-HPLC. Overall, the reaction was completed in about 5 hours with the final library of vaccines (**13-15**, Figure 3-11) and control constructs (**16-18**, Figure 3-11) successfully synthesised.

To answer hypotheses 2: In vitro analysis of this construct library revealed their specificity towards the MR. The analysis involved (1) uptake/binding studies on macrophages and dendritic cells which are two important types of APCs; (2) a mannan competition assay (where mannan is a known ligand for the MR) investigating receptor-mediated uptake; (3) a SPR assay investigating the binding of these constructs to a recombinant human macrophage MR using Biacore technology; and (4) a T cell activation proliferation assay investigating potential T cell activation upon uptake. These *in vitro* assays were performed to show how the designed construct library specifically interacted with the MR and how the alanine spacers (or distance between each mannose unit) affected their binding and/or uptake affinity. Further, the *in vitro* T cell activation was specifically investigated following uptake of these constructs which are all important factors for any vaccine development.

Uptake studies performed on macrophages and dendritic cells showed a significantly higher uptake for the constructs containing both mannose and lipid (**13-15**) and the control peptide with only a lipid (no mannose, **16**) when compared to other vaccine constructs and the negative control group (PBS). The mannan inhibition assay showed that a significant amount of uptake of the mannosylated constructs (**13-16**, 60-70%) was mediated through the lectin receptors. Interestingly, uptake for the control lipopeptide that contained no mannose was also shown to be lectin-receptor mediated (**16**, 60%). It was concluded that although mannan had blocked the CLRs, other receptors present on these cell (e.g. TLRs) were still capable of processing the vaccine constructs.

The *in vitro* OT-II cell proliferation assay on the OVA sensitive T cells isolated from OT-II transgenic mice showed that the vaccine constructs affected proliferation of the OT-II cells when compared with the PBS negative control. This observed proliferation confirmed that vaccine constructs which contained both mannose and lipids, and the control vaccine with only lipids present could significantly increase the number of OT-II cells *in vitro*.

SPR studies (using Biacore technology) were developed and successfully optimised using the recombinant human MR to study the specific affinity/binding of vaccine constructs and the role of spacer length on receptor binding ability. Here, mannan was used as the positive control and had a strong binding affinity towards the MR (KD: 0.15 µM, Rmax: 47). Mannosylated vaccine constructs with a single alanine spacer between the mannose groups (**14**) had a high affinity and level of binding to the MR (KD: 0.83 µM, Rmax: 425), while the vaccine construct with only a lipid (no mannose, **16**) showed a high affinity to the MR, but the level of binding was very low (KD: 2.91 µM, Rmax: 5). Additionally, the vaccine construct with mannose but no lipids (**17**) also showed a high affinity for the MR but again the binding level was low (KD: 0.12 µM, Rmax: 8). It can be concluded that the presence of both mannose and lipids enhance binding and affinity for this receptor.

Interestingly, the overall *in vitro* findings suggest that vaccine constructs that contain both mannose and lipids have increased APC uptake, affinity and binding for the MR but were equally successful in regulatory T cell activation with vaccine constructs containing only lipid. This is supported by a study by Rauen *et al.* They confirmed that the capacity of OT-II cells proliferation was unchanged in the presence of mannose, but the presence of lipids was found to be the key factor in T cell proliferation [188].

To answer hypotheses 3: In vivo studies were designed to assess the ability of the vaccine constructs in T cell proliferation, cytokine release and antibody response in a mouse model. Here, OT-II cells from transgenic mice were purified and injected into C57BL/6 mice. These mice were then vaccination three times (days 2, 21 and 42) with the vaccine constructs. Ten days post each immunisation, blood was collected and analysed using both ELISA and T cell proliferation assays; ICS and CBS assays were used to measure cytokine release and Th pathway activation.

In the T cell activation/proliferation assay, the OT-II cells transferred to C57BL/6 mice diminished and their proliferation ability was not affected by vaccination. It was also observed that mannosylation enhanced cytokine production related to the Th2 pathway, while lipidation of the constructs (no mannose) enhanced cytokine production indicative of a Th1 pathway. In line with the lack of OT-II cell proliferation, the ELISA results were poor and only the vaccine construct with a lipid (no mannose) was able to induce an antibody response (although small, OD < 1), where further assessment on sera from each mouse per group showed a huge variation in antibody levels between the individual mice. This lack of *in vivo* OT-II proliferation, despite being proved in *in vitro* proliferation by mannosylated peptides, was reported previously by Kel *et al.* [335]. In addition, impaired antibody production with the $OVA_{323-339}$ epitope has also been reported by Leung *et al.* who concluded that $OVA_{323-339}$ did not potentiate an antibody response and did not activate OT-II T cells

[288]. Despite these results, one interesting finding was the relationship between the structural properties and cytokine release pathway as shown in the CBA assay. Here, the vaccine construct with two alanine spacers (**15**) induced specificity towards the Th2 pathway as confirmed by IL-5 and IL-10 production.

The trivial task of purifying carbohydrate moieties from pathogenic cell walls can be overcome by the synthesis of mannosylated peptides that bear effective moieties for vaccine development [364]. Recent advances in adjuvant development have proved that the addition of lipid(s) to an antigenic structure can improve antigen delivery, and in some cases, enhance an immune response. Further, addition of carbohydrates and lipid moieties to an antigenic peptide epitope can be easily achieved with the use of organic chemistry resulting in pure, high yields [365]. Additionally, mannosylation can be a helpful method to increase specific uptake by the immune system's responsible cells such as macrophages and DCs through lectin receptors. Recent advances in the development of methods to enhance and characterise the binding affinity of peptides or proteins to specific receptors have changed the understanding of the requirements for successful targeting of vaccines and drugs. Among these methods, SPR has proved to be a recent methodology used in this type of study, enhancing drug and vaccine screening through *in vitro* binding and affinity measurements.

Many studies have reported failure in *in vivo* T cell activation by mannosylated peptides however, there are studies that have shown success in the development of therapies against delayed type hypersensitivity reactions (which are a type of an autoimmune disease caused by T cell malfunction). Studies have reported success in destroying T cells involved in this disease [335]. In the case of preparing protein and peptides with targeting ability, an understanding of methods that use this specific ability of mannosylation in T cell destruction as well as further progress in application of such qualities in autoimmune diseases would be valuable.

Vaccine development is composed of many aspects and has many hurdles to overcome. These hurdles pertain to the selection of an appropriate antigen and the design of vaccines that can effectively induce the desired therapeutic response. In many cases, vaccines struggle to thrive/advance where mouse models fail to accurately represent the disease and/or immune response when replicated in humans. As a result, more intensive studies are required to solve these variabilities.

References

1. Aguilar, J. and E. Rodriguez, *Vaccine adjuvants revisited.* Vaccine, 2007. **25**(19): p. 3752-3762.
2. Sivakumar, S., et al., *Vaccine adjuvants–Current status and prospects on controlled release adjuvancity.* Saudi Pharmaceutical Journal, 2011. **19**(4): p. 197-206.
3. Germain, R.N., *Vaccines and the Future of Human Immunology.* Immunity, 2010. **33**(4): p. 441-450.
4. De Gregorio, E. and R. Rappuoli, *Vaccines for the future: learning from human immunology.* Microbial Biotechnology, 2012. **5**(2): p. 149-155.
5. Gamvrellis, A., et al., *Vaccines that facilitate antigen entry into dendritic cells.* Immunology and cell biology, 2004. **82**(5): p. 506-516.
6. Burgdorf, S., et al., *Distinct pathways of antigen uptake and intracellular routing in CD4 and CD8 T cell activation.* science, 2007. **316**(5824): p. 612-616.
7. Ramkumar, T.P., D. Hammache, and P.D. Stahl, *The macrophage mannose receptor and innate immunity*, in *Innate Immun.* 2003, Springer. p. 191-204.
8. Weis, W.I., M.E. Taylor, and K. Drickamer, *The C-type lectin superfamily in the immune system.* Immunol. Rev., 1998. **163**: p. 19-34.
9. Irache, J.M., et al., *Mannose-targeted systems for the delivery of therapeutics.* 2008.
10. Royer, P.-J., et al., *The mannose receptor mediates the uptake of diverse native allergens by dendritic cells and determines allergen-induced T cell polarization through modulation of IDO activity.* J. Immunol., 2010. **185**(3): p. 1522-1531.
11. Taylor, M.E., K. Bezouska, and K. Drickamer, *Contribution to ligand binding by multiple carbohydrate-recognition domains in the macrophage mannose receptor.* J. Biol. Chem., 1992. **267**(3): p. 1719-1726.
12. Keler, T., V. Ramakrishna, and M.W. Fanger, *Mannose receptor-targeted vaccines.* Expert opinion on biological therapy, 2004. **4**(12): p. 1953-1962.
13. Lam, J.S., et al., *A model vaccine exploiting fungal mannosylation to increase antigen immunogenicity.* J. Immunol., 2005. **175**(11): p. 7496-7503.
14. Janeway, C.A., et al., *Immunobiology: the immune system in health and disease*. Vol. 2. 2001: Churchill Livingstone London.
15. Iwasaki, A. and R. Medzhitov, *Control of adaptive immunity by the innate immune system.* Nature immunology, 2015. **16**(4): p. 343-353.
16. Levitz, S.M. and C.A. Specht, *Recognition of the fungal cell wall by innate immune receptors.* Curr Fungal Infect Rep, 2009. **3**(3): p. 179-185.
17. Banchereau, J. and R.M. Steinman, *Dendritic cells and the control of immunity.* Nature, 1998. **392**(6673): p. 245-252.

18. Medzhitov, R., *Toll-like receptors and innate immunity.* Nature Reviews Immunology, 2001. **1**(2): p. 135-145.
19. Wu, J. and Z.J. Chen, *Innate immune sensing and signaling of cytosolic nucleic acids.* Annual review of immunology, 2014. **32**: p. 461-488.
20. Villablanca, E.J., V. Russo, and J.R. Mora, *Dendritic cell migration and lymphocyte homing imprinting.* Histol Histopathol, 2008. **23**(7): p. 897-910.
21. Burgdorf, S., et al., *Distinct pathways of antigen uptake and intracellular routing in CD4 and CD8 T cell activation.* Science, 2007. **316**(5824): p. 612-6.
22. Sun, J.C. and M.J. Bevan, *Defective CD8 T cell memory following acute infection without CD4 T cell help.* Science, 2003. **300**(5617): p. 339-42.
23. Bourgeois, C. and C. Tanchot, *Mini-review CD4 T cells are required for CD8 T cell memory generation.* European journal of immunology, 2003. **33**(12): p. 3225-3231.
24. Bourgeois, C., et al., *CD8 lethargy in the absence of CD4 help.* European journal of immunology, 2002. **32**(8): p. 2199-2207.
25. Martinez-Pomares, L., *The mannose receptor.* J. Lukocyte Biol., 2012. **92**(6): p. 1177-1186.
26. Saalmüller, A., et al., *Overview of the Second International Workshop to define swine cluster of differentiation (CD) antigens.* Vet. Immunol. Immunop., 1998. **60**(3): p. 207-228.
27. East, L. and C.M. Isacke, *The mannose receptor family.* Biochim. Biophys. Acta., 2002. **1572**(2-3): p. 364-86.
28. East, L., et al., *Characterization of sugar binding by the mannose receptor family member, Endo180.* J Biol Chem, 2002. **277**(52): p. 50469-75.
29. Wileman, T.E., M.R. Lennartz, and P.D. Stahl, *Identification of the macrophage mannose receptor as a 175-kDa membrane protein.* Proc. Natl. Acad. Sci. USA, 1986. **83**(8): p. 2501-2505.
30. Ezekowitz, R.A.B., et al., *Molecular characterization of the human macrophage mannose receptor: demonstration of multiple carbohydrate recognition-like domains and phagocytosis of yeasts in Cos-1 cells.* J. Exp. Med., 1990. **172**(6): p. 1785-1794.
31. Taylor, M.E., et al., *Primary structure of the mannose receptor contains multiple motifs resembling carbohydrate-recognition domains.* J. Biol. Chem., 1990. **265**(21): p. 12156-12162.
32. Boskovic, J., et al., *Structural model for the mannose receptor family uncovered by electron microscopy of Endo180 and the mannose receptor.* J. Biol. Chem., 2006. **281**(13): p. 8780-8787.
33. Napper, C.E., K. Drickamer, and M.E. Taylor, *Collagen binding by the mannose receptor mediated through the fibronectin type II domain.* Biochem. J., 2006. **395**(Pt 3): p. 579.

34. Taylor, P.R., S. Gordon, and L. Martinez-Pomares, *The mannose receptor: linking homeostasis and immunity through sugar recognition.* Trends Immunol., 2005. **26**(2): p. 104-110.
35. Su, Y., et al., *Glycosylation influences the lectin activities of the macrophage mannose receptor.* J. Biol. Chem., 2005. **280**(38): p. 32811-32820.
36. Taylor, M.E. and K. Drickamer, *Structural requirements for high affinity binding of complex ligands by the macrophage mannose receptor.* J. Biol. Chem., 1993. **268**(1): p. 399-404.
37. Drickamer, K., *Two distinct classes of carbohydrate-recognition domains in animal lectins.* J. Biol. Chem., 1988. **263**(20): p. 9557-9560.
38. Ng, K.K.-S., K. Drickamer, and W.I. Weis, *Structural analysis of monosaccharide recognition by rat liver mannose-binding protein.* J. Biol. Chem., 1996. **271**(2): p. 663-674.
39. Stahl, P.D., *The macrophage mannose receptor - current status.* Am. J. Respir. Cell Mol. Biol., 1990. **2**(4): p. 317-318.
40. Fiete, D.J., M.C. Beranek, and J.U. Baenziger, *A cysteine-rich domain of the "mannose" receptor mediates GalNAc-4-SO4 binding.* Proc. Natl. Acad. Sci. USA, 1998. **95**(5): p. 2089-2093.
41. Kornblihtt, A.R., et al., *Primary structure of human fibronectin: differential splicing may generate at least 10 polypeptides from a single gene.* EMBO J., 1985. **4**(7): p. 1755-9.
42. Lepenies, B., J. Lee, and S. Sonkaria, *Targeting C-type lectin receptors with multivalent carbohydrate ligands.* Adv. Drug Deliv. Rev., 2013.
43. Drickamer, K. and M.E. Taylor, *Biology of Animal Lectins.* Annu. rev. cell biol. , 1993. **9**: p. 237-264.
44. Ezekowitz, R.A.B., et al., *Uptake of Pneumocystis-Carinii Mediated by the Macrophage Mannose Receptor.* Nature, 1991. **351**(6322): p. 155-158.
45. Su, Z., et al., *Opsonin-independent phagocytosis: An effector mechanism against acute blood-stage Plasmodium chabaudi AS infection.* J. Infect. Dis., 2002. **186**(9): p. 1321-1329.
46. Mullin, N.P., K.T. Hall, and M.E. Taylor, *Characterization of ligand binding to a carbohydrate-recognition domain of the macrophage mannose receptor.* J. Biol. Chem., 1994. **269**(45): p. 28405-28413.
47. Weis, W.I., K. Drickamer, and W.A. Hendrickson, *Structure of a C-type mannose-binding protein complexed with an oligosaccharide.* Nature., 1992. **360**(6400): p. 127-34.
48. Napper, C.E., M.H. Dyson, and M.E. Taylor, *An extended conformation of the macrophage mannose receptor.* J. Biol. Chem., 2001. **276**(18): p. 14759-14766.
49. Takahashi, K. and R.A.B. Ezekowitz, *The role of the mannose-binding lectin in innate immunity.* Clin. infect. dis., 2005. **41**(Supplement 7): p. S440-S444.

50. Fraser, I.P., H. Koziel, and R.A.B. Ezekowitz. *The serum mannose-binding protein and the macrophage mannose receptor are pattern recognition molecules that link innate and adaptive immunity*. in *Semin. immunol.* 1998. Elsevier.
51. Wilson, M.E. and R. Pearson, *Roles of CR3 and mannose receptors in the attachment and ingestion of Leishmania donovani by human mononuclear phagocytes.* Infect. Immun., 1988. **56**(2): p. 363-369.
52. Schlesinger, L., *Macrophage phagocytosis of virulent but not attenuated strains of Mycobacterium tuberculosis is mediated by mannose receptors in addition to complement receptors.* J. Immunol., 1993. **150**(7): p. 2920-2930.
53. Upham, J.P., et al., *Macrophage Receptors for Influenza A Virus: Role of the Macrophage Galactose-Type Lectin and Mannose Receptor in Viral Entry.* Journal of Virology, 2010. **84**(8): p. 3730-3737.
54. Apostolopoulos, V. and I.F. McKenzie, *Role of the mannose receptor in the immune response.* Curr Mol Med, 2001. **1**(4): p. 469-74.
55. Chieppa, M., et al., *Cross-linking of the mannose receptor on monocyte-derived dendritic cells activates an anti-inflammatory immunosuppressive program.* J. Immunol., 2003. **171**(9): p. 4552-4560.
56. Quah, B.J. and C.R. Parish, *Innate immune mechanisms: nonself recognition.* eLS, 2005.
57. Epstein, J., et al., *The collectins in innate immunity.* Curr. Opin. Immunol., 1996. **8**(1): p. 29-35.
58. Lorenz, R., J. Blum, and P. Allen, *Constitutive competition by self proteins for antigen presentation can be overcome by receptor-enhanced uptake.* J. Immunol., 1990. **144**(5): p. 1600-1606.
59. Prigozy, T.I., et al., *The mannose receptor delivers lipoglycan antigens to endosomes for presentation to T cells by CD1b molecules.* Immunity, 1997. **6**(2): p. 187-197.
60. Engering, A.J., et al., *The mannose receptor functions as a high capacity and broad specificity antigen receptor in human dendritic cells.* Eur. J. of Immunol., 1997. **27**(9): p. 2417-2425.
61. Levitz, S.M. and C.A. Specht, *The molecular basis for the immunogenicity of Cryptococcus neoformans mannoproteins.* FEMS yeast res., 2006. **6**(4): p. 513-524.
62. Tan, M., et al., *Mannose receptor-mediated uptake of antigens strongly enhances HLA class II-restricted antigen presentation by cultured dendritic cells.* Eur. J. of Immunol., 1997. **27**(9): p. 2426-2435.
63. Trombetta, E.S. and I. Mellman, *Cell biology of antigen processing in vitro and in vivo.* Annu. Rev. Immunol., 2005. **23**: p. 975-1028.

64. De Saint-Vis, B., et al., *A novel lysosome-associated membrane glycoprotein, DC-LAMP, induced upon DC maturation, is transiently expressed in MHC class II compartment.* J. Immunol., 1998. **9**(3): p. 325-336.
65. Giddam, A.K., et al., *Liposome-based delivery system for vaccine candidates: constructing an effective formulation.* Nanomedicine, 2012. **7**(12): p. 1877-1893.
66. Brooks, N.A., et al., *Cell-penetrating peptides: application in vaccine delivery.* Biochim Biophys Acta, 2010. **1805**(1): p. 25-34.
67. Chatterjee, D., et al., *Structural basis of capacity of lipoarabinomannan to induce secretion of Tumor-Necrosis-Factor.* Infect. Immun., 1992. **60**(3): p. 1249-1253.
68. Singh, S.K., et al., *Design of neo-glycoconjugates that target the mannose receptor and enhance TLR-independent cross-presentation and Th1 polarization.* Eur. J. of Immunol., 2011. **41**(4): p. 916-925.
69. Apostolopoulos, V., et al., *Ex vivo targeting of the macrophage mannose receptor generates anti-tumor CTL responses.* Vaccine, 2000. **18**(27): p. 3174-3184.
70. Apostolopoulos, V., et al., *Aldehyde-mannan antigen complexes target the MHC class I antigen-presentation pathway.* Eur. J. Immunol., 2000. **30**(6): p. 1714-23.
71. Apostolopoulos, V., et al., *Oxidative/reductive conjugation of mannan to antigen selects for T1 or T2 immune responses.* Proc. Natl. Acad. Sci. USA, 1995. **92**(22): p. 10128-32.
72. Apostolopoulos, V., et al., *Pilot phase III immunotherapy study in early-stage breast cancer patients using oxidized mannan-MUC1* Breast Cancer Res., 2006. **8**(3): p. 27.
73. Ahlen, G., et al., *Mannosylated Mucin-Type Immunoglobulin Fusion Proteins Enhance Antigen-Specific Antibody and T Lymphocyte Responses.* Plos One, 2012. **7**(10).
74. Apostolopoulos, V., G.A. Pietersz, and I.F. McKenzie, *Cell-mediated immune responses to MUC1 fusion protein coupled to mannan.* Vaccine, 1996. **14**(9): p. 930-8.
75. Tan, M.C., et al., *Mannose receptor-mediated uptake of antigens strongly enhances HLA class II-restricted antigen presentation by cultured dendritic cells.* Eur. J. of Immunol., 1997. **27**(9): p. 2426-35.
76. Gustafsson, A., et al., *Pichia pastoris-produced mucin-type fusion proteins with multivalent O-glycan substitution as targeting molecules for mannose-specific receptors of the immune system.* Glycobiology, 2011. **21**(8): p. 1071-1086.
77. Brimble, M.A., et al., *Synthesis of fluorescein-labelled O-mannosylated peptides as components for synthetic vaccines: comparison of two synthetic strategies.* Org. Biomol. Chem., 2008. **6**(1): p. 112-121.

78. Kel, J.M., et al., *Immunization with mannosylated peptide induces poor T cell effector functions despite enhanced antigen presentation.* Int. Immunol., 2008. **20**(1): p. 117-127.
79. Gao, J., et al., *Novel monodisperse PEGtide dendrons: design, fabrication and evaluation of mannose receptor-mediated macrophage targeting.* Bioconjugate Chemistry, 2013.
80. Biessen, E.A.L., et al., *Lysine-based cluster mannosides that inhibit ligand binding to the human mannose receptor at nanomolar concentration.* J. Biol. Chem., 1996. **271**(45): p. 28024-28030.
81. Kinzel, O., et al., *Synthesis of a functionalized high affinity mannose receptor ligand and its application in the construction of peptide-, polyamide- and PNA-conjugates.* J. Pept. Sci., 2003. **9**(6): p. 375-385.
82. Kantchev, E.A.B., et al., *Direct solid-phase synthesis and fluorescence labeling of large, monodisperse mannosylated dendrons in a peptide synthesizer.* Org. Biomol. Chem., 2008. **6**(8): p. 1377-1385.
83. Apostolopoulos, V., *Interview. Cancer vaccines and immunotherapy of autoimmune diseases.* J. Immunother., 2009. **1**(1): p. 15-7.
84. Apostolopoulos, V., et al., *Gallium-diffused waveguides in sapphire.* Opt Lett, 2001. **26**(20): p. 1586-8.
85. Apostolopoulos, V., E. Lazoura, and M. Yu, *MHC and MHC-like molecules: structural perspectives on the design of molecular vaccines.* Adv. Exp. Med. Biol., 2008. **640**: p. 252-67.
86. Apostolopoulos, V. and F.M. Marincola, *Methods to measure vaccine immunity*. Expert Rev. Vaccines, 2010. **9**(6): p. 545-6.
87. Apostolopoulos, V., et al., *Applications of peptide mimetics in cancer*. Curr Med Chem, 2002. **9**(4): p. 411-20.
88. Nelson, R.D., et al., *Candida mannan - chemistry, suppression of cell-mediated-Immunity, and possible mechanisms of action.* Clin. Microbiol. Rev., 1991. **4**(1): p. 1-19.
89. Raschke, W.C., et al., *Genetic control of yeast mannan structure. Isolation and characterization of mannan mutants.* J Biol Chem, 1973. **248**(13): p. 4660-6.
90. Drickamer, K., *C-type lectin-like domains.* Curr. Opin. Struct. Biol., 1999. **9**(5): p. 585-590.
91. Sheng, K.C., et al., *Mannan derivatives induce phenotypic and functional maturation of mouse dendritic cells.* Immunology, 2006. **118**(3): p. 372-83.
92. Vasudevan, D.M., S. Sreekumari, and K. Vaidyanathan, *Textbook of Biochemistry for medical students*. 2010, JP Brothers. p. 74.

93. Ranta, K., et al., *Evaluation of Immunostimulatory Activities of Synthetic Mannose-Containing Structures Mimicking the beta-(1 -> 2)-Linked Cell Wall Mannans of Candida albicans.* Clin. Vaccine. Immunol., 2012. **19**(11): p. 1889-1893.
94. Apostolopoulos, V., et al., *Pilot phase III immunotherapy study in early-stage breast cancer patients using oxidized mannan-MUC1* Breast Cancer Res., 2006. **8**(3): p. 27.
95. Apostolopoulos, V., M.S. Sandrin, and I.F. McKenzie, *Carbohydrate/peptide mimics: effect on MUC1 cancer immunotherapy.* J Mol Med (Berl), 1999. **77**(5): p. 427-36.
96. Apostolopoulos, V., D.B. Weiner, and J. Gong, *Cancer vaccines: methods for inducing immunity.* Expert Rev. Vaccines, 2008. **7**(7): p. 861-2.
97. Johnson, M.A. and D.R. Bundle, *Designing a new antifungal glycoconjugate vaccine.* Chem. Soc. Rev., 2013. **42**(10): p. 4327-4344.
98. Dube, D.H., K. Champasa, and B. Wang, *Chemical tools to discover and target bacterial glycoproteins.* Chemical Communications, 2011. **47**(1): p. 87-101.
99. Romero, P.A., et al., *Ktr1p is an alpha-1,2-mannosyltransferase of Saccharomyces cerevisiae Comparison of the enzymic properties of soluble recombinant Ktr1p and Kre2p/Mnt1p produced in Pichia pastoris.* Biochemical Journal, 1997. **321**: p. 289-295.
100. Cao, B., J.M. White, and S.J. Williams, *Synthesis of glycoconjugate fragments of mycobacterial phosphatidylinositol mannosides and lipomannan.* Beilstein Journal of Organic Chemistry, 2011. **7**: p. 369-376.
101. Cao, B., J.M. White, and S.J. Williams, *Synthesis of glycoconjugate fragments of mycobacterial phosphatidylinositol mannosides and lipomannan.* Beilstein journal of organic chemistry, 2011. **7**(1): p. 369-377.
102. Karanikas, V., et al., *Antibody and T cell responses of patients with adenocarcinoma immunized with mannan-MUC1 fusion protein.* J Clin Invest, 1997. **100**(11): p. 2783-92.
103. Karanikas, V., et al., *High frequency of cytolytic T lymphocytes directed against a tumor-specific mutated antigen detectable with HLA tetramers in the blood of a lung carcinoma patient with long survival.* Cancer Res., 2001. **61**(9): p. 3718-3724.
104. Singh, S.K., et al., *Design of neo-glycoconjugates that target the mannose receptor and enhance TLR-independent cross-presentation and Th1 polarization.* European Journal of Immunology, 2011. **41**(4): p. 916-925.
105. Schlesinger, L., *Macrophage phagocytosis of virulent but not attenuated strains of Mycobacterium tuberculosis is mediated by mannose receptors in addition to complement receptors.* The Journal of Immunology, 1993. **150**(7): p. 2920-2930.

106. Wittmann, V. and S.J. Danishefsky, *Glycopeptides and Glycoproteins: Synthesis, Structure, and Application*. Glycopeptides and Glycoproteins: Synthesis, Structure, and Application. Vol. 267. 2007. 1-265.
107. Bernardi, A., et al., *Multivalent glycoconjugates as anti-pathogenic agents.* Chem. Soc. Rev., 2013. **42**(11): p. 4709-4727.
108. Otvos, L., et al., *Glycosylation of synthetic T-helper cell epitopic peptides influences their antigenic potency and conformation in a sugar location-specific manner.* BBA-Mol Cell Res., 1994. **1224**(1): p. 68-76.
109. White, K., et al., *Increased adjuvant activity of minimal CD8 T cell peptides incorporated into lipid-core-peptides.* Immunol. Cell Biol., 2004. **82**(5): p. 517-522.
110. Vegad, H., et al., *Glycosylation of Fmoc amino acids: Preparation of mono- and di-glycosylated derivatives and their incorporation into Arg-Gly-Asp (RGD)-containing glycopeptides.* Perkin Trans. 1 and Perkin 1997(9): p. 1429-1441.
111. Zhang, Y.L., et al., *Enhanced epimerization of glycosylated amino acids during solid-phase peptide synthesis.* J. Am. Chem. Soc., 2012. **134**(14): p. 6316-6325.
112. Szabo, T.G., et al., *Critical role of glycosylation in determining the length and structure of T cell epitopes.* Immunome Res., 2009. **5**: p. 4.
113. Kong, F., et al., *Mannosylated liposomes for targeted gene delivery.* Int J Nanomedicine, 2012. **7**: p. 1079-1089.
114. Vyas, S.P., A.K. Goyal, and K. Khatri, *Mannosylated liposomes for targeted vaccines delivery*, in *Liposomes*. 2010, Springer. p. 177-188.
115. Kelly, C., C. Jefferies, and S.-A. Cryan, *Targeted liposomal drug delivery to monocytes and macrophages.* Journal of drug delivery, 2010. **2011**.
116. Kragol, G. and L. Otvos, *Orthogonal solid-phase synthesis of tetramannosylated peptide constructs carrying three independent branched epitopes.* Tetrahedron, 2001. **57**(6): p. 957-966.
117. Liu, M.A., et al., *Conformational consequences of protein glycosylation: Preparation of O-mannosyl serine and threonine building blocks, and their incorporation into glycopeptide sequences derived from alpha-dystroglycan.* Biopolymers, 2008. **90**(3): p. 358-368.
118. Engering, A.J., et al., *The mannose receptor functions as a high capacity and broad specificity antigen receptor in human dendritic cells.* European Journal of Immunology, 1997. **27**(9): p. 2417-2425.
119. Burgdorf, S., V. Lukacs-Kornek, and C. Kurts, *The mannose receptor mediates uptake of soluble but not of cell-associated antigen for cross-presentation.* J. Immunol., 2006. **176**(11): p. 6770-6776.

120. Sheng, K.C., et al., *The adjuvanticity of a mannosylated antigen reveals TLR4 functionality essential for subset specialization and functional maturation of mouse dendritic cells.* J Immunol, 2008. **181**(4): p. 2455-2464.
121. Frison, N., et al., *Oligolysine-based oligosaccharide clusters - Selective recognition and endocytosis by the mannose receptor and dendritic cell-specific intercellular adhesion molecule 3 (ICAM-3)-grabbing nonintegrin.* J. Biol. Chem., 2003. **278**(26): p. 23922-23929.
122. Drickamer, K. and R.A. Dwek, *Carbohydrates and Glycoconjugates - Editorial Overview.* Curr. Opin. Struct. Biol., 1995. **5**(5): p. 589-590.
123. Napper, C.E. and M.E. Taylor, *The mannose receptor fails to enhance processing and presentation of a glycoprotein antigen in transfected fibroblasts.* Glycobiology, 2004. **14**(10): p. 7C-12C.
124. Liu, C.F., et al., *Bacterial protein-O-mannosylating enzyme is crucial for virulence of Mycobacterium tuberculosis.* Proc. Natl. Acad. Sci. U.S.A., 2013. **110**(16): p. 6560-6565.
125. Espitia, C., L. Servin-Gonzalez, and R. Mancilla, *New insights into protein O-mannosylation in actinomycetes.* Mol. Biosyst., 2010. **6**(5): p. 775-781.
126. Ifrim, D.C., et al., *Candida albicans primes TLR cytokine responses through a Dectin-1/Raf-1-mediated pathway.* J. Immunol., 2013. **190**(8): p. 4129-4135.
127. Nandakumar, S., et al., *O-mannosylation of the Mycobacterium tuberculosis Adhesin Apa Is Crucial for T Cell Antigenicity during Infection but Is Expendable for Protection.* PLoS pathogens, 2013. **9**(10): p. e1003705.
128. Apostolopoulos, V., et al., *Targeting antigens to dendritic cell receptors for vaccine development.* Journal of drug delivery, 2013. **2013**.
129. Tang, C.K., et al., *Oxidized and reduced mannan mediated MUC1 DNA immunization induce effective anti-tumor responses.* Vaccine, 2008. **26**(31): p. 3827-3834.
130. Brimble, M.A., et al., *Synthesis of fluorescein-labelled O-mannosylated peptides as components for synthetic vaccines: comparison of two synthetic strategies.* Org. Biomol. Chem., 2007. **6**(1): p. 112-121.
131. Kowalczyk, R., *Synthesis of mannosylated peptides as components for synthetic vaccines*. 2008, Published Doctoral Dissertation University of Auklan, Auklan New Zealand.
132. Moyle, P.M., et al., *Toward the development of prophylactic and therapeutic human papillomavirus type-16 lipopeptide vaccines.* J. Med. Chem., 2007. **50**(19): p. 4721-4727.
133. Raiber, E.A., et al., *Targeted Delivery of Antigen Processing Inhibitors to Antigen Presenting Cells via Mannose Receptors.* Acs Chemical Biology, 2010. **5**(5): p. 461-476.
134. Reddy, S.T., et al., *Exploiting lymphatic transport and complement activation in nanoparticle vaccines.* Nature biotechnology, 2007. **25**(10): p. 1159-1164.

135. Arens, R., et al. *Prospects of combinatorial synthetic peptide vaccine-based immunotherapy against cancer*. in *Seminars in immunology*. 2013. Elsevier.
136. Skwarczynski, M. and I. Toth, *Peptide-based synthetic vaccines.* Chemical Science, 2015.
137. Doherty, T.M. and P. Andersen, *Vaccines for tuberculosis: novel concepts and recent progress.* Clinical microbiology reviews, 2005. **18**(4): p. 687-702.
138. Toussaint, N.C. and O. Kohlbacher, *OptiTope-a web server for the selection of an optimal set of peptides for epitope-based vaccines.* Nucleic Acids Research, 2009. **37**(suppl_2): p. W617-W622.
139. Moss, D.J., C. Schmidt, and S. Elliott, *Strategies Involved in Developing.* Advances in cancer research, 1996. **69**: p. 213.
140. Pruksakorn, S., et al., *Identification of T cell autoepitopes that cross-react with the C-terminal segment of the M protein of group A streptococci.* International Immunology, 1994. **6**(8): p. 1235-1244.
141. Purcell, A.W., J. McCluskey, and J. Rossjohn, *More than one reason to rethink the use of peptides in vaccine design.* Nature reviews Drug discovery, 2007. **6**(5): p. 404-414.
142. Kastin, A., *Handbook of biologically active peptides*. 2013: Access Online via Elsevier.
143. Fischer, E., *Synthese von Derivaten der Polypeptide.* Berichte der deutschen chemischen Gesellschaft, 1903. **36**(2): p. 2094-2106.
144. Coin, I., M. Beyermann, and M. Bienert, *Solid-phase peptide synthesis: from standard procedures to the synthesis of difficult sequences.* Nature protocols, 2007. **2**(12): p. 3247-3256.
145. du Vigneaud, V., et al., *The synthesis of oxytocin1*. Journal of the American Chemical Society, 1954. **76**(12): p. 3115-3121.
146. Stewart, J.M. and J.D. Young, *Solid phase peptide synthesis*. 1969, San Francisco - Book: W. H. Freeman.
147. Vaino, A.R. and K.D. Janda, *Solid-phase organic synthesis: a critical understanding of the resin.* Journal of combinatorial chemistry, 2000. **2**(6): p. 579-596.
148. Stawikowski, M. and G.B. Fields, *Introduction to peptide synthesis.* Current Protocols in Protein Science, 2012: p. 18.1. 1-18.1. 13.
149. Carpino, L.A. and G.Y. Han, *9-Fluorenylmethoxycarbonyl function, a new base-sensitive amino-protecting group.* Journal of the American Chemical Society, 1970. **92**(19): p. 5748-5749.
150. Schneider, J.P., et al., *Responsive hydrogels from the intramolecular folding and self-assembly of a designed peptide.* Journal of the American Chemical Society, 2002. **124**(50): p. 15030-15037.

151. Reche, P.A., et al., *Peptide-based immunotherapeutics and vaccines.* Journal of immunology research, 2014. **2014**.
152. Vogel, F.R., M.F. Powell, and C.R. Alving, *A compendium of vaccine adjuvants and excipients.* Vaccine design: the subunit and adjuvant approach, 1995. **6**: p. 141-228.
153. Zhong, W., M. Skwarczynski, and I. Toth, *Lipid Core Peptide System for Gene, Drug, and Vaccine Delivery.* Australian Journal of Chemistry, 2009. **62**(9): p. 956-967.
154. Azmi, F., et al., *Recent progress in adjuvant discovery for peptide-based subunit vaccines.* Human vaccines & immunotherapeutics, 2014. **10**(3): p. 778-796.
155. Chianese-Bullock, K.A., et al., *MAGE-A1-, MAGE-A10-, and gp100-derived peptides are immunogenic when combined with granulocyte-macrophage colony-stimulating factor and montanide ISA-51 adjuvant and administered as part of a multipeptide vaccine for melanoma.* The Journal of Immunology, 2005. **174**(5): p. 3080-3086.
156. Petrovsky, N., *Novel human polysaccharide adjuvants with dual Th1 and Th2 potentiating activity.* Vaccine, 2006. **24**: p. S26-S29.
157. Wallrapp, C., et al., *Cell-based delivery of glucagon-like peptide-1 using encapsulated mesenchymal stem cells.* Journal of Microencapsulation, 2013. **30**(4): p. 315-324.
158. Zhang, L. and G. Bulaj, *Converting peptides into drug leads by lipidation.* Current medicinal chemistry, 2012. **19**(11): p. 1602-1618.
159. Moyle, P.M. and I. Toth, *Self-adjuvanting lipopeptide vaccines.* Curr Med Chem, 2008. **15**(5): p. 506-16.
160. Fagan, V., I. Toth, and P. Simerska, *Convergent synthetic methodology for the construction of self-adjuvanting lipopeptide vaccines using a novel carbohydrate scaffold.* Beilstein J Org Chem, 2014. **10**: p. 1741-8.
161. Renaudet, O., et al., *Linear and branched glyco-lipopeptide vaccines follow distinct cross-presentation pathways and generate different magnitudes of antitumor immunity.* PLoS One, 2010. **5**(6): p. e11216.
162. Brown, L. and D. Jackson, *Lipid-based Self-Adjuvanting Vaccines.* Current Drug Delivery, 2005. **2**(4): p. 383-393.
163. Deres, K., et al., *In vivo priming of virus-specific cytotoxic T lymphocytes with synthetic lipopeptide vaccine.* 1989.
164. Moyle, P.M. and I. Toth, *Self-adjuvanting lipopeptide vaccines.* Current medicinal chemistry, 2008. **15**(5): p. 506-516.
165. Skwarczynski, M. and I. Toth, *Lipid-Core-Peptide System for Self-Adjuvanting Synthetic Vaccine Delivery*, in *Bioconjugation Protocols: Strategies and Methods, Second Edition*, S.S. Mark, Editor. 2011, Humana Press Inc: Totowa. p. 297-308.

166. Toth, I., et al., *A combined adjuvant and carrier system for enhancing synthetic peptides immunogenicity utilising lipidic amino acids.* Tetrahedron letters, 1993. **34**(24): p. 3925-3928.
167. Phillipps, K.S.M., et al., *A novel synthetic adjuvant enhances dendritic cell function.* Immunology, 2009. **128**(1): p. e582-e588.
168. Zeng, W., et al., *Highly Immunogenic and Totally Synthetic Lipopeptides as Self-Adjuvanting Immunocontraceptive Vaccines.* The Journal of Immunology, 2002. **169**(9): p. 4905.
169. Skwarczynskim, M., M. Zaman, and I. Toth, *Lipo-peptides/saccharides in peptide vaccine delivery*. 2013.
170. Abdel-Aal, A.-B.M., et al., *Design of three-component vaccines against group A streptococcal infections: importance of spatial arrangement of vaccine components.* Journal of medicinal chemistry, 2010. **53**(22): p. 8041-8046.
171. BenMohamed, L., S.L. Wechsler, and A.B. Nesburn, *Lipopeptide vaccines--yesterday, today, and tomorrow.* Lancet Infect Dis, 2002. **2**(7): p. 425-31.
172. Fitzmaurice, C.J., et al., *The geometry of synthetic peptide-based immunogens affects the efficiency of T cell stimulation by professional antigen-presenting cells.* International immunology, 2000. **12**(4): p. 527.
173. Brahimi, K., et al., *Protection against Plasmodium falciparum malaria in chimpanzees by immunization with the conserved pre-erythrocytic liver-stage antigen 3.* Nature Medicine, 2000. **6**(11): p. 1258-1263.
174. Moyle, P.M., et al., *Toward the development of prophylactic and therapeutic human papillomavirus type-16 lipopeptide vaccines.* Journal of medicinal chemistry, 2007. **50**(19): p. 4721-4727.
175. Zhu, X., et al., *Lipopeptide epitopes extended by an Nϵ-palmitoyl-lysine moiety increase uptake and maturation of dendritic cells through a Toll-like receptor-2 pathway and trigger a Th1-dependent protective immunity*. European journal of immunology, 2004. **34**(11): p. 3102-3114.
176. Lau, Y.F., et al., *Lipid-containing mimetics of natural triggers of innate immunity as CTL-inducing influenza vaccines.* International immunology, 2006. **18**(12): p. 1801-1813.
177. Zhang, L., et al., *Structural requirements for a lipoamino acid in modulating the anticonvulsant activities of systemically active galanin analogues.* Journal of medicinal chemistry, 2009. **52**(5): p. 1310-1316.
178. Takeda, K., T. Kaisho, and S. Akira, *Toll-like receptors.* Annual review of immunology, 2003. **21**(1): p. 335-376.
179. Akira, S., K. Takeda, and T. Kaisho, *Toll-like receptors: critical proteins linking innate and acquired immunity.* Nature immunology, 2001. **2**(8): p. 675-680.

180. Schnare, M., et al., *Toll-like receptors control activation of adaptive immune responses.* Nature immunology, 2001. **2**(10): p. 947-950.
181. Basto, A.P., et al., *Immune response profile elicited by the model antigen ovalbumin expressed in fusion with the bacterial OprI lipoprotein.* Mol Immunol, 2015. **64**(1): p. 36-45.
182. Huntington, J.A. and P.E. Stein, *Structure and properties of ovalbumin.* Journal of Chromatography B, 2001. **756**(1-2): p. 189-198.
183. Courant, T., et al., *Lipid nanoparticles for enhancing immune responses to protein antigens.* une, 2016. **13**: p. 15.
184. McFarland, B.J., et al., *Ovalbumin(323-339) peptide binds to the major histocompatibility complex class III-A(d) protein using two functionally distinct registers.* Biochemistry, 1999. **38**(50): p. 16663-16670.
185. Holen, E. and S. Elsayed, *Specific T cell lines for ovalbumin, ovomucoid, lysozyme and two OA synthetic epitopes, generated from egg allergic patients' PBMC.* Clinical & Experimental Allergy, 1996. **26**(9): p. 1080-1088.
186. McFarland, B.J., et al., *Ovalbumin (323-339) peptide binds to the major histocompatibility complex class II I-Ad protein using two functionally distinct registers.* Biochemistry, 1999. **38**(50): p. 16663-16670.
187. Brooks, N.A., et al., *A membrane penetrating multiple antigen peptide (MAP) incorporating ovalbumin CD8 epitope induces potent immune responses in mice.* Biochimica et Biophysica Acta (BBA)-Biomembranes, 2010. **1798**(12): p. 2286-2295.
188. Rauen, J., et al., *Enhanced Cross-Presentation and Improved CD8(+) T Cell Responses after Mannosylation of Synthetic Long Peptides in Mice.* Plos One, 2014. **9**(8).
189. Sun, L.Z., et al., *Comparison between Ovalbumin and Ovalbumin Peptide 323-339 Responses in Allergic Mice: Humoral and Cellular Aspects.* Scandinavian Journal of Immunology, 2010. **71**(5): p. 329-335.
190. Lam, J.S., H.B. Huang, and S.M. Levitz, *Effect of Differential N-linked and O-linked Mannosylation on Recognition of Fungal Antigens by Dendritic Cells.* Plos One, 2007. **2**(10).
191. Matzelle, M.M. and J.E. Babensee, *Humoral immune responses to model antigen co-delivered with biomaterials used in tissue engineering.* Biomaterials, 2004. **25**(2): p. 295-304.
192. Apostolopoulos, V. and I. McKenzie, *Role of the mannose receptor in the immune response.* Current molecular medicine, 2001. **1**(4): p. 469-474.
193. Leavy, O., *Planning your route from the start.* Nature Reviews Immunology, 2007. **7**(6): p. 416-417.
194. Shedlock, D.J. and H. Shen, *Requirement for CD4 T cell help in generating functional CD8 T cell memory.* Science, 2003. **300**(5617): p. 337-339.

195. Joshi, M.D., et al., *Targeting tumor antigens to dendritic cells using particulate carriers.* Journal of Controlled Release, 2012. **161**(1): p. 25-37.
196. Garnett, M.C. and P. Kallinteri, *Nanomedicines and nanotoxicology: some physiological principles.* Occupational Medicine, 2006. **56**(5): p. 307-311.
197. Reddy, S.T., et al., *Exploiting lymphatic transport and complement activation in nanoparticle vaccines.* Nature Biotechnology, 2007. **25**(10): p. 1159-1164.
198. Swartz, M.A., S. Hirosue, and J.A. Hubbell, *Engineering approaches to immunotherapy.* Science translational medicine ournal Article, 2012. **4**(148): p. 148rv9.
199. Murthy, N., et al., *A Macromolecular Delivery Vehicle for Protein-Based Vaccines: Acid-Degradable Protein-Loaded Microgels.* Proceedings of the National Academy of Sciences of the United States of America, 2003. **100**(9): p. 4995-5000.
200. Ho Um, S., et al., *Interbilayer-crosslinked multilamellar vesicles as synthetic vaccines for potent humoral and cellular immune responses.* Nature Materials, 2011. **10**(3): p. 243-251.
201. Irvine, D.J., M.A. Swartz, and G.L. Szeto, *Engineering synthetic vaccines using cues from natural immunity.* Nature materials, 2013. **12**(11): p. 978-990.
202. Kovacsovics-Bankowski, M. and K.L. Rock, *A Phagosome-to-Cytosol Pathway for Exogenous Antigens Presented on MHC Class I Molecules.* Science, 1995. **267**(5195): p. 243-246.
203. Pumpens, P. and E. Grens, *HBV core particles as a carrier for B cell/T cell epitopes.* Intervirology, 2001. **44**(2-3): p. 98-114.
204. Green, N., et al., *Immunogenic structure of the influenza virus hemagglutinin.* Cell, 1982. **28**(3): p. 477-487.
205. Chen, L. and D.B. Flies, *Molecular mechanisms of T cell co-stimulation and co-inhibition.* Nature Reviews Immunology, 2013. **13**(4): p. 227-242.
206. Kowalczyk, R., M.A. Brimble, and R. Dunbar, *Synthesis of mannosylated glycopeptides as components for synthetic vaccines.* Biopolymers, 2007. **88**(4): p. 539-539.
207. Kragol, G. and L. Otvos Jr, *Orthogonal solid-phase synthesis of tetramannosylated peptide constructs carrying three independent branched epitopes.* Tetrahedron, 2001. **57**(6): p. 957-966.
208. Brimble, M.A., et al., *Synthesis of fluorescein-labelled O-mannosylated peptides as components for synthetic vaccines: comparison of two synthetic strategies.* Organic & biomolecular chemistry, 2008. **6**(1): p. 112-121.
209. Christensen, T., *Qualitative test for monitoring coupling completeness in solid phase peptide synthesis using chloranil.* Acta Chem Scand Ser B, 1979. **33**.

210. Dyke, J., et al., *Study of the thermal decomposition of 2-azidoacetic acid by photoelectron and matrix isolation infrared spectroscopy*. J. Am. Chem. Soc., 1997. **119**(29): p. 6883-6887.
211. Alewood, P., et al., *Rapid in situ neutralization protocols for Boc and Fmoc solid-phase chemistries.* Methods in enzymology, 1997. **289**: p. 14.
212. Ross, B.P., R.A. Falconer, and I. Thot, *N-1-(4, 4-dimethyl-2, 6-dioxocyclohex-1-ylidene) ethyl (N-Dde) Lipoamino Acids.* Molbank, 2008. **2008**(2): p. M566.
213. Gibbons, W.A., et al., *Lipidic peptides, I. Synthesis, resolution and structural elucidation of lipidic amino acids and their homo-and hetero-oligomers.* Liebigs Annalen der Chemie, 1990. **1990**(12): p. 1175-1183.
214. Ahmad Fuaad, A.A., et al., *Peptide Conjugation via CuAAC 'Click'Chemistry.* Molecules, 2013. **18**(11): p. 13148-13174.
215. Yanagawa, Y. and K. Onoe, *CCR7 ligands induce rapid endocytosis in mature dendritic cells with concomitant up-regulation of Cdc42 and Rac activities.* Blood, 2003. **101**(12): p. 4923-9.
216. Gao, J., et al., *Novel monodisperse PEGtide dendrons: design, fabrication and evaluation of mannose receptor-mediated macrophage targeting.* Bioconjugate Chem., 2013. **24 (8)**: p. 1332–1344.
217. Burkhard, K.A. and P. Shapiro, *Quantitative analysis of ERK2 interactions with substrate proteins.* The FASEB Journal, 2011. **25**(1_MeetingAbstracts): p. 749.1.
218. Cornish-Bowden, A., *Detection of errors of interpretation in experiments in enzyme kinetics.* Methods, 2001. **24**(2): p. 181-190.
219. Doolan, D.L., *Malaria methods and protocols*. Vol. 72. 2002: Springer Science & Business Media.
220. Apte, S.H., et al., *High-throughput multi-parameter flow-cytometric analysis from micro-quantities of Plasmodium-infected blood.* International journal for parasitology, 2011. **41**(12): p. 1285-1294.
221. Blanchfield, J.T. and I. Toth, *Modification of peptides and other drugs using lipoamino acids and sugars.* Methods Mol Biol, 2005. **298**: p. 45-61.
222. Taylor, C.M., *Glycopeptides and glycoproteins: Focus on the glycosidic linkage.* Tetrahedron, 1998. **54**(38): p. 11317-11362.
223. Skwarczynski, M., et al., *Lipid peptide core nanoparticles as multivalent vaccine candidates against Streptococcus pyogenes.* Australian Journal of Chemistry, 2012. **65**(1): p. 35-39.
224. Chatterjee, D., et al., *Structural basis of capacity of lipoarabinomannan to induce secretion of tumor necrosis factor.* Infection and immunity, 1992. **60**(3): p. 1249-1253.

225. Chen, L. and Z. Tan, *A convenient and efficient synthetic approach to mono-, di-, and tri-O-mannosylated Fmoc amino acids.* Tetrahedron Letters, 2013. **54**(17): p. 2190-2193.
226. Bouillon, C., et al., *Microwave assisted "click" chemistry for the synthesis of multiple labeled-carbohydrate oligonucleotides on solid support.* The Journal of organic chemistry, 2006. **71**(12): p. 4700-4702.
227. Bertozzi, C.R. and L.L. Kiessling, *Chemical glycobiology.* Science, 2001. **291**(5512): p. 2357-2364.
228. Simanek, E.E., et al., *Selectin-carbohydrate interactions: from natural ligands to designed mimics.* Chemical reviews, 1998. **98**(2): p. 833-862.
229. Liu, M., G. Barany, and D. Live, *Parallel solid-phase synthesis of mucin-like glycopeptides.* Carbohydrate research, 2005. **340**(13): p. 2111-2122.
230. Liu, M., et al., *Conformational consequences of protein glycosylation: Preparation of O-mannosyl serine and threonine building blocks, and their incorporation into glycopeptide sequences derived from α-dystroglycan.* Peptide Science, 2008. **90**(3): p. 358-368.
231. Buskas, T., S. Ingale, and G.-J. Boons, *Glycopeptides as versatile tools for glycobiology.* Glycobiology, 2006. **16**(8): p. 113R-136R.
232. Gray, C., P. Somers, and A. Dutta, *Glycosylation of Fmoc amino acids: preparation of mono- and di-glycosylated derivatives and their incorporation into Arg-Gly-Asp (RGD)-containing glycopeptides.* Journal of the Chemical Society, Perkin Transactions 1, 1997(9): p. 1429-1442.
233. Wang, Z.D., et al., *A simple preparation of 2, 3, 4, 6-tetra-O-acyl-gluco-, galacto-and mannopyranoses and relevant theoretical study.* Molecules, 2010. **15**(1): p. 374-384.
234. Weis, W.I. and K. Drickamer, *Trimeric structure of a C-type mannose-binding protein.* Structure, 1994. **2**(12): p. 1227-1240.
235. Boumrah, D., et al., *Spacer molecules in peptide sequences: incorporation into analogues of atrial natriuretic factor.* Tetrahedron, 1997. **53**(20): p. 6977-6992.
236. Chantell, C.A., M.A. Onaiyekan, and M. Menakuru, *Fast conventional Fmoc solid-phase peptide synthesis: a comparative study of different activators.* Journal of Peptide Science, 2012. **18**(2): p. 88-91.
237. Li, X. and J.S. Taylor, *General strategy for the preparation of membrane permeable fluorogenic peptide ester conjugates for in vivo studies of ester prodrug stability.* Bioorganic & medicinal chemistry, 2004. **12**(3): p. 545-552.
238. Tan, Z., et al., *Toward Homogeneous Erythropoietin: Non-NCL-Based Chemical Synthesis of the Gln78− Arg166 Glycopeptide Domain.* Journal of the American Chemical Society, 2009. **131**(15): p. 5424-5431.

239. Dyke, J., et al., *Study of the thermal decomposition of 2-azidoacetic acid by photoelectron and matrix isolation infrared spectroscopy.* Journal of the American Chemical Society, 1997. **119**(29): p. 6883-6887.
240. Amblard, M., et al., *Methods and protocols of modern solid phase peptide synthesis.* Molecular biotechnology, 2006. **33**(3): p. 239-254.
241. Gruber, P. and T. Hofmann, *Chemoselective synthesis of peptides containing major advanced glycation end-products of lysine and arginine.* The Journal of peptide research, 2005. **66**(3): p. 111-124.
242. Zom, G.G., et al., *7 TLR Ligand—Peptide Conjugate Vaccines: Toward Clinical Application.* Advances in immunology, 2012. **114**: p. 177.
243. Moyle, P.M., et al., *Site-specific incorporation of three toll-like receptor 2 targeting adjuvants into semisynthetic, molecularly defined nanoparticles: Application to group A streptococcal vaccines.* Bioconjugate chemistry, 2014. **25**(5): p. 965-978.
244. Moyle, P.M., et al., *Development of lipid-core-peptide (LCP) based vaccines for the prevention of group A streptococcal (GAS) infection.* Letters in Peptide Science, 2003. **10**(5-6): p. 605-613.
245. Robertson, J.M., P.E. Jensen, and B.D. Evavold, *DO11. 10 and OT-II T cells recognize a C-terminal ovalbumin 323–339 epitope.* The Journal of Immunology, 2000. **164**(9): p. 4706-4712.
246. Simerska, P., et al., *Ovalbumin lipid core peptide vaccines and their CD4+ and CD8+ T cell responses.* Vaccine, 2014. **32**(37): p. 4743-4750.
247. Tam, J.P., *Synthetic peptide vaccine design: synthesis and properties of a high-density multiple antigenic peptide system.* Proceedings of the National Academy of Sciences, 1988. **85**(15): p. 5409-5413.
248. Kowalczyk, W., et al., *Synthesis of multiple antigenic peptides (MAPs)—strategies and limitations.* Journal of Peptide Science, 2011. **17**(4): p. 247-251.
249. Wiesmüller, K.-H., B. Fleckenstein, and G. Jung, *Peptide vaccines and peptide libraries.* Biological chemistry, 2001. **382**(4): p. 571-579.
250. BenMohamed, L., S.L. Wechsler, and A.B. Nesburn, *Lipopeptide vaccines—yesterday, today, and tomorrow.* The Lancet infectious diseases, 2002. **2**(7): p. 425-431.
251. Isidro-Llobet, A., M. Alvarez, and F. Albericio, *Amino acid-protecting groups.* Chemical reviews, 2009. **109**(6): p. 2455-2504.
252. Chandrudu, S., P. Simerska, and I. Toth, *Chemical methods for peptide and protein production.* Molecules, 2013. **18**(4): p. 4373-4388.

253. Angell, Y.L. and K. Burgess, *Peptidomimetics via copper-catalyzed azide–alkyne cycloadditions.* Chemical Society Reviews, 2007. **36**(10): p. 1674-1689.
254. Kolb, H.C., M. Finn, and K.B. Sharpless, *Click chemistry: diverse chemical function from a few good reactions.* Angew Chem Int Ed Engl, 2001. **40**(11): p. 2004-2021.
255. Stephenson, R., et al., *Effect of lipidated gonadotropin-releasing hormone peptides on receptor mediated binding and uptake into prostate cancer cells in vitro.* Nanomedicine: Nanotechnology, Biology and Medicine, 2014. **10**(8): p. 1799-1808.
256. Zaric, V., et al., *Inhibition of endothelial cell proliferation by per-O-acetylated mannose conjugates.* Anticancer research, 2007. **27**(3A): p. 1331-1335.
257. Skwarczynski, M., M. Zaman, and I. Toth, *Lipo-peptides/saccharides in peptide vaccine delivery*. 2013. p. 571-579.
258. Michelow, I.C., et al., *A novel L-ficolin/mannose-binding lectin chimeric molecule with enhanced activity against Ebola virus.* J. Biol. Chem., 2010. **285**(32): p. 24729-24739.
259. Hadjichristidis, N., *Complex macromolecular architectures: synthesis, characterization, and self-assembly*. 2011, Hoboken, N.J: Wiley.
260. Zhao, X., F. Pan, and J.R. Lu, *Recent development of peptide self-assembly.* Progress in Natural Science, 2008. **18**(6): p. 653-660.
261. Zhang, S. and X. Zhao, *Design of molecular biological materials using peptide motifs.* Journal of Materials Chemistry, 2004. **14**(14): p. 2082-2086.
262. Lee, Y.S., *Self-assembly and nanotechnology: a force balance approach*. 2008: John Wiley & Sons.
263. Eskandari, S., et al., *Synthesis and Characterisation of Self-Assembled and Self-Adjuvanting Asymmetric Multi-Epitope Lipopeptides of Ovalbumin.* Chemistry–A European Journal, 2015. **21**(3): p. 1251-1261.
264. Hume, D.A., *Macrophages as APC and the dendritic cell myth.* The Journal of Immunology, 2008. **181**(9): p. 5829-5835.
265. Itano, A.A. and M.K. Jenkins, *Antigen presentation to naive CD4 T cells in the lymph node.* Nature immunology, 2003. **4**(8): p. 733-739.
266. Carbone, F.R. and W.R. Heath, *The role of dendritic cell subsets in immunity to viruses.* Current opinion in immunology, 2003. **15**(4): p. 416-420.
267. Apostolopoulos, V., et al., *Ex vivo targeting of the macrophage mannose receptor generates anti-tumor CTL responses.* Vaccine, 2000. **18**(27): p. 3174-3184.
268. Sedaghat, B., R. Stephenson, and I. Toth, *Targeting the Mannose Receptor with Mannosylated Subunit Vaccines.* Curr Med Chem, 2014.

269. Gupta, A., R.K. Gupta, and G. Gupta, *Targeting cells for drug and gene delivery: emerging applications of mannans and mannan binding lectins.* Journal of Scientific and Industrial Research, 2009. **68**(6): p. 465.

270. Taylor, M.E., K. Bezouska, and K. Drickamer, *Contribution to ligand binding by multiple carbohydrate-recognition domains in the macrophage mannose receptor.* J Biol Chem, 1992. **267**(3): p. 1719-26.

271. Ramakrishna, V., et al., *Mannose receptor targeting of tumor antigen pmel17 to human dendritic cells directs anti-melanoma T cell responses via multiple HLA molecules.* J. Immunol., 2004. **172**(5): p. 2845-2852.

272. Willer, T., et al., *O-mannosyl glycans: from yeast to novel associations with human disease.* Curr Opin Struct Biol, 2003. **13**(5): p. 621-630.

273. Wei, H., et al., *Targeted delivery of tumor antigens to activated dendritic cells via CD11c molecules induces potent antitumor immunity in mice.* Clinical Cancer Research, 2009. **15**(14): p. 4612-4621.

274. Stagg, A.J., et al., *Isolation of mouse spleen dendritic cells,* in *Dendritic Cell Protocols*. 2001, Springer. p. 9-22.

275. Bond, E., et al., *Techniques for time-efficient isolation of human skin dendritic cell subsets and assessment of their antigen uptake capacity.* Journal of Immunological Methods, 2009. **348**(1): p. 42-56.

276. Narendran, P., et al., *Dendritic cell-based assays, but not mannosylation of antigen, improves detection of T-cell responses to proinsulin in type 1 diabetes.* Immunology, 2004. **111**(4): p. 422-429.

277. Lin, H.-H., et al., *The macrophage F4/80 receptor is required for the induction of antigen-specific efferent regulatory T cells in peripheral tolerance.* The Journal of experimental medicine, 2005. **201**(10): p. 1615-1625.

278. Hu, M., et al., *Different antigen presentation tendencies of granulocyte-macrophage colony-stimulating factor-induced bone marrow-derived macrophages and peritoneal macrophages.* In Vitro Cellular & Developmental Biology. Animal, 2012. **48**(7): p. 434-440.

279. Medina-Kauwe, L.K., et al., *Assessing the binding and endocytosis activity of cellular receptors using GFP-ligand fusions.* BioTechniques, 2000. **29**(3): p. 602-609.

280. Hertzén, E., et al., *M1 protein-dependent intracellular trafficking promotes persistence and replication of Streptococcus pyogenes in macrophages.* J. Innate. Immun., 2010. **2**(6): p. 534-545.

281. van Kooten, C., et al., *Handbook of Experimental Pharmacology "Dendritic Cells"*, in *Dendritic Cells*. 2009, Springer. p. 233-249.

282. Wang, J.C., et al., *An 11-color flow cytometric assay for identifying, phenotyping, and assessing endocytic ability of peripheral blood dendritic cell subsets in a single platform.* J Immunol Methods, 2009. **341**(1-2): p. 106-16.
283. Dasgupta, S., et al., *A role for exposed mannosylations in presentation of human therapeutic self-proteins to CD4+ T lymphocytes.* Proceedings of the National Academy of Sciences, 2007. **104**(21): p. 8965-8970.
284. Lam, J.S., et al., *A model vaccine exploiting fungal mannosylation to increase antigen immunogenicity.* The Journal of Immunology, 2005. **175**(11): p. 7496-7503.
285. Furukawa, A., et al., *Structural analysis for glycolipid recognition by the C-type lectins Mincle and MCL.* Proceedings of the National Academy of Sciences, 2013. **110**(43): p. 17438-17443.
286. Lepenies, B., J. Lee, and S. Sonkaria, *Targeting C-type lectin receptors with multivalent carbohydrate ligands.* Adv. Drug Deliv. Rev., 2013. **65**(9): p. 1271-1281.
287. Paddock, S.W. and K.W. Eliceiri, *Laser scanning confocal microscopy: History, applications, and related optical sectioning techniques*. 2014: Springer.
288. Leung, S., et al., *OT-II TCR transgenic mice fail to produce anti-ovalbumin antibodies upon vaccination.* Cellular immunology, 2013. **282**(2): p. 79.
289. Wilson, T., *Confocal microscopy.* Academic Press: London, etc, 1990. **426**: p. 1-64.
290. Madani, F., et al., *Mechanisms of cellular uptake of cell-penetrating peptides.* Journal of Biophysics, 2011. **2011**.
291. Rich, R.L. and D.G. Myszka, *Survey of the year 2007 commercial optical biosensor literature.* Journal of Molecular Recognition, 2008. **21**(6): p. 355-400.
292. Day, E.S., et al., *Determining the affinity and stoichiometry of interactions between unmodified proteins in solution using Biacore.* Analytical biochemistry, 2013. **440**(1): p. 96-107.
293. Gustafsson, A., et al., *Pichia pastoris-produced mucin-type fusion proteins with multivalent O-glycan substitution as targeting molecules for mannose-specific receptors of the immune system.* Glycobiology, 2011. **21**(8): p. 1071-1086.
294. Duverger, E., et al., *Carbohydrate–lectin interactions assayed by SPR*, in *Surface Plasmon Resonance*. 2010, Springer. p. 157-178.
295. Van Der Merwe, P.A., *Surface plasmon resonance*. 2001, Oxford University Press: New York, NY, USA. p. 137-170.
296. Murphy, M., L. Jason-Moller, and J. Bruno, *Using Biacore to Measure the Binding Kinetics of an Antibody-Antigen Interaction.* Current Protocols in Protein Science, 2006: p. 19.14. 1-19.14. 17.

297. Drescher, D.G., M.J. Drescher, and N.A. Ramakrishnan, *Surface plasmon resonance (SPR) analysis of binding interactions of proteins in inner-ear sensory epithelia*, in *Auditory and Vestibular Research*. 2009, Springer. p. 323-343.
298. Olson, L.J., et al., *Structural Insights into the Mechanism of pH-dependent Ligand Binding and Release by the Cation-dependent Mannose 6-Phosphate Receptor.* Journal of Biological Chemistry, 2008. **283**(15): p. 10124-10134.
299. Schuck, P. and H. Zhao, *The role of mass transport limitation and surface heterogeneity in the biophysical characterization of macromolecular binding processes by SPR biosensing.* Surface plasmon resonance: methods and protocols, 2010: p. 15-54.
300. Phillips, K.S. and Q.J. Cheng, *Surface plasmon resonance*, in *Molecular Biomethods Handbook*. 2008, Springer. p. 809-820.
301. Zamze, S., et al., *Recognition of bacterial capsular polysaccharides and lipopolysaccharides by the macrophage mannose receptor.* J. Biol. Chem., 2002. **277**(44): p. 41613-23.
302. Beckman, E.M., et al., *CD1c restricts responses of mycobacteria-specific T cells. Evidence for antigen presentation by a second member of the human CD1 family.* J. Immunol., 1996. **157**(7): p. 2795-2803.
303. Moody, B.D., *T cell activation by CD1 and lipid antigens*. Vol. 314. 2007: Springer Science & Business Media.
304. Espuelas, S., et al., *Influence of ligand valency on the targeting of immature human dendritic cells by mannosylated liposomes.* Bioconjugate chemistry, 2008. **19**(12): p. 2385-2393.
305. Drickamer, K. and M.E. Taylor, *Biology of animal lectins.* Annual review of cell biology, 1993. **9**(1): p. 237-264.
306. Mogensen, T.H., *Pathogen recognition and inflammatory signaling in innate immune defenses.* Clinical microbiology reviews, 2009. **22**(2): p. 240-273.
307. Alberts, B., et al., *Helper T cells and Lymphocyte activation.* 2002.
308. Coffman, R.L., A. Sher, and R.A. Seder, *Vaccine adjuvants: putting innate immunity to work.* Immunity, 2010. **33**(4): p. 492-503.
309. Weis, W.I., M.E. Taylor, and K. Drickamer, *The C-type lectin superfamily in the immune system.* Immunological reviews, 1998. **163**(1): p. 19-34.
310. Singh, S.K., et al., *Design of neo-glycoconjugates that target the mannose receptor and enhance TLR-independent cross-presentation and Th1 polarization.* European journal of immunology, 2011. **41**(4): p. 916-925.
311. Martinez-Pomares, L., *The mannose receptor*. Journal of leukocyte biology, 2012. **92**(6): p. 1177-1186.

312. Super, M., et al., *Association of low levels of mannan-binding protein with a common defect of opsonisation.* The Lancet, 1989. **334**(8674): p. 1236-1239.
313. Flacher, V., et al., *Mannoside Glycolipid Conjugates Display Anti-inflammatory Activity by Inhibition of Toll-like Receptor-4 Mediated Cell Activation.* ACS chemical biology, 2015.
314. Apostolopoulos, V., et al., *Oxidative/reductive conjugation of mannan to antigen selects for T1 or T2 immune responses.* Proceedings of the National Academy of Sciences, 1995. **92**(22): p. 10128-10132.
315. Geijtenbeek, T.B., et al., *Mycobacteria target DC-SIGN to suppress dendritic cell function.* The Journal of experimental medicine, 2003. **197**(1): p. 7-17.
316. Gazi, U. and L. Martinez-Pomares, *Influence of the mannose receptor in host immune responses.* Immunobiology, 2009. **214**(7): p. 554-561.
317. Zaman, M., M.F. Good, and I. Toth, *Nanovaccines and their mode of action.* Methods, 2013. **60**(3): p. 226-231.
318. Azmi, F., et al., *Self-adjuvanting vaccine against group A streptococcus: Application of fibrillized peptide and immunostimulatory lipid as adjuvant.* Bioorganic & medicinal chemistry, 2014. **22**(22): p. 6401-6408.
319. Mineo, T.W., et al., *Recognition by Toll-like receptor 2 induces antigen-presenting cell activation and Th1 programming during infection by Neospora caninum.* Immunology and cell biology, 2010. **88**(8): p. 825-833.
320. Kuchroo, V., et al., *B7-1 and B7-2 costimulatory molecules activate differentially the Thl/Th2 developmental pathways: application to autoimmune disease therapy.* Cell. **80**: p. 707-718.
321. Radecke, V., H. Hacker, and S. Datta, *Activation of Toll-like receptor 2 induces a Th2 immune response and promotes experimental asthma.* J Immunol, 1994. **172**: p. 2739-43.
322. Eisenbarth, S.C., et al., *Lipopolysaccharide-enhanced, toll-like receptor 4–dependent T helper cell type 2 responses to inhaled antigen.* The Journal of experimental medicine, 2002. **196**(12): p. 1645-1651.
323. Kasten, K.R., et al., *T-cell activation differentially mediates the host response to sepsis.* Shock, 2010. **34**(4): p. 377-383.
324. Wisnoski, N., et al., *The contribution of CD4+ CD25+ T-regulatory-cells to immune suppression in sepsis.* Shock (Augusta, Ga.), 2007. **27**(3): p. 251.
325. Haas, A., K. Zimmermann, and A. Oxenius, *Antigen-dependent and-independent mechanisms of T and B cell hyperactivation during chronic HIV-1 infection.* Journal of virology, 2011. **85**(23): p. 12102-12113.
326. Crotty, S., *A brief history of T cell help to B cells.* Nature Reviews Immunology, 2015. **15**(3): p. 185-189.

327. Sun, L.Z., et al., *Comparison between Ovalbumin and Ovalbumin Peptide 323-339 Responses in Allergic Mice: Humoral and Cellular Aspects.* Scandinavian journal of immunology, 2010. **71**(5): p. 329-335.
328. Kuchroo, V.K., et al., *B7-1 and B7-2 costimulatory molecules activate differentially the Th1/Th2 developmental pathways: application to autoimmune disease therapy.* Cell, 1995. **80**(5): p. 707-718.
329. Ciabattini, A., et al., *Primary activation of antigen-specific naive CD4+ and CD8+ T cells following intranasal vaccination with recombinant bacteria.* Infection and immunity, 2008. **76**(12): p. 5817-5825.
330. Fraser, C.C., et al., *Generation of a universal CD4 memory T cell recall peptide effective in humans, mice and non-human primates.* Vaccine, 2014. **32**(24): p. 2896-2903.
331. Atassi, M.Z., et al., *Epitope-specific suppression of antibody response in experimental autoimmune myasthenia gravis by a monomethoxypolyethylene glycol conjugate of a myasthenogenic synthetic peptide.* Proceedings of the National Academy of Sciences, 1992. **89**(13): p. 5852-5856.
332. Trépanier, P. and R. Bazin, *Intravenous immunoglobulin (IVIg) inhibits CD8 cytotoxic T-cell activation.* Blood, 2012. **120**(13): p. 2769-2770.
333. Mirenda, V., et al., *Tolerant T cells display impaired trafficking ability.* European journal of immunology, 2005. **35**(7): p. 2146-2156.
334. Lechler, R., et al., *The contributions of T-cell anergy to peripheral T-cell tolerance.* Immunology, 2001. **103**(3): p. 262-269.
335. Kel, J.M., *Immune modulation by mannosylated peptides*. 2008: Department of Immunohematology and Blood Transfusion, Faculty of Medicine, Leiden University Medical Center (LUMC), Leiden University.
336. Yang, S., et al., *The shedding of CD62L (L-selectin) regulates the acquisition of lytic activity in human tumor reactive T lymphocytes.* PLoS One, 2011. **6**(7): p. e22560.
337. Thomas, P.G., et al., *Physiological numbers of CD4+ T cells generate weak recall responses following influenza virus challenge.* The journal of immunology, 2010. **184**(4): p. 1721-1727.
338. Peschon, J.J., et al., *An essential role for ectodomain shedding in mammalian development.* Science, 1998. **282**(5392): p. 1281-1284.
339. Richards, H., et al., *CD62L (L-selectin) down-regulation does not affect memory T cell distribution but failure to shed compromises anti-viral immunity*. The Journal of Immunology, 2008. **180**(1): p. 198-206.

340. Sun, J.B., C. Czerkinsky, and J. Holmgren, *Sublingual 'oral tolerance' induction with antigen conjugated to cholera toxin B subunit generates regulatory T cells that induce apoptosis and depletion of effector T cells.* Scand J Immunol, 2007. **66**(2-3): p. 278-86.
341. Kel, J.M., et al., *Immunization with mannosylated peptide induces poor T cell effector functions despite enhanced antigen presentation.* International immunology, 2008. **20**(1): p. 117-127.
342. Clem, A.S., *Fundamentals of vaccine immunology.* Journal of global infectious diseases, 2011. **3**(1): p. 73.
343. Murphy, K.M., et al., *Signaling and transcription in T helper development.* Annual Review of Immunology, 2000. **18**: p. 451-494.
344. Liew, F.Y., *T(H)1 and T(H)2 cells: a historical perspective.* Nature Reviews Immunology, 2002. **2**(1): p. 55-60.
345. Borish, L.C. and J.W. Steinke, *2. Cytokines and chemokines.* J Allergy Clin Immunol, 2003. **111**(2 Suppl): p. S460-75.
346. Karulin, A.Y., et al., *Neuroantigen-Specific CD4 Cells Expressing Interferon-γ (IFN-γ), Interleukin (IL)-2 and IL-3 in a Mutually Exclusive Manner Prevail in Experimental Allergic Encephalomyelitis (EAE).* Cells, 2012. **1**(3): p. 576-596.
347. Biosciences, B., *Detection of Intracellular Cytokines in T Lymphocytes using the BD FastImmune™ Assay on the BD FACSVerse™ System.* Cytokine, 2011. **101**: p. 100.
348. Zimmer, H., S. Riese, and A. Regnier-Vigouroux, *Functional characterization of mannose receptor expressed by immunocompetent mouse microglia.* Glia, 2003. **42**(1): p. 89-100.
349. Bettahi, I., et al., *Antitumor activity of a self-adjuvanting glyco-lipopeptide vaccine bearing B cell, CD4+ and CD8+ T cell epitopes.* Cancer Immunology, Immunotherapy, 2009. **58**(2): p. 187-200.
350. Braumüller, H., et al., *T-helper-1-cell cytokines drive cancer into senescence.* Nature, 2013. **494**(7437): p. 361-365.
351. Eriksson, K., et al., *Cholera toxin and its B subunit promote dendritic cell vaccination with different influences on Th1 and Th2 development.* Infect Immun, 2003. **71**(4): p. 1740-7.
352. Sheng, K.C., et al., *Delivery of antigen using a novel mannosylated dendrimer potentiates immunogenicity in vitro and in vivo.* European Journal of Immunology, 2008. **38**(2): p. 424-436.
353. Taneichi, M., et al., *Induction of differential T-cell epitope by plain-and liposome-coupled antigen.* Bioconjugate chemistry, 2006. **17**(4): p. 899-904.

354. Stelmaszczyk-Emmel, A., et al., *The usefulness of flow cytometric analysis of cytokines in peripheral blood and bone marrow plasma.* Postepy Hig Med Dosw (online), 2013. **67**: p. 879-886.
355. Chieppa, M., et al., *Cross-linking of the mannose receptor on monocyte-derived dendritic cells activates an anti-inflammatory immunosuppressive program.* Journal of Immunology, 2003. **171**(9): p. 4552-4560.
356. Anjuère, F., et al., *Transcutaneous immunization with cholera toxin B subunit adjuvant suppresses IgE antibody responses via selective induction of Th1 immune responses.* The Journal of Immunology, 2003. **170**(3): p. 1586-1592.
357. Netea, M.G., et al., *From the Th1/Th2 paradigm towards a Toll-like receptor/T-helper bias.* Antimicrobial agents and chemotherapy, 2005. **49**(10): p. 3991-3996.
358. Singh, M. and D. O'Hagan, *Advances in vaccine adjuvants.* Nature biotechnology, 1999. **17**(11): p. 1075-1081.
359. O'Hagan, D.T. and N.M. Valiante, *Recent advances in the discovery and delivery of vaccine adjuvants.* Nature Reviews Drug Discovery, 2003. **2**(9): p. 727-735.
360. Cordeiro, A.S. and M.J. Alonso, *Recent advances in vaccine delivery.* Pharmaceutical patent analyst, 2016. **5**(1): p. 49-73.
361. Radcliff, F.J., et al., *Antigen Targeting to Major Histocompatibility Complex Class II with Streptococcal Mitogenic Exotoxin Z-2 M1, a Superantigen-Based Vaccine Carrier.* Clinical and Vaccine Immunology, 2012. **19**(4): p. 574-586.
362. Sellers, R., et al., *Immunological Variation Between Inbred Laboratory Mouse Strains Points to Consider in Phenotyping Genetically Immunomodified Mice.* Veterinary Pathology Online, 2012. **49**(1): p. 32-43.
363. Leung, S., et al., *OT-II TCR transgenic mice fail to produce anti-ovalbumin antibodies upon vaccination.* Cellular immunology, 2013. **282**(2): p. 79-84.
364. Buskas, T., P. Thompson, and G.-J. Boons, *Immunotherapy for cancer: synthetic carbohydrate-based vaccines.* Chemical communications (Cambridge, England) Journal Article, 2009(36): p. 5335.
365. Goodwin, D., *Lipid and carbohydrate-based systems to enhance the bioavailability and immunogenicity of therapeutic peptides*. 2013, The University of Queensland, School of Chemistry and Molecular Biosciences Dissertation.

Appendices: RP-HPLC Trace, NMR and Mass spectrometry Data

Appendix 1. N-Fmoc-O-(2,3,4,6-tetra-O-acetyl-α,β-D-mannopyranosyl)-L-serine (2)

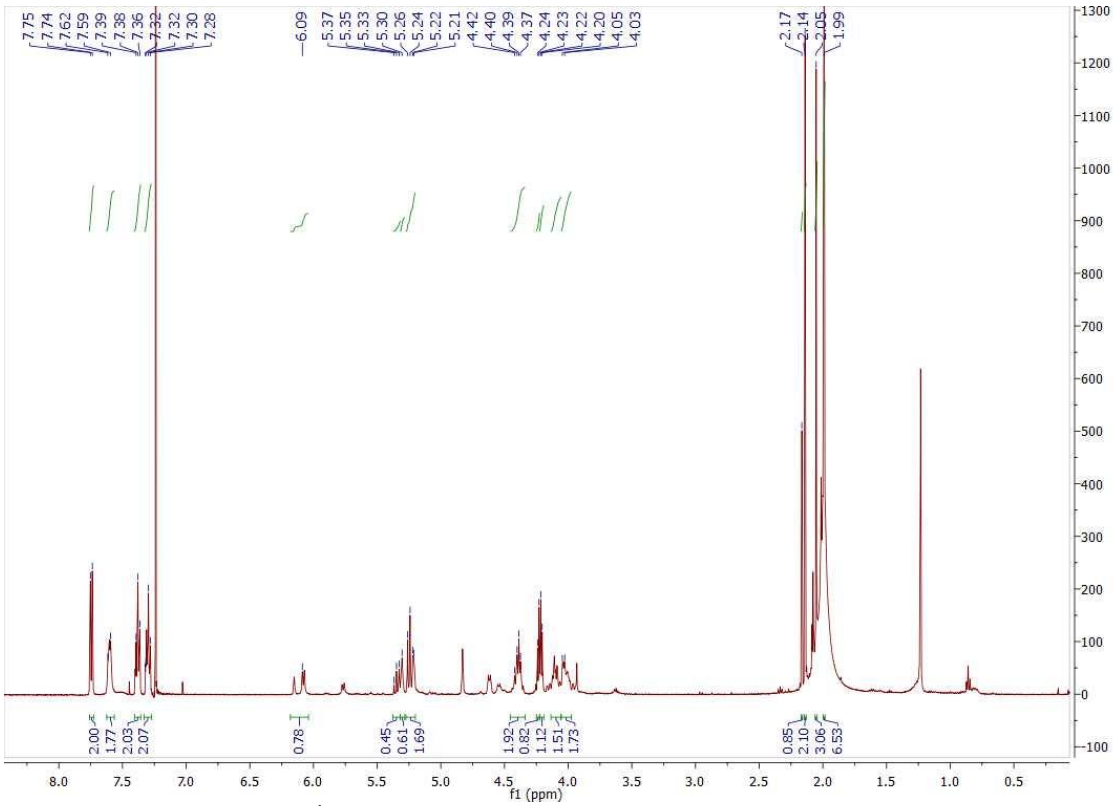

Appendix 1a. Yield = 42%, ^{1}HNMR (500 MHz, $CDCl_3$): δ 7.75-7.60, 7.40–7.36, 7.32–7.28, (8H, ArH), 6.17 (d, 1H, *O*-ester), 5.77 (d, 1H, NH), 5.37 (t, H4), 5.32 (bs, H2), 5.26 (dd, 1H), 4.58 (bd, 1H, CH), 4.25 (complex, H6), 4.17 (bd, 1H, CH), 4.13 (bd, 2H, H5, H6), 3.98 (bd, 1H), 2.19, 2.10, 2.03, 2.01 (4s, 12H, $4CH_3$)

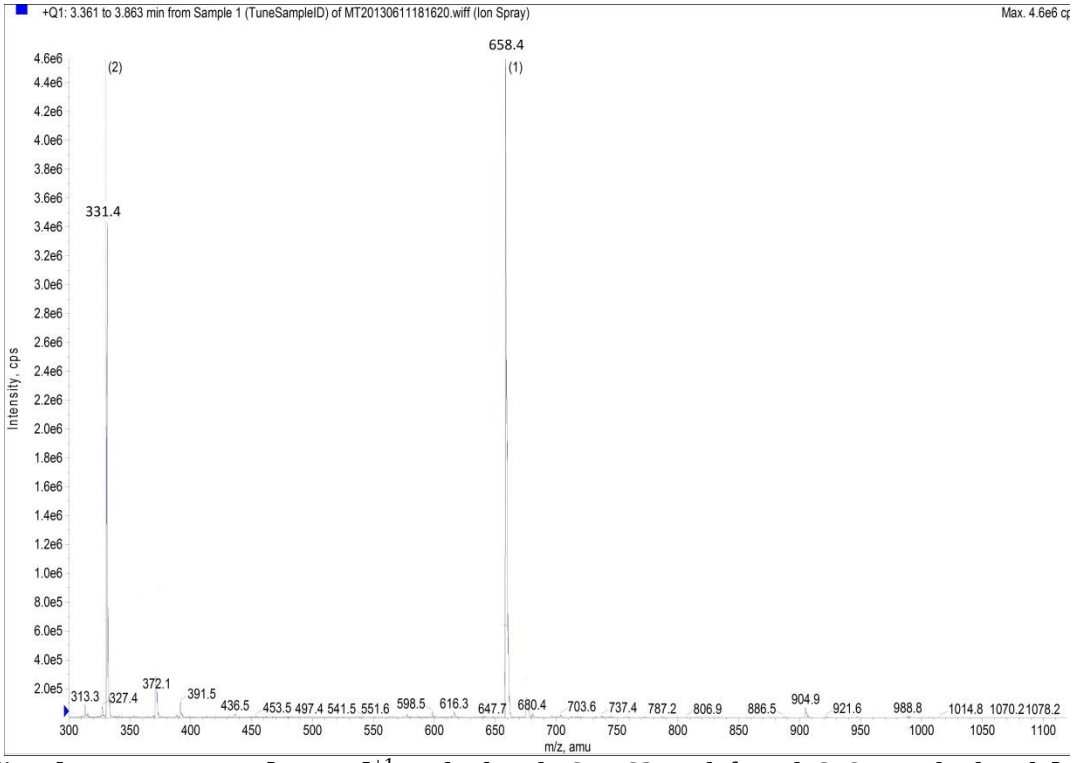

Appendix 1b. Exact mass, $[M+1H]^{+1}$ calculated: 657.63 and found 658.4; calculated $[M+2H]^{+2}$ 329.81 and found 331.4. Found 675.7 referring to calculated mass+Na

Appendix 2. Mannosylated peptide 4

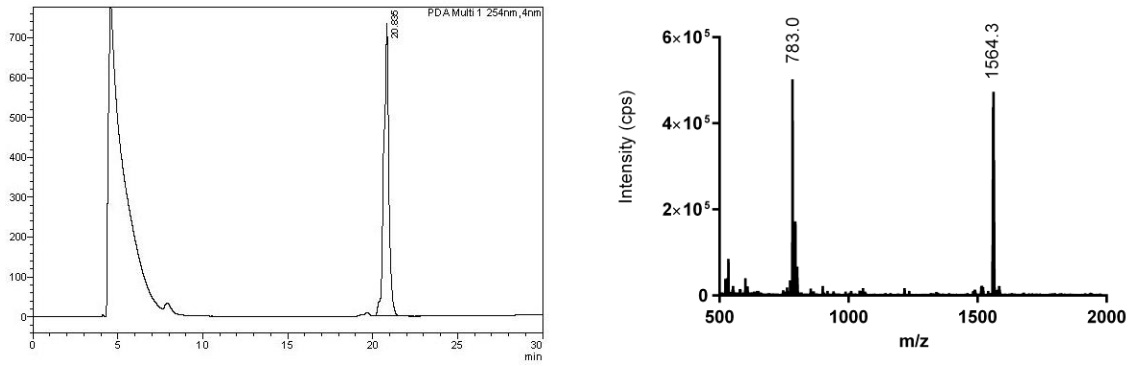

Appendix 2. RP-HPLC trace and mass spectra for Peptide **4** (54 % yield). Rt=20.835 min (C8 column, 0-100% solvent B, 30 min). A solvent peak was observed between 4-10 min. Exact mass of Peptide **4** $[M+1H]^{+1}$ calculated: 1562.51 and found 1564.3; calculated $[M+2H]^{+2}$ 782.255 and found 783.0. Purity ≥ 95%.

Appendix 3. Mannosylated peptide 5

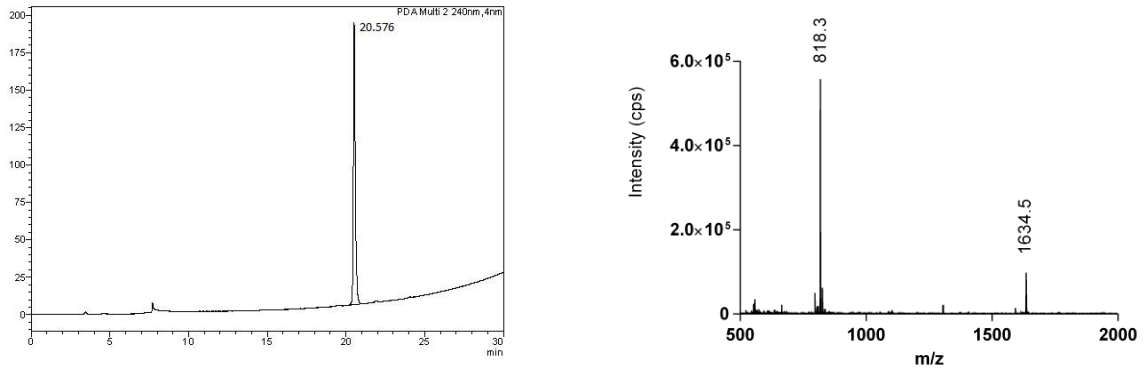

Appendix 3. RP-HPLC trace and mass spectra for Peptide **5** (62 % yield). Rt=20.576 min (C8 column, 0-100% solvent B, 30 min). A solvent peak was observed at 8 min. Exact mass of Peptide **5** $[M+1H]^{+1}$ calculated: 1633.55 and found 1634.5; calculated $[M+2H]^{+2}$ 8173.77 and found 818.3. Purity ≥ 95%.

Appendix 4. Mannosylated peptide 6

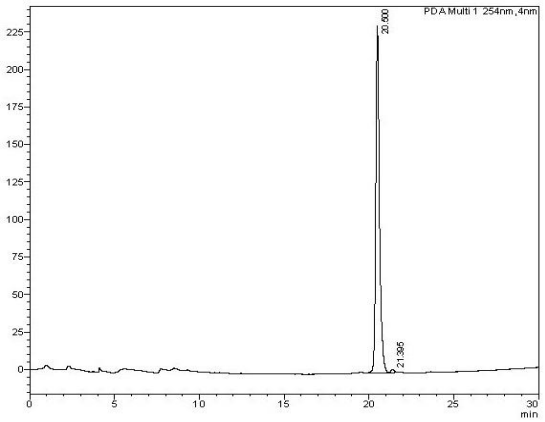

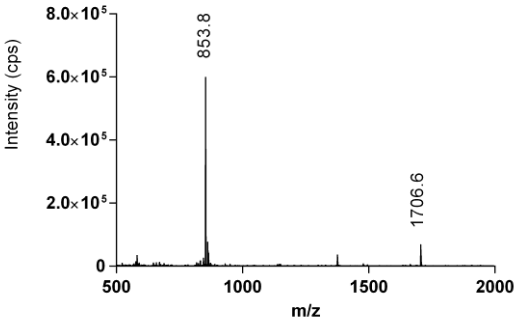

Appendix 4. RP-HPLC trace and mass spectra for Peptide **6** (68 % yield). Rt=20.50 min (C8 column, 0-100% solvent B, 30 min). Exact mass of Peptide **6** $[M+1H]^{+1}$ calculated: 1704.58 and found 1706.6; calculated $[M+2H]^{+2}$ 853.29 and found 853.8. Purity ≥ 95%.

Appendix 5. Mannosylated peptide 7

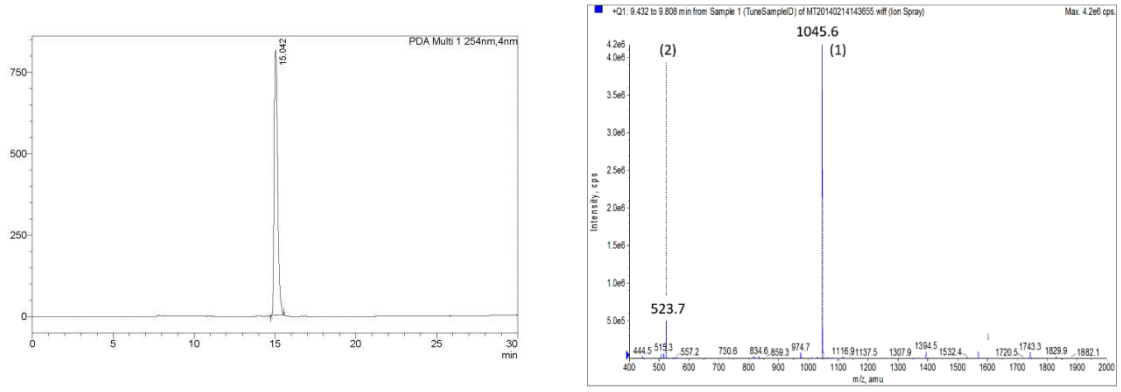

Appendix 5. RP-HPLC trace and mass spectra for Peptide **7** (48 % yield). Rt=15.042 min (C8 column, 0-100% solvent B, 30 min). Exact mass of Peptide **7** $[M+1H]^{+1}$ calculated: 1044.39 and found 1045.6; calculated $[M+2H]^{+2}$523.195 and found 528.7. Purity ≥ 95%.

Appendix 6. 2-(4, 4-Dimethyl-2, 6-Dioxocyclohex-1-ylidene) ethylaminododecanoic acid (Dde-C12-OH) (10)

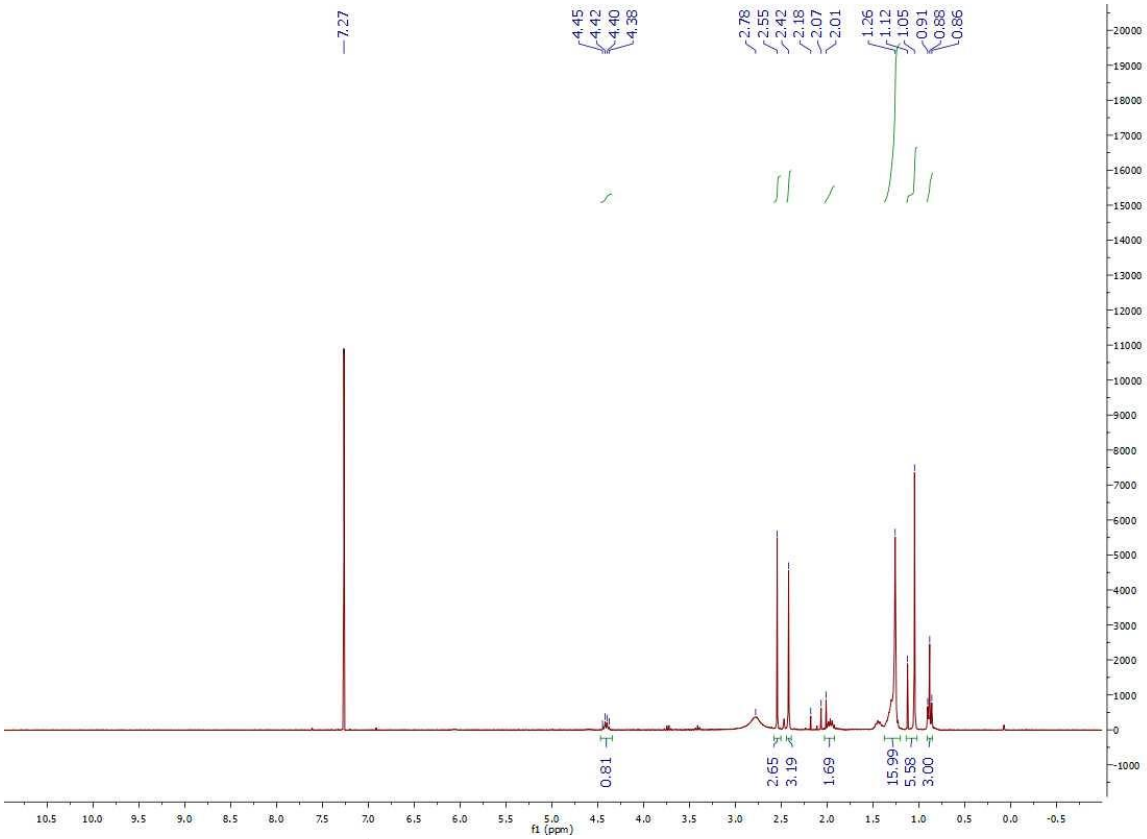

Appendix 6. Yield = 30%, ^{1}H NMR (500 MHz, $CDCl_3$): 0.86 (3H, t, CH3), 1.05 (6H, s, $C(CH_3)2$), 1.12-1.26 (16H, m, $8CH_2$), 2.01-1.87 (2H, m, CH_2), 2.42 (4H, s, $2CH_2CO$), 2.55 (3H, s, $C(NH)CH_3$), 4.38 (1H, m, CH).

Appendix 7. Peptide 11

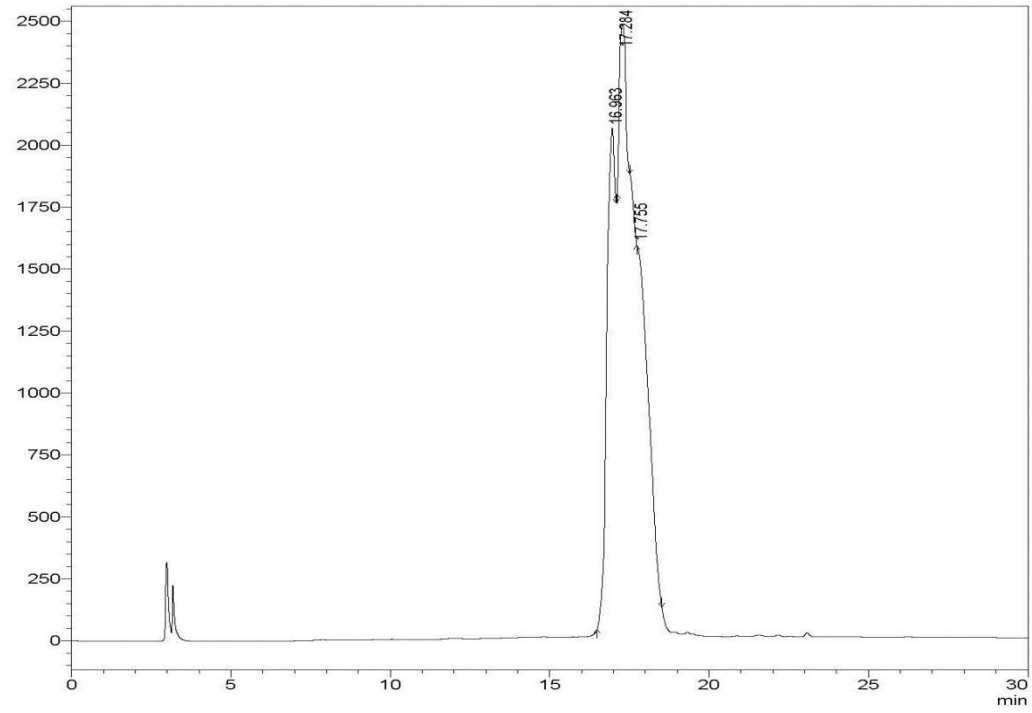

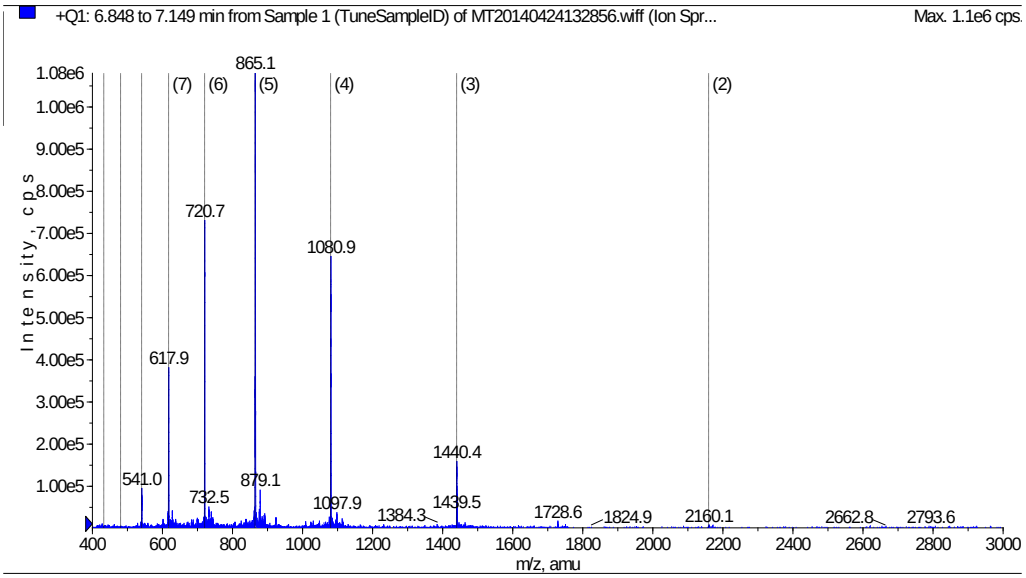

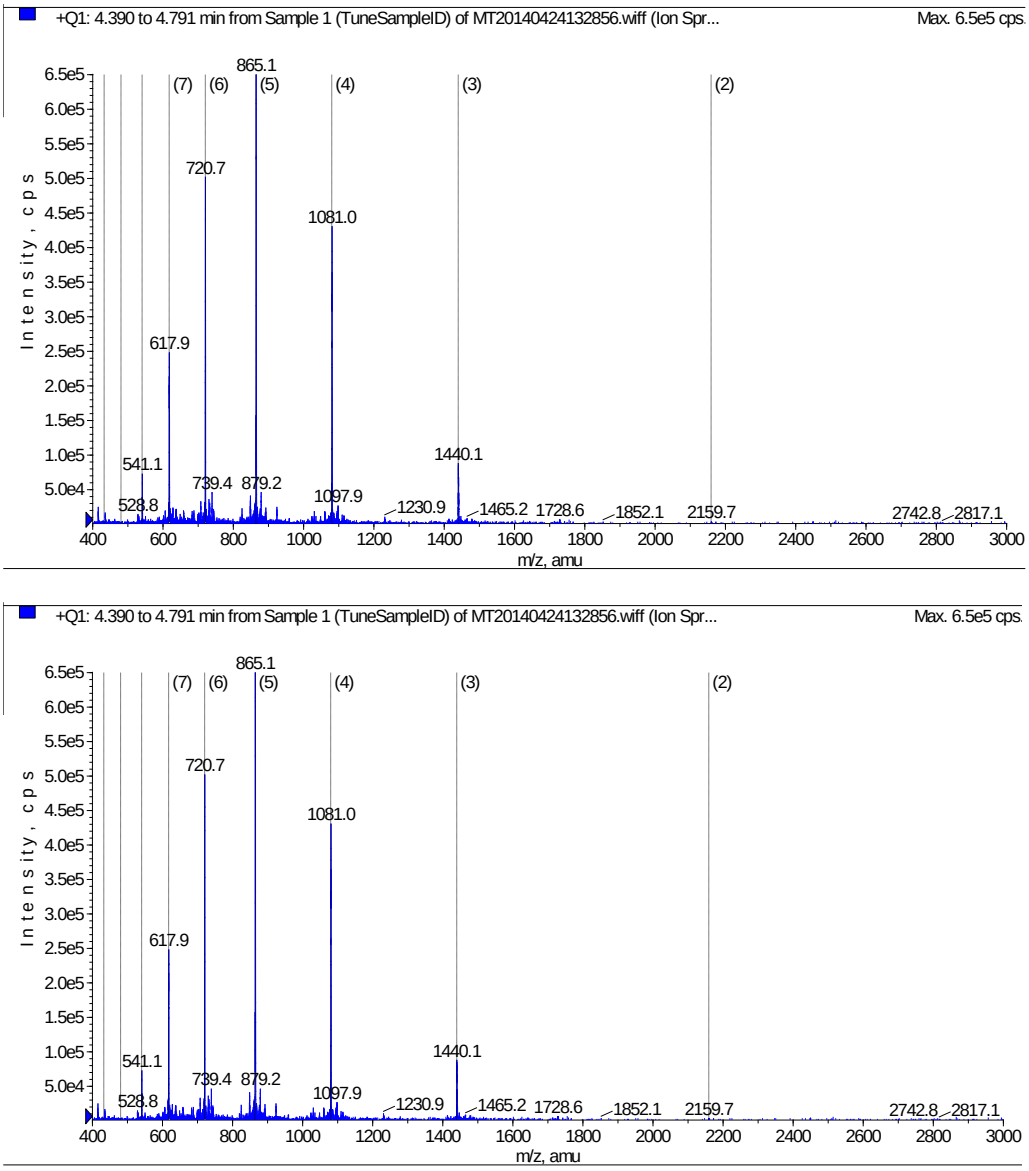

Appendix 7. RP-HPLC trace and mass spectra for Peptide **11** (73 % yield). Rt=16.96, 17.28 and 17. 75 min (C4 column, 0-100% solvent B, 30 min). Exact mass of Peptide **11** $[M+1H]^{+1}$ calculated: 4316.39; calculated $[M+2H]^{+2}$ 2159.195 and found 2159.7, 2160.1 and 2160.7; calculated $[M+3H]^{+3}$ 1439.8 and found 1440.1, 1440.1, 1440.6; calculated $[M+4H]^{+4}$ 1080.09 and found 1081.0, 1080.9, 1080.0; calculated $[M+5H]^{+5}$ 864.38 and found 865.6, 865.1, 865.2. Purity ≥ 95%.

Appendix 8. Peptide 12

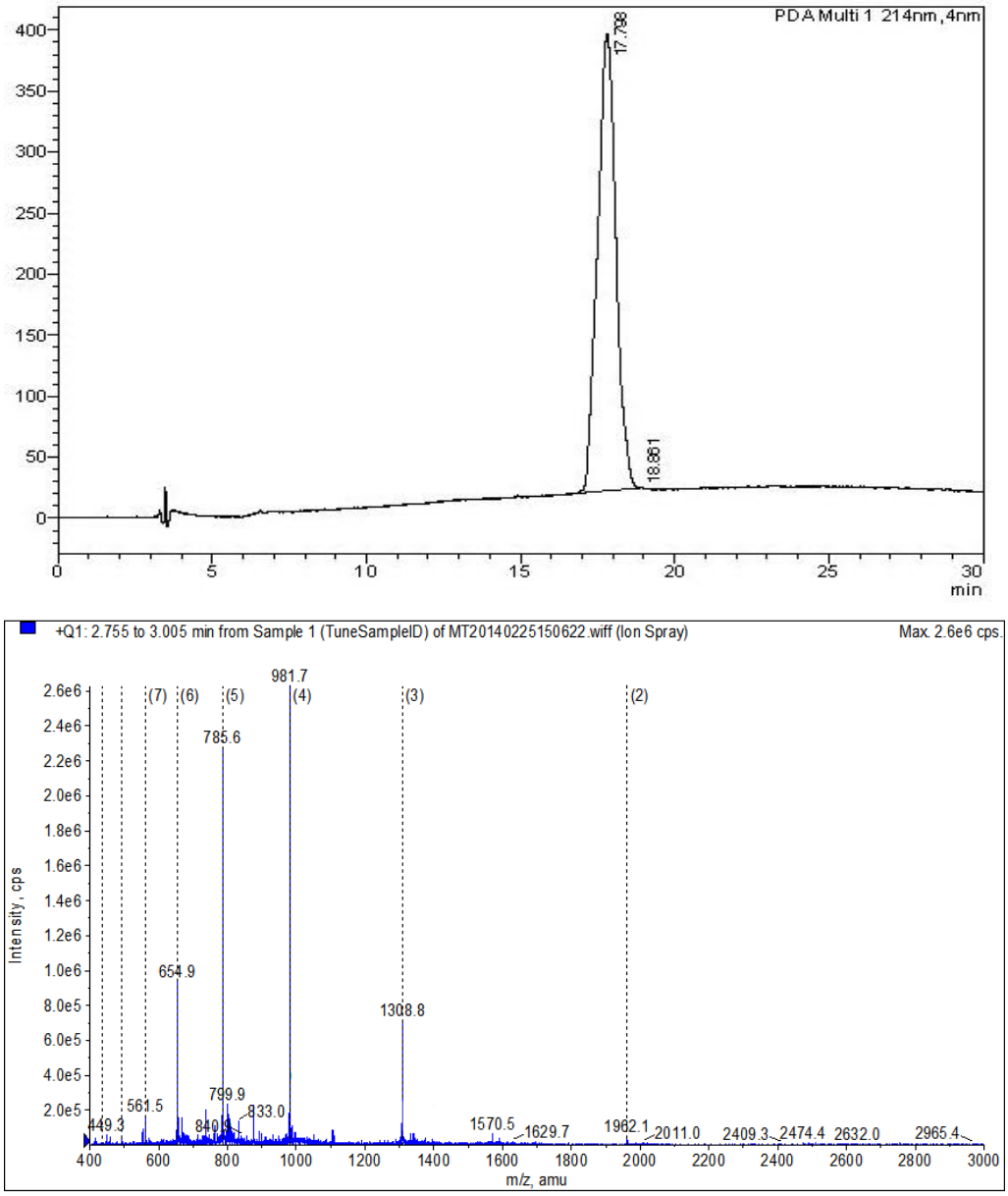

Appendix 8. RP-HPLC trace and mass spectra for Peptide **12** (83 % yield). Rt=17.79 min (C18 column, 0-100% solvent B, 30 min). Exact mass of Peptide **12** $[M+1H]^{+1}$ calculated: 3922.03; calculated $[M+2H]^{+2}$ 1962.01 and found 1962.1; calculated $[M+3H]^{+3}$ 1308.34 and found 1308.8; calculated $[M+4H]^{+4}$ 981.50 and found 981.7; calculated $[M+5H]^{+5}$ 785.40 and found 785.6. Purity ≥ 95%.

Appendix 9. Vaccine construct 13

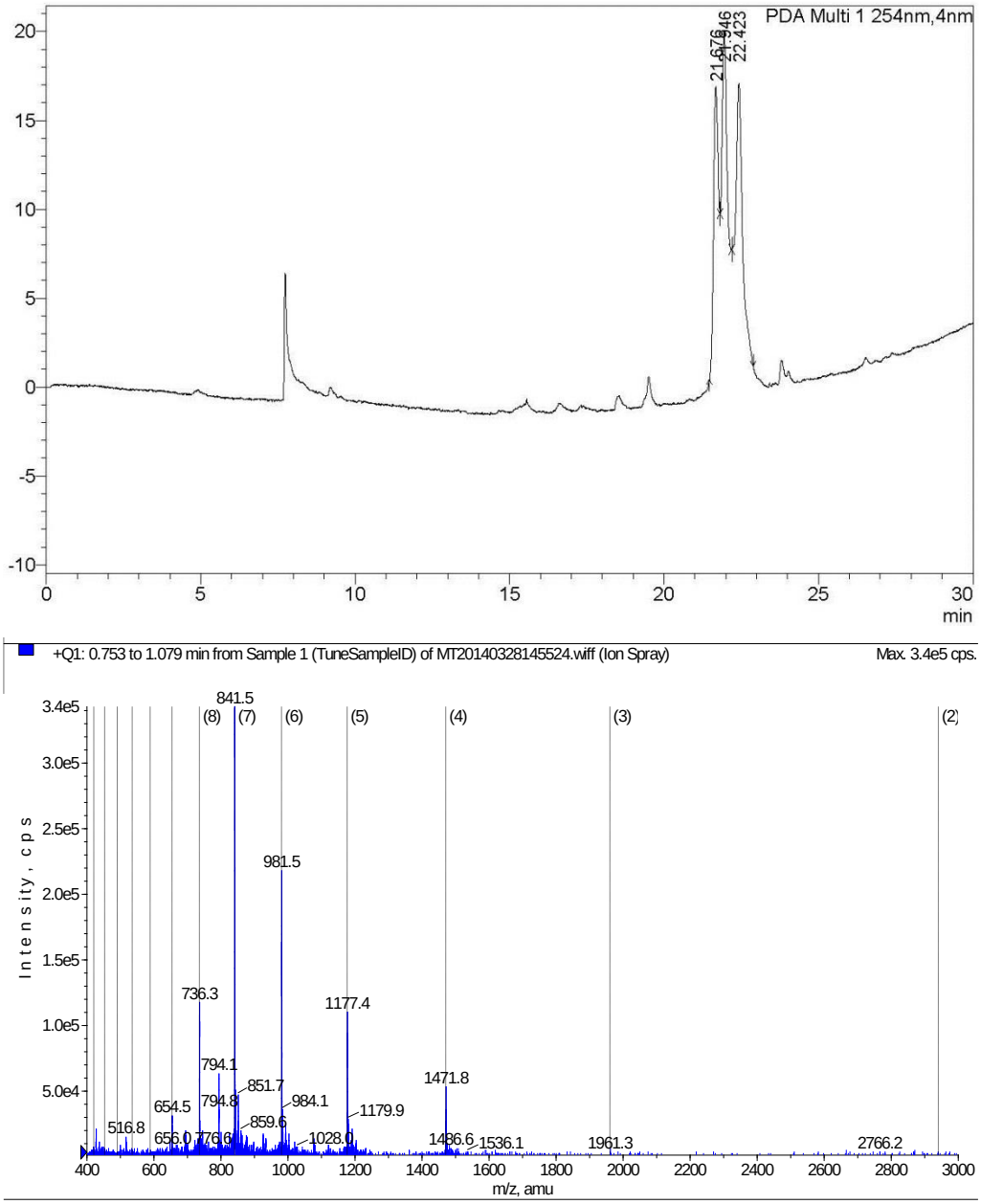

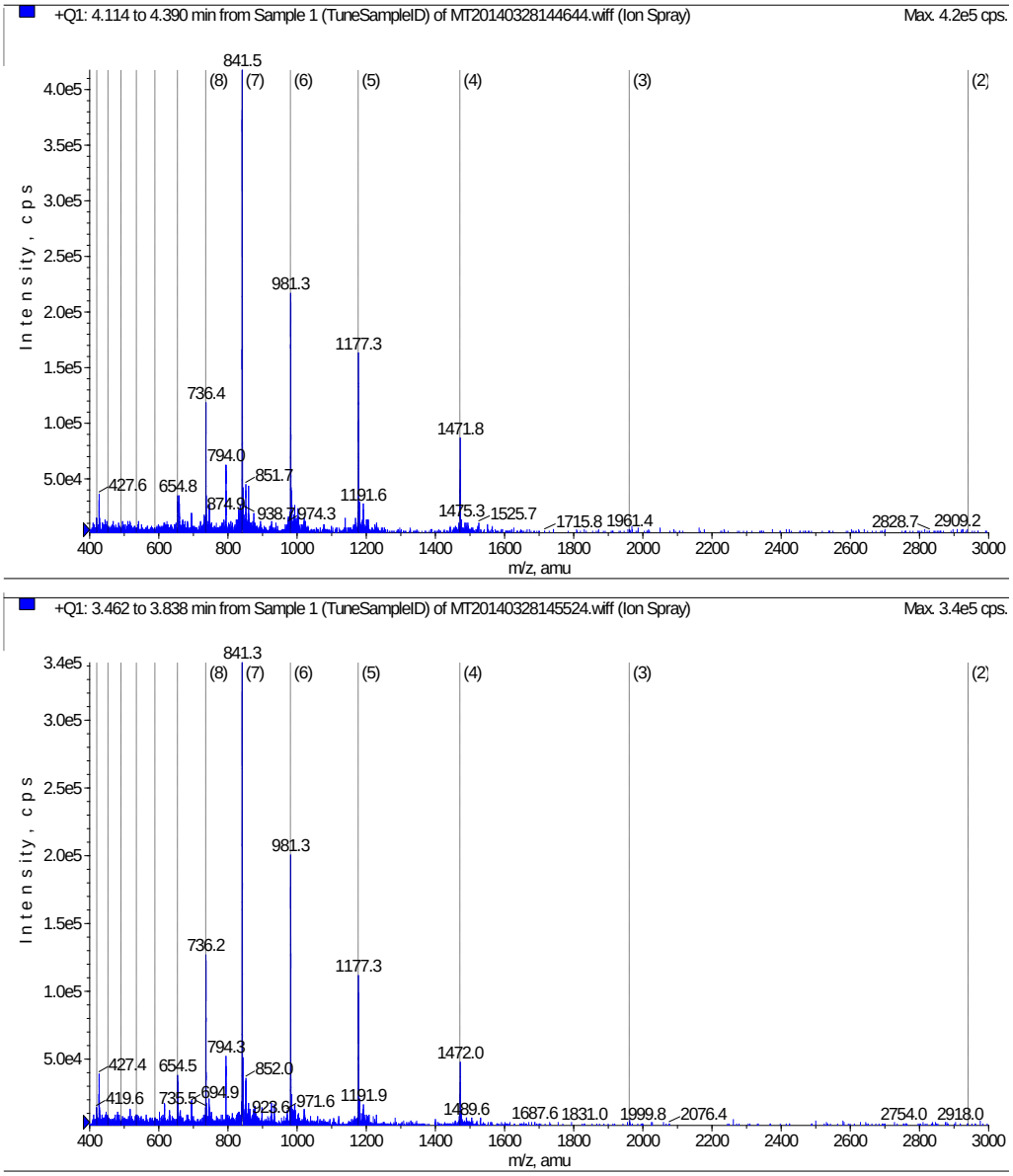

Appendix 9. RP-HPLC trace and mass spectra for Peptide **13** (33 % yield). Rt=21.67, 21.94 and 22.42 min (C8 column, 0-100% solvent B, 30 min). Exact mass of Peptide **13** $[M+1H]^{+1}$ calculated: 5876.89; calculated $[M+2H]^{+2}$ 2939.45; calculated $[M+3H]^{+3}$ 1959.96 and found 1961.3 and 1961.4; calculated $[M+4H]^{+4}$ 1470.22 and found 1471.8 and 1472; calculated $[M+5H]^{+5}$ 1176.37 and found 1177.3 and 1177.4. Purity ≥ 90%.

Appendix 10. Vaccine construct 14

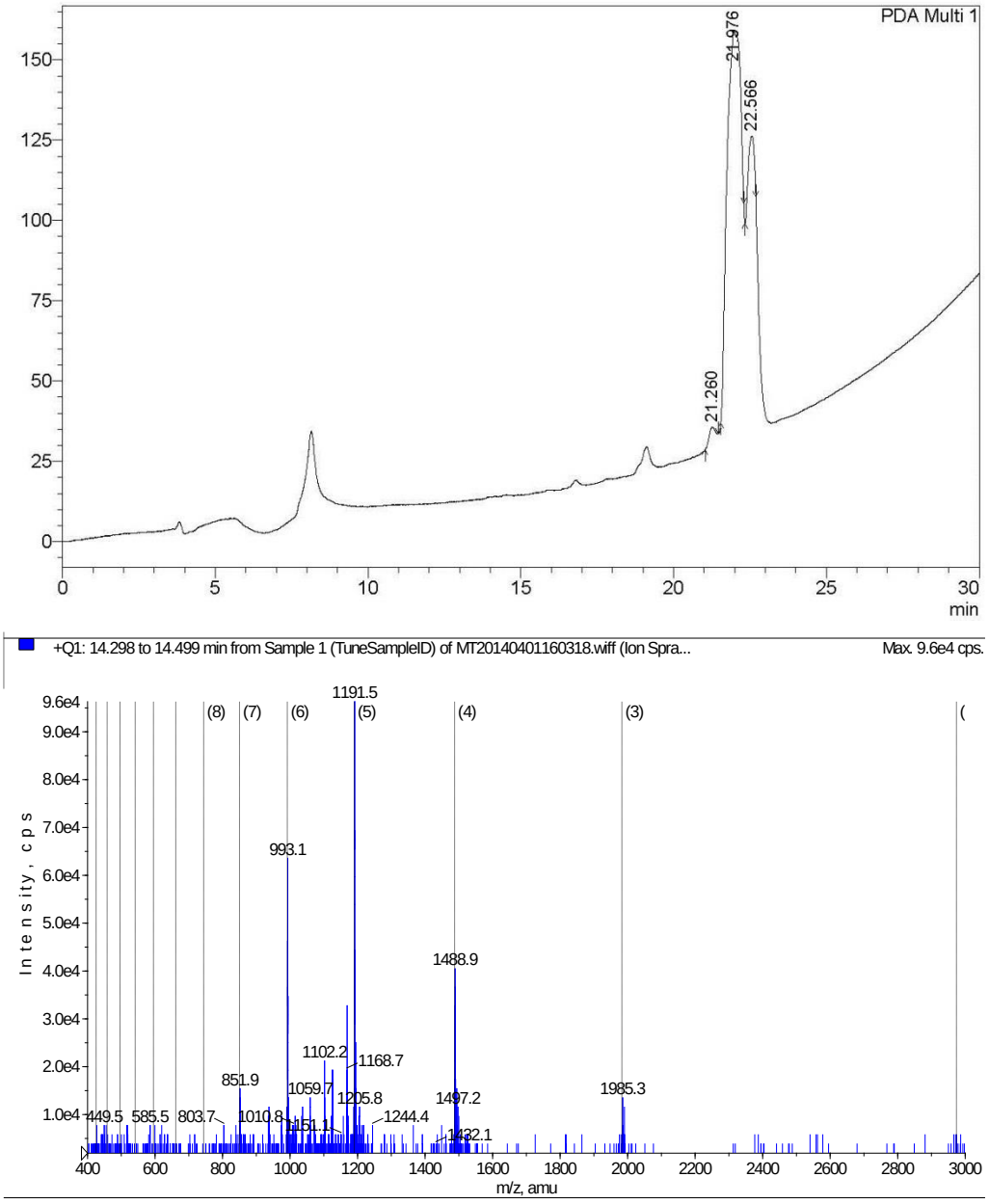

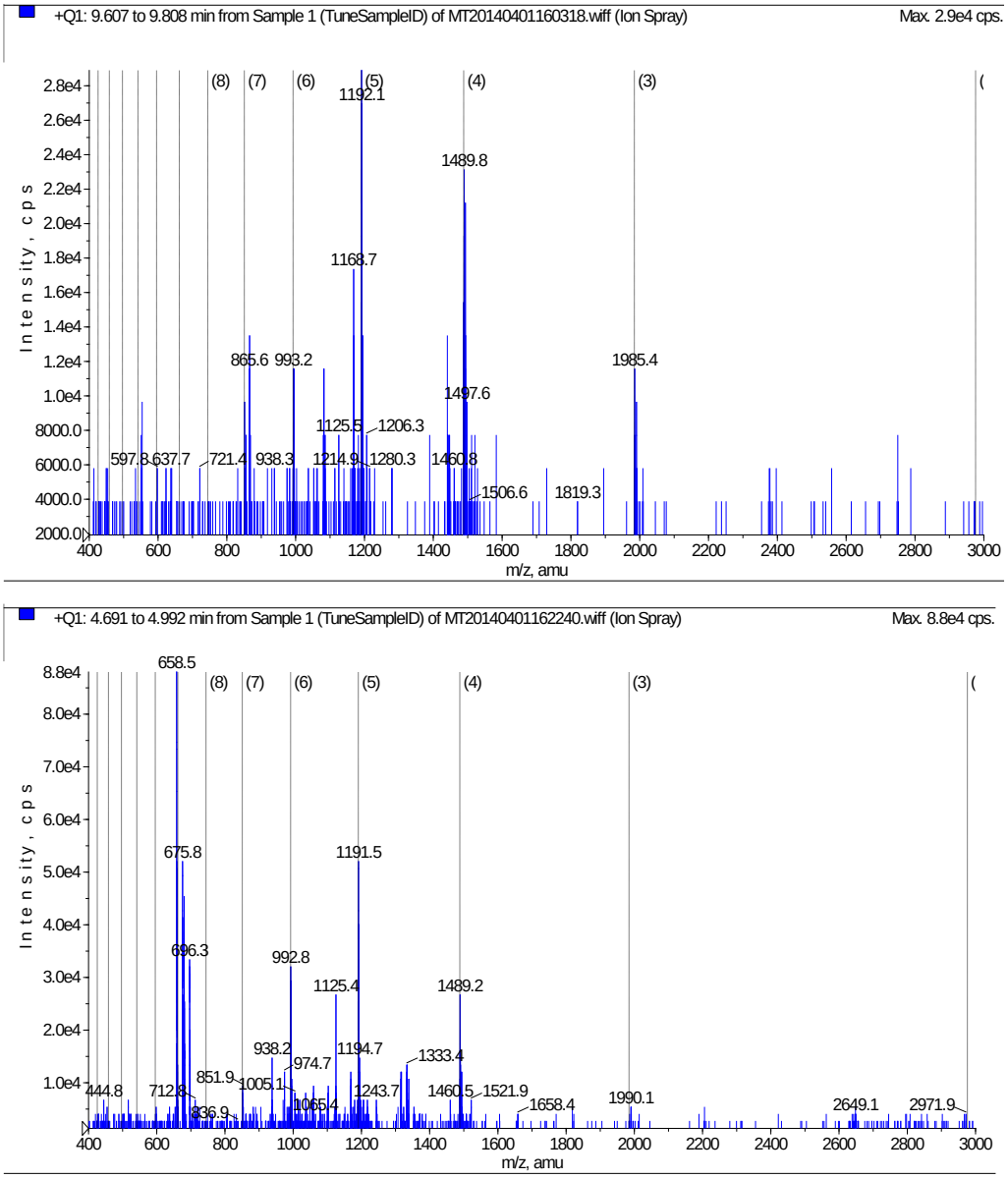

Appendix 10. RP-HPLC trace and mass spectra for Peptide **14** (35 % yield). Rt=21.26, 21.97 and 21.56 min (C8 column, 0-100% solvent B, 30 min). Exact mass of Peptide **14** $[M+1H]^{+1}$ calculated: 5947.93; calculated $[M+2H]^{+2}$ 2974.965 and found 2971.9; calculated $[M+3H]^{+3}$ 1983.64 and found 1985.4, 1985.3 and 1990.1; calculated $[M+4H]^{+4}$ 1487.98 and found 1489.8, 1488.9 and 1489.2; calculated $[M+5H]^{+5}$ 1190.58 and found 1192.1 and 1191.5. Purity ≥ 90%.

Appendix 11. Vaccine construct 15

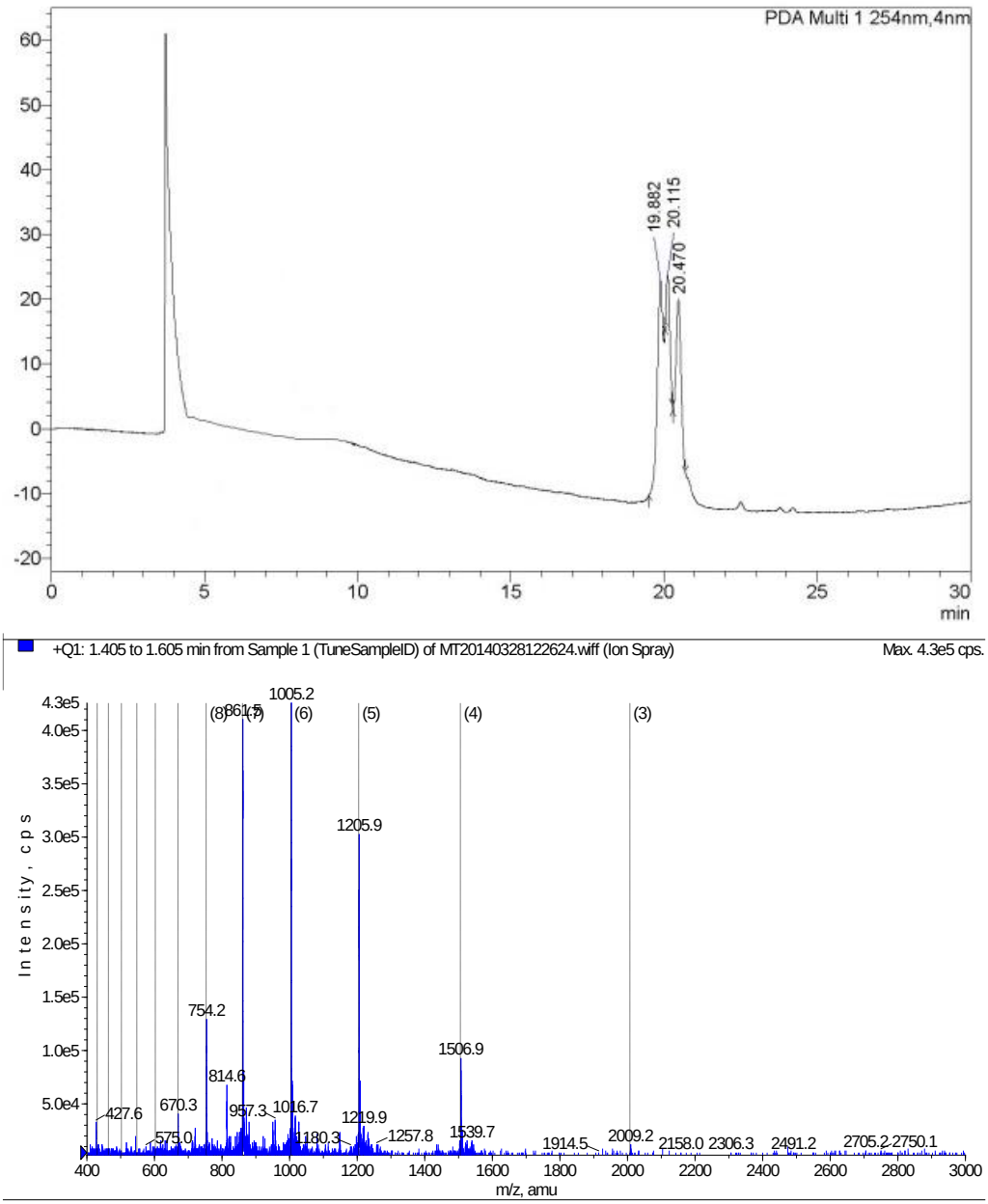

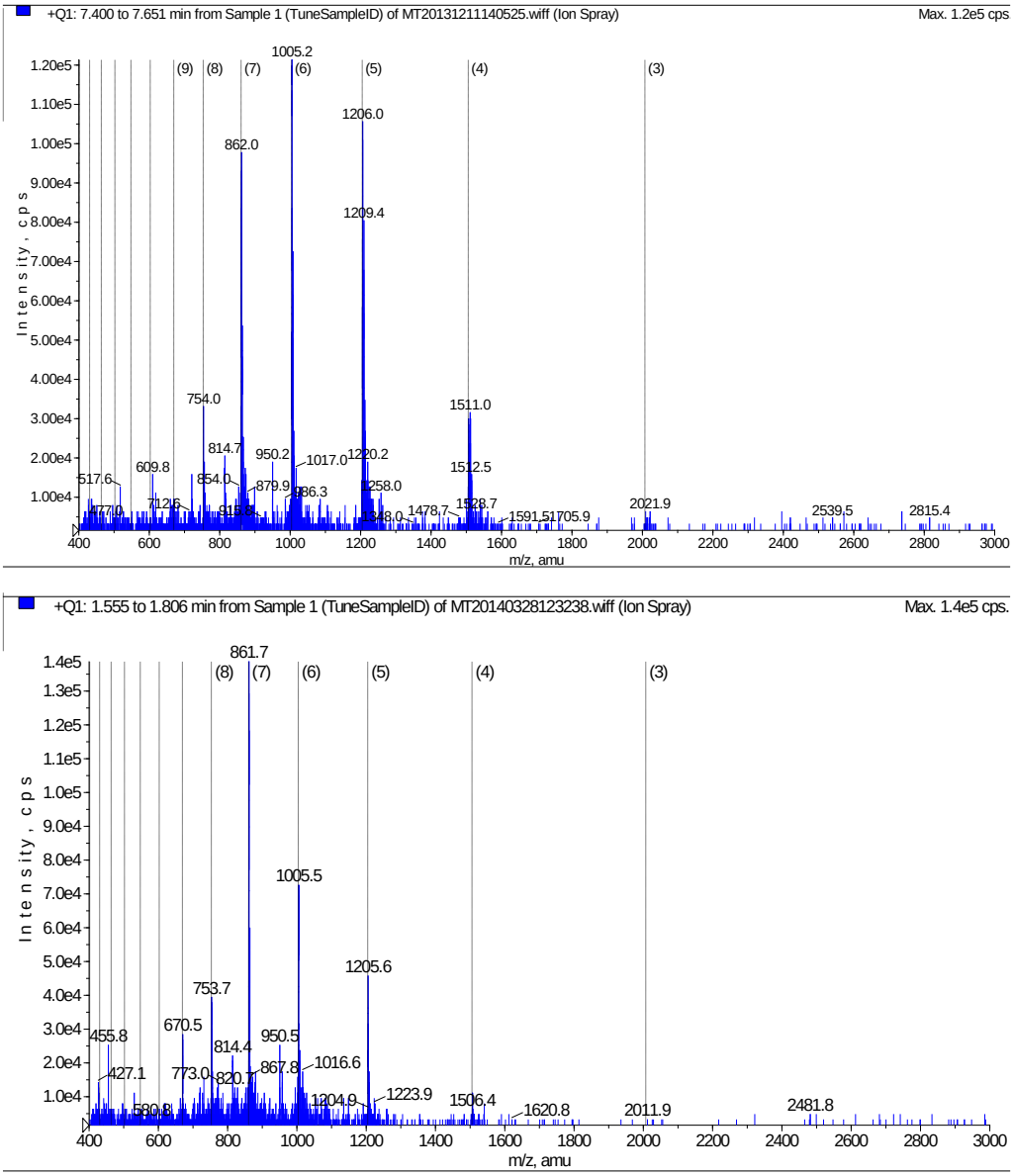

Appendix 11. RP-HPLC trace and mass spectra for Peptide **15** (34 % yield). Rt=19.88, 20.11 and 20.47 min (C8 column, 0-100% solvent B, 30 min). Exact mass of Peptide **15** $[M+1H]^{+1}$ calculated: 6018.97; calculated $[M+2H]^{+2}$ 3009.98; calculated $[M+3H]^{+3}$ 2007.32 and found 2009.2 and 2011.9; calculated $[M+4H]^{+4}$ 1505.74 and found 1511, 1506.9 and 1506.4; calculated $[M+5H]^{+5}$ 1204.79 and found 1206, 1205.9 and 1205.6. Purity ≥ 90%.

Appendix 12. Vaccine construct 16

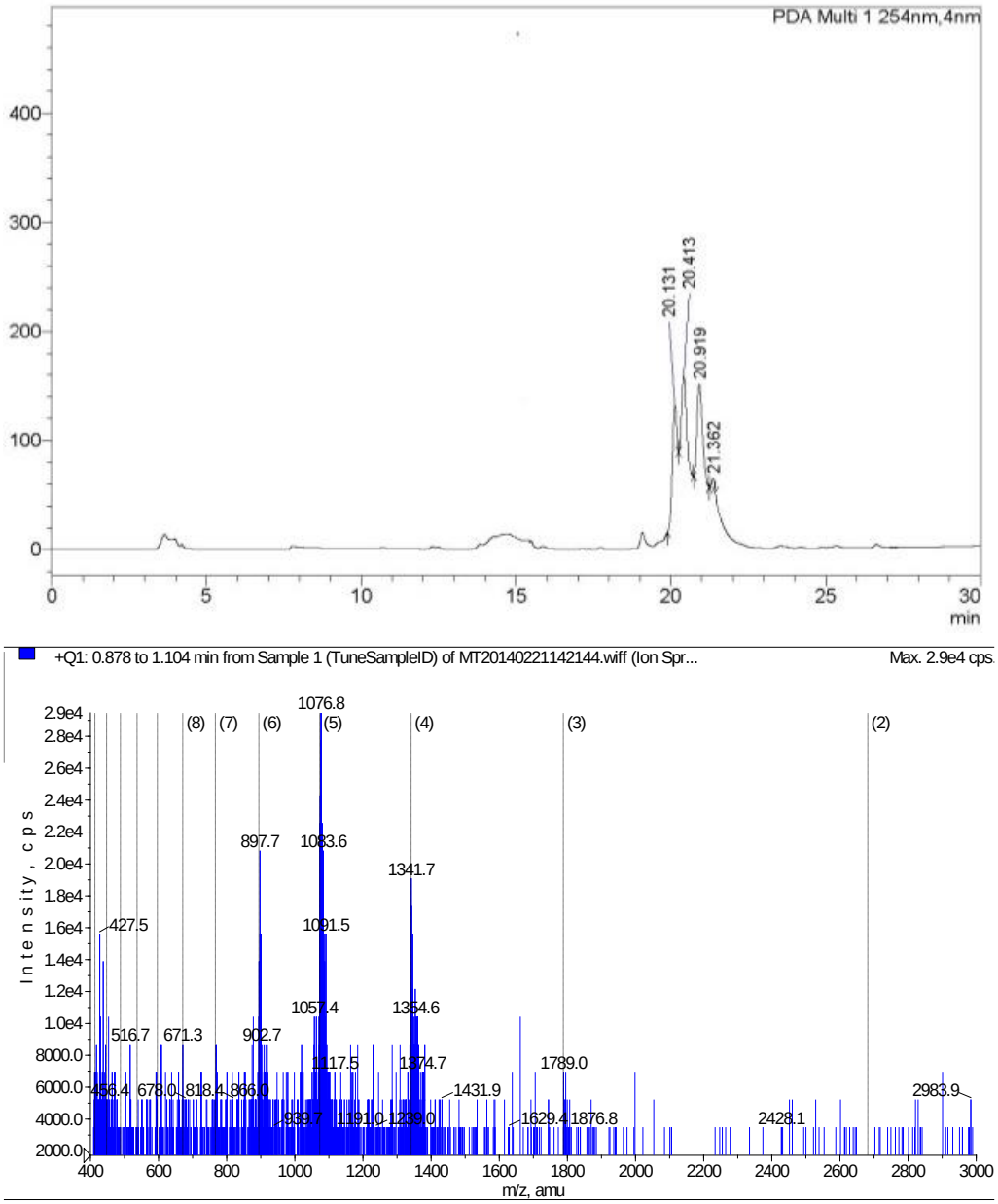

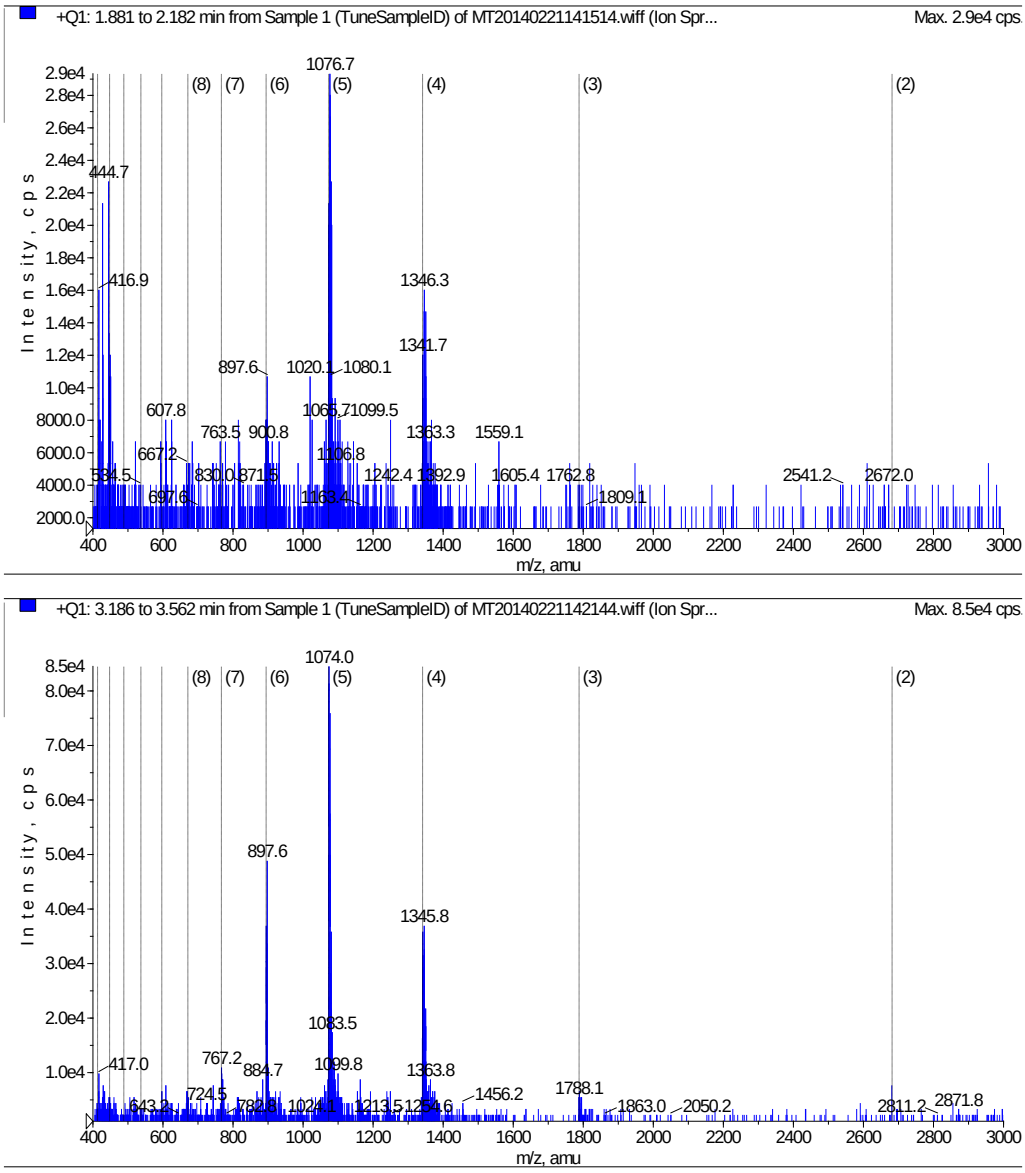

Appendix 12. RP-HPLC trace and mass spectra for Peptide **16** (45 % yield). Rt=20.13, 20.41 and 21.36 min (C8 column, 0-100% solvent B, 30 min). Exact mass of Peptide **16** $[M+1H]^{+1}$ calculated: 5358.78; calculated $[M+3H]^{+3}$ 1787.26 and found 1789 and 1788.1; calculated $[M+4H]^{+4}$ 1340.69 and found 1341.7 and 1345.8; calculated $[M+5H]^{+5}$ 1072.75 and found 1076.7, 1076.8 and 1074. Purity ≥ 90%.

Appendix 13. Vaccine construct 17

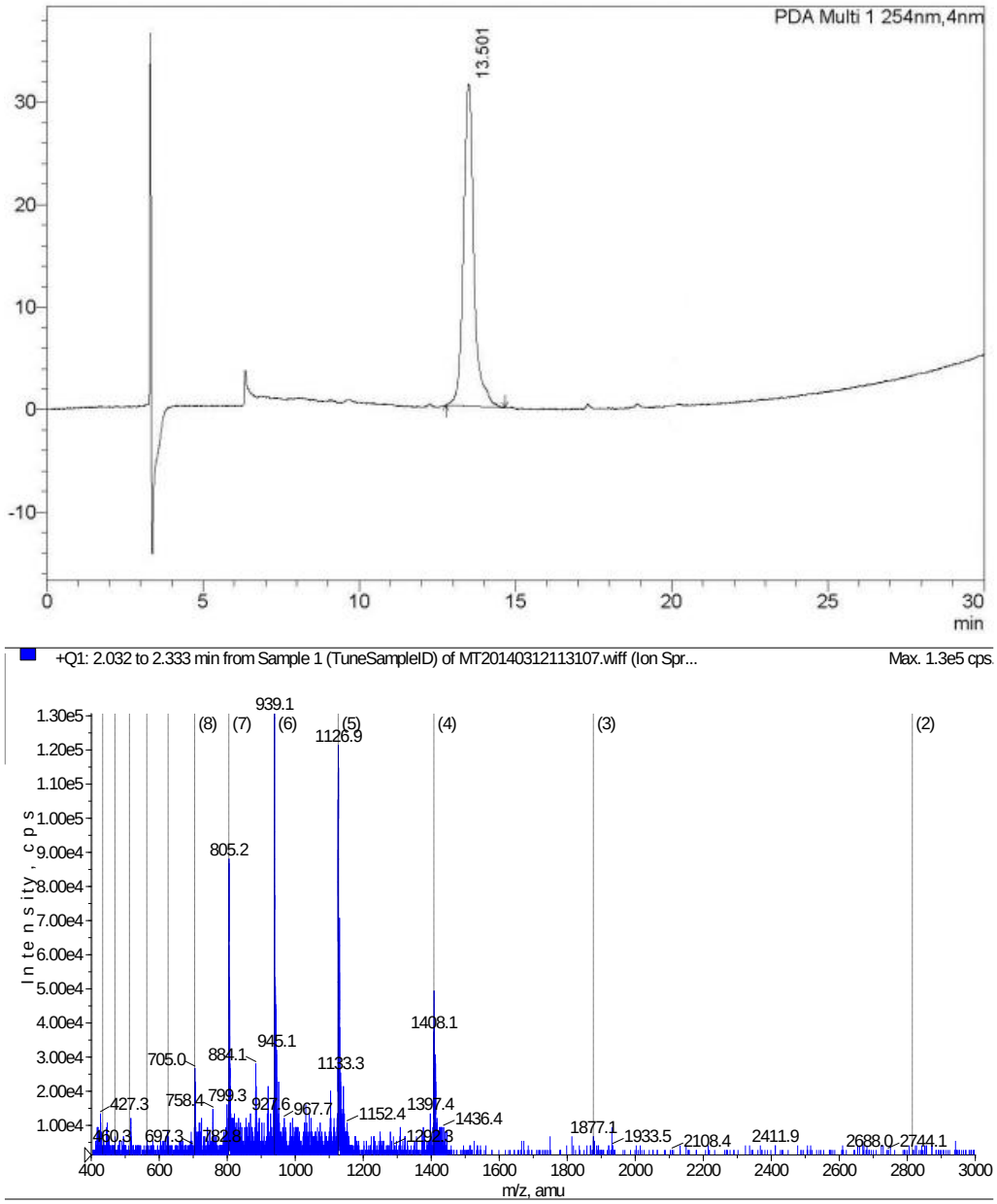

Appendix 13. RP-HPLC trace and mass spectra for Peptide **17** (51 % yield). Rt=13.501 min (C8 column, 0-100% solvent B, 30 min). Exact mass of Peptide **17** $[M+1H]^{+1}$ calculated: 5624.61; calculated $[M+3H]^{+3}$ 1875.78 and found 1877.1; calculated $[M+4H]^{+4}$ 1407.15 and found 1408.1; calculated $[M+5H]^{+5}$ 1125.92 and found 1126.9. Purity ≥ 92%.

Appendix 14. Vaccine construct 18

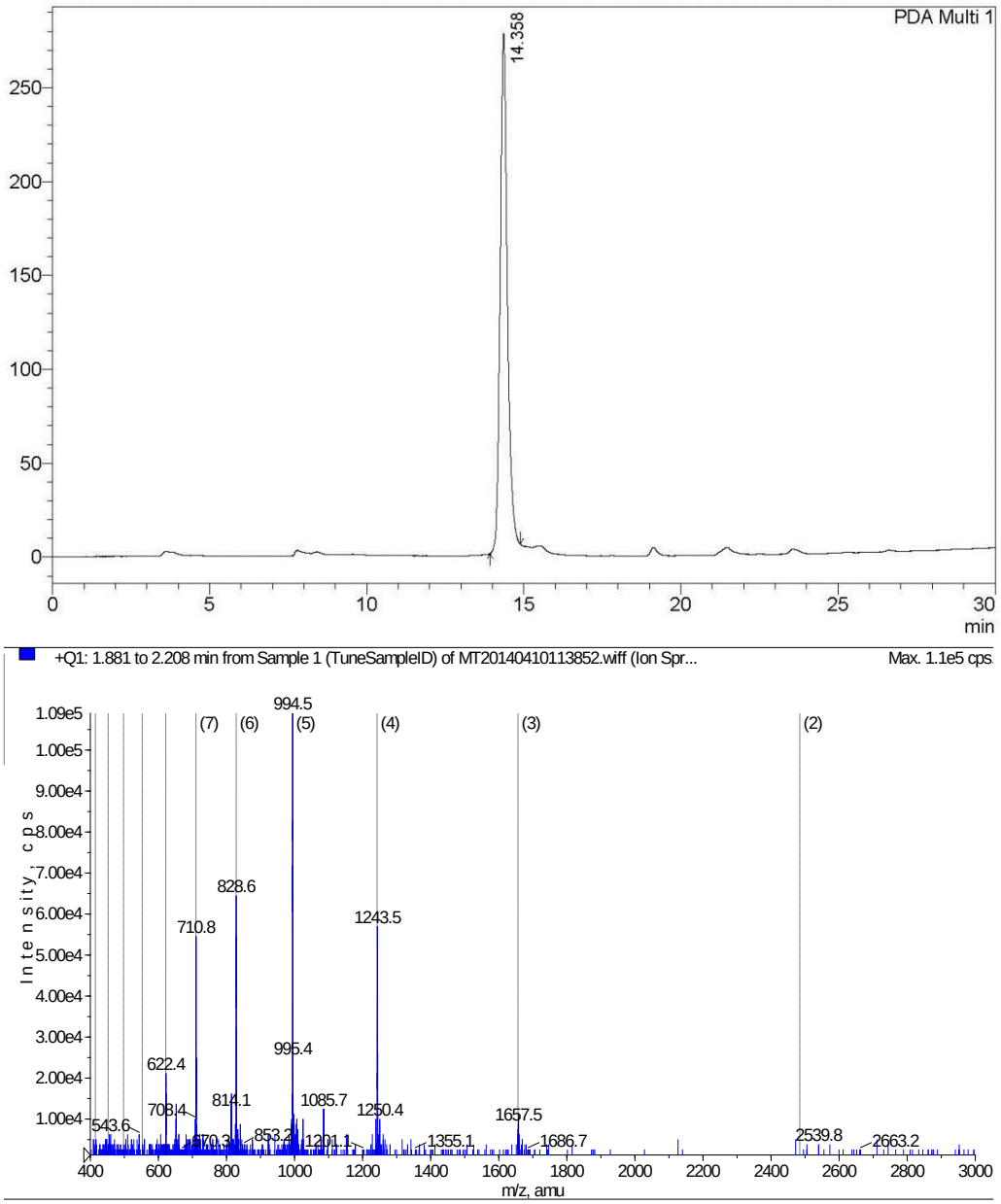

Appendix 14. RP-HPLC trace and mass spectra for Peptide **18** (35 % yield). Rt=13.501 min (C8 column, 0-100% solvent B, 30 min). Exact mass of Peptide **18** $[M+1H]^{+1}$ calculated: 4964.42; calculated $[M+3H]^{+3}$ 1655.8 and found 1657.5; calculated $[M+4H]^{+4}$ 1242.1 and found 1243.5; calculated $[M+5H]^{+5}$ 993.88 and found 994.5. Purity ≥ 92%.

Appendix 15. Flow Cytometry Concentration Selection

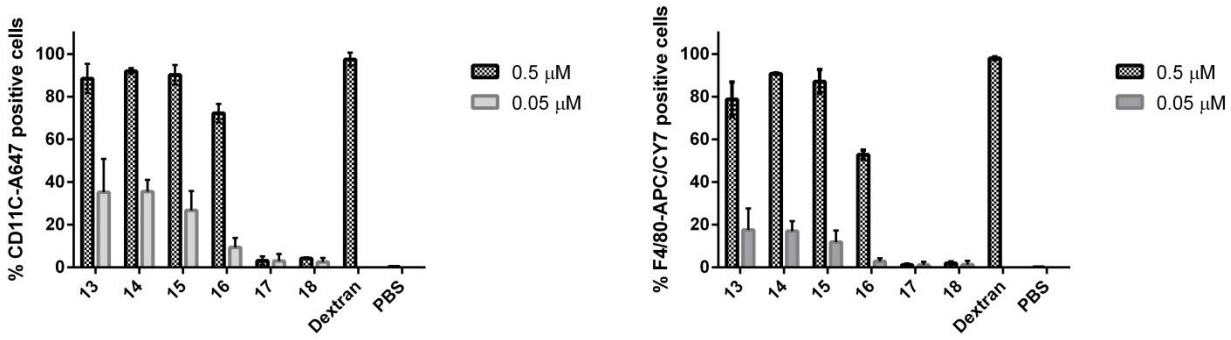

Appendix 15. Concentration (μM) selection using flow cytometry at 0.5 μM and 0.05 μM for the Vaccine Constructs (A) $CD11c^+$ and (B) $F4/80^+$ cells in triplicate. Dextran-FITC (1 mg/ml) was the positive control. PBS was the negative control. The study was performed in triplicate and the results were analysed with mean ± SD.

Appendix 16. Mass transfer limitation study on vaccine constructs 15 and 16

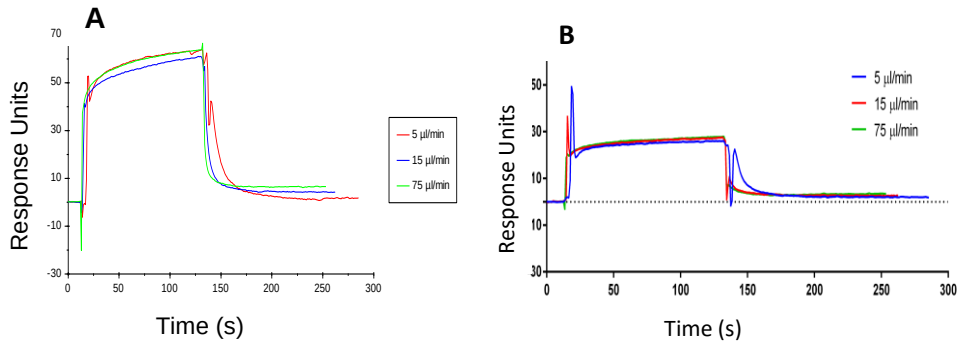

Appendix 16. Mass transfer limitation for (A) Peptide 11 and (B) Peptide 12 measured at 50 µM using different flow rates (5 µl/min, 15 µl/min, 75 µl/min) to determine changes in the level of response units using Biacore® 3000. Human recombinant mannose receptor (MR) immobilized on the CM-5 chip was used as the ligand. No change was observed in the response level (RU) between each of these runs indicating that mass transfer was not a limiting factor in this study.

Appendix 17. R_{max}, K_D and *in vitro* OT-II relation of vaccine constructs 13-18

Vaccine construct	K_D	R_{max}	OT-II *in vitro* prolifration count
13	5.31	15.2	1.12E+01
14	0.83	425	1.47E+02
15	22.8	51.3	2.97E+01
16	2.91	5.31	8.07E+00
17	0.12	27.5	1.49E+01
18	128	2.28	4.94E+01

Appendix 17. R_{max}, K_D and *in vitro* OT-II relation of vaccine constructs 13-18

This table summarises the information presented in **Chapter 4, Section 4.2.4.1.3, Figure 4-15** on binding measurements by SPR, and also the results provided in **Chapter 4, Section 4.2.3, Figure 4-3** from the average of three repeats of *in vitro* OT-II proliferation assay results**.**